MECHANISMS OF O_2-CHEMOSENSING IN DEVELOPING CHROMAFFIN CELLS

MECHANISMS OF O_2-CHEMOSENSITIVITY IN ADRENAL MEDULLARY

CHROMAFFIN CELLS FROM THE DEVELOPING RAT AND MOUSE

By

ROGER J. THOMPSON, B.Sc.(H).

A Thesis

Submitted to the School of Graduate Studies

in Partial Fulfilment of the Requirements

for the Degree

Doctor of Philosophy

McMaster University

Doctor of Philosophy   McMaster University
(Biology)   Hamilton, Ontario

TITLE: Mechanisms of O_2-Chemosensitivity in Adrenal Medullary Chromaffin Cells
      from the Developing Rat and Mouse

AUTHOR: Roger J. Thompson, B.Sc.(H). (Queen's University)

SUPERVISOR: Professor Colin A. Nurse

NUMBER OF PAGES: xxi, 270

ABSTRACT

The mammalian adrenal gland (or suprarenal gland) is a small organ located on the superior aspect of the kidney. The central region of the gland, the medulla, consists of chromaffin cells, which release catecholamines into the blood during periods of stress. This is best known as the 'fight or flight' response and is regulated, in the adult animal, by neuronal signals from the cholinergic sympathetic fibres of the splanchnic nerve. Interestingly, in some mammals, such as rat and human, sympathetic innervation is immature at birth, yet the chromaffin cells can still secrete catecholamines in response to physiological stessors, e.g. hypoxia. Increased plasma catecholamines is thought to provide a vital protective role for the neonatal animal during, and following birth. This is mediated in part by promoting lung fluid absorption, surfactant secretion, heart rate stabilization, and brown fat mobilization. The observation that, in the neonate, catecholamines are secreted in the absence of functional sympathetic innervation suggests that the chromaffin cells posses other mechanisms for directly 'sensing' a fall in blood O_2 tension (hypoxia).

The primary goal of this thesis was to uncover the mechanisms of oxygen-sensing in developing chromaffin cells from the rat and mouse, using primary short-term cell cultures of chromaffin cells. The experimental approaches relied on patch clamp techniques to record ionic currents and membrane potential, carbon fibre electrochemistry to record catecholamine

secretion from cell clusters, and fluorescent indicators to measure reactive oxygen species generation.

Hypoxic chemosensitivity was found in embryonic and neonatal, but *not* juvenile chromaffin cells from both the rat and mouse. Exposure to hypoxia or anoxia caused a reversible suppression of whole-cell current, which was comprised of the differential modulation of three K^+ currents: (1) suppression of a large-conductance Ca^{2+}-dependent K^+ current; (2) suppression of a delayed rectifier K^+ current; and (3) activation of an ATP-sensitive K^+ current. Hypoxia also induced membrane depolarization that was not initiated by any of these three voltage-dependent K^+ currents. Additionally, hypoxia broadened action potentials in chromaffin cells that showed spontaneous activity, and this was mediated by a prolongation of the time course of membrane repolarization. All of these factors likely contribute to catecholamine secretion by enhancing the influx of Ca^{2+} through depolarization-activated L-type Ca^{2+} channels.

Two sets of experiments were designed to identify the oxygen sensor in neonatal chromaffin cells. First, cells from transgenic mice, deficient in the gp91^{phox} component of the putative O_2-sensor protein, NADPH oxidase, responded to hypoxia in the same way as wild type cell, indicating that NADPH oxidase is not primarily responsible for oxygen sensitivity in these cells. Second, inhibitors of the proximal electron transport chain (e.g. rotenone and antimycin A) mimicked and attenuated the hypoxic response, while inhibitors of the distal electron transport chain (cyanide) and uncouplers of oxidative

v

phosphorylation (2,4-dinitrophenol) had no effect. Furthermore, reactive oxygen species production, primarily H_2O_2, decreased during exposure to hypoxia or inhibitors of the proximal electron transport chain, revealing a potential mitochondrial mechanism for 'sensing' of the hypoxic stimulus.

Reduced oxygen availability to the electron transport chain is proposed to cause a fall in cellular reactive oxygen species (ROS), principally H_2O_2. This fall in ROS signals closure of Ca^{2+}-dependent and Ca^{2+}-independent K^+ channels, which causes broadening action potentials and increases Ca^{2+} influx. The later is further enhanced by the hypoxia-induced membrane depolarization, which in turn increases the probability of cell firing. The rise in intracellular Ca^{2+} then acts as the signal for catecholamine release from the chromaffin cells.

Acknowledgements

Firstly, I would like to thank Dr. Colin Nurse for his excellent supervision, conversations, and faith in my abilities. His passion for science and research served as an excellent guideline for my graduate work. I also greatly acknowledge the technical assistance of Cathy Vollmer, without whom the smooth functioning of the lab would surely cease and whose yearly 'newspapers' always brought a smile. My gratitude goes out to past and present members of the lab, Hui Zhong, Min Zhang, Adele Jackson, Suzie Farragher, Veronica Campannucci, Nicole Inglis, and others that I have forgotten here, whose collaborations and contributions to a fantastic work environment were greatly appreciated. Thank you to the members of my committee, Dr. Mike O'Donnell, Dr. Gord McDonald, and Dr. Luke Janssen for your valuable criticisms and insights. I also gratefully acknowledge the Natural Science and Engineering Research Council of Canada and the Heart and Stroke Foundation of Canada for their continued support, and I thank the International Society for Arterial Chemoreception for the honour bestowed upon me when I was awarded the Heymans-deCastro-Neil Award for young investigators.

I would like to thank my great friends Jonothan Audia, Todd Bulmer, and Mike 'Ritchie' Cunningham for great golf games, hockey parties and an indeterminate number of breaks at the Phoenix (at which science was surely the major topic of conversation). I thank Vanessa Lougheed for her support and friendship. Of course my eternal gratitude goes out to my family for their support and love, and words alone could never describe

TABLE OF CONTENTS

Chapter 3...120

Oxygen-chemosensitivity in adrenal chromaffin cells: Comparison between developing wild type and NADPH oxidase deficient mice

O_2-sensing in neonatal rat adrenal chromaffin cells: Role of mitochondrial electron transport chain and reactive oxygen species

List of Figures

Introduction

Chapter 1

Chapter 2

Chapter 3

Chapter 4

Discussion

Appendix 1

Appendix 2

List of Abbreviations

4-AP	4-aminopyridine
A	adrenaline
AC	adenylate cyclase
ACh	acetylcholine
AChE	acetylcholine esterase
ACTH	adrenocorticotropic hormone
ADP	adenine diphosphate
AMC	adrenomedullary chromaffin cells
ATP	adenine triphosphate
BBSS	bicarbonate-buffered saline solution
bHLH	basic helix-loop-helix
BK	large-conductance Ca^{2+}-dependent K^+ channel
CA	catecholamines
CCAC	Canadian council on animal care
CGRP	calcitonin-gene related peptide
ChTX	charybdotoxin
CN	cyanide
DA	dopamine
DCF	2,7-dichlorodihydrofluorescine
DHBA	di-3,4-hydroxybenzylamine hydrobromide

xviii

DNP	2,4-dinitrophenol
DPI	diphenylene iodonium
E	epinephrine
E14.5-20	embryonic day
ETC	mitochondrial electron transport chain
FGF	fibroblast growth factor
GAP-43	growth-associated protein 43
GC	glucocorticoids
GC-1	glucocorticoid-1 receptor
H_2O_2	hydrogen peroxide
Heb3B	human embryonic erythropoeitn producing kidney cells
HERG	Human ether-a-go-go related gene
HIF-1	hypoxia-inducible factor
HPLC	high performance liquid chromatography
IbTX	iberiotoxin
IK_{O_2}	oxygen-sensitive outward current
I-V	current-voltage / current density-voltage relationship
$K_v 1.2$	*Shaker* potassium channels
L	lumbar
mAChR	muscarinic acetylcholine receptor
MAH	*v-myc* oncogene MASH1 positive immortalized adrenal cells
MASH1	mammalian *achete-schute* homologous gene

NA	noradrenaline
nAChR	nicotinic acetylcholine receptor
NE	norepinephrine
NEBs	neuroepithelial bodies
NGF	nerve growth factor
NMDG	N-methyl-D-glucamine
O_2^-	superoxide radical
P	postnatal day
PACAP	pituitary adenylate-cyclase activating peptide
PASMC	pulmonary artery smooth muscle cells
PBS	phosphate-buffered saline
PC12	phaeochromocytoma cells
P_{CO_2}	partial pressure of carbon dioxide
PNMT	phenylethanolamine-N-methyl transferase
P_{O_2}	partial pressure of oxygen
Q_{CA}	catecholamine charge
R_f	feedback resistor
R_{in}	input resistance
ROS	reactive oxygen species
R_s	series resistance
SA	sympathoadrenal
SDHD	succinate-ubiquinone oxidoreductase subunit D gene

SIF	small-intensely fluorescent
SK	small-conductance Ca^{2+}-dependent K^+ channel
SN	sympathetic neuron
SP	substance P
T	thoracic
TEA	tetraethylammonium
TTX	tetrodotoxin
VIP	vasoactive intestinal peptide

GENERAL INTRODUCTION

The availability of adequate tissue oxygenation is crucial for the survival of all mammals. Oxygen primarily functions as the terminal electron acceptor in the electron transport chain (ETC), which is a vital molecule in the oxidative phosphorylation of adenosine diphosphate (ADP) to adenosine triphosphate (ATP). In adult mammals, adequate oxygen is supplied to blood by the respiratory system and delivered to tissues by the circulatory system. In fetal animals, the maternal circulation delivers oxygen to the fetus via gas transfer across the placenta. Normally, oxygen levels are kept within strict limits, even during times of increased oxygen demand (e.g. exercise). The normal arterial partial pressure of oxygen (Po_2) in the adult is ~105 mmHg. Due to diffusion constraints, the Po_2 in normal fetal tissue is reduced to ~ 30 mmHg, but is still adequate for proper fetal oxygenation and development (Guyton, 1991).

Fetal mammals have evolved several strategies that allow them to enhance O_2 delivery to tissues. These include expression of fetal hemoglobin that shifts the O_2-hemoglobin dissociation curve to the left and allows the fetal blood to carry 20-30% more O_2 than the adult. Fetal hemoglobin concentration per red cell is also ~50% greater than in the adult. Finally, the Bohr effect, which describes the inverse relationship between O_2 and CO_2 binding to hemoglobin in the adult, is reversed in the fetus, so that fetal blood can carry more O_2 at higher CO_2 concentrations (Guyton, 1991).

In adult mammals, a series of events is thought to maintain blood Po_2 levels. Oxygen partial pressure (Po_2) is measured by strategically located peripheral

chemoreceptors, of which the best characterised are the glomus or type 1 cells of the carotid body. A fall in arterial P_{O_2}, P_{CO_2}, or $[H^+]$, as may occur during ascent to high altitude or respiratory disease, is thought to evoke secretion of neurotransmitters from glomus cells onto the synaptic terminals of petrosal sensory neurons. The chemical, neurotransmitter signals are then thought to be relayed to the central pattern generator of the brain stem via a change in firing frequency of the carotid sinus nerve (Gonzalez, 1994). Thus, blood homeostasis is maintained via activation of the respiratory reflex, which increases ventilation. The carotid chemoreceptor reflex is also thought to initiate catecholamine release from the chromaffin cells of the adult adrenal medulla via activation of cholinergic sympathetic fibres in the splanchnic nerve (Biesold et al., 1989). In the neonatal animal however, glomus cell function in the carotid body is immature and undergoing 'resetting' to function in the higher oxygen tension of the extrauterine environment (Gonzalez et al., 1994; Wasiko et al., 1999). Additionally, sympathetic innervation of target organs, such as the adrenal gland and heart, is relatively immature in some species, e.g. rat and human (Lagercrantz and Slotkin, 1986). Thus, a problem arises for the neonate, in that normal mechanisms for P_{O_2} homeostasis are immature, yet the animal must still respond appropriately to hypoxic stress, as frequently occurs during birth and extrauterine apnoea. It is now thought that the chromaffin cells of the adrenal medulla function as O_2-sensors in preparing the neonate for extrauterine life.

1. Historical implications of chromaffin cells as oxygen sensors.

West and colleagues (1953) suggested the first physiological role for fetal chromaffin tissue when they proposed that the high catecholamine (CA) content of the adrenal medulla functions to maintain fetal blood pressure and circulation. It was confirmed in later experiments that norepinephrine (NE), released from adrenomedullary chromaffin cells (AMC) and the extrachromaffin cells of Zuckerkandl can redistribute fetal blood flow in the lamb to the brain, heart and adrenal gland at the expense of less vital organs (Campbell et al., 1967). Further, Seidler and Slotkin (1985) demonstrated a vital role for epinephrine (E) release during hypoxia in the survival of neonatal rats (see section 4.1 below). These studies suggested that the adrenal chromaffin cells, in the absence of mature sympathetic innervation, are able to detect changes in arterial oxygen levels and secrete CA to make appropriate physiological adjustments in response to hypoxic stress.

A direct role of AMC in oxygen sensing was first suggested by Comline and Silver (1961), who showed that the CA content of the early term fetal lamb adrenal gland was reduced during hypoxia. They also demonstrated a progressive increase in CA output during fetal maturation that was accompanied by a shift in the NE to E content of the adrenal medulla. Studies on human infants who experienced complicated births, such as breech presentation and fetal asphyxia, revealed a depletion of CA content in the adrenal medulla (Lagercrantz and Bistoletti, 1973), suggesting a direct response of the human fetal AMC to hypoxia. Additionally, other studies have shown that neonatal rat AMC release CA during exposure to hypoxia (Seidler and Slotkin, 1985). However, after

maturation of sympathetic innervation to the adrenal gland, hypoxia-evoked CA release becomes dependent on splanchnic nerve activation. This has been observed in rat (Seidler and Slotkin, 1985, 1986), ovine (Jones et al., 1988; Cheung, 1990; Rychkov et al., 1998), and bovine (Dry et al., 1991) adrenal glands. Taken together, these studies suggest that AMC possess a developmentally regulated mechanism for sensing a fall in arterial Po_2 (hypoxia).

2. Structure and function of the adrenal gland

The mammalian adrenal, or suprarenal glands, are located on the superior aspect of the kidneys (Figure 1A), and have two main structures (Figure 1B). The outer layer, or adrenal cortex, is comprised of the cortical cells, which are responsible for hormone production (e.g. corticosteroids, mineralocorticoids and gonadocorticoids). The inner layer, or adrenal medulla, consists of chromaffin cells, which synthesise and release catecholamines (epinephrine, norepinephrine, and to a lesser extent dopamine) into the blood.

2.1 The adrenal cortex

The cortical (outer) layer of the adrenal gland is comprised of three main structures: 1) the zona glomerulosa, which secretes primarily mineralocorticoids; 2) the zona fasciculata, which secretes the glucocorticoids, and; 3) the zona reticularis, which secretes gonadocorticoids. The zona glomerulosa is the outermost layer and the

Figure 1. Anatomy of the adrenal gland and its innervation.

A. the adrenal gland (AD) is found on the superior side of the kidney (K; left side shown) and receives innervation from the splanchnic nerve (sp), which arises, in part, from the sympathetic chain (SC) and spinal cord. Other abbreviations in the figure are A; aorta, a and b; anterior and posterior divisions of the splanchnic nerve, cg; coeliac ganglia, D; diaphragm, PS; psoas muscle, sg; suprarenal ganglion (from Keese et al., 1988). B. diagram of a cross section of the adrenal gland, illustrating the main structures (From Hole, 1993).

A
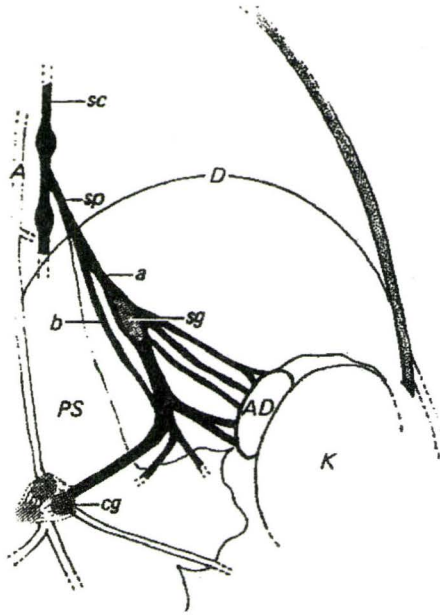
B
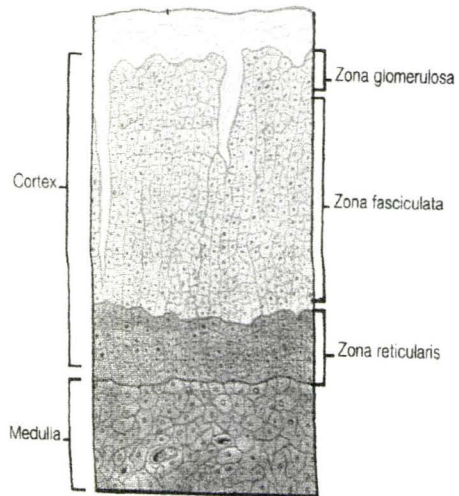
cationic balance of the blood regulates secretion of mineralocorticoids from these cortical cells. Specifically, when plasma sodium ions (Na^+) decrease, the renin-angiotensin pathway is activated, leading to angiotensin II release from lung capillaries. Angiotensin II activates aldosterone secretion from cortical cells in the zona glomerulosa, which promotes Na^+ reabsorbtion in the nephrons of the kidney (Tortora and Grabowski, 1992).

The middle layer of the adrenal cortex, the zona fasciculata, is principally responsible for the synthesis and secretion of glucocorticoids (GC). Approximately, 95% of the GC produced is hydrocortisone (Tortora and Grabowski, 1992). The secretion of GC is under negative control by hypothalamus-pituitary-adrenal axis, such that low GC levels stimulate release of corticotropin releasing hormone from the hypothalamus, which in turn causes secretion of adrenocorticotropic hormone (ACTH) from the anterior pituitary. ACTH is carried by the blood to the zona fasciculata where it activates GC secretion from the zona fasciculata (Hole, 1993).

The actions of GC (primarily hydrocortisone is considered here) are varied and evoke tissue-specific responses. Hydrocortisone 1) promotes ATP production in skeletal muscle through gluconeogenesis; 2) provides an anti-inflammatory action through inhibition of histamine secretion (mediated through the H_1 receptor) from Mast cells, and; 3) regulates gene expression, e.g. increase phenolethanolamine-N-methyltransferase (PNMT) expression, which is the enzyme responsible for E synthesis from NE in the adrenal medulla (Tortora and Grabowski, 1992). GCs have

also been reported to provide trophic and differentiation roles for adrenal chromaffin cells (see section *3.1* below; Doupe et al., 1985).

The innermost layer of the adrenal cortex, the zona reticularis, produces and secretes several male sex hormones. Cortical cells in the zona reticularis produce androgens, and possibly estrogens (Tortora and Grabowski, 1992), which are thought to assist the gonad-produced sex hormones during puberty and menopause, but the specific functions of the gonadocorticoids are not well understood.

2.2 *The adrenal medulla*

The adrenal medulla is the innermost layer of the adrenal gland (see figure 1B) and is comprised mainly of the adrenomedullary chromaffin cells (AMC). These cells received their name because they stain brown with chromic acid, like other catecholamine-containing cells derived from the neural crest (e.g. glomus cells of the carotid body; Tsapatsaris et al., 1989). AMC are responsible for the synthesis of the catecholamines (CA), E and NE, and, to a lesser extent dopamine (DA). Approximately 80% of AMC found in the adult rat adrenal gland are E secreting, and the remaining ~20% secrete primarily NE, but this composition of AMC subtypes varies among species. DA release during stimulation is likely a consequence of its role as a precursor in E and NE synthesis, though an autocrine or paracrine function cannot be ruled out (Phillippe, 1983). AMC are arranged in small clusters of 10-20 cells, surrounded by blood vessels and axons of sympathetic origin (Hole, 1993).

The AMC are electrically excitable (see section 5 below), and release CA upon activation by the cholinergic sympathetic fibres of the splanchnic nerve (see figure 1A and section *3.2* below). Acetylcholine (ACh) release from sympathetic nerve terminals activates nicotinic acetylcholine receptors (nAChR) and muscarinic acetylcholine receptors (mAChR) on the chromaffin cell. The net result of ACh stimulation is cell depolarization through activation of cation channels or K^+ channel inhibition via mAChR activation. These in turn are coupled to Ca^{2+} influx and/or release of Ca^{2+} from intracellular stores (Chowdhury et al., 1994). Increased intracellular Ca^{2+} during cholinergic stimulation of AMC is thought to be the main mechanism for CA release.

In the adult, CA secretion from AMC usually occurs during physiological (e.g. hypoxia) or environmental (e.g. predator-prey interaction) stress. Detection of stress involves activation of the hypothalamus or other brain centres, which stimulate the sympathetic nervous system (Hole, 1993). CA released from AMC during stress mediate the 'fight-or-flight' response, which comprises multiple physiological changes that are designed to prepare the animal to combat the stress. These include, increases in heart rate and force of contraction, vasodilation, and increased glucose production from glycogen (Hole, 1993); these effects are mediated through α and β adrenergic receptors (see section 4 below).

Interestingly, in some mammals (e.g. rat) the sympathetic nervous system is immature at birth (see section *3.2* below), yet there is still a requirement for adrenal CA in the stress response. It appears that developing AMC express adaptations to directly measure the physiological status of the blood (e.g. O_2 tension or pH) and

consequently to secrete CA during stress (see Lagercrantz and Slotkin, 1986). In addition to these transiently-expressed chemosensory properties, the neonatal animal also has a different tissue distribution of adrenergic receptors than the adult, which alters the 'fight-or-flight' response so that neonatal survival is promoted through physiological protective effects (see section *4.2* below for more detail).

3. Origin and development of chromaffin cells and chromaffin cell function

3.1 Embryonic origin of chromaffin cells

Chromaffin cells are adrenergic (primarily epinephrine containing) endocrine cells that are derived from sympathoadrenal (SA) precursor cells of the neural crest. The SA progenitors are multipotent cells that can develop into sympathetic neurons (SN), small-intensely fluorescent (SIF) cells, extra-adrenal chromaffin cells or adrenal chromaffin cells. The final developmental fate of the SA progenitor may be guided by a number of sequential events, e.g. exposure to specific growth factors, that occur during ontogeny (reviewed by Anderson, 1993).

The first identifiable stage indicating commitment of neural crest-derived cells to the SA lineage is thought to be the expression of mammalian *achaete-schute* homologous (MASH1) gene (Lo et al., 1991). The MASH1 gene is a transcription factor that is a homologue of the *Drosophila* gene, *achaete-schute*, which is required for development of specific neuroblasts in the fly larvae (Ghysen and Dambly-Chaudiere, 1988). Twenty-four hours after the appearance of MASH1, the neural crest

cells begin to express SA differentiation genes, e.g. tyrosine hydroxylase, which likely marks their commitment to the SA lineage (Anderson, 1993).

Sympathoadrenal precursors migrate from the neural crest to their target sites, such as the adrenal primordia, carotid body, and paravertebral sympathetic ganglia. A combination of soluble factors (e.g. growth factors), extracellular matrix and the timing of cell dispersal are thought to commit the migrating SA cells to their final developmental fate. SA progenitors from the neural crest are initially unresponsive to nerve growth factor (NGF), based on measurements of neurite outgrowth and mitotic rate (Anderson, 1993). This is further reflected in the observation that SA progenitors do not express mRNA for the NGF receptors, p75 and p140^{trk} (Birren and Anderson, 1990). However, they show responsiveness to fibroblast growth factor (FGF), which can promote neurite outgrowth, but fails to act as a long-term survival factor (Stemple et al., 1988). FGF dependence in SA progenitors migrating to the sympathetic trunk is followed by development of NGF dependence. At this stage, the SA progenitors begin to show a SN phenotype and become dependent on NGF for survival (Anderson, 1993).

In the case of AMC, there appears to be a specific sequence of growth factor dependence and interdependence that ultimately commits the SA cell to a chromaffin phenotype. SA progenitors that migrate to the developing adrenal medulla are exposed to high levels of glucocorticoid (GC), which have two main effects on the development and differentiation of AMC. First, low concentrations (~10^{-8} M) of GC, produced by the developing adrenal cortex, inhibit the development of the neuronal

phenotype. This is achieved through suppression of neuron-specific genes, such as GAP-43 (Federoff et al., 1988). This first action of GC is thought to be a prerequisite for the second function, which is to induce the expression of PNMT, the enzyme responsible for E synthesis (Michelsohn and Anderson, 1992). After induction of PNMT, chromaffin cells require GC for survival, since ~80% of cultured rat neonatal chromaffin cells die in the absence of exogenous dexamethasone or hydrocortisone (Doupe et al., 1985). It is interesting to note that the second effect of GC on chromaffin cell differentiation requires much higher concentrations of GC ($\sim10^{-3}$ M), similar to levels found in the adult adrenal gland, and may reflect a switchover of GCs role from suppressing neuronal genes to providing trophic support. Induction of PNMT synthesis is thought to be the marker for commitment of the SA progenitor to the chromaffin phenotype (Anderson, 1993).

Although the SA progenitors in the developing adrenal medulla express a predominantly chromaffin phenotype at embryonic day > 14.5 in the rat, they are able to change into other SA-derived cell types by exposure to the appropriate growth factors, indicating maintenance of pleuripotency. For example, GC (e.g. dexamethasone, a synthetic analogue of hydrocortisone) is required to maintain the chromaffin phenotype, and withdrawal of GC and concomitant addition of NGF to cultured rat neonatal chromaffin cells produces a switch from the chromaffin phenotype to a neuronal one without associated cell death (Doupe et al., 1985). Dexamethasone is frequently used to replace hydrocortisone in culture media because it is more stable than the natural GC. Interestingly, the transition from AMC to SN

passes through an intermediate stage where the cells appear SIF-like, illustrating the importance of growth factors in determining the final developmental fate of SA progenitors during ontogeny (Doupe et al., 1995). However, AMC from the adult rat are much more resistant to the effects of GC withdrawal and NGF administration, suggesting that at some point during development AMC become committed to their chromaffin phenotype (Doupe et al., 1985).

3.2 Innervation of chromaffin cells

Two main types of nerve fibres, cholinergic sympathetic fibres (efferent innervation) from the splanchnic nerve, and peptidergic fibres (afferent innervation) innervate the chromaffin cells of the adrenal medulla. Functional innervation of AMC by these two types of fibres develops along quite different time courses; efferent innervation is not mature in the rat until ~ 10 days postnatally, while functional afferent innervation can be detected as early as postnatal day 2 (Holgertet al., 1994).

The neuronal cells that give rise to the splanchnic nerve have complex origins throughout the central and peripheral nervous systems, and have been extensively mapped using the retrograde tracer, fast blue (Kesse et al., 1988; Mohamed et al., 1988; Coupland et al., 1989; Parker et al., 1993). By far the most abundant innervation of AMC originates from pre-ganglionic sympathetic neurons, whose cell bodies are found in the spinal cord within thoracic (T) segments 8 and 9, but range from T1 to lumbar segment (L) 1 (Keese et al., 1988). There is also an innervation from a population of postganglionic sympathetic fibres that arise from the paravertebral

sympathetic chain between T4 and T12, with the maximal contribution from T9 and T10 (Keese et al., 1988). A few postganglionic neurons are found in the suprarenal ganglion, but none in the coeliac ganglion have been identified (see Figure 1A). Parasympathetic innervation to the medulla is also present and likely functions to oppose the effects of sympathetic stimulation that has activated the fight-or-flight response (Parker et al., 1993).

In addition to the pre- and post-ganglionic sympathetic efferent fibres that innervate the adrenal medulla there is also an afferent component. Cell bodies of afferent fibres were traced with fast blue and arise primarily from the dorsal root ganglia between T3 and L2, with the largest component from T10 (Mohamed et al., 1988). Interestingly, there is also a small component of afferent fibres (~14% of the total afferents labelled) arising from the vagal sensory nodose ganglion (Coupland et al., 1989). Characterization of the afferent innervation of the medulla by immunocytochemistry has revealed at least three types of peptidergic sensory neurons. These contain substance P (SP; Khalil et al., 1986), vasoactive intestinal peptide (VIP; Malhotra and Wakade, 1987) or pituitary adenylate cyclase activating peptide (PACAP; Dun et al , 1996), all of which are proposed modulators of adrenal medullary CA secretion.

SP has been proposed to prevent desensitization of the nAChR by binding to a site different from the ACh binding domain or by regulating phosphorylation of the protein, thus allowing the nAChR to continue responding to prolonged stimulation (Khalil et al., 1987). VIP and PACAP are hypothesised to act as peptidergic

transmitters within the medulla. PACAP has been shown to cause greater CA release from AMC than both ACh and VIP, and is activated by low frequency stimulation (0.5 to 3 Hz) of the splanchnic nerve. In contrast, high frequency (10 to 50 Hz) stimulation appears to evoke ACh release (Malhotra and Wakade, 1987). VIP release is also induced by low frequency stimulation of the splanchnic nerve, but appears only to activate secretion from epinephrine containing AMC (Guo and Wakade, 1994).

Development of the efferent and afferent components of adrenal innervation follows distinct time courses. Peptidergic (CGRP-containing) sensory fibres are detectable by immunocytochemistry 2 days after birth, but decline in number by the 6th postnatal day (Holgert et al., 1994). These fibres are degraded by treatment of the animal with capsaicin, which selectively destroys C-type or nociceptive sensory neurons (Pelto-Huikko et al., 1984) but are not affected by monoclonal antibodies against ACh esterase, suggesting that these fibres are non-cholinergic (Holgert et al., 1994). Further, peptidergic transmitters are potent modulators of CA secretion from AMC during the perinatal period (Slotkin and Seidler, 1988), suggesting that the sensory (afferent) component of adrenal innervation is functional at birth.

In contrast, the preganglionic sympathetic innervation to the adrenal medulla does not mature until approximately 10 days after birth in the rat. This is supported by the observation that GAP-43 and neurofilament-10, markers of axonal growth, decrease with postnatal age (Holgert et al., 1994). Additionally, AChE positive fibres are observed to project into the medulla on the second postnatal day, but AChE staining is relatively weak and increases dramatically by postnatal day 16 (Holgert et

al., 1994). Interestingly, the increase in AChE staining is accompanied by a decrease in the number of sensory fibres and an increase in the expression of CA synthesising enzymes (dopamine-β-hydroxylase and tyrosine hydroxylase) in AMC, suggesting that chromaffin cell maturation and sensory innervation are under the control of sympathetic innervation (Holgert et al., 1994).

The existence of sympathetic fibres in the neonatal medulla (though fewer in number compared to the adult) raises the question whether these are functional. Several lines of evidence suggest that sympathetic innervation to the adrenal medulla is indeed immature or non-functional at birth. First, reflex stimulation of AMC normally occurs when stress (e.g. hypoglycemia) is detected by the central nervous system, followed by activation of the hypothalamus, stimulation of pre-ganglionic sympathetic fibres and CA secretion from AMC. In adult but not neonatal rats, this reflex is blocked by the nAChR antagonist, chlorisondamine, suggesting that functional nerve connections are absent in the neonate (Seidler and Slotkin, 1985). Second, hypoxia-induced CA release from AMC, can be blocked by chlorisondamine in the adult but not neonate (Seidler and Slotkin, 1985). Third, maternal stress, such as alkaline shock, which accelerates development of sympathetic innervation results in premature loss of the 'direct' hypoxia-induced CA secretory response in rat AMC, while splanchnic denervation of the adult results in its return (Slotkin and Seidler, 1986). Finally, markers of sympathetic innervation, ornithine decarboxylase activity and acetylcholine transferase levels are low or absent in neonatal animals, but increase ~ 4 fold by the 10th postnatal day (Slotkin and Seidler, 1988). Since, nicotine and high

extracellular K^+ evoke Ca^{2+}-dependent CA secretion from neonatal AMC the secretory machinery is intact (Slotkin and Seidler, 1988). Taken together, these studies suggest that sympathetic innervation of the adrenal medulla is immature or non-functional during early postnatal life.

3.3 Development of stimulus-secretion coupling

Both the cholinergic and peptidergic neurons that innervate adult AMC can evoke robust CA secretion. Pre-ganglionic sympathetic fibres release ACh, which activates both the nicotinic and muscarinic acetylcholine receptors on AMC. The nicotinic receptors found in adult AMC are of the neuronal type (nAChR), with a single channel conductance of ~45 pS and show rapid (~ 2ms) activation. Muscarinic receptors on the other hand, are classical G-protein coupled receptors, that can either modulate ion channels directly or mobilize release of Ca^{2+} from intracellular stores. Using specific inhibitors and activators of these two classes of receptors, several differences in receptor coupling to secretion in AMC have been observed.

In AMC, nicotine activates a rapid inward current via a cation channel permeable to Ca^{2+}, Na^{2+} and to a lesser extent, K^+ (Fenwick et al., 1982). The resulting inward current causes membrane depolarization, activation of voltage-dependent Na^+ and Ca^{2+} channels and cell firing. During the action potential, Ca^{2+} influx causes CA secretion by promoting vesicle fusion with the plasma membrane (Aunis and Langley, 1999). The rise in intracellular Ca^{2+} and CA secretion evoked by nicotine is rapid (< 2 ms) and terminates within ~10 sec (Chowdhury et al., 1994).

In addition, AMC express either the M_3 or M_4 muscarinic receptors, as assayed by measurements of changes in intracellular Ca^{2+} upon binding of the M_3/M_4 antagonist, 4-diphenylacetoxy-4-methyl-piperidine (4-DAMP). Muscarine evokes secretion with a delay (0.5-2 sec), but its effects last up to 30 sec following stimulation (Chowdhury et al., 1994). Muscarinic stimulation of CA secretion may involve a dual mechanism where the rise in intracellular Ca^{2+} is mediated via K^+ channel inhibition and membrane depolarization or release from intracellular stores. The mAChR's can stimulate secretion through inhibition of large conductance Ca^{2+} dependent K^+ channels, which are thought to prolong action potential duration and enhance Ca^{2+} influx (Herrington et al., 1995). Alternatively, it has been proposed that mAChR stimulation inhibits an inward rectifier K^+ channel, which depolarizes the membrane and activates Ca^{2+} influx through voltage-dependent Ca^{2+} channels (Akaikeet al., 1990). In addition to modulation of ion channels, mAChR stimulation has also been shown to cause release of intracellular Ca^{2+} from inositol trisphosphate-sensitive stores in bovine AMC (Eberhard and Holz, 1987).

Catecholamine release by ACh stimulation of AMC, mediated through the two classes of ACh receptors, shows a developmental profile that likely reflects the maturation of innervation. AMC from embryonic rats aged E14-16 days were unresponsive to ACh stimulation and the nerve fibres projecting to the adrenal medulla contained few detectable synaptic vesicles viewed by electron microscopy (Oomori et al., 1998). By embryonic day E18-20, synaptic vesicles in neurons and AMC were more numerous, but AMC responded only to nAChR stimulation and not mAChR

stimulation (Seidler and Slotkin, 1986; Oomori et al., 1998). Immediately after birth (postnatal days, P1-2), adult levels of CA secretion could be evoked by both types of ACh receptor agonists (Oomori et al., 1998). Interestingly, these changes in AChR-coupled secretion also parallel changes in the expression of the CA synthesizing enzymes, as assayed by immunocytochemistry. Dopamine-β-hydroxylase activity, which is required for NE synthesis, is seen as early as embryonic day E14. However, PNMT expression, an indicator of E synthesis, is absent until E18 and continues to increase until ~ 16 days after birth (Verhofstad et al., 1985; Oomori et al., 1998).

Although it is generally thought that the signal for CA release during the stress response in mammals arises from ACh release from sympathetic fibres, several peptidergic neurotransmitters are potent stimulators of CA secretion. Secretion evoked by VIP, PACAP and ACh has been observed in a single rat AMC, but some cells are responsive only to ACh (Chowdhury et al., 1994). Thus, CA secretion is under strict developmental control and is regulated by a number of different neurotransmitters. Opiate peptides have also been found in rat AMC, and are released during nervous stimulation or during direct stimulation of neonatal cells by hypoxia. They are proposed to play a modulatory role in CA secretion (Chantry et al., 1982). It is thought that different brain centres stimulate specific populations of spinal neurons, leading to preferential release of CA from sub-populations of AMC. This ensures the proper amount and type of CA enters the blood in response to different stressors (Anuis and Langley, 1999).

4. Catecholamines, adrenergic receptors and their physiological roles

The first step in the synthesis of CA in the adrenal medulla (and other adrenergic tissues) is the hydroxylation of tyrosine to Dopa, by the rate-limiting enzyme tyrosine hydroxylase (TH). Dopa is then converted by dopa-decarboxylase to dopamine, which is subsequently hydroxylated by dopamine-β-hydroxylase to norepinephrine (NE). NE is then N-methylated by phenylethanolamine-N-methyltransferase to produce epinephrine.

CA are functionally coupled to adrenergic receptors, which consist of two general classes, α-adrenergic receptors and β-adrenergic receptors. To date, nine subunits of these receptors (α_{1a}, α_{1b}, α_{1c}, α_{2a}, α_{2b}, α_{2c}, β_1, β_2 β_3) have been classified based on rank order of potency for adrenergic drugs and genetic sequence (reviewed by Strosberg, 1993). These receptor subtypes have both tissue specific and overlapping distributions, in addition to a specific developmental profile (see below). Generally, both E and NE function as ligands for α and β receptors, but NE has a higher affinity for the α subtypes, while E can activate both classes equally well (Guyton, 1991). The overall tissue response to adrenergic receptor stimulation is a combination of the relative proportion of receptor subtypes and the degree to which they are coupled to their effector systems.

The adrenergic receptors are considered to be the prototypical G-protein coupled receptors, and since the first proposal of two receptor subtypes in 1948 by Ahlquist, much information on their function has appeared in the literature. The α_1 receptors are positively coupled to phospholipase C by the G-protein, G_q, and increase

phosphatidyl-inositol turnover, which in turn mediates changes in intracellular Ca^{2+} levels (Summers and McMartin, 1993). The α_2 receptors are negatively coupled to adenylate cyclase (AC) activity via G_i or directly to ion channels, and activation causes a decrease in cellular cyclic AMP (cAMP) or ion channel inhibition. On the other hand, all three classes of β receptors are positively coupled to AC through G_s and therefore, increase cAMP levels (Summers and McMartin, 1993). The physiological role of adrenoreceptor stimulation varies from tissue to tissue. However, adrenergic-receptor stimulation is generally accepted to be the main receptor type that mediates the stress, or 'fight-or-flight' response in mammals.

4.1 Adrenergic receptors and the stress response in the mature mammal

During stress, whether physiological (e.g. hypoxia) or environmental (e.g. predation), the hypothalamus signals the descending fibres of the reticular formation to activate the sympathetic nervous system. The pre-ganglionic sympathetic fibres of the splanchnic nerve then release ACh onto AMC, evoking CA secretion into the blood. Circulating CA then acts on adrenergic receptors in target tissues to activate the stress response. Generally, the stress response consists of a series of physiological responses that prepare the animal to either combat or flee the stress.

These responses include: 1) increased strength of heart contraction and heart rate, mediated through β_1 and β_2 receptors; 2) shunting of blood flow from the periphery and less vital organs (e.g. digestive track and kidneys) to more vital ones (e.g. heart and brain), which is mediated by both α and β receptors; 3) glycogenolysis

and heat generation, mediated through β receptors; and 5) bronchiodilation and increased respiration, which is also mediated through β receptors in the lung. The initial response is mediated by sympathetic neurons that synapse directly with target tissues, but prolonged responses are mediated by CA release from the adrenal medulla (Guyton, 1991).

The basal rate of CA release from the adrenal medulla is approximately 0.2 μg/kg/min of E and 0.05 μg/kg/min of NE (Guyton, 1991), which yields typical plasma concentrations in the human between 1 and 2 ng/litre (Lagercrantz and Slotkin, 1986). These levels of circulating CA help maintain blood pressure at almost normal levels, and likely function in concert with the sympathetic nervous system to provide physiological redundancy in the production of sympathetic tone. During stress, plasma CA concentration can reach between 5 and 10 ng/litre in the adult and ~50 ng/litre in the newborn (Lagercratz and Slotkin, 1986). Sustained basal release of CA into the blood likely allows for both increases and decreases in sympathetic tone, giving the animal a broad dynamic range of responses to varying stress situations.

4.2   Adrenergic receptors and the stress response in neonates and the fetus

It had been known before the pioneering study of Comline and Silver (1961) on adrenal responses of fetal sheep to hypoxia that administration of exogenous NE to early term animals can shunt blood flow from the periphery to the heart and brain. This suggests that the stress response is intact at early developmental stages. Work in the 1980's by Slotkin and colleagues demonstrated that the fetus and neonatal rat

express specific adaptations to the stress response, which allow the animal to cope with a lack of functional sympathetic innervation. The most dramatic was the observation that the fetal rat heart expresses predominantly α receptors, as opposed to β receptors found in the adult heart (Slotkin and Seidler, 1986). This allows the fetus to avoid life threatening (due to energy depletion) increases in heart rate and strength of contraction that normally occur during the adult stress response. Administration of α antagonists during exposure of the neonatal rat to hypoxia results in a rapid increase in heart rate, followed by a loss of normal heart rhythm and eventual death (Seidler et al., 1987). In contrast, during hypoxia in the absence of adrenergic inhibitors, the fetal heart rate is maintained at a constant level, which provides a protective effect against the oxidative stress.

The role of β receptors in the stress response, especially that elicited by hypoxia, is similar to, but more diverse than that seen in adult rats. During hypoxia CA released from the adrenal medulla act on β receptors in the lung to induce bronchiodilation and increased respiration (as in the adult). Most importantly, in preparation for air breathing, CA change the lung from a net fluid secreting epithelium to one of net fluid absorption. In addition, CA induce surfactant secretion, which facilitates breathing by decreasing surface tension forces in the lung (Seidler and Slotkin, 1986). This is especially important during birth and in the immediate postnatal period, since blockade of β receptors results in respiratory failure and death in neonatal rats exposed to hypoxia. Additionally, human infants born by Caesarean section before the onset of labour have reduced plasma CA levels and this is correlated

with decreased lung compliance and cyanosis (Lagercrantz and Bistoletti, 1973). Thus, the specific profile in receptor expression allows the neonatal rat to display a modified stress response that is tailored to promoting survival, as opposed to inducing the adult fight-or-flight response.

4.3   Regulation of adrenergic receptor expression and function

As illustrated in the sections above (4.1 and 4.2), the response of a specific tissue to adrenergic receptor stimulation during the stress response is determined by the expression of specific α and β receptors. Additionally, the specific effects of the stress response reflect a combination of several factors including, relative levels of receptor expression and density, extent of receptor desensitization, and efficiency of coupling to effector systems.

The transcription of adrenergic genes is regulated in a biphasic manner by the presence of agonist. Acute increases in agonist concentration (1-2 hours) increases expression of β_2 receptor mRNA, however, prolonged exposure to agonist results in a dramatic decrease in mRNA and protein levels. These effects are thought to be mediated through changes in intracellular cAMP levels, which act on the cAMP-response element located in the 5' flanking region of the gene to transiently increase of decrease mRNA stability (Hadcock and Malbon, 1993). Similar effects of agonist concentration on expression of α_1 mRNA have been observed, but the opposite effect is seen for the α_2 receptor (Strosberg, 1993). Interestingly, activation of different receptor subtypes by agonist can also influence coupling of adrenergic receptors to G-

proteins and the effector molecules, (e.g. adenylate cyclase). For example, activation of the α_1 receptor can lead to increased coupling of the β_2 receptor to G_s in cardiomyocytes (Castellano and Bohn, 1997).

In addition to the 'direct' regulation of adrenergic receptor expression by their agonists, cross-talk between other G-protein coupled receptors may also regulate their expression and function. For example, stimulation of the glucocorticoid-1 (GC-1) receptor by dexamethasone can upregulate β_2 mRNA in the heart through activation of the cAMP response element (Strosberg, 1993). Interestingly, GC levels are quite low in the fetus because the adrenal cortex is relatively immature (see section *2.1*) and the heart seems to lack β receptors at this time (Seidler et al., 1987). Thus, it is difficult to predict the effects of basal levels of CA on receptor function during development, because the adrenergic receptors are regulated by a number of independent and overlapping mechanisms. Studies of physiological responses to CA have provided the best information on the types and functions of adrenergic receptors during development (see above). However, the factors that regulate development and expression of adrenergic receptors in the fetus are complex and presently are not fully understood.

5. Electrophysiology of adrenal chromaffin cells

The patch clamp technique is an experimental protocol that was invented in 1976 by Erwin Neher and Bert Sackman, for which they received the Nobel Prize in Physiology and Medicine in 1991 (see Sackman and Neher, 1995). This powerful

experimental technique uses a small glass electrode ($\sim$ 1 μm diameter) to form a tight electrical seal (GΩ; gigaseal) with the plasma membrane of the cell. The patch clamp technique is advantageous over traditional sharp electrode voltage clamp recordings because it allows for accurate measurements of ionic currents from small cells, which are often damaged during impalement. After gigaseal formation, application of a small amount of suction (conventional whole cell configuration) allows the researcher to precisely control membrane potential using a low-noise high-bandwidth feedback amplifier (Figure 2A). The amplifier uses a single electrode to control the membrane potential by injection of an equal and opposite current to the normal ionic current fluctuations in the cell. Thus, the experimenter can measure ionic currents at controlled voltages as the voltage drop across a high resistance (500 MΩ to 10 GΩ) feedback resistor (R_f; see figure 2).

In addition to whole-cell recording, several other configurations of the patch-clamp technique have been utilized (Figure 2B). Before application of suction to establish the whole-cell configuration, ionic currents can be recorded in the 'cell-attached' mode, or withdrawing the electrode can remove a 'patch' of membrane and allow recording of the current through channels in the 'inside-out' configuration (Hamill et al., 1981). Alternatively, after establishment of the whole-cell configuration, the electrode can be withdrawn to form an outside-out patch (see Figure 2B). In this way, the solution bathing the cytoplamic or extracellular sides of the membrane can be manipulated, allowing precise descriptions of ion channel selectivity, conductance, open probability, and gating properties in a variety of

excitable and non-excitable cell types. AMC have been one of the most extensively characterised cell types using this technique, and they are generally thought to be a prototypical model for studying excitable membranes and neurosecretion (e.g. Fenwick et al., 1984).

In classical whole-cell recording (used for ~ ½ of the recordings in Chapter 1 of this thesis), the intracellular milieu is replaced with the solution in the electrode, allowing for precise control of the fluid environment in the cell. Unfortunately, cell dialysis leads to loss of the normal cytoplasmic constituents, so that many second messenger systems are no longer intact. To overcome this experimental limitation, Horn and Marty (1988) invented a new whole-cell recording technique, the perforated-patch configuration, which utilized the pore-forming antibiotic, nystatin, to achieve electrical access to the cell. In the perforated-patch technique (used for the majority of recordings in this thesis), nystatin is placed into the patch pipette, and after seal formation, the antibiotic inserts into the plasma membrane to form 'perforations' that are permeable to monovalent, but not divalent cations and, to a lesser extent, anions (Kleinberg and Finklestein, 1984). Thus, this technique allows the monovalent ions inside the cell to be precisely controlled with minimal washout of second messengers, metabolites and buffers. The main disadvantage of the perforated-patch technique is that the series resistance (R_s), which is a sum of the pipette and membrane patch resistances, is ~ 3 fold higher than traditional whole cell recordings and can introduce substantial voltage errors (Jones, 1990). However, if care is taken to cancel the majority of series resistance, and if input resistance (R_{in}) of the cell is high (>1 GΩ), as

Figure 2. Electronic design of the patch clamp amplifier and configurations for patch clamp recordings.

A, simplified schematic of the electronic design of a patch clamp amplifier. The command voltage (Vc) is used to precisely control the potential across the cell membrane resistance (r) and capacitance (c). The electrode alternates between current injection and current measurements so that the cell's potential is held constant at Vc. Fluctuations in Vc at the cell, due to ionic currents, is measured across the feedback resistance (Rf) as a voltage drop. Rs represents the series combination of the pipette and patch resistances. B, typical configurations of the patch clamp technique. After the initial seal formation, the cell-attached configuration is achieved. Progression to the three other possible states are shown in the figure. Both and A and B are modified from Jones (1990).

A

R_f

Amplifier

V_c

Electrode

R_s

R

Cell

C

Ground

B

INSIDE—OUT

OUTSIDE—OUT

pull ↑

↑ pull

CELL—ATTACHED

suction →

WHOLE—CELL
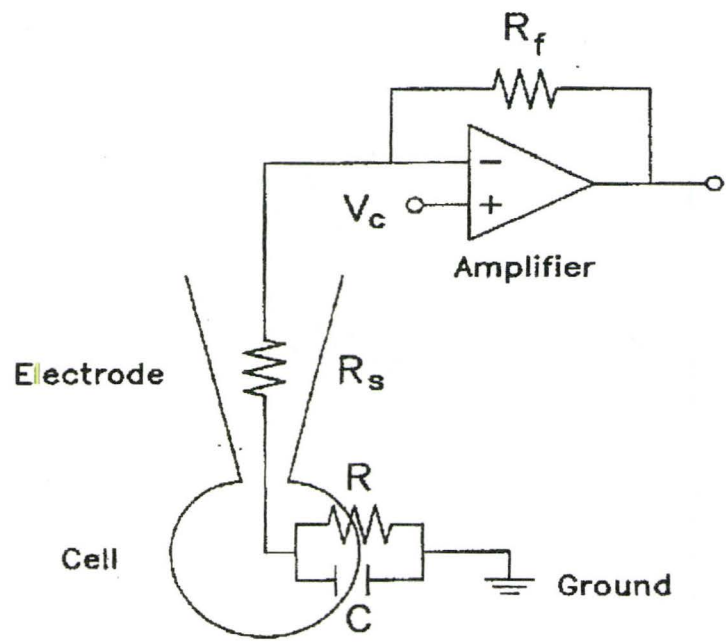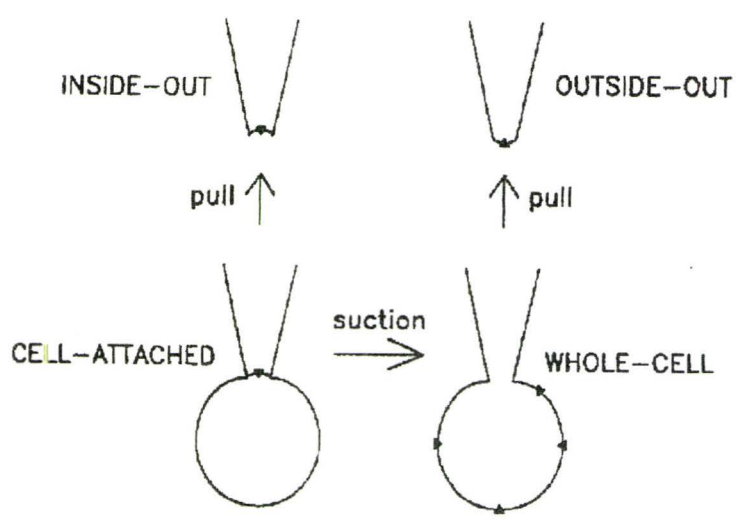
is the case for AMC, these voltage errors are minimal (Jones, 1990).

5.1 Amperometric determination of amine release

An interesting and powerful extension of voltage clamp utilises the low-noise amplifier and single carbon fibre microelectrodes (5-30 μm diameter) to monitor exocytosis of amines from single cells. In this technique, carbon fibre electrodes are placed adjacent to cells and polarized to ~ 600 mV to detect CA release (Leszczyszyn et al., 1990). This potential is well above the oxidation potential for CA (~ 300 mV), and amines released from the cell are rapidly oxidized following contact with the electrode surface. Oxidized amines release two electrons per molecule, which are measured as a current by the electrode. Carbon fibre electrochemistry has two main recording configurations. In the first, amperometry, the electrode is held at a constant potential and secreted amines can be monitored in real time as their oxidation current. Unfortunately, amperometry does not allow identification of individual amine species. The second configuration, cyclic voltammetry, utilizes a rapid (~ 10 ms) triangular waveform to repeatedly oxidize and reduce amines. In this way, individual species of amines can be identified by their characteristic oxidation-reduction curve (Chow and von Ruden, 1995). However, since most amine secreting cells release more than one species during a secretory event, the oxidation-reduction curve is a hybrid of the individual profiles of each oxidizable chemical released and quantification of specific amines is impossible. Despite these limitations, carbon fibre electrochemistry has been

a powerful addition to electrophysiology because it allows correlation of secretion with changes in other cell properties, such as ionic conductances or intracellular Ca^{2+}.

5.2 Inward currents in chromaffin cells

As summarized below, the majority of electrophysiological studies on AMC have been performed on cells isolated from adult animals. The inward current is carried predominantly by classical voltage-dependent, tetrodotoxin (TTX)-sensitive Na^+ channels (Fenwick et al., 1982). These channels are similar to those underlying the original Na^+ conductance described by Hodgkin and Huxley (1952) for the squid giant axon, and play an important role in action potential generation in AMC (Hollins and Ikeda, 1996).

In addition, rat AMC possess at least three types of Ca^{2+} channels, which control CA secretion to different extents: The long-lasting (L-type) channel is activated by depolarization and sensitive to dihydropyridines (e.g. nifedipine). The rapidly inactivating (N-type) Ca^{2+} channel is open at depolarized membrane potentials and is sensitive to ω-conotoxin-GIVA. Persistent (P-type) Ca^{2+} channels are non-inactivating and blocked by ω-agatoxin-IVA (Hess, 1990; Artalejo et al., 1994).

The ability to monitor membrane capacitance as an index of secretion concomitantly with voltage clamping has allowed Artalejo and colleagues (1994) to determine that L-type Ca^{2+} channels are most efficiently coupled to CA secretion in rat AMC. The L-type channel likely contributes to CA release during action potentials evoked by sympathetic stimulation of AMC during stress because it is non-

inactivating, opened by membrane depolarization, and may be closely linked to the exocytotic machinery (Artalejo et al., 1994). The N-and P- type channels appear to play important roles in CA secretion in the absence of action potentials and are thought to be more diffusely distributed in the cell (Artelejo et al., 1994; Kim et al., 1995). Similar Ca^{2+} channel subtypes have been described in cat (Lopez et al., 1995), dog (Gaspo et al., 1993), mouse and bovine (Hernandez-Guijo et al., 1998) AMC. Interestingly, in the rat, mouse and cat, L-type channels predominate, comprising ~50% of the total Ca^{2+} current. In bovine and porcine AMC, L-type channels comprise only about 15% of the total Ca^{2+} current (Hernandez-Guijo et al., 1998). These differences may reflect the extent to which Ca^{2+} currents are modulated by peptide co-transmitters (e.g. opiates) released from AMC during stimulation, but further work is required to validate this point.

5.3 Outward currents in chromaffin cells

The outward currents of AMC consist primarily of large-conductance Ca^{2+}-dependent K^+ channels (BK) that are blocked by the scorpion toxins, charybdotoxin (ChTX) and iberiotoxin (IbTX; Solaro et al., 1992). Two subtypes of BK current have been described in adult rat AMC, one inactivating (BK_i) in about 75% of cells, and the other non-inactivating or sustained (BK_s) in ~10% of AMC. The remaining ~15% express mixed BK currents (Solaro et al., 1992). The proportion of BK channels is somewhat different in neonatal AMC, where ~70% express BK_s and the remaining 30% have either BK_i or both currents (Thompson and Nurse, 1997; Chapter 2 in this

thesis). Thus, expression of these BK current subtypes may be modified postnatally (see also Appendix 1 in this thesis).

Regardless of the subtype, BK channels are activated by a combination of membrane depolarization and an increase in intracellular Ca^{2+}. This makes them ideally suited to function in a negative feedback role during CA secretion, since Ca^{2+} influx through L-type Ca^{2+} channels during an action potential can activate the BK channels, aiding repolarization and curtailing secretion. Thus, subtle changes in the activation or inactivation of BK channels can dramatically change the shape of an action potential and modulate CA secretion. Pancrazio et al. (1994) have described the importance of BK channels for membrane repolarization during the action potential in rat AMC. They showed that inhibition of BK channels with ChTX caused a marked broadening of the action potential, and that increasing intracellular Ca^{2+} levels shortened action potentials in a ChTX-sensitive manner. Additionally, expression of BK_i channels appears crucial for the ability of AMC to fire repetitive action potentials, whereas cells expressing predominantly BK_s fire only single action potentials in response to depolarizing stimuli (Solaro et al., 1995).

Similar types of BK currents have been described in bovine AMC, with some interesting differences. A much smaller proportion of bovine AMC express inactivating BK currents with markedly different gating properties. They acitvate and inactivate more slowly, and have an activation potential that is more positive (Lovell et al., 2000). These properties likely reflect different combinations of the subunits that form the tetrameric structure of a functional K^+ channel.

In addition to BK channels, rat AMC also possess a number of other K^+ channel subtypes. These include a small-conductance Ca^{2+} dependent K^+ channel that is sensitive to apamin (Neeley and Lingle, 1992) and a delayed rectifier K^+ channel that is slowly inactivating and similar to the K_z channel described in the chromaffin derived pheochromocytoma (PC12) cell line (Hoshi and Aldrich, 1988; Solaro et al., 1992).

6. O_2-chemotransduction in carotid body chromaffin cells

This thesis is concerned with investigating the mechanisms of O_2-chemotransduction in adrenal chromaffin cells. Thus, it is pertinent to contrast the properties of O_2-chemosensitivity in a related, well-studied neural crest derived O_2-chemoreceptor, the type 1 or glomus cell of the carotid body. Glomus cells are prototypical O_2, CO_2, and acid chemoreceptors that are located in the carotid body, a small organ found at the bifurcation of the common carotid artery. The carotid body is a densely vascularized organ that is ideally located to sample changes in the chemical composition of arterial blood. A fall in arterial Po_2, Pco_2 or acidity is 'sensed' by the glomus cell and thought to evoke neurotransmitter secretion onto afferent terminals of the petrosal neurons that innervate them. Neurotransmitters then excite the petrosal neurons and alter action potential frequency, which is relayed to the central pattern generator of the brain stem (see Gonzalez et al., 1994 for a review of carotid body function). The output from the central pattern generator ultimately controls firing of

other neurons that innervate the diaphragm. Thus, in response to a hypoxic stimulus, ventilation is increased leading to a restoration of blood Po_2.

6.1 Effects of hypoxia on ion channels and membrane potential in glomus cells

The first characterization of O_2-sensitive K^+ channels in rabbit glomus cells demonstrated hypoxic inhibition of a slowly inactivating, 4-aminopyridine-sensitive delayed rectifier K^+ channel (Lopez-Barneo et al., 1988). Subsequently, it was shown that rat glomus cells also express O_2-sensitive K^+ channels that are reversibly inhibited by hypoxia (Peers, 1990; Stea and Nurse, 1991). Interestingly, these are Ca^{2+}-dependent K^+ or BK channels, evidenced by their sensitivity to extracellular Cd^{2+} and ChTX (Peers, 1990). Other O_2-sensitive ion channels have been described in glomus cells from the rat and rabbit. These include a voltage-insensitive 'leak' K^+ channel that is TEA, 4-AP, ChTX, and Ca^{2+}-insensitive, which may belong to the acid-sensitive TASK or TRAK family of K^+ channels (Buckler, 1997; Kim et al., 1999; Buckler et al., 2000). These channels have not yet been described in the rabbit, but an O_2-sensitive, inward rectified K^+ conductance that belongs to the human ether-a-go-go related gene (HERG) family, and may be O_2-sensitive, has recently been identified in this species (Overholt et al., 2000). In addition, glomus cells of the rabbit carotid body express an O_2-sensitive L-type Ca^{2+} channel that is inhibited by hypoxia at low voltages, but augmented at higher voltages (Montoro et al., 1996); this channel is not present in the rat glomus cell (Lopez-Lopez et al., 1997).

The exact mechanism of ion channel inhibition/activation by hypoxia that leads to neurotransmitter release from glomus cells, as well as the specific neurotransmitters involved remain controversial (see however, Zhang et al., 2000). Generally, if glomus cells are quiescent (not firing action potentials), as rat glomus cells seem to be when singly isolated, inhibition of the 'leak' K^+ channel is thought to depolarize the membrane and increase Ca^{2+} influx through voltage-sensitive Ca^{2+} channels, evoking neurosecretion (Buckler, 1997). However, if glomus cells are spontaneously active, as may occur in some large clusters in the rat (Zhang and Nurse, 2000), then inhibition of BK currents by hypoxia may broaden action potentials or increase firing frequency and thereby enhance neurosecretion (see Peers, 1990; Zhang and Nurse, 2000). Interestingly, in a recent study on thin slices of adult rat carotid body, inhibition of BK channels by iberiotoxin (IbTX) evoked CA secretion, suggesting these channels are open during normoxia in more intact preparations (Pardal et al., 2000)

7. Theories on the identity of the O_2-sensor

For a cell to be sensitive to changes in Po_2, it is reasonable to assume that there is a mechanism for detecting O_2. The nature of this O_2-sensor has been the focus of much research, yet remains controversial, as attempts to identify a ubiquitous sensor protein remain elusive. Several hypotheses have been raised and are described below. However, it appears that all cells do not sense O_2 by the same mechanism, so it is imperative that the O_2-sensor be investigated for each type of O_2-chemosensitive cell.

7.1 The plasma membrane hypothesis of O_2-chemotransduction

It was first suggested by Acker et al. (1989) that the O_2-sensor in the rat glomus cell is a complex of proteins similar to the NAD(P)H oxidase responsible for the oxidative burst used in pathogenic defence by neutrophils. In this model of O_2-chemoreception, the reduced availability of O_2 results in reduced H_2O_2 generation by the gp91^{phox} subunit of the oxidase. A reduction in cellular H_2O_2 is then proposed to cause inhibition of K^+ channels, depolarization of glomus cells, and neurosecretion (Acker et al., 1989). Expression of subunits of the NAD(P)H oxidase has been detected, by immunocytochemisty, in glomus cells (Kummer and Acker, 1995; Youngson et al., 1997), and diphenylene iodonium (DPI), an inhibitor of the oxidase has been shown to mimic the effects of hypoxia in these cells (Acker et al., 1989; see however Obeso et al., 1999). Additionally, the NAD(P)H oxidase has been implicated as the O_2-sensor in pulmonary myocytes (Grimminger et al., 1995) and neuroepithelial bodies (NEBs) of the lung (Wang et al., 1996).

Perhaps the best evidence for NAD(P)H oxidase functioning as the O_2-sensor is from studies on pulmonary NEBs. First, low concentrations of DPI (~1 μM), which are thought to be specific for the oxidase (see however, Li and Trush, 1998), mimicked and ablated the effects of hypoxia on K^+ currents (Wang et al., 1996). Second, it was recently shown that NEBs obtained from a knockout mouse model deficient in the O_2-binding gp91^{phox} subunit of the oxidase, failed to show hypoxic suppression of K^+ currents, even though the corresponding K^+ channels appeared to be expressed (Fu et

al., 2000). In contrast, Archer et al. (1999) demonstrated that pulmonary myocytes derived from the *same* oxidase deficient mice have normal O_2-sensitivity, suggesting that different tissues have distinct O_2-sensing mechanisms.

An alternative membrane delimited mechanism for O_2-sensing has been proposed. It suggests that the K^+ channels themselves, or closely associated subunits may function directly as O_2-sensors (Lopez-Barneo, 1996). This theory is based on the observation K^+ channels in isolated membrane patches from rabbit glomus cells showed reduced open probability during hypoxia (Ganfornia and Lopez-Barneo, 1992). In contrast, O_2-sensitive BK channels from *rat* glomus cells showed modulation by hypoxia, only when perforated vesicles, but not isolated membrane patches were used (Wyatt and Peers, 1995). The perforated vesicle is thought to retain a small component of the cytoplasm, so these authors concluded that a soluble second messenger is required for O_2-sensing in rat glomus cells. Interestingly, sequence analysis of the *shaker* K^+ channel secondary subunit, $\beta 1$, suggests that it belongs to the oxido-reductase family of enzymes. Thus, secondary subunits could function as O_2-sensors, directly linked to K^+ channels (McCormack and McCormack, 1994)

7.2 The mitochondrial hypothesis of O_2-chemotransduction

An alternative hypothesis for sensing hypoxia involves inhibition of mitochondrial respiration, leading to either a change in reactive oxygen species (ROS) generation or alteration of intracellular ATP. This was first proposed for the glomus cells of the rabbit by Duchen and colleagues (1989), who suggested that the

cytochrome oxidase in the glomus cell has a lower affinity for O_2 than that normally seen in cells or isolated mitochondria. A similar role for mitochondria in O_2-sensing has been suggested in neonatal rat AMC (Mojet et al., 1997), cardiomyocytes (Duranteau et al., 1998), human kidney 3B cell lines (Hep3B; Chandel et al., 1998) and rat pulmonary myocytes (Archer et al., 1993).

In Hep3B cells and cardiomyocytes, it is proposed that inhibition of the proximal (upstream of complex IV in figure 3) and not the distal electron transport chain (ETC) increases reactive oxygen species (Chandel et al., 1998). This is because antimycin A (an inhibitor of complex III) but not cyanide (CN; an inhibitor of complex IV) mimics the effects of hypoxia. Furthermore, cobalt, which disrupts heme formation in the cell, mimicked hypoxia in activating the transcription factor, Hypoxia Inducible Factor (HIF-1) in Hep3B cells. These effects appear to be mediated through an increase in ROS generation by the mitochondria as assayed by fluorometric measurements using 2,7-dichlorofluorescein (Chandel et al., 1998). In contrast, an alternative mechanism of O_2-chemotransduction has been proposed for isolated cardiomyocytes. Hypoxia, antimycin A, H_2O_2, and azide (an inhibitor of complex IV) produced contractions in the isolated cardiomyocyte through increases in ROS generation, suggesting that inhibition of the distal ETC at complex IV (cytochrome oxidase) is the O_2-sensor in these cells (Duranteau et al., 1998).

The complexity of the ETC functioning as the O_2-sensor is further illustrated by the fact that pulmonary myocytes show a decrease in ROS generation by hypoxia and antimycin A, but an increase in ROS with CN (Archer et al., 1993). This suggests that

Figure 3. Composition of the electron transport chain.

Inhibition of the electron transport chain has been implicated as an O_2-sensor in many cell types (see section *7.2* in the introduction). The well characterised components, complexes I, II, III, IV, and V are surrounded by square parenthesis and individual subunits are contained within. Sites of action of specific inhibitors are indicated by the waved arrow and the top scale represents the voltage scale for driving protons (H^+) across the inner mitochondrial membrane, which is coupled to the synthesis of ATP from ADP and inorganic phosphate (modified from Hatefi, 1985).

NADH

Succinate

(Complex I)

$[\text{FMN, FeS}_{N-1}, \text{FeS}_{N-3}, \text{FeS}_{N-2}]$

$\begin{bmatrix} \text{FeS}_{-2} & \text{FeSs}_{-1} \\ \text{B}_{560} & \text{FeS}_{-3} \end{bmatrix}$ (Complex II)

Rotenone

Ubiquinone

Antimycin A

(Complex III)

B_{562},
b_{566},
FeS,
C1

Cytochrome C

(Complex IV) $\begin{bmatrix} \text{a}_3 & \text{a} \\ \text{Cu} & \text{Cu} \end{bmatrix}$

O_2

H_2O

CN
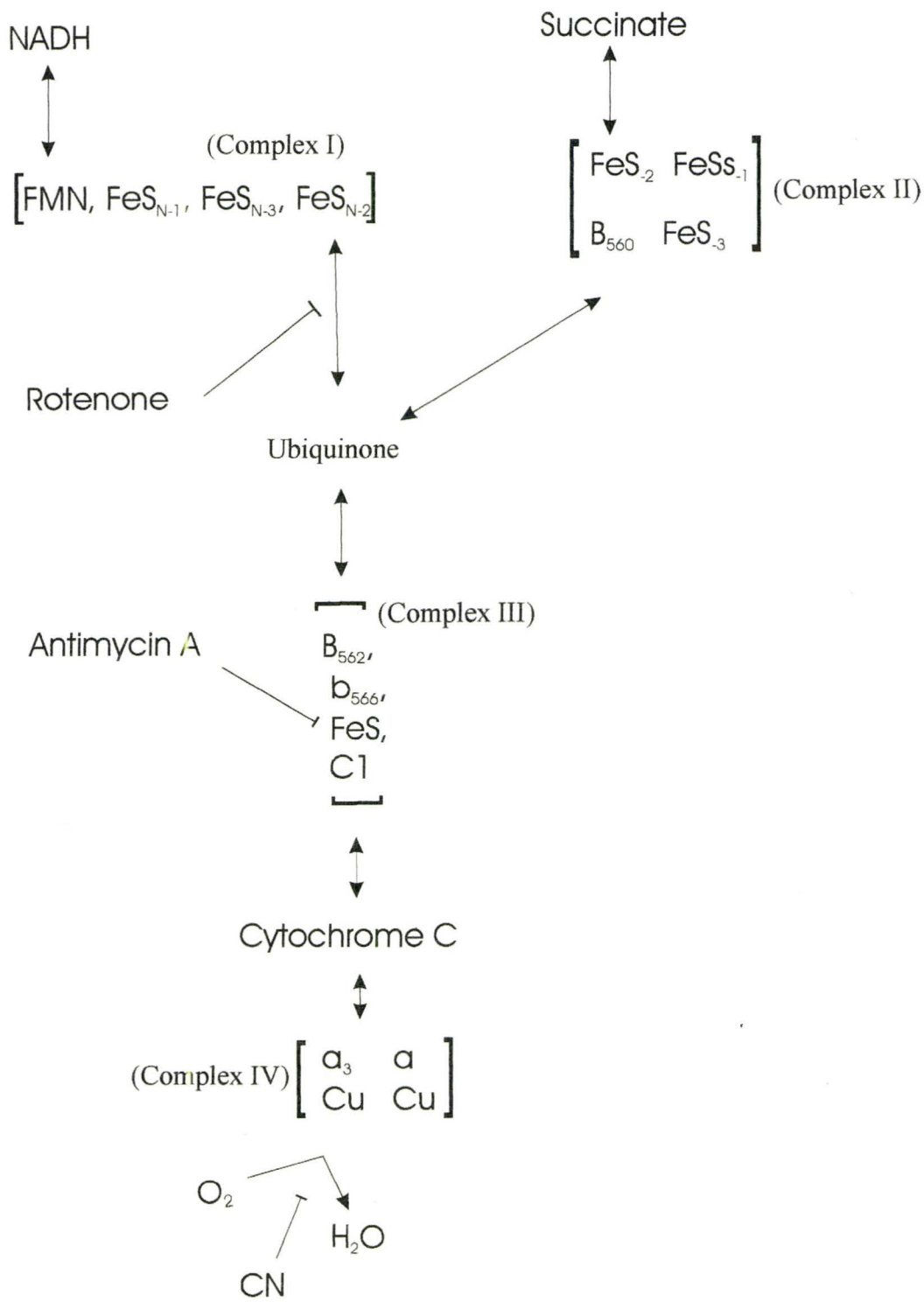
inhibition of the ETC during hypoxia or treatment with proximal inhibitors (e.g. antimycin A or rotenone) decreases ROS generation, which shifts redox status to the more reduced form and results in closure of delayed rectifier type K^+ channels that are open at the resting membrane potential. The ensuing depolarization induces Ca^{2+} influx and constriction of the blood vessels, resulting in shunting of blood to more oxygenated areas of the lung (Archer et al., 1993).

Alternative second messengers in O_2-chemotransduction generated by the mitochondria include a change in ATP production. During hypoxia or metabolic inhibition with CN a decrease in ATP has been suggested to play this role (Mojet et al., 1997; Duchen, 1999). It is proposed that rabbit glomus cells express a novel cytochrome oxidase that has lower affinity for oxygen ($K_m \sim$ 20-30 torr, compared to ~5 torr in most cells; Hatefi, 1985; Duchen, 1999). Thus, during hypoxia the ETC is inhibited leading to depolarization of the mitochondrial membrane potential, reduced ATP production by the F_o/F_1 ATPase, and Ca^{2+} release from both mitochondrial and intracellular stores (Duchen and Biscoe, 1992a,b). These results are supported by the observations that CN may mimic hypoxia in rabbit glomus cells and by measurements of changes in cytochrome absorption spectra during hypoxia and metabolic inhibition (Lahiri et al., 1999). Biscoe and Duchen (1989) also demonstrated that CN activates K^+ channels in rabbit glomus cells. These results are controversial, especially when compared to work from other laboratories, demonstrating that Ca^{2+} influx is required for neurotransmitter release from glomus cells during hypoxia (Lopez-Barneo, 1996; Jackson and Nurse, 1997), and that K^+ currents are inhibited by hypoxia in rabbit

(Lopez-Barneo et al., 1989) and rat (Peers, 1990; Stea and Nurse, 1991) glomus cells. It is possible that CN has non-specific effects and may not completely mimic hypoxia. For example, CN could act as a general inhibitor of heme-containing proteins (e.g. NAD(P)H oxidase and hemoglobin) and may not be specific for cytochrome oxidase alone (Hatefi, 1985).

The metabolic hypothesis of O_2-chemoreception is interesting because the O_2-sensor appears to vary among cell types. It appears that ETC inhibition can be functionally coupled to different cellular responses during hypoxia through a variety of potential second messengers. Alternatively, some cell types (e.g. NEBs) appear to utilize a different O_2-sensor, the NADPH oxidase. Thus, it is important to investigate each O_2-sensitive cell type individually in order to determine whether the ETC functions as an O_2-sensor, and the specific signalling pathway involved in chemoreception.

8. Goals and organization of thesis

The primary goal of this thesis was to elucidate the development of the electrophysiological and molecular mechanisms of O_2-chemosensitivity in adrenomedullary chromaffin cells (AMC). Dissociated cell cultures of embryonic, neonatal and juvenile (2-3 week old) rat and mouse AMC were exposed to hypoxia while measuring ionic currents and membrane potential responses with the patch clamp technique. In addition, amine secretion was monitored by carbon fibre electrochemistry, and ROS by fluorometric imaging using DCF fluorescence. This

experimental approach offers distinct advantages over an *in vivo* approach, because it avoids complications that could arise from circulating systemic or humoral factors. The thesis also has particular relevance to the fields of O_2-chemoreception, developmental neurobiology, and biochemistry of K^+ channel function. Three developmentally regulated K^+ currents that are differentially sensitive to hypoxia have been identified, and a biochemical mechanism for the modulation of these channels by hypoxia and metabolic inhibition is proposed.

The main body of this thesis is written in a 'sandwich' style, comprising a series of five papers that are either published in peer-reviewed journals, or are in preparation for submission. Some of the papers are multi-authored, so a short preface appears at the beginning of each chapter that describes my contributions. Work from the other collaborators involved is included because it provides a more complete analysis and serves to emphasize the importance of this work.

Chapter 1 addresses the development of O_2-chemosensitivity in rat chromaffin cells and emphasises the difference in O_2-sensing properties between neonatal and juvenile AMC. Chapter 2 is an electrophysiological characterization of the types of K^+ currents involved in hypoxia-sensing by neonatal rat AMC. The last two Chapters, 3 and 4, are concerned with identifying the O_2-sensor in neonatal AMC. A knockout mouse model, deficient in the putative O_2-sensor, NAD(P)H oxidase gp91^{phox} subunit, is utilized in Chapter 3 to investigate the potential role of this membrane protein complex in O_2-sensing. Chapter 4 contrasts the electrophysiological properties and changes in ROS levels in AMC during metabolic inhibition and/or hypoxia, and tests

the hypothesis that the mitochondrial electron transport chain functions as the O_2-sensor in AMC. The contents of Appendix 1 describe the development of the O_2-sensitive K^+ currents in perinatal rat AMC and indicate that hypoxic sensitivity is not fully developed in embryonic E16-18 cells. Finally, there is a general discussion of these results and a model is proposed to explain O_2-chemosensitivity in adrenal chromaffin cells.

CHAPTER 1

Developmental Loss of Hypoxic Chemosensitivity in Rat Adrenomedullary Chromaffin Cells

The majority of work in this chapter has been previously published as:

I was responsible for preparation of the text and all electrophysiology and carbon fibre electrochemistry experiments, which comprise Figures 1, 2 and 4. Adele Jackson performed the HPLC experiments (Figure 3).

SUMMARY

1. We investigated whether adrenomedullary chromaffin cells (AMCs) derived from neonatal (postnatal day (P)1-P2) and juvenile (P13-P20) rats, and maintained in short-term culture (1-3 days), express O_2-chemoreceptive properties.

2. In whole-cell recordings, the majority (~70%; n=47) of neonatal AMCs were sensitive to hypoxia. Under voltage clamp, acute hypoxia (Po_2= ~ 40 mmHg) suppressed voltage-dependent K^+ current by 25.1 ± 3.4 % (mean ± s.e.m.; n=22); under current clamp, acute hypoxia caused a membrane depolarization of 14.1 ± 1.3 mV (n=13) from a resting membrane potential of -54.8 ± 2.8 mV (n=13), and this was often sufficient to trigger action potentials.

3. Exposure of neonatal AMC cultures to a moderate (Po_2= ~75 mmHg) or severe (Po_2= ~ 35 mmHg) hypoxia for 1 hr caused a dose-dependent stimulation (~ 3x or 6x normoxia, respectively) of catecholamine (CA) release, mainly adrenaline, determined by HPLC. This induced CA release was abolished by the L-type calcium channel blocker, nifedipine (10 µM).

4. In contrast to the above results in neonates, hypoxia had no significant effects on voltage-dependent K^+ current, membrane potential, or CA release in juvenile AMCs.

5. We conclude that rat adrenal chromaffin cells possess a developmentally regulated O_2-sensing mechanism, similar to carotid body type I cells.

Introduction

In the perinatal period, catecholamine (CA) release from adrenomedullary chromaffin cells (AMCs) is critical for the animal's ability to survive stresses associated with delivery and the transition to extrauterine life. This release plays a vital role in the modulation of cardiovascular, respiratory and metabolic responses to stressors such as hypoxia (Lagercrantz & Slotkin, 1986; Slotkin & Seidler, 1988). In some species such as rat and man, sympathetic innervation of the adrenal medulla is immature or absent in the neonate, yet the animal can still elicit the vital catecholamine surge in response to hypoxic challenge (Seidler & Slotkin, 1985). Seidler & Slotkin (1985) showed that in the newborn rat, acute hypoxia reduces adrenal catecholamines through a `non-neurogenic' mechanism, which disappears postnatally with a rough correlation to the maturation of the sympathetic innervation to the adrenal medulla. Furthermore, they demonstrated that sympathetic denervation of the adrenal medulla in mature animals causes a gradual re-appearance of this non-neurogenic mechanism (Seidler & Slotkin, 1986).

The mechanisms underlying the non-neurogenic response of the adrenal medulla to hypoxia are unknown. One possibility is that it is mediated indirectly, via humoral factors released into the circulation during hypoxia. Alternatively, adrenomedullary chromaffin cells might themselves possess O_2-sensing mechanisms, similar to their neural crest counterparts in the carotid body, i.e. glomus or type 1 cells, which are the prototype for O_2

chemoreceptors in mammals (Gonzalez, Almaraz, Obeso & Rigual, 1994). These cells respond to hypoxia by suppression of an outward K^+ current (Lopez-Barneo, Lopez-Lopez, Urena & Gonzalez, 1988; Delpiano & Hescheler, 1989; Peers, 1990; Stea & Nurse, 1991), membrane depolarization and/or increased action potential frequency (Lopez-Barneo *et al.*, 1988; Buckler & Vaughan-Jones, 1994), leading to entry of extracellular calcium and enhanced CA release (Buckler & Vaughan-Jones, 1994; Montoro, Urena, Fernandez-Chacon, Alvarez DE Toledo & Lopez-Barneo, 1996). In this study, using whole-cell recording techniques and HPLC determination of CA release, we tested the hypothesis that newborn rat AMC share similar O_2-sensing properties to carotid body type 1 cells, and that these properties are lost with postnatal maturation.

METHODS AND MATERIALS

Pregnant or lactating Wistar rats (Charles River, Quebec) and pups were housed in our animal facility under constant light-dark cycle, according to the guidelines of the Canadian Council on Animal Care (CCAC). All procedures for animal handling and tissue removal were carried according to CCAC guidelines. Prior to removal of adrenal glands, animals were killed by decapitation or cervical dislocation, immediately after being rendered unconscious by a blow to the head (1-14 day-old pups) or by inhalation of the anaesthetic, Somnothane (15-20 day-old pups). The pups were then killed by decapitation or cervical dislocation and the adrenal glands removed.

Cultures

Primary cultures enriched in dissociated rat AMCs were prepared by a modification of methods previously described (Doupe, Landis & Patterson, 1985). Briefly, adrenal glands were dissected from rat pups of two age-groups, i.e. neonatal (postnatal day (P)1-P2) or juvenile (P13-P20). Most of the surrounding cortical tissue was trimmed and discarded, whereas the remaining central medulla was incubated in an enzymatic solution, containing 0.1% trypsin (Sigma), 0.1% collagenase (GIBCO), and .01% deoxyribonuclease (Millipore) for 1 hr at 37 °C. Following incubation, most of the enzyme was removed with a pipette and the remainder was inactivated with growth medium consisting of F-12 nutrient medium

(GIBCO) supplemented with 10% fetal calf serum (GIBCO), 80 U/l insulin (Sigma Chemical Co., St. Louis, Mo), 0.6% glucose, 2mM glutamine, 1% penicillin/streptomycin (GIBCO), and 0.01% dexamethasone (Sigma). In most experiments, after mechanical dissociation of the tissue with forceps and trituration with a Pasteur pipette, the resulting cell suspension was pre-plated for 24 hr on collagen to remove most of the cortical cells. The non-adherent chromaffin cells were then re-plated on the central wells of modified culture dishes (Nurse, 1990), coated with Matrigel (Collaborative Research, Bedford, MA, USA). The cells were grown at 37 °C in a humidified atmosphere of 95% air: 5% CO_2 for 1-3 days before they were used in the patch clamp experiments, or for determination of CA release.

Electrophysiology

Voltage clamp data were obtained using either conventional whole-cell or Nystatin perforated-patch techniques as previously described (see Stea & Nurse, 1991). Membrane potential measurements under current clamp were obtained with the latter method. The seal resistance was in the range 2-10 GΩ and most (~75%) of the series resistance (range 10-25 MΩ) was compensated in voltage clamp experiments. Junction potentials (2-10 mV) were nulled at the beginning of each experiment. Voltage and current clamp records were obtained using an extracellular fluid with the following composition (mM): NaCl, 135; KCl, 5; $CaCl_2$, 2; $MgCl_2$, 2; glucose, 10; HEPES, 10; adjusted to pH 7.4 with NaOH. The pipette solution for conventional whole-cell recording contained (mM): KCl, 135; NaCl, 5; $CaCl_2$, 0.1; EGTA, 11; HEPES, 10; Mg-ATP, 2 at pH 7.2. For perforated-patch recording the pipette

solution contained (mM): KGluconate, 105; KCl, 30; NaCl 5; CaCl$_2$, 0.1; HEPES, 10 at pH 7.2, plus nystatin (300 μg/ml). All recordings were obtained at room temperature (20-23 °C) with an Axopatch-1D patch clamp amplifier equipped with a 500 MΩ headstage feedback resistor, digitized with a Digidata 1200 computer interface (Axon Instruments), and stored on disk in an IBM-compatible computer using pCLAMP software version 6.0 (Axon Instruments). Solutions were exchanged by perfusion under gravity and simultaneous removal by suction. Hypoxia was generated by bubbling 100% N$_2$ into the perfusion chamber, occasionally with the O$_2$ scavenger, 1 mM Na dithionite, present (Peers, 1990). During stimulus application the Po$_2$ at the recording site was within 4 mmHg of that measured with an oxygen electrode placed in the perfusion chamber. During stimulus application, the Po$_2$ at the recording site was within 4 mmHg of that measured with an oxygen electrode placed in the perfusion chamber. The effects of hypoxia on voltage-activated outward currents were determined by comparing peak currents from four records taken at each step potential, before (control), during, and after (wash) stimulus application. Currents or current densities were compared using the Student's t test and the level of significance was set at $P<0.05$. Membrane capacitance was obtained by integration of the capacitative transient during a hyperpolarizing voltage step from -60 to -100 mV. Voltage clamp traces shown in text are leak subtracted.

Catecholamine determination by HPLC

Catecholamines (CA) released from living cultures, were separated by HPLC

(Waters, model 510) with a Spherisorb-ODS2 column (10x 0.46 cm, 3 μm particle size; Chromatography Sciences Co., Montreal, Quebec, Canada), coupled with an electrochemical detector (Coulochem II detector, model 5200; ESA, Inc., Bedford, MA, USA). The first detector in the analytical cell was set at 0.05 V to reduce interference by contaminating electroactive compounds at the second detector which was set at -0.3 V, the potential required for electro-reduction of (-)-arterenol (noradrenaline), (-)-adrenaline, 3-hydroxytyramine (dopamine) and the internal standard, di-3,4-hydroxybenzylamine hydrobromide (DHBA). The mobile phase consisted of NaH_2PO_4 (6.9 g/L; Sigma), Na_2EDTA (80 mg/L; BDH Chemicals), and heptanesulfonic acid (250 mg/L; Sigma) in water and 5% methanol; pH was adjusted to 3.5 with concentrated H_3PO_4. Chromatograms were analysed with the aid of a Waters 740 Data Module (Millipore, Milford, MA) and quantified by the peak area ratio method, using known external standards (25 nM) and the internal standard, DHBA.

In studies of CA release, cultures, grown on a circular area of ~8 mm diameter, were first rinsed in 1:1 Dulbecco's modified Eagle's medium/F12 medium before a 1hr incubation at 37 °C in 100 μl bicarbonate-buffered salt solution (BBSS), under an atmosphere of 5% CO_2 plus either normoxia (Po_2= 160 mmHg), moderate hypoxia (Po_2= ~75 mmHg), or severe hypoxia (Po_2= ~35 mmHg) , using a Forma Scientific O_2/CO_2 incubator. The BBSS contained in mM: NaCl 116, KCl 5, $NaHCO_3$ 24, $CaCl_2$ 2, $MgCl_2$ 1.1, HEPES 10, glucose 5.5 at pH 7.4; for high K^+ experiments 25 mM NaCl was replaced by equimolar KCl. In a few experiments the calcium channel blocker, nifedipine (10 μM; Sigma), was added to the

BBSS. Each release sample was mixed with an equal volume of 0.1 M $HClO_4$ containing 2.7 mM Na_2EDTA and then stored at $-80^\circ C$ prior to HPLC analysis. CA release was compared between different treatments using Student's t test with the level of significance set at $P< 0.05$. Results are presented as mean $\pm$ s.e.m.

Immunofluorescence

At the end of release experiments cultures were processed for tyrosine hydroxylase (TH) immunofluorescence , to obtain an absolute count of the number of chromaffin cells present. Procedures for TH-immunostaining were similar to those described previously (Nurse, 1990); the primary TH-antibody (rabbit; Chemicon, El Segundo, CA, USA) was visualized with a fluorescein-conjugated goat anti-rabbit IgG secondary antibody (Cappel, Malvern, PA, USA).

Carbon fibre amperometry

Catecholamine secretion was monitored using single carbon-fibre microelectrodes, prepared according to a modification of the procedure of Zhou and Misler (1995). Briefly, a single carbon-fibre (diameter 10 µm) was inserted into a glass capillary tube (type 7052, Corning) and pulled on a horizontal microelectrode puller. The fibre was trimmed, sealed with epoxylite resin and heat cured overnight at $100\ ^\circ C$. Electrical connection between the fibre and silver wire in the electrode holder was obtained with the aid of conductive silver paint. The electrode was connected to a standard patch-clamp headstage and polarized to a

potential of 600 mV, i.e, above the oxidation potential for catecholamines. After stabilization of the baseline (~15 min), the electrode was positioned near a small cluster of AMC. Extracellular solutions were the same as those described above, except that Na dithionite was always omitted from the hypoxic solution since it interfered with the electrochemical signal. The Po_2 of the hypoxic solution (in the absence of dithionite) ranged from 0-5 torr in the recording chamber as measured with a Clark-style O_2-electrode.

RESULTS

Conventional whole-cell or nystatin perforated-patch techniques were used to study the effects of hypoxia on ionic currents or membrane potential of rat AMCs, after 1-3 days in culture. In the majority (~70%) of AMC (33/47) derived from *neonatal* (P1-P2) rat pups, acute hypoxia caused either a suppression of voltage-dependent K^+ current (voltage clamp) or membrane depolarization (current clamp). In contrast, most AMC (29/30) from juvenile (P13-P20) pups were unresponsive to hypoxia during similar measurements.

Age-dependent effects of acute hypoxia on voltage-activated K^+ currents in AMC

In voltage clamp studies using conventional whole-cell recording, reducing Po_2 from 160 mmHg (normoxia) to ~40 mmHg (hypoxia) caused a suppression of the outward K^+ current in neonatal AMC by 24.4 ± 3.1 % (n=11), measured during voltage steps from -60 to +20 mV. With perforated-patch recording, a similar K^+ current suppression occurred during hypoxia (26.0 ± 3.4 %; n= 11). In many cases (e.g. Figure 1A), recovery of control responses after hypoxia was complete, and generally was within 90 - 100% of control values. A plot of the outward current, normalized to cell size or input capacitance (pA/pF), versus membrane potential before (open circles), and during (filled circles) acute hypoxia ($Po_2 \sim 40$ mmHg) is illustrated in Figure 1B for a group of 4 cells with similar current densities, investigated with conventional whole-cell recording. For each of these cells recovery of control current was 95-100% complete following wash with normoxic solution, but is omitted from Fig. 1B for clarity. Statistical analysis revealed that during hypoxia K^+ current

Figure 1. Contrasting effects of acute hypoxia on outward K$^+$ currents of neonatal versus juvenile rat adrenal chromaffin cells (AMC).

A and B, effect of reducing Po$_2$ from 160 mmHg (control; normoxia) to ~40 mmHg (hypoxia) in neonatal (P1-P2) AMC. In A, the outward K$^+$ current, recorded with the conventional whole-cell technique, is reversibly suppressed by hypoxia; voltage step is shown below traces. Each current trace is an average of 4 recordings to the same step potential, and is leak subtracted. The small downward deflection at the beginning of the control current record is due to incomplete subtraction of the capacitative transience. In B, the I-V relation for the peak outward current, recorded with conventional whole-cell methods and plotted as current density (pA/pF) vs membrane potential (voltage), is shown for a group (n=4) of neonatal AMC before (open circles) and during (filled circles) hypoxia. After hypoxia, outward currents recovered to >95% of control values in B, but are omitted for clarity. C and D, effect of reducing Po$_2$ from 160 mmHg (control) to ~40 mmHg (hypoxia) in juvenile (P13-P20) AMCs. Hypoxia had no effect on outward current (C), in contrast to neonatal cells in A and B. In D, the I-V relation is similar before and during hypoxia, and is shown for a group (n=5) of juvenile cells. Recording conditions in C and D are similar to those described above for A and B. * P<0.05 and ** P<0.01, current density is significantly different from control (Student's *t* test).

Neonatal

A

Control/wash

Hypoxia

100 pA

10 ms

+20 mV

-60 mV

B

Current density (pA pF^{-1})

60

40

20

0

-40   0   40   80

Juvenile

C

Control/wash

Hypoxia

200 pA

10 ms

+20 mV

-60 mV

D

Current density (pA pF^{-1})

160

120

80

40

0

-40   0   40   80
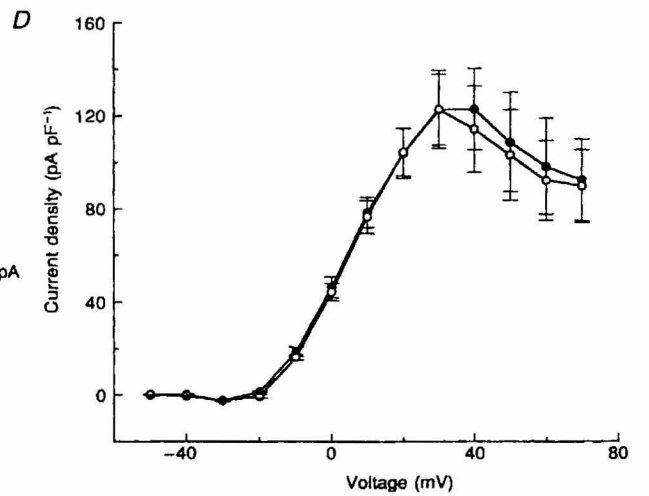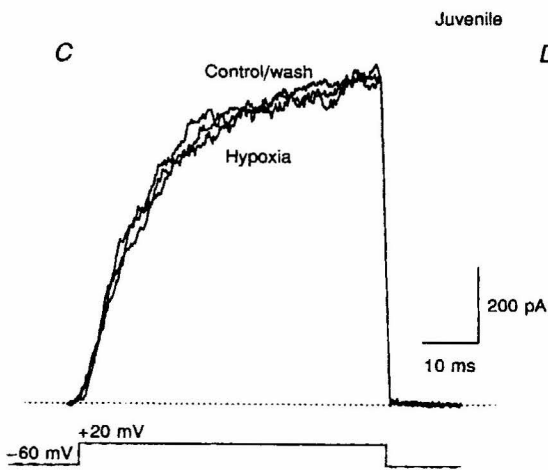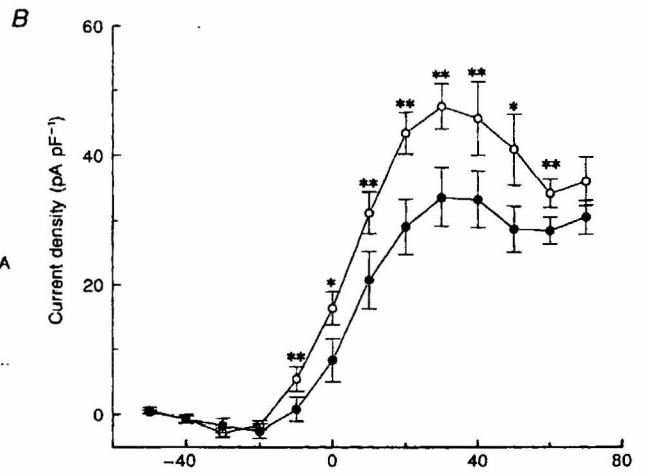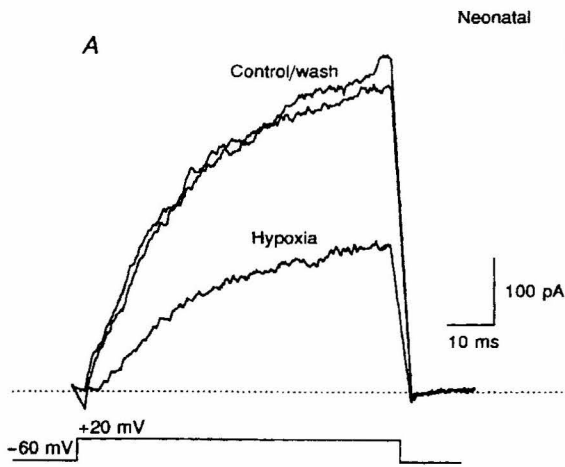
Voltage (mV)

density (e.g. Fig. 1B) was significantly (P< 0.05) reduced at all voltage steps between -10 and +60 mV.

During conventional whole-cell recordings from rat AMC, there was usually a characteristic 'hump' or shoulder in the I-V relation between +20 and +50 mV (see Neely & Lingle, 1992), suggesting the presence of a prominent Ca^{2+}-dependent K^+ current. Interestingly, for neonatal AMC, K^+ current suppression was largest in this region (Figure 1B), as previously observed in the hypoxic response of rat carotid body type 1 cells (Peers, 1990). However, with perforated-patch recording the shoulder in the I-V relation was less prominent, and usually absent (not shown); this may be related to differences in intracellular calcium buffering during the two recording conditions.

In contrast to the above results on neonates, the same level of hypoxia failed to elicit significant K^+ current suppression at any test potential in twenty-six out of twenty-seven AMC derived from juvenile rats of ages P13- P20 (Figure 1C, D). As expected (Neely & Lingle, 1992), these juvenile cells displayed a prominent hump in the I-V relation during conventional whole cell recording (see Fig. 1D), suggesting that they too expressed a Ca^{2+}-dependent K^+ current. However, there was no significant effect of hypoxia even in the hump region of the I-V relation in these juvenile cells (Fig. 1D).

Over 1-3 days in culture, the mean input capacitance (± s.e.m.) of neonatal AMC was 8.5 ± 0.7 pF (n=20), a value significantly (P<0.01) larger than that for juvenile AMC , i.e. 5.9 ± 0.2 pF (n=20). It is not clear whether this difference is attributable to differences in shape changes as the cells flatten out over time in culture, since there was no significant

difference between the two (7.5 ± 0.8 pF; n=5 for neonatal, versus 6.0 ± 0.6 pF; n=5 for

juvenile) after only one day in culture. The mean outward current density, calculated at

voltage steps to +50 mV, was significantly (P<0.05) higher in juvenile (126.0 ± 15.1 pA/pF;

n=20) compared to neonatal (78.9 ± 11.8 pA/pF; n=20) AMC.

Age-dependent effects of hypoxia on membrane potential

In order to test whether acute hypoxia can alter the membrane potential and /or

excitability of AMC, nystatin perforated-patch recordings were carried out in current clamp

mode. The mean resting potential (± s.e.m.) in neonatal AMC was -54.8 ± 2.8 mV (n=13),

a value not significantly different from that in juvenile AMC, i.e. -54.1 ± 3.0 mV (n=12).

Exposure to hypoxia, however, had quantitatively different effects on cells from the two age

groups. Whereas hypoxia (Po_2= ~ 40 mmHg) depolarized neonatal AMC by 14.1 ± 1.3 mV

(n=11; e.g. Figure 2 A, B), it produced no detectable change in membrane potential of

juvenile AMC (Figure 2C, D). In eight out of thirteen neonatal AMC, the hypoxia-induced

depolarization was sufficient to elicit action potentials at room temperature (e.g. Figure 2A).

Application of brief, constant hyperpolarizing current pulses indicated that the depolarization

during hypoxia in neonatal AMC was accompanied by a significant (P<0.05) increase in

input resistance (e.g. Figure 2B), consistent with the closure of ion channels that were open

under resting normoxic conditions. The mean (± s.e.m.) input resistance in four neonatal

AMC was 2.0 ± 0.6 GΩ, 2.9 ± 0.7 GΩ and 1.9 ± 0.5 GΩ, before, during and after acute

hypoxia, respectively. In contrast, the input resistance of juvenile AMC was unaffected

Figure 2. Contrasting effects of acute hypoxia on resting membrane potential and input resistance of neonatal versus juvenile rat adrenal chromaffin cells (AMC). Membrane potential was recorded in current clamp mode, using the perforated-patch, whole-cell technique. A and B. Perfusion of a hypoxic solution ($Po_2 = \sim 40$ mmHg), during the time indicated by lower horizontal bar, causes ~10 mV depolarization of neonatal (P1-P2) AMCs, from a resting potential of −63 (A) and -53 mV (B), respectively. In A, hypoxia elicited active responses which are superimposed on the depolarization. In B, injection of constant hyperpolarizing current pulses (downward vertical deflections) indicates that the membrane resistance is increased during hypoxia. C and D, in contrast to its effects on neonatal cells, a similar hypoxic stimulus failed to affect either the resting membrane potential (C and D), or input resistance (D) in juvenile (P13-P20) AMC. Details are as for A and B.

Neonatal

A

−63 mV ⋯⋯

Hypoxia

B

−53 mV ⋯⋯

Hypoxia

Juvenile

C

−70 mV ⋯⋯

Hypoxia

D

−50 mV ⋯⋯

Hypoxia

10 mV

25 s
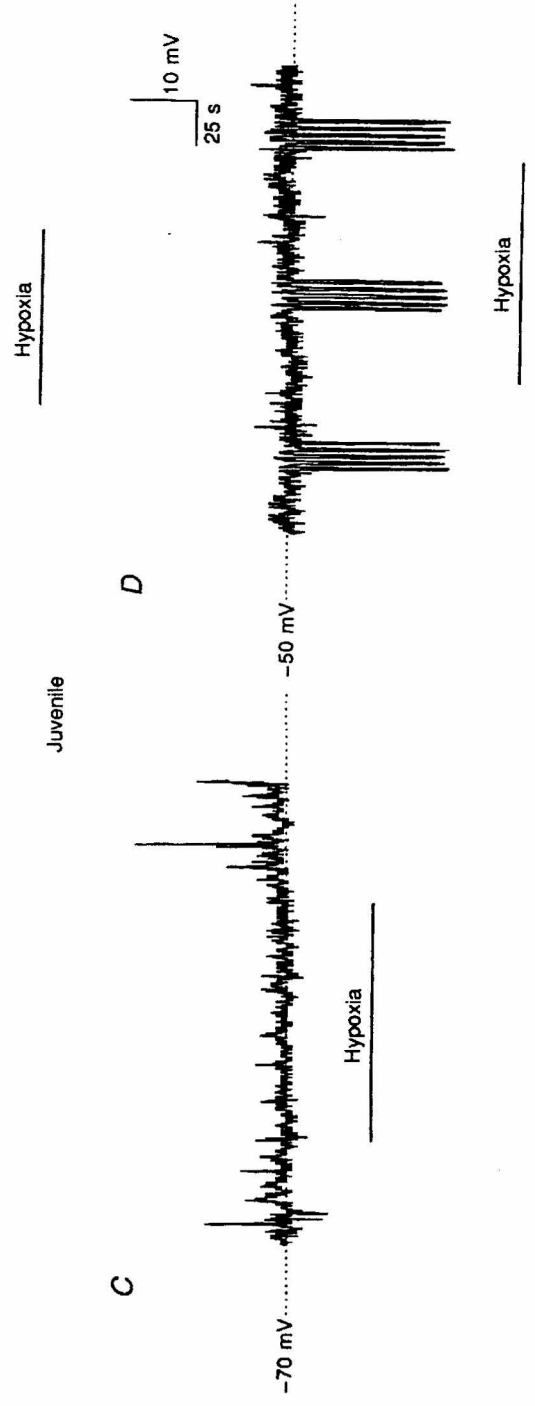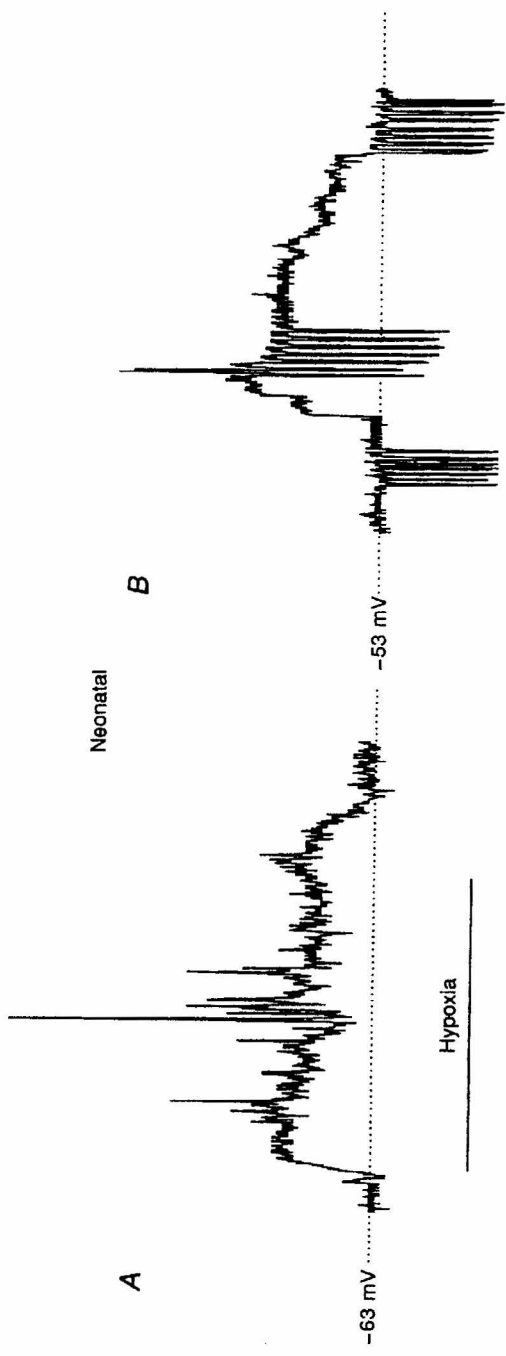
by hypoxia (Figure 2D); in 5 juvenile cells the mean input resistance was 2.9 ± 0.7 GΩ, 2.9 ± 0.7 GΩ, and 2.8 ± 0.7 GΩ, before, during and after acute hypoxia, respectively.

Age-dependent effects of hypoxia on catecholamine release from AMC cultures

Do the contrasting membrane responses of neonatal versus juvenile AMC correlate with their secretory activities during acute hypoxia? To test this we used High Performance Liquid Chromatography (HPLC) with electrochemical detection and compared catecholamine (CA) secretion (Figure 3A) in neonatal and juvenile AMC cultures, following 1 hr exposure to moderate ($P_{O_2}= \sim 75$ mmHg) or severe ($P_{O_2}= \sim 35$ mmHg) hypoxia. We avoided the use of *anoxia* (0 mmHg) since this stimulus is known to deplete CA from adult bovine chromaffin cells (e.g., Dry, Phillips & Dart, 1991), conceivably by a different mechanism involving calcium release from intracellular compartments, e.g. mitochondria (see Duchen & Biscoe, 1992). As shown in Figure 3C, in neonatal cultures CA release per hour, normalized to 10,000 AMC, was stimulated ~3 and 6 times above normoxic ($P_{O_2} = 160$ mmHg) basal release when cultures were exposed to a P_{O_2} of ~75 and ~35 mmHg respectively. Counts of AMC were obtained at the end of each release experiment following immunofluorescence staining for tyrosine hydroxylase (TH), a cytoplasmic marker (Figure 3B). Though adrenaline (A) was the major CA released (Figure 3C), hypoxia also stimulated noradrenaline (NA) and dopamine (DA) release (Figure 3C). However, the ratio of released A: NA was similar for normoxia and moderate hypoxia. The CA release induced by both hypoxic stimuli was abolished by the L-type calcium channel blocker, nifedipine (10 μM;

Figure 3. **Comparison of normalized catecholamine release in neonatal and juvenile chromaffin cell cultures.**

A, HPLC record of a release sample (Po_2=160 mmHg) from a neonatal AMC culture indicating peaks corresponding to the catecholamines: noradrenaline (NA), adrenaline (A), dopamine (DA), as well as to the internal standard DHBA (vertical scale readings in minutes). B, an example of rat chromaffin cells (diameter ~ 10 μm each) in a 2-day-old culture that was stained for tyrosine hydroxylase (TH)-immunoreactivity, and visualized with a fluorescein-conjugated secondary antibody; cultures prepared in this way were used to obtain absolute chromaffin cell counts at the end of the release experiments, and for normalizing release to 10,000 TH^+ cells in C and D. C, histogram illustrating the stimulatory effects of moderate (~75 mmHg) and severe (~35 mmHg) hypoxia, and high extracellular K^+ (30 mM) on catecholamine (NA, A, DA) release in *neonatal* AMC cultures after 1 hr exposure; basal release is represented by 160 mmHg (normoxia). Hypoxia-induced catecholamine release is abolished by the L-type calcium channel blocker, nifedipine (Nif; 10 μM). D, histogram illustrating the lack of effect of moderate and severe hypoxia on catecholamine release in *juvenile* AMC cultures; in these cultures, however, high extracellular K^+ (30 mM) significantly stimulated catecholamine release. Bars in C and D represent mean ± s.e.m. for number of cultures indicated; ** $P < 0.01$ and * $P < 0.05$, release is significantly different from basal (Student's *t* test).

A

0

DHBA

12·5 min

NA
Adr

Dop

B

C   Neonatal

CA release (pmol (10000 TH⁺ AMC)⁻¹ h⁻¹)

100

80

60

40

20

0

160   160 +   75   75 +   35   35 +   160 +
        Nif   Nif   Nif   high K⁺

P_{O_2} (mmHg)

D   Juvenile

CA release (pmol (10000 TH⁺ AMC)⁻¹ h⁻¹)

70

60

50

40

30

20

10

0

160   160 +   75   75 +   35   35 +   160 +
        Nif   Nif   Nif   high K⁺

P_{O_2} (mmHg)
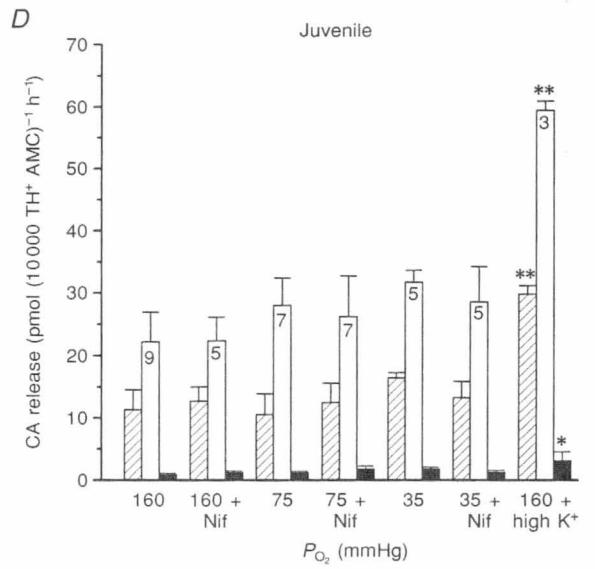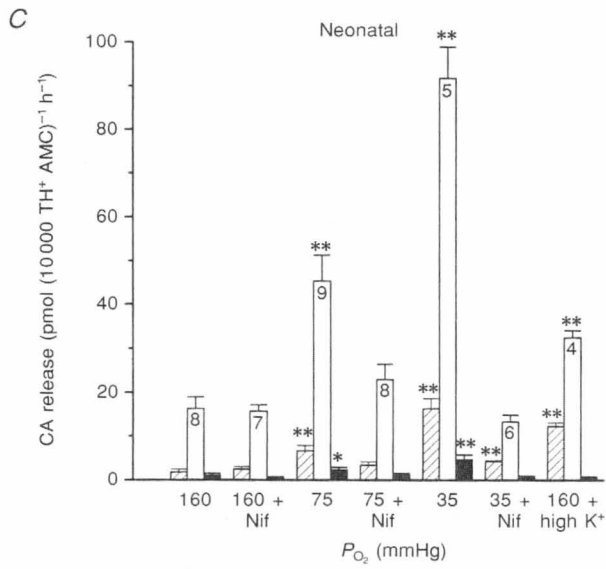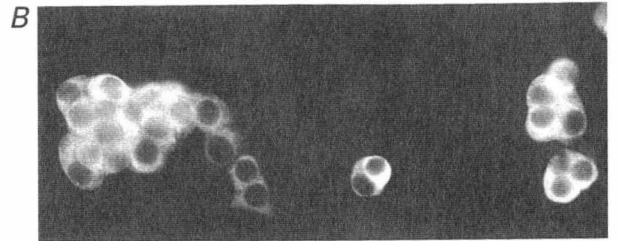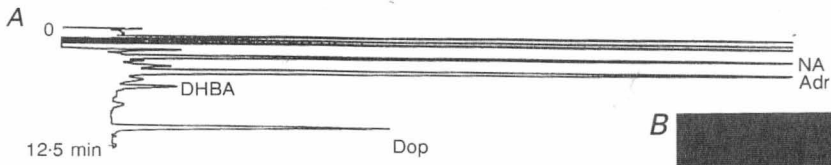
Figure 3C), suggesting a requirement for the entry of extracellular calcium through voltage-gated Ca^{2+} channels.

In contrast, exposure of juvenile AMC cultures to either hypoxic stimulus ($Po_2 = \sim$ 35 or 75 mmHg) had no effect on the normalized CA release relative to basal (Figure 3D). In addition, CA release in juvenile AMC cultures was unaffected by nifedipine at the oxygen tensions tested (Figure 3D). These results indicate that the ability of AMC to secrete CA in response to an acute hypoxic stimulus is lost by 2 weeks of postnatal life. This is likely due to a developmental loss of hypoxic chemosensitivity in AMC, rather than a failure of the secretory machinery, since in juvenile (and neonatal) AMC cultures CA release could be stimulated more than 2 times basal by a different stimulus, i.e. high extracellular K^+ (30 mM; Figure 3C, D).

Amperometric Determination of Catecholamine Release from Neonatal AMC

It was shown above that catecholamine (CA) release, as monitored by HPLC, was enhanced by hypoxia in a dose-dependent manner in neonatal but not juvenile AMC. This hypoxia-induced CA release from chromaffin cells can also be monitored in real time using carbon fibre microelectrodes. Fig 4A shows an amperometric recording of CA release from a small cluster of neonatal AMC under basal (normoxic) conditions ($Po_2 \sim$ 150 torr; top trace), during exposure to hypoxia ($Po_2 \sim$ 5 torr; middle trace), and after recovery in normoxia (lower trace). Note that the CA spike frequency and amplitude, as well as the baseline current, are reversibly increased following exposure to severe

hypoxia ($Po_2 \sim 5$ torr). Similar results were obtained in 5 of 8 cell clusters treated in this way.

Though it is evident from Fig 4A that CA spike frequency was augmented during hypoxia, an independent estimate of secretion can be obtained from the integrated area (Q_{CA}) under the amperometric spike records (see Lopez-Barneo, 1996). Fig 4B illustrates that hypoxia dramatically increases Q_{CA} over a 60 second interval, and that the effects are reversible (data obtained from the cell in Fig 4A).

Fig. 4. Catecholamine (CA) release from adrenal chromaffin cells monitored by carbon fibre microelectrodes.

A, representative 15 second amperometric recordings of CA current spikes from a cluster of 8-10 chromaffin cells after 24 hrs in culture. Traces from top to bottom represent respectively, basal CA release during normoxia ($Po_2 \sim 140$ torr), evoked release during severe hypoxia ($Po_2 = 0\text{-}5$ torr), and basal release after return to normoxia. Numbers indicated at right of each trace represent Po_2 in torr. B, total catecholamine charge (Q_{CA}), determined by integrating the area under the amperometric traces over a 60 second recording period. Note that hypoxia reversibly increases the amplitude and frequency of CA spikes in A, and this is correlated with an increase in Q_{CA}. Similar results were obtained from 5 of 8 cell clusters treated this way. Vertical scale bar represents 10 pA, and horizontal scale 1.5 sec.

A

140

~ 5

140

10 pA

2 sec

B

Q_{CA} (nC)

250

200

150

100

50

0

140   ~ 5   140

Po_2 (mmHg)
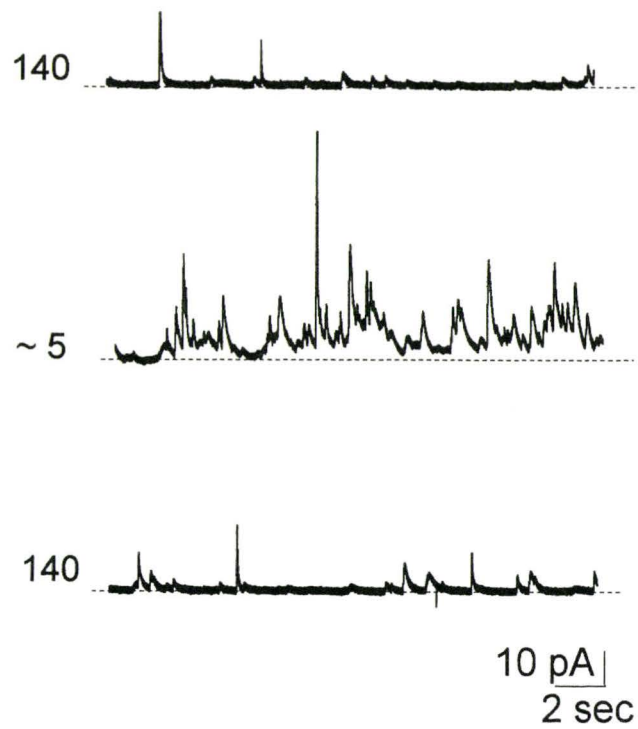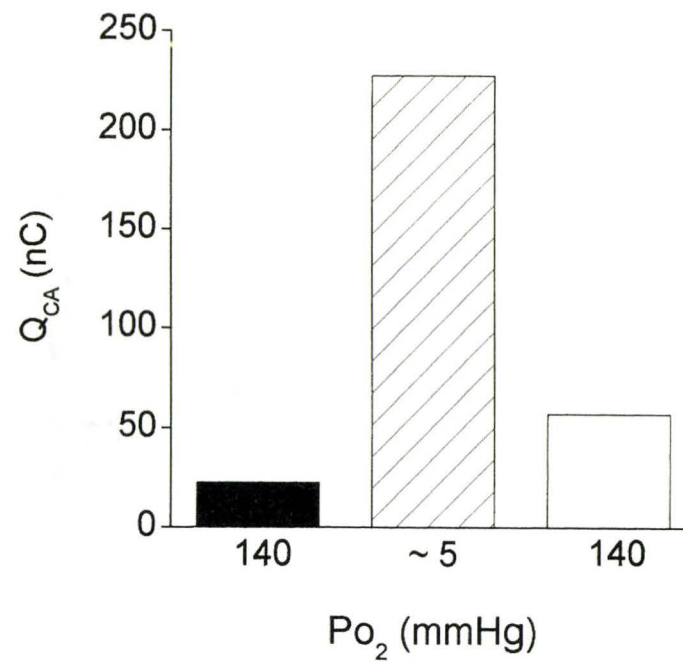
DISCUSSION

O₂-chemoreceptive properties is present in neonatal but not juvenile AMC

In this study we demonstrate that acute hypoxia causes suppression of a voltage-dependent K^+-current, membrane depolarization, and stimulation of CA release in neonatal (P1-P2) AMCs. Significantly however, these properties were virtually absent in juvenile AMCs, suggesting that the mechanisms for sensing oxygen in these cells are transiently expressed in the perinatal period. In this respect, they differ from chromaffin-like (type 1) cells of the carotid body, a major O_2- chemosensory organ which, throughout postnatal life, continues to sense oxygen and regulate arterial Po_2 via reflex input to the respiratory centre (Gonzalez *et al.*, 1994). The fact that the hypoxia-evoked CA release in neonatal AMC was abolished by the L-type calcium channel blocker, nifedipine, and that the depolarization was often sufficient to trigger action potentials, suggests that the hypoxia-sensing mechanism in these cells is similar to that described in other cell types including, carotid body type 1 cells (Lopez-Barneo *et al.*, 1988; Delpiano & Hescheler, 1989; Peers, 1990; Stea & Nurse, 1991; Buckler & Vaughan-Jones, 1994; Gonzalez *et al.*, 1994; Montoro *et al.*, 1996), and neuroepithelial bodies (Youngson, Nurse, Yeger & Cutz, 1993).

The depolarization of neonatal AMC by hypoxia was accompanied by a decrease in membrane conductance, consistent with the closing of ion channels that were open at the resting potential. Though closing of K^+ channels is a likely explanation, these may well be different from the ones that were sensitive to hypoxia in our voltage clamp studies. In the

latter case, the voltage-dependent hypoxia-sensitive K^+ current was activated at potentials

positive to -30 mV, well above the observed resting potentials of ~ -55 mV for chromaffin

cells. Thus, the possibility that the hypoxia-induced depolarization in neonatal AMC was due

to closure of a different K^+ channel subtype cannot be excluded, and indeed, there is evidence

in the carotid body that different types of K^+ channels can be regulated by hypoxia (Lopez-

Barneo et al., 1988; Peers, 1990; Ganfornina & Lopez-Barneo, 1992; Wyatt, Wright, Bee &

Peers, 1995). Whatever the origin of the initial depolarization, the hypoxic suppression of

a voltage-dependent K^+ current in this study is still likely to be physiologically important,

perhaps in regulating catecholamine secretion via control of action potential frequency

and/or duration. In neonatal AMC this current was activated at potentials positive to -30

mV, as occurs in other neuroendocrine cell types that sense oxygen (Lopez-Barneo et al.,

1988; Peers, 1990; Stea & Nurse, 1991; Youngson et al., 1993). The fact that with

conventional whole-cell recording, hypoxic suppression was greatest in the region of the I-V

relation where there was a characteristic 'hump', suggests the possible involvement of a Ca^{2+}-

activated K^+ current as occurs in rat type 1 cells (Peers, 1990); however, further studies are

required for validation of this point.

Importance of hypoxic chemosensitivity in neonatal animals

In the context of neonatal physiology, our results suggest a plausible 'non-neurogenic'

mechanism for adrenal catecholamine release during hypoxic stress in the newborn rat, where

sympathetic innervation of the adrenal medulla is immature or absent (Slotkin and Seidler,

1988; Lagercrantz and Slotkin, 1986; see also Cheung, 1990). This catecholamine release is crucial for survival of the neonate, producing multiple systemic effects that facilitate the transition from fetal to extrauterine life. Among these are absorption of lung fluid, secretion of surfactant (a process mediated by β_2-receptors), and regulation of cardiac function via stimulation of α- adrenergic receptors (Slotkin and Seidler, 1988). Thus, our data indicate that the increase in plasma catecholamine associated with birth could arise from the hypoxic-sensing mechanism we have uncovered in neonatal chromaffin cells, leading to membrane depolarization and increased action potential frequency, entry of extracellular calcium, and catecholamine release. Interestingly, our results also account for the observation that this 'non-neurogenic' mechanism disappears in the rat during the first few weeks of postnatal life (Slotkin and Seidler, 1988). At this time adrenal catecholamine release in response to hypoxic stress is abolished by blockers of cholinergic transmission or by short-term denervation of the adrenal medulla (Slotkin and Seidler, 1988). Thus our finding that the hypoxic-sensing mechanism, present in the neonate, disappears in juvenile (P13-P20) chromaffin cells is consistent with a model where O_2-sensing in these cells is a developmentally regulated process. It remains to be determined whether preganglionic sympathetic innervation can directly modulate O_2-chemosensitivity in adrenal chromaffin cells.

Chapter 2

Anoxia differentially modulates multiple K$^+$ currents and depolarizes neonatal rat adrenal chromaffin cells

In this chapter, additions to the published paper include Fig. 8 plus related results and discussion.

Summary

1. Using perforated-patch, whole cell recording, we investigated the membrane mechanisms underlying O_2-chemosensitivity in neonatal rat adrenomedullary chromaffin cells (AMC), bathed in extracellular solution containing tetrodotoxin (TTX; 0.5-1 μM), with or without blockers of calcium entry.

2. Under voltage clamp, low Po_2 (0-15 mmHg) caused a graded and reversible suppression in macroscopic outward K^+ current. The suppression during anoxia ($Po_2 = 0$) was ~35% (voltage step from -60 to +30mV) and was due to a combination of several factors: (i) suppression of a cadmium-sensitive, Ca^{2+}-dependent K^+ current, $IKCao_2$; (ii) suppression of a Ca^{2+}-insensitive, delayed rectifier type K^+ current, $IKVo_2$; (iii) *activation* of a glibenclamide (and Ca^{2+})-sensitive current, IK_{ATP}.

3. During normoxia (Po_2=150 mmMg), application of pinacidil (100 μM), a K_{ATP} activator, increased outward current density by 45.0 ± 7.0 pA pF^{-1} (step from -60 to + 30 mV), whereas the K_{ATP} blocker, glibenclamide (50 μM), caused only a small suppression by 6.3 ± 4.0 pA pF^{-1}. In contrast, during anoxia, the presence of glibenclamide resulted in a substantial reduction in outward current density by 24.9 ± 7.9 pA pF^{-1}, which far exceeded that seen in

its absence. Thus, activation of IK_{ATP} by anoxia appears to reduce the overall K^+ current suppression attributable to the combined effects of $IKCao_2$ and $IKVo_2$.

4. Pharmacological tests revealed that $IKCao_2$ was carried predominantly by maxi K^+ or BK channels, sensitive to 50-100 nM iberiotoxin; this current also accounted for the major portion (~60%) of the anoxic suppression of outward current. Tetraethylammonium (TEA; 10-20 mM) blocked all of the anoxia-sensitive K^+ currents recorded under voltage clamp, i.e., $IKCao_2$, $IKVo_2$ and IK_{ATP}.

5. Under current clamp, anoxia depolarized neonatal AMC by 10-15 mV from a resting potential of ~ -55 mV. At least part of this depolarization persisted in the presence of TEA, Cd^{2+}, 4-aminopyridine, or charybdotoxin, suggesting the presence of anoxia-sensitive mechanisms additional to those revealed under voltage clamp. In Na^+/Ca^{2+}-free solutions, the membrane hyperpolarized, though at least a portion of the anoxia-induced depolarization persisted.

6. In the presence of glibenclamide, the anoxia-induced depolarization increased significantly to ~25 mV, suggesting that activation of K_{ATP} channels may function to attenuate the anoxia- induced depolarization or receptor potential.

Introduction

Adrenomedullary chromaffin cells (AMC) mediate the elevation in plasma catecholamine (CA) that occurs when animals are exposed to stressors, eg. acute hypoxia. In the neonatal rat, this CA surge is vital for the animal's ability to survive hypoxic stress associated with the transition to extrauterine life, but occurs through a 'non-neurogenic' mechanism that is present prior to the onset of mature sympathetic innervation (Seidler & Slotkin, 1985). We recently reported that rat AMC possess a developmentally-regulated oxygen sensing mechanism, since in the majority of cells derived from neonatal (postnatal (P) day 1- P3), but not juvenile (P13-P21) animals, acute hypoxia caused suppression of the outward K^+ current, membrane depolarization, and CA secretion (Thompson et al., 1997). These responses appear qualitatively similar to those of prototypic O_2 chemoreceptors, i.e. type 1 cells of the carotid body (Buckler & Vaughan-Jones, 1994; Gonzalez et al., 1994; Peers & Buckler, 1995; Lopez-Barneo, 1996; Jackson & Nurse, 1997), and interestingly, both cell types derive from a similar lineage, the sympathoadrenal branch of the neural crest. However, hypoxia is known to modulate differentially, several types of K^+ channels and cause either membrane depolarization or hyperpolarization in a number of other cell types (Haddad & Jiang, 1997), including arterial myocytes (Post et al., 1992), pulmonary neuroepithelial bodies (Youngson et al., 1993), PC 12 cells (Zhu et al., 1996), and central neurons (Jiang et al., 1994).

The K^+ channel subtypes that are inhibited by hypoxia in carotid body type 1 cells

include large conductance Ca^{2+}-dependent K^+, or maxi-K^+, channels (Wyatt & Peers, 1995), and voltage-independent, small conductance K^+ 'leak' channels (Buckler, 1997) in the rat, and Ca^{2+}-independent, slow-inactivating, delayed rectifier type K^+ channels in the rabbit (Lopez-Lopez et al., 1989). In PC12 cells, a cell line derived from adrenal chromaffin cells, hypoxia inhibits a slow-inactivating, delayed rectifier type K^+ channel, which mediates membrane depolarization (Zhu et al., 1996). However, in these cells, hypoxia also appears to activate a large conductance Ca^{2+}-dependent K^+ channel (Conforti & Millhorn, 1997). In central neurons, hypoxia activates a glibenclamide-sensitive K_{ATP} current, which is thought to play a protective role in low oxygen conditions, by inducing hyperpolarization and preventing action potential generation (Jiang et al., 1994). These results suggest that hypoxia can modulate multiple K^+ channels in different tissues, and that the effect on a particular channel (i.e. closure vs opening) may be both species and cell-type dependent.

In our initial study (Thompson et al., 1997), it was unclear which K^+ channel types mediate hypoxic chemosensitivity in *neonatal* rat AMC. This is of additional interest, since, as discussed above, hypoxia inhibits K^+ channels with different calcium sensitivities in two cell types, i.e. carotid body type 1 cells and PC 12 cells, that are related developmentally to AMC. Furthermore, in a recent study, K_{ATP} channels were presumed to play a crucial role in hypoxia-induced responses in *adult* rat chromaffin cells (Mochizuki-Oda et al., 1997). In the present study, we used perforated-patch / whole-cell recording and pharmacological tools, to characterize the types of O_2-sensitive K^+ currents in neonatal rat AMC and to investigate whether these currents can account for the hypoxia-induced membrane depolarization or

receptor potential (Thompson *et al.*, 1997). Preliminary results of some of these findings were reported in a recent abstract (Thompson & Nurse, 1997).

Materials and Methods

Cell culture

Pregnant or lactating Wistar rats and pups (Charles River, Quebec, Canada) were housed in our animal facility under a 12 hr light, 12 hr dark cycle. All animal handling and tissue removal conformed to guidelines established by the Canadian Council on Animal Care. Primary cultures enriched in dissociated adrenomedullary chromaffin cells (AMC) were prepared as previously described (Thompson et al., 1997). Adrenal glands were dissected from neonatal rats [i.e. postnatal (P) day P1-P2] that were rendered unconscious by a blow to the head and killed by decapitation. Most of the surrounding cortex was trimmed and discarded. The remaining (medullary) tissue was dissociated by incubation (at 37 °C) in an enzymatic solution containing 0.1% v/v trypsin, 0.1% v/v collagenase (Gibco), and 0.01% v/v deoxyribonuclease (Millipore). After 1 hr incubation, most of the enzyme was removed, and the remainder was inactivated by addition of the growth medium consisting of F-12 nutrient medium (Gibco) supplemented with 10% v/v fetal calf serum (Gibco), 80 UI^{-1} insulin (Sigma), 0.6% v/v glucose, 2mM glutamine, 1% v/v penicillin and streptomycin (Gibco), and 0.01% v/v dexamethasone (Sigma). Tissue was then triturated using a Pasteur pipette, and the final cell suspension was pre-plated for 1-24 hr on a collagen-coated culture dish to remove most of the cortical cells. The non-adherent AMC were then plated onto the central region of "Nunclon" culture dishes, that was previously

coated with a thin layer of matrigel (Collaborative Research, Bedford, MA, USA). The cells were grown at 37 $^{\circ}$C in a humidified atmosphere of 95% air : 5% CO_2 for 3-72 hr before they were used in patch clamp experiments.

Electrophysiology

All voltage and current clamp data were obtained using the perforated-patch configuration of whole-cell technique as previously described (Thompson *et al.*, 1997). The seal resistance was typically 2-10 GΩ, and most (~75%) of the series resistance (range 12-50 MΩ) was compensated in voltage-clamp experiments; voltage errors due to series resistance were minimal due to the high input resistance (~ 2GΩ) of the cells. Junction potentials were typically 2-5 mV in the standard bathing solution, and were cancelled prior to seal formation. The pipette solution for perforated-patch recording contained (in mM): potassium gluconate, 105; KCl, 30; NaCl, 5; $CaCl_2$, 0.1; Hepes, 10; at pH 7.2, plus nystatin (450 μg ml^{-1}). The standard bathing solution for both voltage clamp and current clamp experiments consisted of (in mM): NaCl, 135; KCl, 5; $CaCl_2$, 2; $MgCl_2$, 2; glucose, 10; Hepes, 10; tetrodotoxin (TTX), 0.0005-0.001; the pH was adjusted to 7.4 with NaOH. In experiments where a Ca^{2+}-free bathing solution was required, $CaCl_2$ (2 mM) was replaced with equimolar $MgCl_2$ and 1 mM EGTA. In some experiments, 200 μM $CdCl_2$ was added to block Ca^{2+} currents, and indirectly, Ca^{2+}-dependent K^+ currents. In experiments requiring a Na^+-free solution, Na^+ was replaced with equimolar N-methyl-D-glucamine (NMDG), and the pH was adjusted with HCl.

All recordings were obtained at room temperature (20-23 °C) with an Axopatch-1D amplifier equipped with a 500 MΩ head stage feedback resistor (Axon Instruments). Records were digitized with a Digidata 1200 computer interface (Axon Instruments) and stored on hard disk in an IBM-compatible computer using pCLAMP software version 6.0.3 (Axon Instruments). In the majority of experiments anoxia was used the low Po_2 stimulus. Anoxia was generated by bubbling 100% N_2 into the perfusion reservoir in the presence of the O_2 scavenger sodium dithionite; the pH was adjusted to 7.4 with NaOH. For hypoxic solutions, 100% N_2 was bubbled in the absence of dithionite. Measurements of Po_2 were obtained with an O_2 microelectrode (Diamond Electro-Tech Inc., MI, USA) placed near the recording site. During calibration, 0 mmHg (anoxia) was the designated Po_2 of a solution equilibrated with 100% N_2 in the presence of 1 mM sodium dithionite. The solution in the recording chamber (volume= 750µl - 1 ml) was exchanged by perfusion under gravity and simultaneous removal by suction at a rate of 5-6 ml min^{-1}.

The effects of anoxia and/or hypoxia on voltage-activated currents were examined by comparing peak currents from the average of four records at each step potential, over the range of -50 to +50 mV (10 mV increments), from a holding potential of -60 mV. Records were taken before (control), during, and after (recovery) application of the stimulus, and the averages were obtained either during data collection (on-line), or during subsequent analysis (off-line). All measurements of membrane potential were obtained under current clamp in zero current (I =0) mode. Membrane capacitance (pF) was obtained by first integrating the capacitative transient elicited by a hyperpolarizing voltage step from -60 to -100 mV, and

then dividing by the magnitude of the step. Currents (pA) or current densities (pA pF^{-1}) were compared using either paired or independent Students t tests, with the level of significance set at $P<0.05$. Voltage clamp current traces are shown in the text with 'leak currents' unsubtracted; current or current density vs voltage (I-V) plots are leak subtracted. All data are presented as mean ± S.E.M.

Drugs

In order to block various types of K$^+$ currents (as indicated in the text) the following drugs were added directly to the perfusion fluid: tetraethylammonium (TEA), glibenclamide, and 4-aminopyridine (4-AP) were obtained from Sigma; iberiotoxin (IbTx) and charybdotoxin (ChTx) were obtained from Alomone Laboratories (Jerusalem, Israel). In some experiments the K$_{ATP}$ channel activator, pinacidil, a gift of Dr. Jan Huizinga, was used. Additionally, in some experiments cadmium 200 μM (CdCl$_2$) was used to block Ca^{2+} entry and indirectly Ca^{2+}-dependent K$^+$ currents. To block voltage-dependent Na$^+$ currents, tetrodotoxin (TTX; Sigma) was added to the bathing solution.

Results

Neonatal rat adrenomedullary chromaffin cells (AMC) were first tested for hypoxic sensitivity after 3 hr - 3 days in culture, using the perforated-patch technique for whole-cell recording. Similar to our previous report (Thompson *et al.*, 1997), low Po_2 caused a reversible suppression of outward current (Figs. 1 and 2) and/or membrane depolarization (e.g. Fig. 7) in >80% of cells tested (n = 68/78). As shown in Fig. 1 A and B, the magnitude of the effect was graded, with the maximum current suppression occurring in anoxia (Po_2= 0 mmHg). During a voltage step from -60 mV to +30 mV, the mean ($\pm$ S.E.M.) percent suppression was 12.2 ± 0.02 % during hypoxia ($Po_2 \sim 15$ mmHg), compared to 43.6 ± 0.08 % in anoxia, for the same group of 5 cells examined at both Po_2 levels. Thus, in the experiments reported below an anoxic stimulus was routinely used in order to optimize the cell response. O_2-sensitive AMC were observed after acute cell isolation (i.e. 3 hr in vitro), and in short term cultures (1-3 days), suggesting that the hypoxia-sensing mechanism was expressed *in vivo*, before the cells were brought into culture.

To allow comparisons among cells of different sizes, current density ($pA\ pF^{-1}$) was determined by dividing the steady-state outward current (at 45 msec; step from -60 mV) by the whole-cell capacitance (range: 4-10 pF; see Materials and Methods). Under voltage clamp, the mean ($\pm$ S.E.M.) outward current density during normoxia ($Po_2 = 150$ mmHg)

Figure 1. Po_2-dependent suppression of outward current in neonatal rat adrenal chromaffin cells (AMC).

A, leak-unsubtracted outward currents recorded from a cell exposed sequentially to normoxia (Po_2= 150 mmHg), hypoxia (Po_2~15 mmHg), normoxia again (not shown), anoxia (Po_2= 0 mmHg), and finally normoxia (wash). All traces were obtained during voltage steps from -60 mV to +30mV, and each trace is the average of 4 records; the two top traces are superimposed initial (control) and final (wash) recordings in normoxia. Horizontal scale represents 10 ms, and vertical scale 200 pA. B, current *vs.* voltage plots for the cell in A. Records were taken at 10 mV voltage increments from a holding potential of -60 mV. Symbols are as follows: control, O: hypoxia, ●; anoxia, ▲; wash, Δ. The anoxic stimulus was applied after the cell had recovered from the hypoxic stimulus (not shown). Wash represents recovery after anoxia. Note the magnitude of outward current suppression is Po_2 dependent. Similar results were obtained in 4 other cells exposed to normoxia, hypoxia and anoxia.

A

150 mmHg
15 mmHg
0 mmHg

B

Current (pA)

2000

1000

-40   0   40
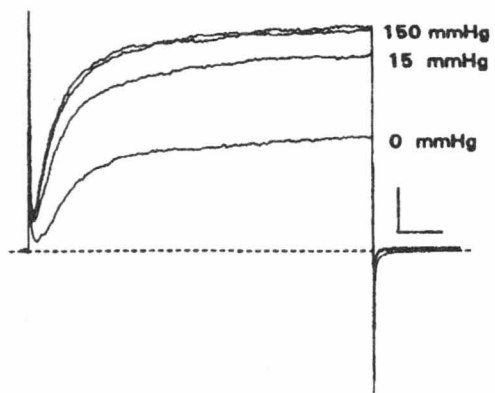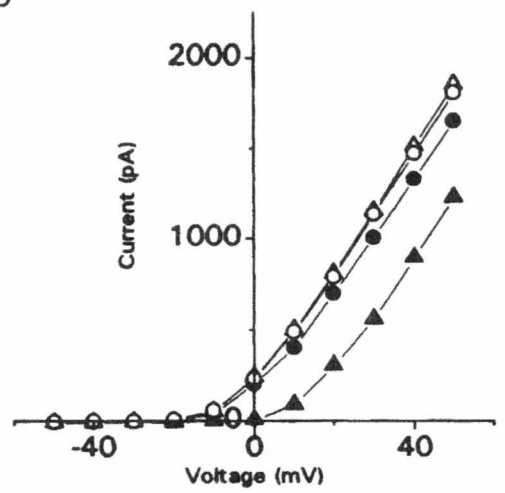
Voltage (mV)

was 115 ± 8.24 pA pF^{-1} (n = 48) for a voltage step from -60 to +30 mV. Exposure to anoxia

caused a significant reduction in outward current density to 74.25 ± 5.96 pA pF^{-1} (n = 48;

P<0.01); after reperfusion with control (normoxic) solution, the current density returned to

100.8 ± 8.8 pA pF^{-1} (n =48), a value not significantly different from control (P>0.2). The

anoxia-sensitive component of outward current (IKo$_2$) comprised an average of 34.5 ± 0.03

% (n = 48) of the total outward K$^+$ current recorded in normoxia, for the voltage step from

-60 to +30 mV. By first testing for the presence of this anoxia- sensitive K$^+$ current, O$_2$-

sensitive AMC were identified, thereby allowing the K$^+$ current subtype(s) that mediate O$_2$-

chemosensitivity to be investigated in greater detail. In the voltage clamp experiments

reported below, cells that failed to show >90% recovery of the control current, after exposure

to anoxia or pharmacological agents (with the exception of the poorly reversible, Ca^{2+}-

dependent K$^+$ channel blocker, iberiotoxin), were excluded.

Anoxia suppresses both Ca^{2+}-dependent and Ca^{2+}-independent K$^+$ currents in neonatal AMC

Closure of a variety of K$^+$ channels, including both Ca^{2+}-dependent and Ca^{2+}-

independent subtypes, mediates hypoxic chemosensitivity in carotid body type 1 cells

(Lopez-Lopez *et al.*, 1989; Peers, 1990; Gonzalez *et al.* 1994; Buckler, 1997), and in PC 12

cells (Conforti & Millhorn, 1997). To test whether both subtypes participate in the anoxic

suppression of K$^+$ current in neonatal AMC, cells were studied in either Ca^{2+}-free or Cd^{2+}-

containing (200 µM) bathing solutions. These conditions have been shown to inhibit Ca^{2+}-

dependent K$^+$ currents in adult rat AMC (Neely & Lingle, 1992) and neonatal rat type 1 cells

(Peers, 1990). Blockade of Ca^{2+} entry by addition of 200 μM Cd^{2+} to the bathing solution, resulted in a reduction in outward current by 64.3 ± 0.06 % relative to control (n =10; step from -60 to +30 mV); an example is shown in Figs. 2A and B (compare left traces). This reduction was not significantly different from that seen in Ca^{2+}-free medium, where the corresponding suppression was 60.1 ± 0.08 % (n =12). Thus, as in adult rat AMC (Neely & Lingle, 1992), the majority (~62%) of the outward current in neonatal, O_2-sensitive AMC is Ca^{2+}-dependent.

Since anoxia suppressed the outward current by ~35% when Ca^{2+} currents were present (see above and. Fig. 2A), it was of interest to determine whether the same stimulus had any effect on the residual K^+ current recorded in Ca^{2+}-free or Cd^{2+}-containing solutions. As shown in Figs. 2B and D, anoxia caused a small, but significant suppression in outward current in the presence of 200 μM Cd^{2+} and the effect was reversible. Also, cells exposed to Ca^{2+}-free solutions were still capable of responding normally to another anoxic stimulus, after return to normal Ca^{2+} (n= 3; Fig. 2E). Experiments similar to Figs. 2B,D and E, allowed a quantitative estimate of $IKVo_2$, i.e. the magnitude of the Ca^{2+}-independent component of the total anoxia-sensitive current, IKo_2. This current, $IKVo_2$, is shown as difference current traces for the cell in Fig. 3A (lower traces), and compared to IKO_2 for the same cell in Fig. 3A (upper traces). Comparisons of current densities (pA pF^{-1}) for groups of cells exposed to anoxia in Ca^{2+}-free or Cd^{2+}-containing solutions are shown in Fig. 3B and C. The difference current traces shown in Fig. 3A, where currents recorded in anoxia are subtracted

Figure 2. Effect on anoxia on Ca^{2+}-dependent and Ca^{2+}-independent outward currents in neonatal rat AMC.

A, leak-unsubtracted outward current traces recorded from a cell in normal (2 mM) Ca^{2+}, before (left; control), during (middle), and after (right; recovery) exposure to anoxia. Traces shown are for voltage steps from a holding potential of -60 to +50 mV in 10 mV increments; top trace in each record represents the step to +50mV. Note anoxia reversibly suppresses outward current. B, Same cell (as in A) was exposed to a similar protocol, except that Ca^{2+}-dependent currents were blocked by inclusion of 200 µM Cd^{2+} in the bathing solution. Note anoxia still had a suppressive effect on the residual Ca^{2+}-independent outward current. C and D, current density *vs.* voltage plots for 10 representative cells, including the one in A. Mean current density (± SEM) is shown for cells recorded in 2 mM Ca^{2+} (C) and 200 µM Cd^{2+} (D). The current density measured during anoxia was significantly different from control (P<0.05) at all voltage steps between -10 and + 50 mV in C, or -10 and +30 mV in D, and recovery was complete at each step. Symbols are as follows: control, O; anoxia, •; and recovery, Δ. E, time course of anoxic inhibition of outward currents (step to +40 mV) in the presence and absence (Ca^{2+}-free) of extracellular Ca^{2+}. Note that the cell responded to a third anoxic stimulus after return to normal Ca^{2+}- containing medium. Outward current is expressed as a percentage of the maximum recorded in normal Ca^{2+}. c, a, and r refer to control, anoxia and recovery respectively. Vertical scale represents 500 pA and horizontal scale represents 10 ms.

A

control   anoxia   recovery

2 mM
Ca^{2+}

B

200 µM
Cd^{2+}

C

Current density (pA pF^{-1})

300

200

100

0

-40   0   40
Voltage (mV)

D

75

50

25

0

-40   0   40
Voltage (mV)

Current density (pA pF^{-1})

E

I (% control)

100

0

c, r   c, r   c, r

a   a   a

a   a   a
Ca^{2+}-free

0   2   4   6   8   10   12   14
time (min)
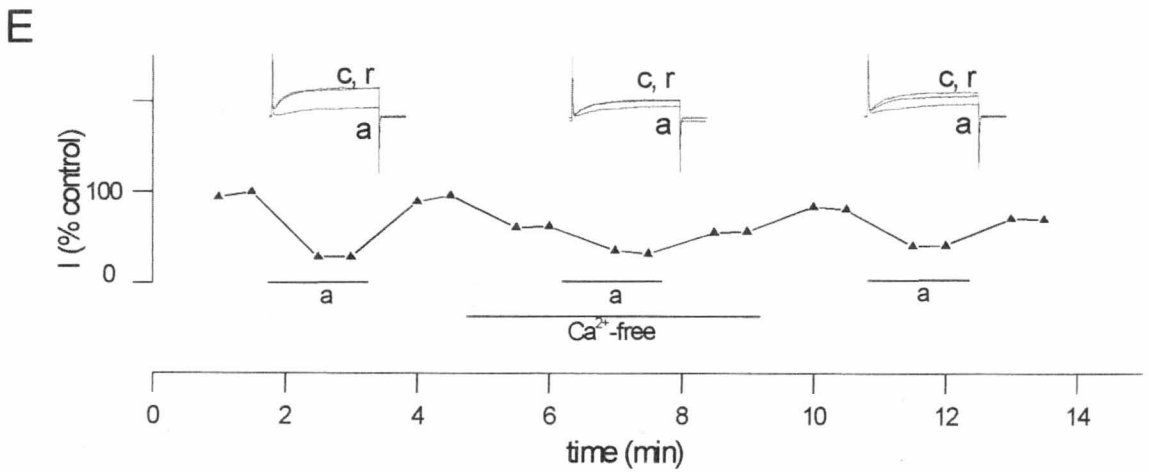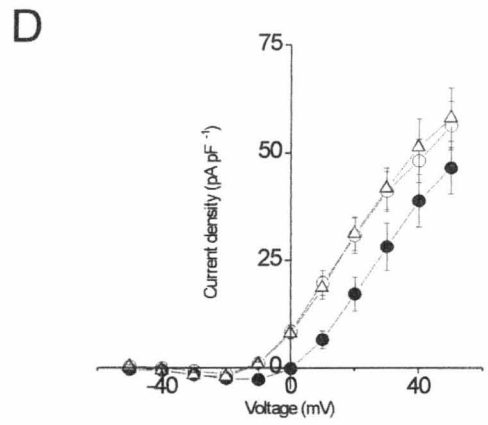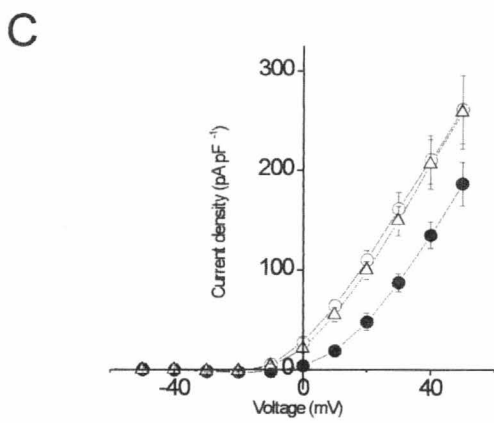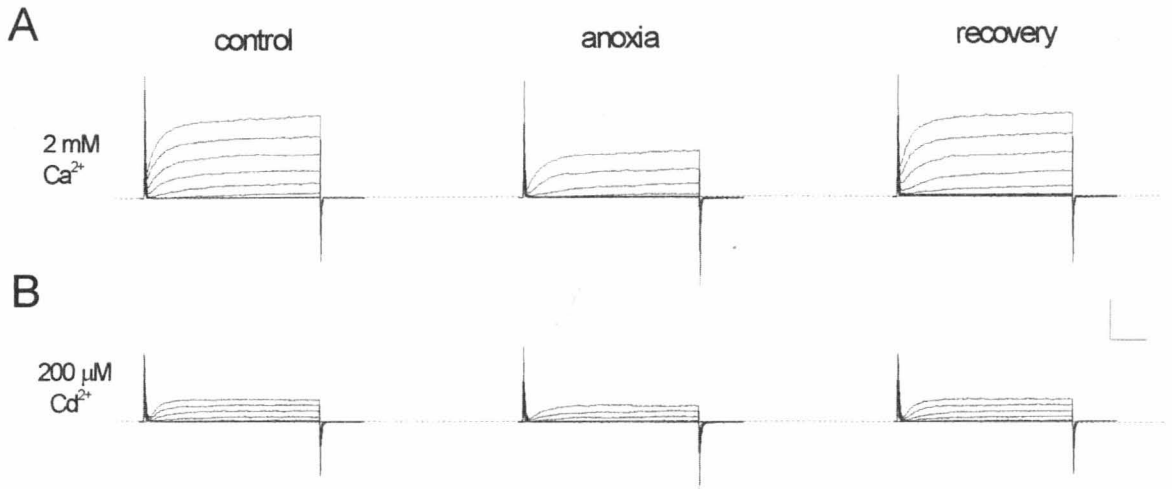
Figure 3. Comparison of anoxia-sensitive difference currents in neonatal chromaffin cells.

A, anoxia-sensitive currents, obtained by subtracting current traces recorded during anoxia from corresponding ones in normoxia, are shown in normal Ca^{2+}-containing (upper traces) and Ca^{2+}-free (lower traces) solutions. Subtracted traces are for 10 mV incremental steps between -50 and +30 mV; holding potential was -60 mV. Note the larger component of the anoxia-sensitive difference current is Ca^{2+}-sensitive; lower traces represent the Ca^{2+}-*independent* O_2-sensitive current, IKV_{O2}. Vertical scale bar represents 100 pA, and horizontal scale bar represents 10 ms. B, current density *vs.* voltage plots for 6 representative cells, showing the total (mean ± SEM) anoxia-sensitive component, IK_{O2} (O), and IKV_{O2} (•; recorded in 200 μM Cd^{2+}). C, comparison of mean (± SEM) outward current density at + 30 mV, for all cells investigated in normal Ca^{2+} (2 mM), Ca^{2+}-free, and Cd^{2+}-containing (200 μM) bathing solutions. * significantly different from control group (P<0.05). The mean current density (at +30 mV) during anoxia in the presence of Cd^{2+}, or in Ca^{2+}-free solutions, was significantly different from that in the presence of 2 mM Ca^{2+} (P<0.01).

A

B

C

control
anoxia
difference

2 mM Ca²⁺   Ca²⁺-free   0.2 mM Cd²⁺
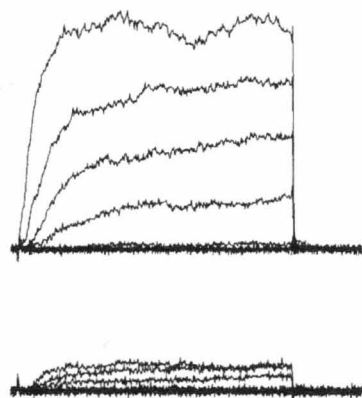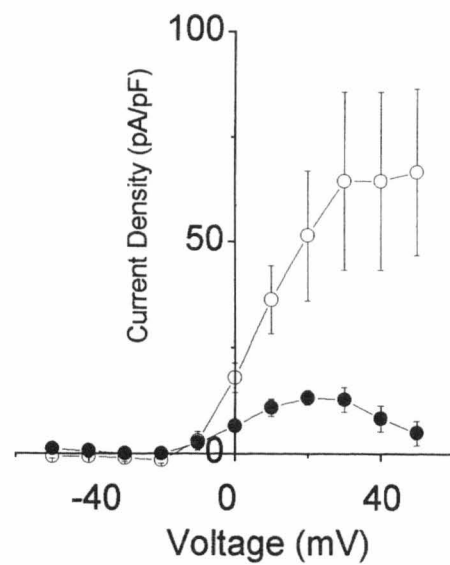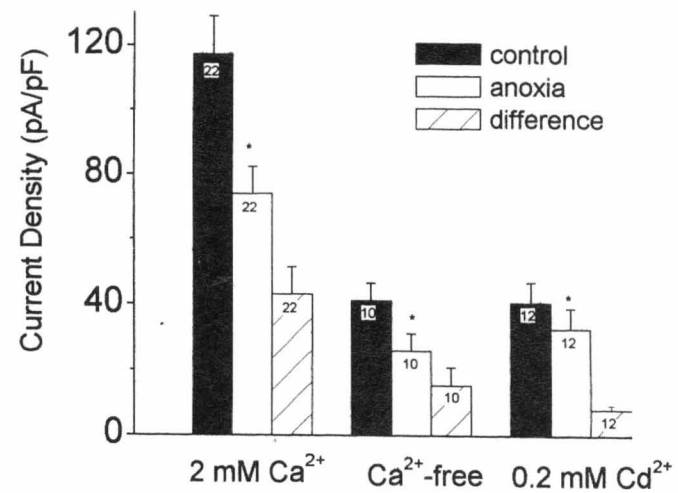
from control (normoxic) currents, allow the anoxia-sensitive component to be isolated in both normal Ca^{2+} (upper traces), and Ca^{2+}-free (lower traces) solutions. It is evident from these traces, as well as the current density *vs.* voltage plot in Fig. 3B, that the Ca^{2+}-independent component, $IKVo_2$, represents only a small fraction of the total IKo_2. For a voltage step from -60 to +30 mV, $IKVo_2$ represents 39.1 ± 0.1 % (n =10) of IKO_2 in Ca^{2+}-free, and 26.1 ± 0.05 % (n =12) in Cd^{2+}-containing solutions. This implies that the remaining ~65% of IKo_2 must be Ca^{2+}-dependent, i.e. $IKCao_2$. Both of these O_2-sensitive K^+ currents were observed in the majority of cells tested (n =21/22). A comparison of the absolute K^+ current densities in normoxia and anoxia, as well as the difference K^+ current density, is shown in Fig. 3C for cells recorded in normal Ca^{2+}, Ca^{2+}-free, and Cd^{2+}-containing solutions. Note that the anoxia-sensitive, or difference K^+ current density, is similar in Ca^{2+}-free and Cd^{2+}-containing solutions (i.e. $IKVo_2$).

Neonatal AMC possess anoxia-sensitive K_{ATP} currents

K_{ATP} channels have been implicated in hypoxic chemosensitivity of *adult* rat AMC, based on the observation that openers of these channels prevented the hypoxia-induced rise in intracellular Ca^{2+} (Mochizuki-Oda *et al.*, 1997). In addition, activation of K_{ATP} channels during hypoxia is hypothesized to play a protective role in some central neurons (Jiang *et al.*, 1994). If similar channels were present in *neonatal* rat AMC, then their activation by anoxia would tend to oppose or reduce the inhibition of outward current resulting from closure of the Ca^{2+}-dependent and Ca^{2+}-independent channels described above. To determine if O_2-

sensitive AMC possess K_{ATP} channels we used both pinacidil (a K_{ATP} activator) and glibenclamide (a K_{ATP} blocker; Ashcroft and Ashcroft, 1990). In Figs. 4Aa and Ab, exposure of AMC to 100 μM pinacidil resulted in a reversible *augmentation* of outward current and current density. For a voltage step from -60 to +30 mV, the outward current density was increased from the control value of 128.3 ± 19.5 pA pF^{-1} to 173.3 ± 16.6 pA pF^{-1} in the presence of 100 μM pinacidil (n =5; P<0.05); after washout of pinacidil the current density recovered to 132.7 ± 25.8 pA pF^{-1}. These results suggest that O_2-sensitive AMC possess K_{ATP} channels.

We then tested whether activity of these K_{ATP} channels was regulated by O_2 tension, using the specific K_{ATP} channel blocker, glibenclamide (50 μM). Figures 4Ba and Bb show the effect of glibenclamide on outward K^+ currents recorded during normoxia (Po_2 = 150 mmHg). In most cells (6/9) cells there was no detectable effect of glibenclamide (Fig. 4Ba), though in the remaining (3/9) cells, a small, reversible suppression in K^+ current was observed (not shown). Pooled data from the 9 cells revealed that for a voltage step to +30 mV, the mean current density for the glibenclamide-sensitive component was 6.3 ± 4.0 pA/pF (range: 0 to 25.2 pA/pF), corresponding to 4.9 ± 0.8 % of the total outward current density. Plots of current density *vs.* voltage under normoxic conditions are shown in Fig. 4Bb for these 9 cells, before, during and after glibenclamide; overall, the latter had negligible effect over the voltage range -30 to +50 mV.

In contrast, exposure to anoxia had a profound effect on glibenclamide sensitivity. For example, in Fig. 4Ca, anoxia alone produced the usual suppression in K^+ current, but

when combined with glibenclamide the suppression was much more dramatic (compare *same* cell in Fig. 4Ba), and the effect was completely reversible. Pooled data from 9 cells revealed that for a voltage step from -60 to +30 mV, the outward current density was reduced from 80.7 ± 17.8 pA pF^{-1} in normoxia, to 57.0 ± 11.6 pA pF^{-1} in anoxia alone, and this was further reduced to 32.0 ± 6.1 pA pF^{-1} in anoxia plus glibenclamide (significantly different from anoxia alone; $P < 0.01$). The mean outward current density after reperfusion with control (normoxic) solution was 75.5 ± 16.7 pA pF^{-1}, a value not significantly different from the initial control response. Current density *vs.* voltage plots are shown in Fig. 4Cb for these cells, which were exposed sequentially to normoxia, anoxia, anoxia plus glibenclamide, and then returned to normoxia. These data indicate that for a step from -60 to +30 mV, the anoxia-sensitive component of outward current IK_{O_2} comprised 29.4 ± 0.1 % (n =9) of the control (normoxic) K^+ current in the absence of glibenclamide, compared to 60.3 ± 0.1 % (n =9) in its presence (difference significant; $P < 0.05$). Measurements of difference current density allowed a direct comparison of the magnitude of the glibenclamide-sensitive component in normoxia and anoxia. For a step to +30 mV, the glibenclamide-sensitive component during anoxia was 24.9 ± 7.9 pA pF^{-1} (n =9), a value significantly different ($P < 0.05$) from that seen in normoxia (6.3 ± 4.0 pA pF^{-1}; n =9).

Are anoxia-sensitive K_{ATP} channels in neonatal AMC also Ca^{2+} sensitive?

In central neurons, the O_2-sensitive K_{ATP} channels are Ca^{2+}-sensitive (Jiang *et al.*, 1994). To investigate whether the same is true for K_{ATP} channels in neonatal AMC, the effect

of glibenclamide on O_2 sensitivity was tested in Cd^{2+}-containing solutions which block Ca^{2+} entry. As shown in Fig. 4Da and Db, the presence of glibenclamide (50 µM) had no *additional* effect on the outward current recorded during anoxia over the voltage range -30 to +30 mV, when Cd^{2+} was present. Under these conditions, the glibenclamide sensitive component was 6.6 ± 4.9 pA pF^{-1} (n =7) in normoxia vs 10.0 ± 3.3 pA pF^{-1} (n =7) in anoxia for a voltage step from -60 to +30 mV (difference not significant; P> 0.1). This contrasts with the results reported above in normal Ca^{2+} (Cd^{2+} -free) solutions (Fig. 4Ca and Cb), where glibenclamide significantly reduced the K^+ current recorded in anoxia. Current density *vs.* voltage plots are compared in Fig. 4Db, for these 7 cells in the continuous presence of Cd^{2+}-containing solutions, during exposure to normoxia (open circles), anoxia alone (closed circles), anoxia plus glibenclamide (closed triangles), and finally normoxia again (open triangles). However, at the voltage steps > +40 there is an apparent activation of IK_{ATP} by anoxia (Fig. 4Db), even in the presence of Cd^{2+}. The underlying mechanism is unclear, but may involve interactions of divalent cations (eg. Cd^{2+} or Mg^{2+}) with the K_{ATP} channel (Ashcroft & Ashcroft, 1990).

Pharmacology of IKC_{aO_2} and IKV_{O_2}

Since the predominant Ca^{2+}-dependent outward current in adult AMC is carried by large conductance maxi-K^+ or BK potassium channels (Neely & Lingle, 1992), which are known to be inhibited by hypoxia in carotid body type 1 cells (Wyatt & Peers, 1995), it was

Figure 4. Comparison of the effects of K_{ATP} channel modulators on K^+ current and K^+ current density recorded during normoxia or anoxia in neonatal AMC.

All current records are shown for cells studied under voltage clamp, and representative traces are shown for the voltage step from -60 to + 30 mV. A_1 and A_2, in normoxia, effects of pinacidil (100 µM) an activator of IK_{ATP}, on outward currents and current density. Note that sequential application of pinacidil (+ pinacidil, ●), increases outward current above control (c, O), and the effect was reversible after washout (w, Δ). Mean (± SEM) K^+ current density is shown for a group of 5 cells, indicating that pinacidil significantly increased K^+ current density relative to control at all voltage steps between 0 and +50 mV (p <0.05). B_1 and B_2, current records in normoxia, for cells (n=9) treated with control saline (c, O), 50 µM glibenclamide (+glib, ●), a blocker of IK_{ATP}, and after washout (w, Δ) of this drug. Mean (± SEM) K^+ current density vs voltage plot for 9 cells shows that glibenclamide did not significantly effect outward current density. C_1 and C_2, effect of simultaneous exposure to anoxia and glibenclamide on outward current for the same 9 cells as in B. Cells were sequentially exposed to normoxia/control (c, O), anoxia (a, ●), anoxia plus glibenclamide (a+glib, ▲), and recovery (r, Δ). Note that the inhibitory effect of anoxia on the outward current (a) was greatly exaggerated in the presence of glibenclamide. Current density in anoxia was significantly less than normoxic control at all voltage steps between 0 and + 50 mV (p <0.01); also, current density in anoxia plus glibenclamide was significantly less than anoxia alone, between -20 and + 30 mV (P<0.05). D_1 and D_2, outward current and current density recorded in the presence of Cd^{2+} (200 µM), to block Ca^{2+}-dependent K^+ currents. Note that anoxia (a) reversibly suppressed the outward current, but addition of 50 µM glibenclamide (a+glib) had no *additional* suppressive effect during anoxia (compare Fig. $4C_1$), suggesting that IK_{ATP} is Ca^{2+}-dependent. Mean (± SEM) K^+ current density vs. voltage plot is for a group of 7 cells and shows that anoxia significantly (P<0.01) suppressed outward currents in the presence of Cd^{2+} at all potentials between -10 and + 50 mV. In the presence of glibenclamide, the additional suppression of outward current by anoxia was absent at all test potentials below +40 mV (P>0.05). Symbols are the same as in C. . This suggests IK_{ATP} is Ca^{2+}-sensitive. Vertical scale represents in 400 pA in A, B and C, and 100 pA in D. Horizontal scale represents 30 ms.
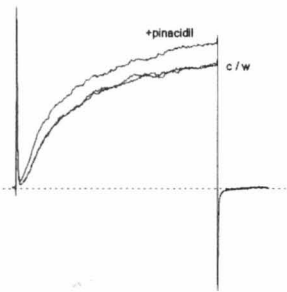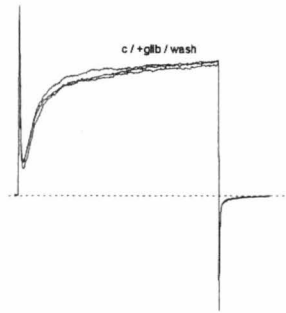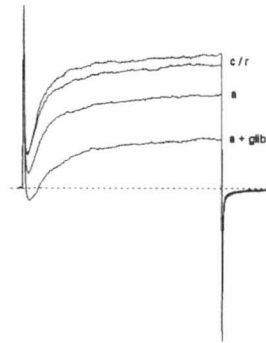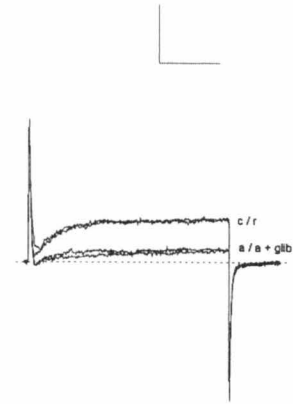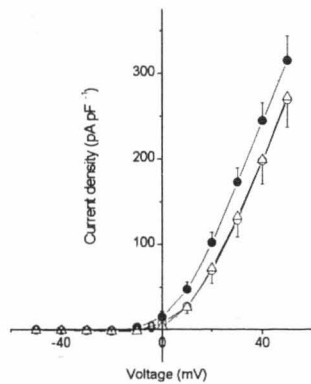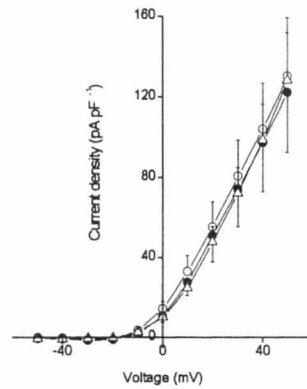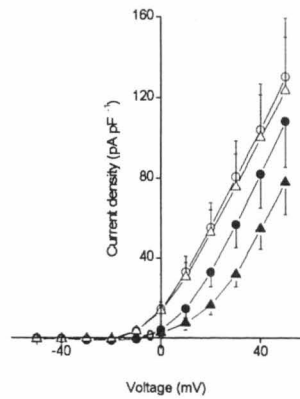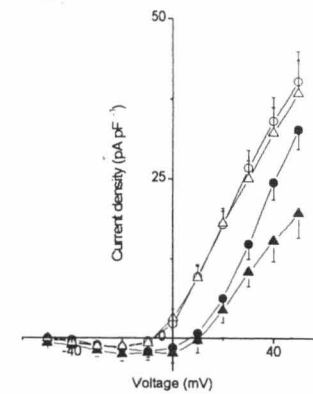
of interest to determine if $IKCao_2$ was also carried by BK channels. To test this we used the specific blocker, iberiotoxin (IbTx), to inhibit the large conductance BK channels (Galvez *et al.*, 1990). Exposure of neonatal AMC to IbTx (50 - 100 nM), resulted in a suppression of the outward current, suggesting the presence of BK channels (Fig. 5A). The IbTx-sensitive component consisted of 47.6 ± 0.04 % (n = 4) of the overall outward current, for a voltage step from -60 to +30 mV. This is slightly less than the values (~62%) reported above for the magnitude of the Ca^{2+}-dependent K^+ currents recorded in Ca^{2+}-free or Cd^{2+}- containing solutions, and is probably due to the persistence of small conductance Ca^{2+}-dependent K^+ channels, which are insensitive to IbTx (Park, 1994). Exposure of neonatal AMC to anoxia, in the presence IbTx (Fig. 5A, middle trace), caused a further suppression in outward current. Plots of current density vs voltage indicate that the suppression in IbTx-containing medium occurred at all voltage steps between -10 and +50 mV, and the effect of anoxia was reversible (Fig. 5B). Generally, washout of the effects of IbTx on the total K^+ current was incomplete, even after reperfusion for 10-15 min with control solution. The contribution of both the IbTx-sensitive and IbTx-insensitive K^+ currents to the total anoxia-sensitive IKo_2 was determined from the difference current measurements for the voltage step to +30 mV. The IbTx-insensitive portion of IKo_2 represented 42.2 ± 0.2 % (n =4) of the total IKo_2, and the remaining 57.8 ± 0.2 % was IbTx-sensitive. Since the IbTx-insensitive component of IKo_2 is similar to that obtained above for the Ca^{2+}-independent portion of IKo_2, i.e. $IKVo_2$, obtained in Ca^{2+}-free (~39%) and Cd^{2+}-containing (~28%) solutions, it appears that $IKCao_2$ is carried almost exclusively by IbTx-sensitive BK channels. To investigate further the

pharmacology of anoxia-sensitive K^+ currents, the non-specific K^+ channel blocker, TEA, was used.

Figure 5C (left traces) shows that 20 mM TEA reduced substantially the outward current in a cell that was previously identified as anoxia-sensitive. In 9 such cells, 10-20 mM TEA caused a mean suppression of outward current by 95.7 ± 1.4 % of control, as measured during a voltage step from -60 to +30 mV. However, in the presence of 10-20 mM TEA, anoxia had no additional effect on the residual K^+ currents in 8 out of 9 cells tested (e.g. Fig. 5C, middle traces; Fig. 5D). Since the cell shown in Fig. 5C contained both $IKCa_{O_2}$ and IKV_{O_2} components of outward current (not shown), it appears that both components are sensitive to 10-20 mM TEA. Figure 5D also indicates that the remaining outward current seen at more depolarized potentials (>20 mV) is anoxia-insensitive. Since anoxia activates IK_{ATP} in these cells, the data also suggest that IK_{ATP} is TEA sensitive.

O_2-sensitivity in AMC with different types of BK currents

In adult rat adrenal chromaffin cells two types of BK currents have been described. One is a non-inactivating current (BK_s; in ~9% of adult AMC) and the other is a slowly inactivating current (BK_i; in ~75% of adult AMC); the remaining ~15 % of cells express both currents (Solaro *et al.*, 1995). Since hypoxic suppression of outward currents was not observed in all neonatal AMC (~ 80% respond), the question arises whether O_2-chemosensitivity was restricted to a specific population of BK-expressing cells (i.e. BK_i or BK_s). To identify BK_i and BK_s expressing cells, a voltage-clamp protocol reported to

Figure 5. Effects of iberiotoxin (IbTx) and tetraethylammonium (TEA) on anoxia-sensitive currents in neonatal AMC.

A, in normoxic conditions, IbTx (100 nM) suppressed outward current at +30 mV (left traces); upper trace is control record before IbTx. In the presence of IbTx, anoxia still suppressed outward current reversibly, though washout of the effects of IbTx was incomplete (not shown). B, mean current density (± SEM) *vs.* voltage plots for 4 cells, in the presence of IbTx. Symbols are same as in Fig. 1. Anoxia significantly suppressed outward current at all voltage steps between 0 and +50 mV (P<0.05). C, effects of TEA on outward currents. Addition of TEA (20 mM) suppressed ~96% of outward current (left traces; upper dotted trace is control current for step to +30 mV). Anoxia had no *additional* effect on outward current in the presence of TEA (middle traces; only steps to +30 and +50 mV shown). D, mean current density vs voltage plots for a group of 6 cells with similar initial densities; TEA was present throughout. Vertical and horizontal scale bars represent 200 pA and 20 ms, respectively, for both A and C.

A

normoxia   anoxia   normoxia

+ IbTx   + IbTx   + IbTx

B

Current density (pA pF^{-1})

200

100

-40   0   40

Voltage (mV)

C

+ TEA   + TEA   + TEA

D

Current density (pA pF^{-1})

50

25

-40   0   40

Voltage (mV)
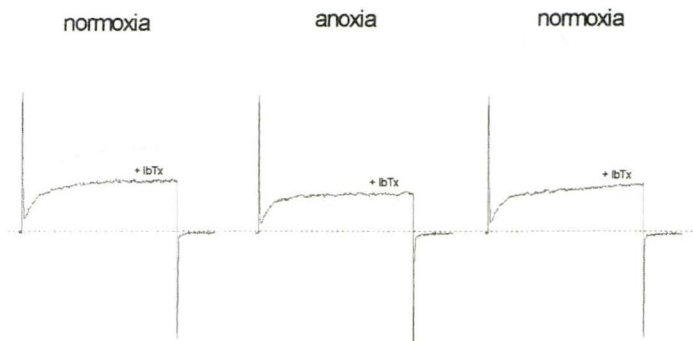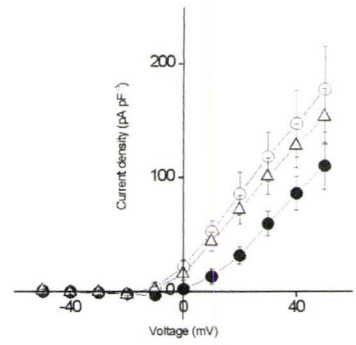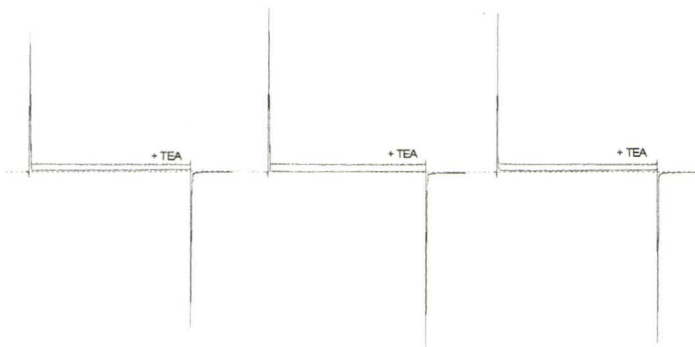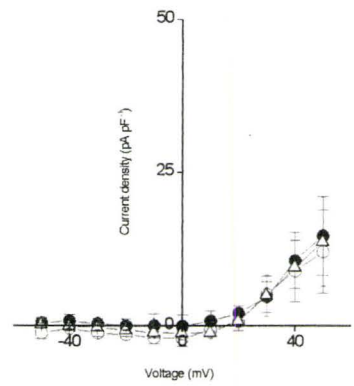
enhance BK currents in these cells, was applied (Solaro *et al.*, 1995). Cells were held at -70 mV and stepped to 0 mV for 50 ms to load them with Ca^{2+}, and then were immediately stepped to +80 mV for 500 ms to identify the type of BK current (see Fig. 6). Out of 17 cells examined, 12 contained predominantly BK_s currents, i.e. they showed no inactivation of outward current during the 500 ms step to +80 mV (e.g. Fig. $6A_1$, upper trace). The remaining 5 cells contained a slowly inactivating component of outward current, presumably due to the presence of BK_i (e.g. Fig. 6Ba, upper trace). It was found that both BK_s (10/12 cells) and BK_i (4/5 cells) containing cells responded to hypoxia with a suppression of outward current (Fig. 6Ab and Bb respectively). These data suggest that O_2-sensitivity can occur in neonatal rat AMC which express either BK_s or BK_i currents.

Do $IKCao_2$ or $IKVo_2$ mediate receptor potential in AMC during anoxia?

We previously reported that neonatal AMC depolarize during hypoxia, and that this depolarization was associated with a conductance *decrease* (Thompson *et al.*, 1997). These observations are consistent with the closure of, e.g. K^+, channels as a general mechanism for hypoxia-induced depolarization in O_2-chemoreceptive cells (Gonzalez *et al.*, 1994). However, given a resting potential in neonatal AMC of ~ -60 mV, it is unclear whether inhibition of the O_2-sensitive currents described above, i.e. $IKCao_2$ and $IKVo_2$, forms the basis of the initial membrane depolarization or receptor potential during hypoxia. To test whether inhibition of $IKCao_2$ and/or $IKVo_2$ may contribute to the initial depolarization, neonatal AMC were exposed to solutions containing Cd^{2+} (200 μM) and/or TEA (20 mM),

Figure 6. Chromaffin cells expressing either sustained or inactivating BK currents are anoxia-sensitive.

A_1 and B_1, protocol used to identify AMC that expressed a sustained BK (A) or inactivating BK (B) current. Cells were initially held at -70 mV and briefly stepped to 0 mV for 50 ms (lower traces), before a final step to +80 mV for 500 ms. Both cells contained outward current that was reversibly suppressed by anoxia as shown in Fig. A_2 (for cell in A_1), and Fig. B_2 (for cell in B_1). Traces shown for voltage step from -60 to +30 mV.

A₁

B₁

400 pA | 500 pA

100 ms

80 mV
0 mV
-70 mV

A₂

B₂

a

350 pA | 400 pA

20 ms

30 mV
-60 mV
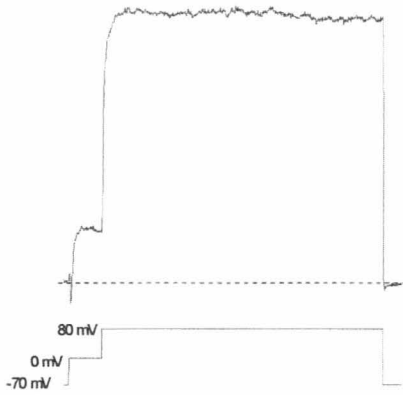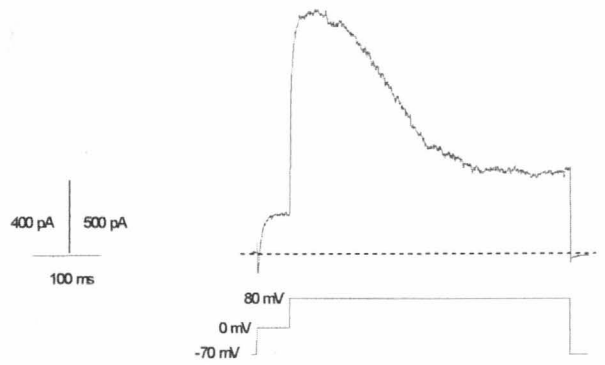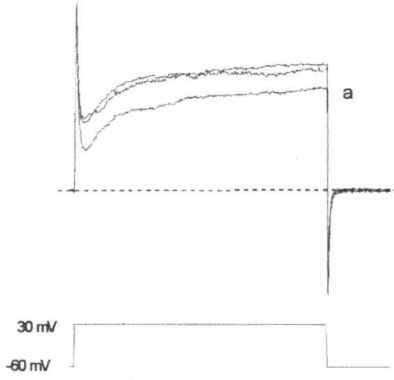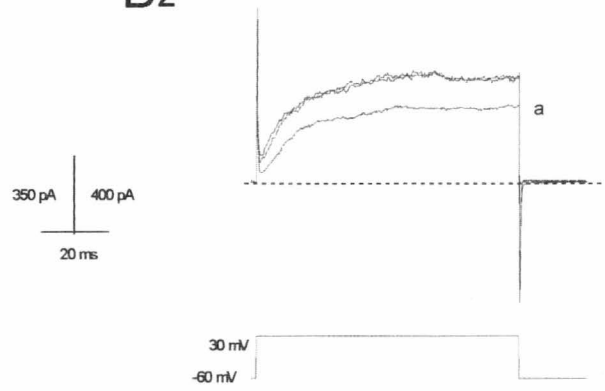
while the membrane potential was monitored using perforated-patch recording in current clamp mode.

As illustrated in Fig. 7A and B (left portion of trace), exposure of neonatal AMC to anoxia caused a significant (and reversible) depolarization from a mean resting potential of -57.6 ± 1.9 mV to -46.3 ± 1.8 mV (n =11; P<0.01). However, subsequent exposure to 200 µM Cd^{2+} had no effect on membrane potential (-58.3 ± 2.6 mV after Cd^{2+}, n =6; see Fig. 7A, right portion of trace), nor did it prevent the anoxia-induced depolarization (mean membrane potential during anoxia in the presence of Cd^{2+} = -49.0 ± 2.5 mV, n =6; difference significant from Cd^{2+} control, P<0.01). Since voltage-dependent Na^+ channels were blocked in these experiments with 0.5 µM TTX, the recorded spike activity in Fig. 7 was likely due to Ca^{2+} entry, and this was abolished in the presence of Cd^{2+} (see Fig. 7A; note spike activity in left but not right portions of the trace). These results suggest that $IKCao_2$ does not contribute significantly to the initial depolarization (or receptor potential) in neonatal AMC during anoxia, nor to the resting membrane potential. Confirmation of this point was obtained using 50 nM charybdotoxin (ChTx), to block the large conductance BK channels that mediate $IKCao_2$. For these experiments ChTx was used (instead of IbTx) since it is a much faster blocker of BK channels (Galvez et al., 1990), and therefore the effects of direct BK channel inhibition could be more easily assessed. In Fig. 7B, 50 nM ChTx failed to depolarize neonatal AMC, and also failed to prevent the anoxia-induced depolarization, even in this cell which had a relatively low initial resting potential (-40 mV). This result was seen in all cells tested (n =3).

In contrast to the above results, the more general K^+ channel blocker, TEA (10-20 mM), depolarized neonatal AMC from -57.6 ± 1.9 mV to -48.1 ± 5.2 mV (n =5; difference significant, P<0.01; see Fig. 7C). However, even in the presence of 20 mM TEA, exposure to anoxia caused a further significant depolarization to -40.8 ± 4.5 mV (P<0.01), and the effect was reversible (Fig. 7C; right portion of trace). Additionally, when TEA and Cd^{2+} were applied together, the membrane depolarized, but the depolarizing effects of anoxia still persisted in the presence of these drugs (n =3; not shown). These data suggest that though some TEA-sensitive K^+ channels are open at rest, they are not responsible for the anoxia-induced depolarization

Blockade of other K^+ channel subtypes with 2 mM 4-AP did not alter resting membrane potential of neonatal AMC (n =4; mean membrane potential was -59.7 ± 6.4 before, and -57.7 ± 5.6 mV after 4-AP). Further, in the presence of 2 mM 4-AP, anoxia still depolarized AMC from -59.7 ± 6.4 to -46.0 ± 5.4 mV (n =4), an effect similar to that seen in the absence of 4-AP, where the membrane potential depolarized to -47.7 ± 6.1 mV (n =4; see Fig. 7D). These observations suggest there is a distinct O_2-sensing mechanism in neonatal AMC that controls at least part of the initial depolarization or receptor potential during anoxia, and that is insensitive to conventional blockers of voltage-dependent K^+ channels.

Does a cationic current or Na/K-ATPase contribute to O_2-sensitivity in rat AMC?

In guinea-pig AMC, concomitant activation of a cationic current and inhibition of a

Na/K-ATPase by hypoxia was recently described and is thought to generate the receptor potential (Inoue *et al.*, 1998). Since during voltage-clamp studies in Cd^{2+}-containing (or Ca^{2+}-free) solutions we often observed a slight enhancement of inward current during hypoxia (e.g. Fig. 2D and 4Db), we wondered whether a similar cationic current, or electrogenic pump may contribute to the receptor potential in rat AMC. To test this possibility we examined the effects of anoxia on AMC under current clamp, while perfusing a Na^{+}/Ca^{2+}-free bathing solution. Interestingly, under these conditions anoxia-sensitive AMC hyperpolarized to -63.1 ± 9.2 mV (n=4) from the control membrane potential of -52.6 ± 6.5 mV (P<0.05; Fig 6E). Since this hyperpolarization was also observed in Na^{+}-free solutions that contained Ca^{2+} (not shown), it appears that a substantial Na^{+} leak current contributes to the resting membrane potential of AMC. Application of an anoxic stimulus in the presence of a Na^{+}/Ca^{2+}-free bathing solution revealed that AMC depolarized from -63.1 ± 9.2 to -51.6 ± 9.4 mV (n = 4; Fig. 7E). Thus, the anoxia-induced depolarization was reduced, but not abolished, in the absence of extracellular Na^{+} and Ca^{2+}. The mean depolarization in the control solution was 24.2 ± 2.6 mV (n=4), compared to 11.5 ± 2.5 mV for the *same* cells studied in the absence of external Na^{+} and Ca^{2+} (e.g. Fig. 7E; P<0.01).

To investigate the possibility that inhibition of an electrogenic Na/K-ATPase contributes to generation of the receptor potential we used 100 µM strophanthidin, an inhibitor of p-type ATPases. In three cells that were identified as O_2-sensitive (Fig 8A), strophanthidin did not affect resting membrane potential (Fig. 8B); mean resting potential was −49.5 ± 4.3 mV before, and −47.7 ± 3.8 mV after strophanthidin. Anoxia reversibly

depolarized these cells by 21.8 ± 1.4 mV (n=3; P<0.05 from control) and the magnitude was unchanged in the presence of strophanthidin (Fig. 8C), where the receptor potential was 19.3 $\pm$ 2.0 mV (n=3; P>0.2). This suggests that hypoxic inhibition of an electrogenic Na/K-ATPase does not contribute significantly to generation of the receptor potential in neonatal AMC.

Activation of K_{ATP} attenuates the anoxia-induced depolarization

We also investigated whether K_{ATP} channels were active at the resting potential of O_2-sensitive AMC, and could therefore influence the magnitude of the receptor potential. Perfusion with extracellular solution containing the K_{ATP} channel blocker, glibenclamide (50 μM), had no significant effect (P> 0.2) on membrane potential (Fig. 7F); the mean resting potential was -52.6 ± 3.2 mV before, and -54.0 ± 3.5 mV after glibenclamide for a group of 11 cells that were O_2-sensitive. Thus, K_{ATP} channels do not appear to contribute significantly to the resting potential of neonatal AMC during normoxia.

To determine if activation of IK_{ATP} by anoxia (see above) functions to attenuate the receptor potential, the anoxia-induced depolarization was compared in the presence and absence of glibenclamide (50 μM). In the absence of glibenclamide, AMC depolarized by an average of 16.6 ± 2.5 mV (n=11) during anoxia. However, this depolarization was significantly (P<0.01) enhanced when anoxia was applied in the presence of glibenclamide (mean = 23.3 ± 3.1 mV; n=11; e.g. Fig. 7F). Since IK_{ATP} also appears to be TEA-sensitive (see above), it was surprising that the anoxia-induced depolarization was not similarly

enhanced in the presence of TEA. Although the reasons for this are unclear, the two drugs block IK_{ATP} via different mechanisms, and unlike TEA, glibenclamide had no effect on resting membrane potential (compare Fig 7C to 7F). These data suggest that although IK_{ATP} does not appear to contribute to the resting potential of AMC during normoxia, its activation by anoxia may serve to reduce the magnitude of the receptor potential.

Figure 7. Effects of anoxia and manipulation of the extracellular fluid on membrane potential of neonatal AMC.

Recordings under current clamp were obtained in the continuous presence of TTX (0.5-1 µM). A, anoxia depolarized AMC, though addition of Cd^{2+} alone did not; further, Cd^{2+} did not prevent the anoxia-induced depolarization, but abolished spike activity (compare right with left portions of trace). B, direct blockade of BK currents with 50 nM ChTx did not significantly alter membrane potential, nor prevent the anoxia-induced depolarization (compare left and right portions of trace). C, addition of TEA (20 mM) caused a slight membrane depolarization (right portion of trace), but did not block the anoxia-induced depolarization. D, addition of 4-AP did not depolarize nor prevent anoxia-induced depolarization of neonatal AMC. E, effects of perfusion with a Na^+/Ca^{2+}-free (NMDG was substituted for Na^+; Ca^{2+} was replaced with 2 mM Mg^{2+} and 1 mM EGTA). Exposure to a Na^+/Ca^{2+}-free bathing solution hyperpolarized AMC and reduced, but did not block, the anoxia-induced depolarization. F, blockade of K_{ATP} channels with 50 µM glibenclamide did not affect resting membrane potential, nor did it prevent the anoxia-induced depolarization. However, in the presence of glibenclamide the anoxia-induced depolarization was significantly ($P<0.05$) enhanced. Vertical scale bars represent 20 mV in A-E and 15 mV in F; horizontal bar represents 25 s.

A

-60 mV

anoxia

anoxia
200 µM Cd²⁺

B

-40 mV

anoxia

anoxia
50 nM ChTx

C

-57 mV

anoxia

20 mM TEA

anoxia

D

-63 mV

anoxia

anoxia
2 mM 4-AP

E

-65 mV

anoxia

anoxia
Na⁺ / Ca²⁺-free

F

-43 mV

anoxia

anoxia
50 µM glibenclamide
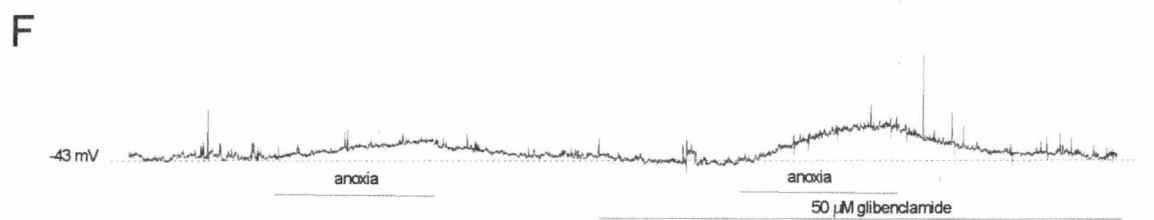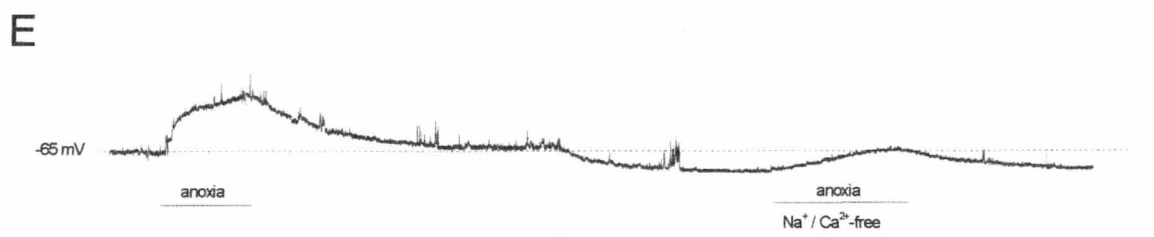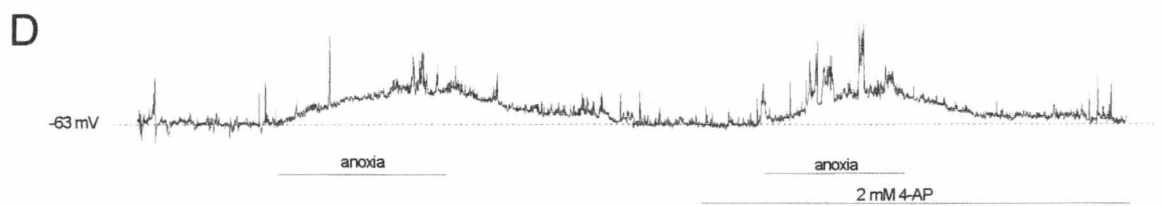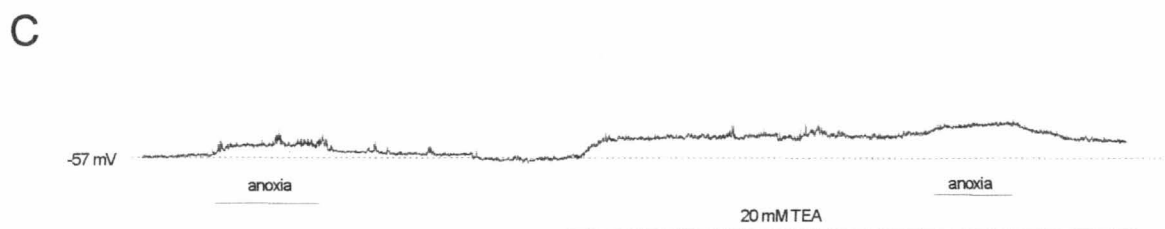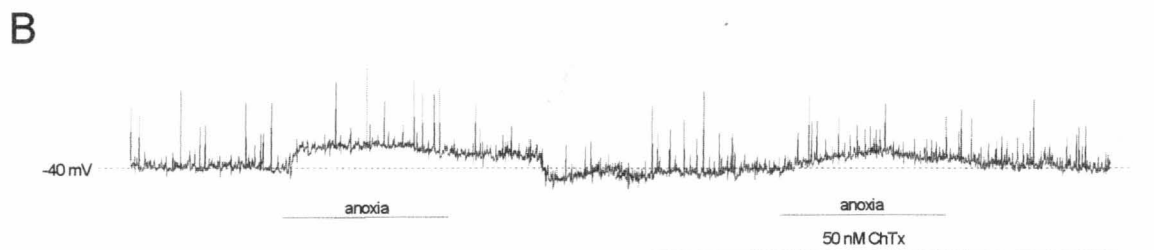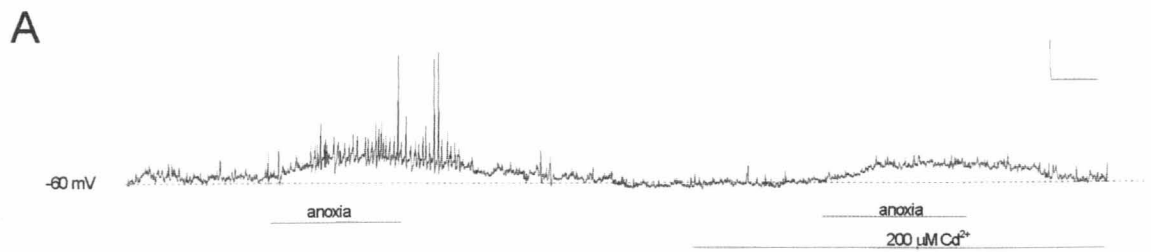
Figure 8. Effects of strophanthidin on membrane potential and hypoxia-induced depolarization in neonatal rat AMC.

All current clamp records were collected in zero current (I=0) mode. In A, anoxia reversibly depolarized this neonatal AMC. B, effects of 100 μM strophanthidin (an inhibitor of the Na/K-ATPase) on the resting membrane potential of the cell in A. Note that this did not affect the resting membrane potential, suggesting that p-type electrogenic pumps make a minimal contribution to the resting membrane potential in neonatal AMC. C, the anoxia-induced depolarization persists in the presence of strophanthidin, indicating that inhibition of electrogenic pumps does not significantly contribute to the generation of the receptor potential.

A

-55 mV

anoxia

20 mV

25 sec

B

-55 mV

100 μM strophanthidin

C

-55 mV

anoxia

100 μM strophanthidin
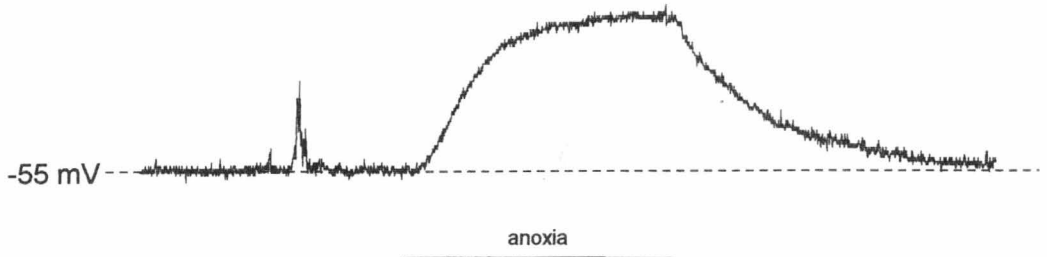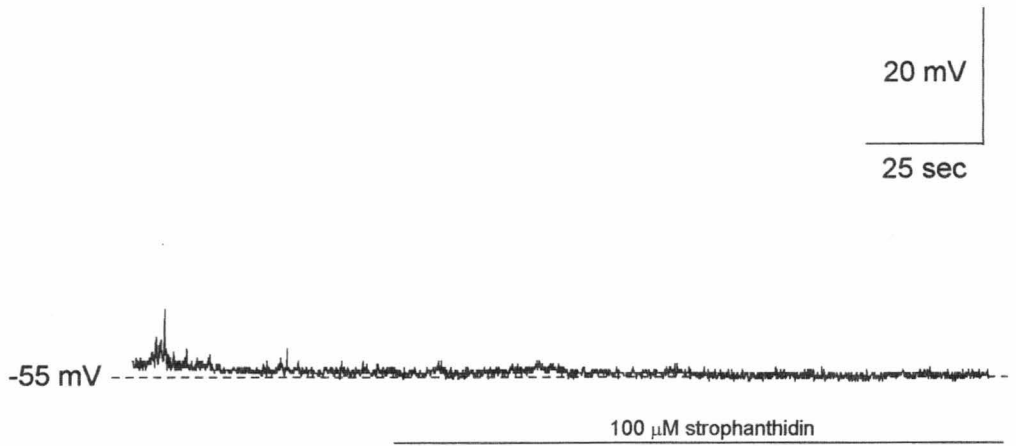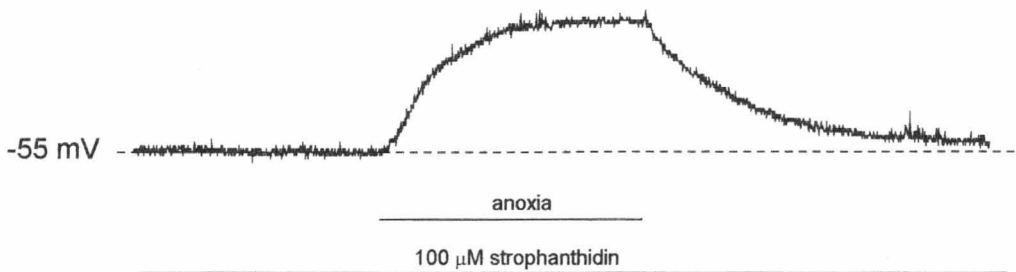
Discussion

The goal of the present study was to investigate the type(s) of voltage- activated K^+ currents that mediate O_2-chemosensitivity in neonatal rat adrenal chromaffin cells (AMC), and to determine whether these currents also contribute to the genesis of the hypoxia-induced depolarization or receptor potential (see Thompson *et al.*, 1997). These hypoxia-sensing mechanisms appear to mediate the vital catecholamine surge that enables the neonate to survive hypoxic stress, associated with the transition to extrauterine life (Seidler & Slotkin, 1985; Slotkin & Seidler, 1988; Thompson *et al.*, 1997). Our results from voltage-clamp studies indicated that the suppression of voltage-dependent outward K^+ current by anoxia is the net result of the differential modulation of several K^+ currents and comprises: i) anoxic suppression of the large conductance Ca^{2+}-dependent K^+ current, $IKCao_2$; ii) anoxic suppression of a Ca^{2+}-independent K^+ current, $IKVo_2$; and iii) anoxic *activation* of a glibenclamide-sensitive K^+ current, IK_{ATP}. Additionally, results from current clamp recordings indicated that alternative mechanisms to these voltage-dependent and anoxia-sensitive K^+ currents must be invoked to account for the genesis of the receptor potential, seen during exposure of neonatal rat AMC to anoxia.

Anoxic suppression of the outward current in neonatal AMC results primarily from the inhibition of large conductance, Ca^{2+}-dependent K^+ channels, i.e. BK or maxi-K

channels, and referred to as $IKCao_2$ in this study. Though we cannot formally rule out an indirect effect due to anoxic suppression of Ca^{2+} currents (see Lopez-Barneo, 1996), in preliminary studies there was no consistent effect of anoxia on Ca^{2+} currents (Thompson & Nurse, unpublished observations), and we previously showed that entry of extracellular calcium and catecholamine secretion was enhanced in these cells by hypoxia (Thompson et $al.$, 1997). When BK currents were eliminated, by using Ca^{2+}-free solutions, or by the addition of either Cd^{2+} or iberiotoxin (IbTx), a smaller Ca^{2+}-independent component ($IKVo_2$) amounting to ~35% of the total anoxia-sensitive outward current (IKo_2), persisted. Since TEA (10-20 mM) abolished almost all of the outward current, and anoxia had negligible effect on the residual currents when TEA was present, it appears that both $IKCao_2$ and $IKVo_2$ are TEA sensitive. It is noteworthy that in PC 12 cells, a cell line with an adrenomedullary chromaffin cell origin, hypoxia suppresses a Ca^{2+}-independent and TEA-sensitive outward current (Zhu et $al.$, 1997), raising the possibility that it is similar to $IKVo_2$ investigated in the present study. In contrast, however, hypoxia was reported to $stimulate$ large conductance, Ca^{2+} dependent K^+ channels in PC 12 cells, though the pharmacology of this current was not reported (Conforti & Millhorn, 1997). It is possible that this anoxia-activated current is similar to IK_{ATP} described here (see below), and in central neurons (Haddad & Jiang, 1997).

Anoxic activation of K_{ATP} currents

In addition to $IKCao_2$ and $IKVo_2$, we observed a third voltage dependent, Ca^{2+}-sensitive K^+ current, IK_{ATP}, which was regulated by Po_2. The presence of this current was

inferred from experiments where the total outward current was enhanced by pinacidil (100 $\square$M), a K_{ATP} activator, and where the anoxic suppression of outward current was augmented by glibenclamide (50 $\square$M), a K_{ATP} blocker (see Ashcroft & Ashcroft, 1990). Unlike the suppressive effects of anoxia on the other two currents, IK_{ATP} was *activated* by anoxia in these cells, suggesting more K_{ATP} channels became available or were opened at low Po_2. Since this augmentation of K_{ATP} by anoxia was absent in a Cd^{2+}- or TEA-containing bathing solutions (but persisted in the presence of the BK channel blocker, ChTx; not shown), it appears that IK_{ATP} is both Ca^{2+} and TEA sensitive. Similar results have been reported for O_2-regulated K_{ATP} channels described in central neurons (Jiang *et al.*, 1994; Haddad & Jiang, 1997). Taken together, these results support the conclusion that anoxia augments K_{ATP} channels, but attenuates both Ca^{2+}-dependent ($IKCao_2$) and delayed rectifier type ($IKVo_2$) K^+ currents in neonatal AMC.

Interestingly, the augmentation of K_{ATP} by anoxia observed in this study is in contrast with a recent suggestion that hypoxia inhibits K_{ATP} currents in adult rat chromaffin cells (Mochizuki-Oda *et al.*, 1997). This interpretation was based on the finding that cromakalim, an activator of K_{ATP} currents, prevented the hypoxia-induced rise in intracellular Ca^{2+}; however, a direct inhibitory effect of hypoxia on K_{ATP} currents was not demonstrated. It is also noteworthy that Mochizuki-Oda *et al.* (1997) observed hypoxic chemosensitivity in adult rat chromaffin cells, whereas we did not (Thompson *et al.*, 1997; see also, Mojet *et al.*, 1997). It is possible that use of longer term cultures (up to 7 days) by Mochizuki-Oda *et al.* (1997), and resulting longer period of denervation in vitro, resulted in recovery of hypoxic

sensing in these cells (see Slotkin & Seidler, 1988).

Possible functional role of anoxic modulation of K^+ currents in neonatal AMC

In the present study, inhibition of Ca^{2+}-dependent K^+ (BK) channels was the major cause of the anoxic suppression of outward current in neonatal AMC. Similar BK channels are thought to participate in hypoxic chemosensitivity in rat carotid body type 1 cells (Wyatt & Peers, 1995; Jackson & Nurse, 1997), and are generally accepted to play important roles in action potential repolarization (Pancrazio *et al.*, 1994), and in the ability of adult rat AMC to fire repetitive action potentials (Solaro *et al.*, 1995). Thus, hypoxic inhibition of $IKCao_2$ may result in broadening of the action potential, leading to the observed rise in intracellular Ca^{2+} and catecholamine release (Thompson *et al.*, 1997; see also Mojet *et al.*, 1997). Additionaly, hypoxic inhibition of the delayed rectifier-type K^+ current, $IKVo_2$, may also contribute to action potential broadening.

On the other hand, anoxia was found to *activate* a Ca^{2+}- and glibenclamide-sensitive, K_{ATP} current in neonatal AMC? This activation tended to counteract or blunt the depolarizing effects of anoxia. Interestingly, in catecholaminergic neurons of the substantia nigra, hypoxic-activation of Ca^{2+}- and glibenclamide-sensitive K_{ATP} channels leads to membrane hyperpolarization, which is presumed to serve a protective role during metabolic stress associated with hypoxia and ischaemia (Jiang *et al.*, 1994, Haddad & Jiang, 1997). Conceivably, hypoxia-sensitive K_{ATP} channels in AMC may play a similar role during periods of prolonged neonatal hypoxia, e.g. during birth or repetitive apnoeic events.

Activation of K_{ATP} channels by the concomitant fall in Po_2, and ATP, and the increase in intracellular Ca^{2+} could limit membrane depolarization and prevent CA depletion from AMC, allowing them to maintain an influence on respiratory and cardiovascular physiology during subsequent hypoxic events (see Seidler & Slotkin, 1985, Slotkin & Seidler, 1988).

Origin of the receptor potential

In this study blockers of voltage-dependent, O_2-sensitive currents did not prevent the anoxia-induced depolarization in neonatal AMC. For example, direct inhibition of BK currents by charybdotoxin (50 nM) did not induce depolarization of neonatal AMC, suggesting that most of these channels are closed at the cell's resting potential (~-58 mV). Further, the presence of the relatively non-specific K^+ channel blocker, TEA, which blocked all anoxia-sensitive K^+ channels in voltage clamp studies, also failed to prevent the anoxia-induced depolarization. However, TEA itself caused a slight depolarization, possibly due to closure of K^+ channels that were open at rest.

During exposure of AMC to anoxia, an apparent activation of a small inward current was frequently observed in voltage clamp studies when most of the outward current was blocked (e.g. Fig. 2D). This current was not studied in detail and its origin remains uncertain. On the one hand, it may result simply from inhibition of the residual outward current; alternatively, it may be due to activation of a cationic current, perhaps similar to the one recently described in hypoxia-sensitive guinea-pig AMC (Inoue *et al.*, 1998). In the present

study, the anoxia-induced depolarization of rat AMC persisted in the absence of extracellular Na^+ and Ca^{2+}, though the magnitude of the depolarization was decreased. Thus, activation of an inward cationic current by anoxia does not appear to be the major mechanism underlying the receptor potential. Furthermore, these experiments suggest that the genesis of the receptor potential does not arise from the inhibition of a Na/K-ATPase, since under Na^+-free conditions this electrogenic pump is likely to be inactive. Indeed, this was confirmed using strophanthidin, (an inhibitor of p-type ATPases), which did not depolarize AMC nor affect the magnitude of the receptor potential.

In summary, it appears that chromaffin cells have evolved complex mechanisms for sensing O_2 and regulating catecholamine secretion in the perinatal period. These mechanisms involve the differential modulation of several K^+ channel subtypes. Additional work, aided by single channel analysis, is required to elucidate the molecular mechanisms by which these channels are regulated by low Po_2, and the basis of the hypoxia-induced depolarization or receptor potential.

Chapter 3

Oxygen-chemosensitivity in developing adrenal chromaffin cells: Comparison between wild type and NADPH oxidase deficient mice.

The work in this chapter is in preparation for submission to the *American Journal of Physiology*.

I was responsible for all electrophysiology, which comprises figures 1-4 in the text. Suzanne Farragher was responsible for the HPLC experiments.

Summary

Catecholamine (CA) release from adrenal chromaffin cells (AMC) in mammals plays a vital role in the adaptability of the neonate to extrauterine life by mediating appropriate cardiovascular and respiratory adjustments during periods of hypoxia or low Po_2. The identity of the primary pO_2 detector in AMC is however, unknown. We compared AMC from wild type and transgenic mice lacking the gp91[phox] subunit of NADPH oxidase. To determine whether the putative O_2-sensor protein (NADPH oxidase) is the O_2 sensor hypoxia-induced suppression of outward K^+ current, membrane depolarization, and stimulation of CA secretion (determined by HPLC) were taken as indicators of O_2-chemosensitivity. Hypoxia (pO_2 ~5mmHg) caused reversible inhibition of outward K^+ current by ~27% (n=6) in wild type (WT) and ~29% (n=9) in oxidase deficient (OD) AMC from newborn (P1-P5) mice. Pharmacological tests revealed two O_2-sensitive K^+ currents in both WT and OD cells, i.e., large conductance Ca^{2+}-dependent K^+ current (I_{BK}) and delayed rectifier-like K^+ current (I_{KV}). Additionally, hypoxia depolarized WT and OD cells to a similar degree and reversibly broadened the action potential. Exposure of neonatal AMC cultures to hypoxia ($5\%O_2$) for 1 hr stimulated CA release (~3 to 4 x normoxia) in both WT and OD cultures as determined by HPLC. Interestingly, roughly equal proportions of norepinephrine (NE) and epinephrine (EPI) were released under all conditions. In contrast, hypoxia had no effect on voltage dependent K^+ currents, membrane potential or CA release in AMC derived from juvenile (P14-P15) mice. However, hypoxic sensitivity was re-established after juvenile AMC were cultured for > 3 days. We conclude that NADPH oxidase is *not* the

oxygen sensor in newborn AMC and that in mice these cells possess a developmentally

regulated O_2-sensing mechanism, similar to that previously described in rat.

.

Introduction

During the perinatal period, adrenal medulla chromaffin cells (AMC) possess an O_2-sensing mechanism which occurs in the absence of mature sympathetic innervation (Slotkin and Seidler, 1986). During postnatal maturation, this 'non-neurogenic' mechanism is lost along a time course similar to the development of sympathetic innervation to the adrenal gland (Seidler and Slotkin, 1985, 1988). Physiological responses to hypoxia in neonatal rat AMC result in increased catecholamine (CA) secretion, primarily epinephrine, into the circulation. This CA release is vital for the animal's transition to extrauterine life since it promotes lung maturation and protects the fetal heart rate (Seidler and Slotkin, 1985; Slotkin and Seidler, 1988).

The mechanisms underlying the non-neurogenic response of AMC to hypoxia are not completely understood. Presently it is thought that hypoxia-induced inhibition of K^+ channels and membrane depolarization lead to CA secretion (Thompson and Nurse, 1998; see however, Mojet et al., 1997). The "membrane model" of O_2-chemoreception predicts that regulation of K^+ channels by hypoxia is indirect and is mediated through a membrane bound O_2-sensor protein (Lopez-Barneo, 1996). One candidate for the O_2-sensor is the NADPH oxidase enzyme complex similar to the burst oxidase found in phagocytic cells (Cross et al, 1990). This NADPH oxidase is a five-subunit enzyme complex that transfers electrons from NADPH to molecular oxygen, producing superoxides (O_2^-), which are thought to be a key source of microbicidal oxidants in the immune response (De Leo and Quinn, 1996). There is strong evidence indicating that the

gp91^{phox} subunit of the NADPH oxidase complex is the heme-containing subunit (Yu et al, 1998). According to the membrane model of O_2-chemoreception, decreased O_2 availability to the gp91^{phox} subunit during hypoxia results in reduced production of reactive oxygen species (ROS; e.g. H_2O_2), which signal modulation of O_2-sensitive K^+ channels (Wang et al., 1998; Fu et al, 2000). Hypoxia-induced K^+ channel closure and membrane depolarization, possibly mediated through the fall in ROS, is then thought to activate voltage-dependent Ca^{2+} channels, Ca^{2+} entry and CA secretion.

In this study we tested the possibility NADPH oxidase is the primary O_2-sensor in neonatal chromaffin cells using a transgenic approach. Excellent evidence exists indicating a role for the oxidase in O_2-chemosensitivy of airway neuroepithelial bodies (NEBs), since the NEBs of transgenic mice (deficient in gp91^{phox}) are unresponsive to hypoxia, in contrast to their wild type (WT) counterparts (Fu et al, 2000). Other studies on endothelial cells (Zulueta et al, 1997) and pulmonary artery myocytes (Archer, 1999) of the gp91^{phox} knockout mouse suggest that the NADPH oxidase is not the primary O_2-sensor in all O_2-chemosensitive cells. In addition, diphenylene iodonium (DPI), a flavoprotein inhibitor that blocks the NADPH oxidase, was ineffective in stimulating rat carotid body glomus cells, suggesting that the oxidase was not the primary O_2-sensor in these well-studied arterial chemoreceptors (Obesso et al, 1999). Taken together, these data suggest that the NADPH oxidase may function as the primary O_2-sensor in specific cell types. Thus, it was of interest to determine whether O_2-chemosensitivity was present in developing WT mouse chromaffin cells and if so, whether it was retained in gp91^{phox} deficient mice.

We therefore used cultures of AMC from neonatal and juvenile WT and oxidase deficient (OD) mice to test for the development of O_2-chemoreceptor function. AMC were assayed for O_2-chemosensitivity using perforated patch clamp whole cell recordings of K^+ current and membrane potential. Additionally, HPLC was used to quantify catecholamine (CA) release from wild type and transgenic AMC. Here we report that neonatal cells from both WT and OD mice are O_2-chemosensitive, indicating that the NADPH oxidase is not the primary O_2-sensor in adrenal chromaffin cells. Further, we show that this property is lost with postnatal maturation, as previously reported for rat chromaffin cells (Thompson et al., 1997; Mojet et al., 1997).

Materials and Methods

Cell culture

Primary cultures of mouse AMC were prepared as previously described for the rat (Thompson et al, 1997). Briefly, adrenal glands were dissected from postnatal day (P) 1-5 (neonatal) and P14-19 (juvenile) day old mice, and trimmed of most of the outer cortex. The tissue was incubated in an enzymatic solution containing 0.1% trypsin, 0.1% collagenase, and 0.01% deoxyribonuclease for 60 to 80 minutes at 37°C. Most of the enzyme was removed, and the remainder was inactivated by addition of growth medium consisting of F-12 nutrient medium (GIBCO) supplemented with 10% fetal calf serum, 80 U 1-1 insulin (Sigma), 0.6% glucose, 1% penicillin and streptomycin, 2mM glutamine and 0.01% dexamethasone. The tissue was then mechanically teased and triturated, producing a cell suspension that was preplated for 24hr on collagen-coated 35 mm culture dishes to remove most of the cortical cells. The supernatant, enriched in chromaffin cells, was then plated on the centre well of Matrigel-coated Nunclon dishes. Cells were grown at 37°C in a humidified atmosphere of 95% air-5% CO_2 for 1-6 days before they were used in patch-clamp experiments, or for determination of CA release using HPLC.

Electrophysiology

All voltage clamp data were obtained at room temperature (21-23 °C) using the Nystatin perforated-patch configuration of the patch clamp technique. Seal resistance ranged from 2-10 GΩ and most (~75%) of the series resistance was compensated.

Junction potentials, typically 2-5 mV, were cancelled prior to seal formation. The pipette solution consisted of (mM) potassium gluconate, 95; KCl, 35; NaCl, 5; CaCl$_2$, 2; HEPES, 10; and Nystatin (300-450 µg/ml) adjusted to pH 7.2 with KOH. The standard bathing solution consisted of (mM) NaCl, 135; KCl, 5; CaCl$_2$, 2; MgCl$_2$, 2; HEPES, 10; glucose, 10; adjusted to pH 7.4 with NaOH and 0.5 µM tetrodotoxin (TTX; Sigma). TTX was omitted during some current clamp experiments in order to investigate the effects of hypoxia on action potential duration.

All recordings were obtained with an Axopatch 1-D patch clamp amplifier equipped with a 500 MΩ head stage feedback resistor (Axon Instruments). Records were lowpass filtered at 2kHz and digitized at 10kHz using a Digidata 1200 A-D converter and pClamp software versions 6.0.3 or 8.0 (Axon). The holding potential was set at –60 mV and current responses to four consecutive 80 msec depolarizations (10 mV steps; range – 100 to +50 mV) were averaged on-line and stored on a personal computer. The magnitude of outward currents was measured at 40 msec for comparison between control (normoxia; 2mM bathing Ca^{2+}) and stimulus-evoked (hypoxia and/or 200 µM CdCl$_2$) responses. Whole cell capacitance was determined by integrating the capacitative transient elicited by a voltage-step to –100 mV, then dividing the resulting charge by the magnitude of the step. Current density (pA/pF) was calculated for each cell by dividing the steady-state current (at 40 msec) by the cell capacitance. Data were compared using the paired Student's t test, with the significance level set at $P < 0.05$. All data are presented as mean ± standard error of the mean.

Hypoxia was generated by bubbling 100% N_2 into 150 ml of standard bathing solution for 1-1.5 hours. Measurement of Po_2 in the recording chamber was periodically carried out with a 25 μm Clark-style O_2 microelectrode (Diamond General Electro-Tech Inc., Ann Arbor, MI) and yielded a bath Po_2 of ~ 150 mmHg during normoxia and ~ 5 mmHg during hypoxia. Solutions were exchanged by perfusion under gravity and removal by suction at a rate of ~ 4 ml/min.

Catecholamine determination by HPLC

Norepinephrine (NE), epinephrine (EPI) and dopamine (DA) release from living cells were analyzed by high performance liquid chromatography (HPLC) using a Waters model 510 pump with a 5 μm Spherisorb analytical column (Waters) and an electrochemical detector (Coulochem II detector, model 5200; ESA Inc., Bedford, MA). Detection of CA was made at a potential of –350 mV versus the Ag/AgCl reference electrode. Flow rate was set at 1.0 ml/min at approximately 1800 psi. Using NE, EPI, and DA standards and using the peak area ratio method, the amount of CA was quantitatively determined by integration of the area under the peaks. In addition, an internal standard 3,4-dihydroxybenzylamine hydrobromide (DHBA, Sigma), was added to each sample to correct for variation in injection volume. The mobile phase consisted of $Na_2H_2PO_4$ (6.9 g/L; Sigma), Na_2EDTA (80 g/L; BDH Chemicals, Toronto, Can.), distilled H_2O and 5% MeOH; adjusted to a pH of 3.5 with concentrated H_2PO_4.

The release experiments began with a quick rinse of the cultures with Dulbecco's modified Eagle's medium/F12 or DMEM/F12 (50:50; Gibco), supplemented with 5%

glucose. A basal release sample (20% O_2) or a hypoxia-induced release sample (5% O_2) was collected after one hour incubation in 105 µl bicarbonate-buffered salt solution (BBSS) in a 5% CO_2 atmosphere. The BBSS consisted of (in mM): 116 NaCl; 5 KCl; 24 $NaHCO_3$; 2 $CaCl_2$; 1.1 $MgCl_2$; 10 HEPES; 5.5 glucose; at pH 7.4. BBSS containing high extracellular K^+ (30 mM K^+) was prepared by equimolar replacement of NaCl with KCl. Release samples were mixed 1:1 with 1M $HClO_4$ containing 2.7 mM Na_2EDTA and stored at $-80^{\circ}C$ until HPLC analysis (typically performed within 1 week).

Immunofluorescence

After collection of the release sample, chromaffin cells were identified and the number of cells in each culture dish were determined by immunocytochemistry for an antibody against tyrosine hydroxylase (TH). The procedure has been previously reported (Thompson et al., 1997).

RESULTS

Hypoxia suppresses Ca^{2+}-dependent and independent components of outward current in neonatal wild type and NADPH oxidase deficient AMC

In order to determine whether wild type (WT) AMC from the neonatal mouse are O_2-chemosensitive, we first carried out voltage clamp studies. This provided the basis for comparison of NADPH oxidase deficient (OD) cells from transgenic mice lacking the $gp91^{phox}$ subunit. Figure 1 shows the effects of hypoxia on outward currents and current density-voltage (I-V) relationships in WT (Fig. 1A and C) and OD (Fig. 1B and D) cells in culture for 1-5 days. Exposure to hypoxia ($Po_2 \sim 5$ mmHg) reduced outward current density in wild type AMC from the normoxic ($Po_2 \sim 150$ mmHg) value of 107.83 ± 22.5 pA/pF to 81.0 ± 21.44 pA/pF (n=6; $p<0.05$); the control response recovered to 106.0 ± 18.5 pA/pF followin reperfusion with a normoxic solution. Similarly, hypoxia suppressed outward current density in AMC from OD neonatal mice from the normoxic value of 90.4 ± 17.4 pA/pF (not significantly different from WT mice during normoxia) to 66.0 ± 14.5 pA/pF (n=9; $p<0.01$) and the effect was reversible (89.9 ± 21.2 pA/pF) after return to normoxia. Thus, hypoxia inhibited outward currents to a similar extent in WT (27.2 ± 0.09 %) and OD (29.6 ± 0.04 %) mice, suggesting that a mechanism for O_2-sensing is present in the mouse AMC and NADPH oxidase is not the O_2-sensor.

We previously showed that neonatal rat AMC express two K^+ currents that are inhibited by hypoxia, i.e., a large-conductance Ca^{2+}-dependent K^+ current (I_{BK}) and a

Fig. 1. Hypoxia suppresses outward current in neonatal wild type and oxidase deficient mouse AMC.

All current traces are shown for the voltage step to +30 mV from the holding potential of −60 mV. A, effects of hypoxia on outward current (top panel) and current density *vs.* voltage plots (lower panel) recorded from wild type mouse AMC in culture for 1-5 days. Note that hypoxia (h) suppresses outward current from the control (c) value, and the effects are reversible (r). Lower panel in A is a current-density *vs.* voltage plot for a group of 7 cells exposed to normoxia (open triangles), hypoxia (open circles) and then normoxia again (closed squares). B, effects of hypoxia on outward current (top panel) and current density *vs.* voltage relationship recorded from neonatal transgenic mouse AMC. Symbols are as in A. Hypoxia reversibly inhibits outward currents at voltages where currents are activated (step to +30 mV is shown in the top panel).

A   B
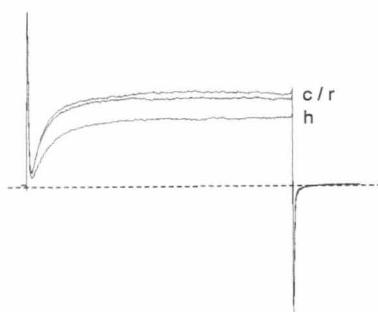
control   transgenic
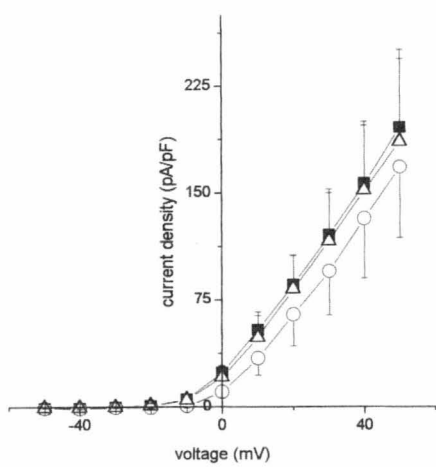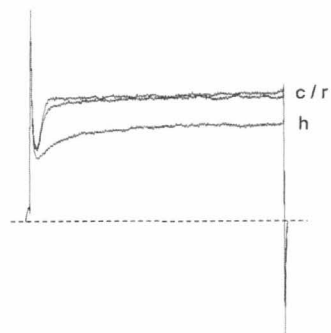
delayed rectifier-like K^+ current (IK_V; Thompson and Nurse, 1998). To determine whether these K^+ currents played a similar role in hypoxic sensitivity of mouse AMC, the non-specific Ca^{2+} channel blocker, cadmium (Cd^{2+}; 200 μM) was used to block Ca^{2+} entry and indirectly, I_{BK}. Figure 2 shows the effects of $Cd^{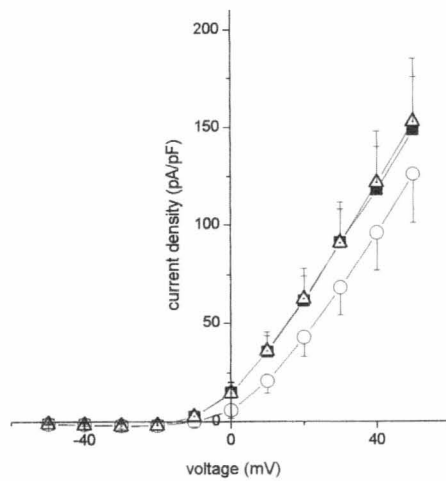2+}$, and hypoxia plus Cd^{2+}, on outward currents (step to +30 mV) and I-V plots from WT and OD chromaffin cells. Outward currents were suppressed in WT cells from 116.5 ± 25.4 pA/pF to 62.0 ± 7.5 pA/pF (n=5; p<0.05) in the presence of Cd^{2+}. However, hypoxia caused a further inhibition of the current in presence of Cd^{2+} to 49.1 ± 4.3 pA/pF (Fig. 2A C; n=5; p<0.05). Thus, the total O_2-sensitive outward current density (IKo_2), estimated from different current measurements, was reduced from 25.9 ± 9.0 pA/pF (n=6) without Cd^{2+} to 10.7 ± 4.2 pA/pF (n=5) in the presence of Cd^{2+}, indicating that both I_{BK} and IK_V are present in WT cells and are O_2-sensitive.

The effects of Cd^{2+}, and hypoxia plus Cd^{2+}, on outward current of OD cells is shown in Figs. 2B and D. The outward current (at +30 mV) was reduced from 106.8 ± 26.5 pA/pF to 40.4 ± 8.2 pA/pF (n=5; p<0.05) by 200 μM Cd^{2+}. Hypoxia caused a further significant suppression of this Ca^{2+}-*independent* outward current to 32.2 ± 6.5 pA/pF (n=5; p<0.05). Thus, similar to neonatal WT cells, 200 μM Cd^{2+} reduced IKo_2 in the OD cells from 26.9 ± 8.2 pA/pF to 7.6 ± 2.4 pA/pF (n=5; p<0.05). Taken together, these data suggest that both I_{BK} and IK_V are present and inhibited by hypoxia in both the WT and OD chromaffin cells from neonatal mice.

Fig. 2. Neonatal wild type and oxidase deficient chromaffin cells express Ca^{2+}-independent, hypoxia-sensitive outward currents.

A, extracellular Cd^{2+} (200 μM) suppresses outward current (+Cd/c), indicating the presence of Ca^{2+}-dependent K^+ currents in mouse AMC. Exposure to hypoxia in the presence of Cd^{2+} (+Cd/h) causes a further suppression of outward current, and the effects of hypoxia are reversible (+Cd/r). Lower panel in A is a current density *vs.* voltage plot for a group of 7 cells, note that a portion of the O_2-sensitive outward current persists in the absence of Ca^{2+}-dependent K^+ current at all voltages where currents are activated. B, effects of Cd^{2+} (+Cd/c) and hypoxia in the presence of Cd^{2+} (+Cd/h) on outward currents recorded from a neonatal transgenic AMC. Note that the effects of hypoxia are reversible (+Cd/r). Lower panel in B is a current density *vs.* voltage plot for a group of 7 transgenic AMC in the presence of Cd^{2+}. Hypoxia reversibly inhibits outward current at all test potentials, indicating the presence of O_2-sensitive Ca^{2+}-independent K^+ current in transgenic AMC. Symbols are the same as in Fig. 1. and all voltage steps in the top panels are to +30 mV from a –60 mV holding potential.

A   control

c

+ Cd / c,r

+ Cd / h

B   transgenic

c

+ Cd / c,r
+ Cd / h

400 pA

10 ms

current density (pA/pF)

150

100

50

-40   0   40

voltage (mV)

current density (pA/pF)

100

75

50

25

-40   0   40

voltage (mV)
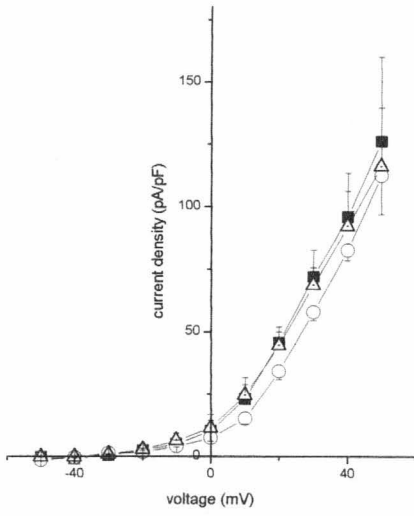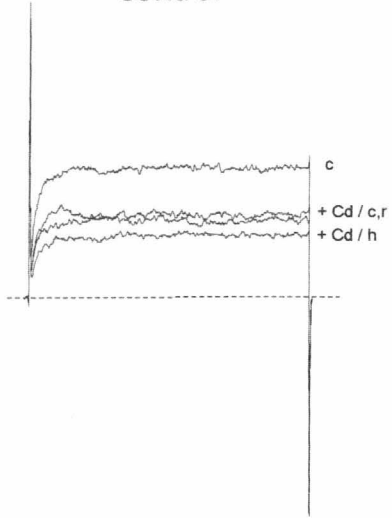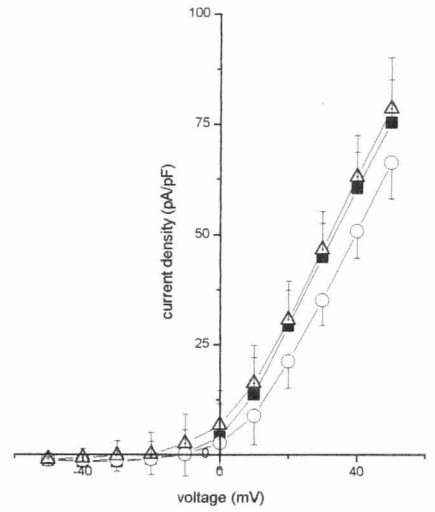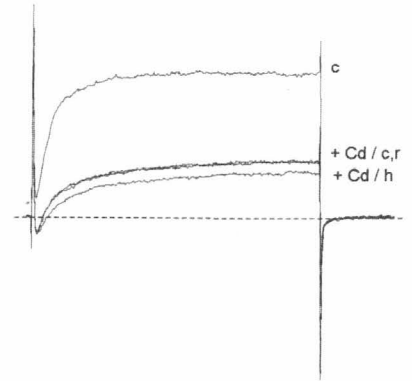
Juvenile mouse AMC are not hypoxia-sensitive.

A further goal of this study was to determine if the expression of O_2-chemosensitivity in mouse AMC was developmentally regulated, as previously reported for rat (Thompson et al, 1997; Mojet et al., 1997) and sheep (Rhykov et al, 1998) chromaffin cells. Figure 3 shows the effects of hypoxia on outward currents (step to +30 mV) in juvenile WT cells in culture for 1-3 days (Figs. 3A and C) and 4-6 days (Figs. 3B and D). The majority (5/6 cells tested) of juvenile AMC in culture for 1-3 days did not respond to hypoxia; outward current density was 97.0 ± 19.0 pA/pF in control (normoxia), and 94.8 ± 19.0 pA/pF (n=6; p=0.8) during hypoxia, and 98.0 ± 24.4 pA/pF after return to normoxia. Interestingly however, hypoxic sensitivity was detectable when juvenile cells were maintained in culture for more than 3 days (Figs 3B and D). For a group of 4 juvenile WT cells, cultured for 4-6 days, the outward current density (step to +30 mV) was 137.5 ± 49.7 pA/pF in normoxia, 114.7 ± 46.5 pA/pF (n=4; p<0.05) during hypoxia and 141.1 ± 51.7 pA/pF after return to normoxia. Thus, the hypoxia-sensitive difference current (IK_{O_2}) was 2.2 ± 2.5 pA/pF and 22.8 ± 5.3 pA/pF for juvenile AMC in culture for 1-3 days and 4-6 days, respectively. These data correspond to a non-significant hypoxia-induced suppression of outward current by 1.3 ± 0.03 % for cells in culture for 1-3 days, but a significant one of 20.0 ± 0.03 % for cells in culture for 4-6 days. It therefore appears that the O_2-sensing mechanism is absent soon after isolation of *juvenile* WT cells, but gradually re-appears following isolation *in vitro*, probably as a result of denervation.

Fig. 3. Juvenile wild type AMC are not O_2-sensitive when first brought into culture, but hypoxic sensitivity returns after four days of isolation.

A, hypoxia does not affect outward current (top panel; step to +30 mV) in juvenile wild type AMC in culture for 1-3 days. Lower panel is a current density *vs.* voltage plot for a group of 5 juvenile AMC in culture for 1-3 days. Note that hypoxia does not affect outward currents in these cells. Symbols are as in Fig. 1. B, hypoxia-induced suppression is present in juvenile AMC in culture for 4-6 days. On day 3, ~ half of AMC are O_2-sensitive (n=2/4 cells tested). Lower panel in B is a current density *vs.* voltage plot for a group of 6 cells, in culture for 4-6 days, that were hypoxia-sensitive. Although the effects of hypoxia on outward current were variable (not the large S.E.M. in the lower panel), hypoxia significantly suppressed outward current in these cells at all test potentials where current is activated. Symbols are the same as Fig. 1.

A   1-3 days

B   3-6 days

c / h / r

c / r

h

350 | 250 mV

10 ms

current density (pA/pF)

250

200

150

100

50

0

-40   0   40

voltage (mV)

current density (pA/mV)

400

300

200

100

0

-40   0   40
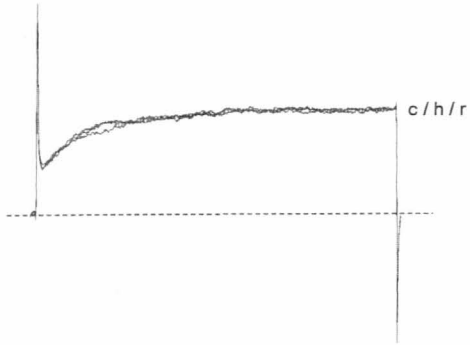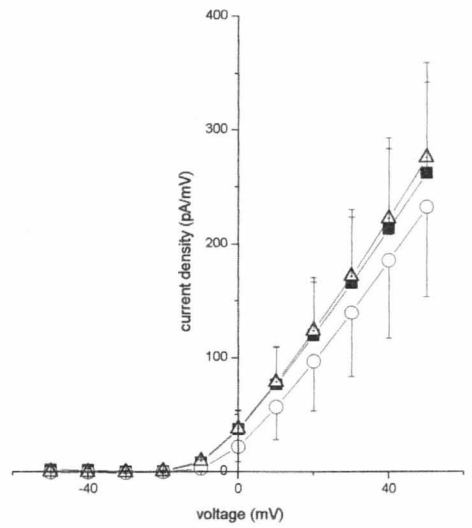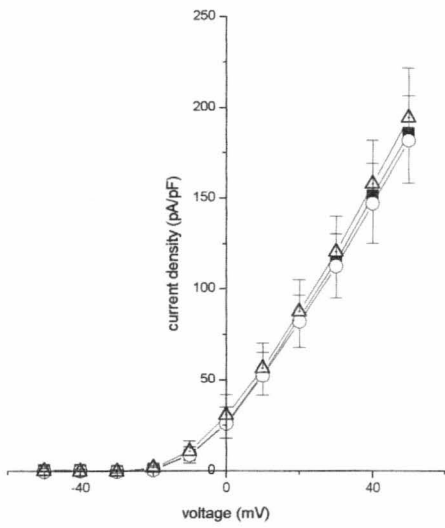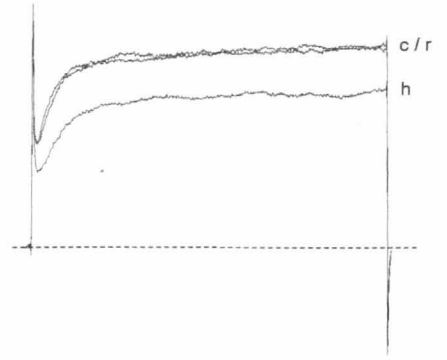
voltage (mV)

Effects of hypoxia on membrane potential and action potential duration in neonatal AMC

A component of the hypoxia-sensing mechanism in rat AMC involves membrane depolarization, which is not initiated by the voltage-dependent channels described above (Thompson and Nurse, 1998), and increased action potential duration (see Chapter 4 of this thesis). Thus, it was of interest to test whether these properties are shared with mouse AMC. Neonatal WT cells had a mean resting membrane potential of -50.0 ± 10.1 mV (n=3). During hypoxia, the membrane potential depolarized to -43.3 ± 11.3 mV (n=3; p<0.05) and returned to -49 ± 11 mV (n=3) following return to a normoxic solution. Similarly, in OD neonatal AMC the resting potential was -44.1 ± 1.7 mV (n=5) in normoxia, -36.0 ± 2.9 mV (n=5; p<0.05) during hypoxia, and returned to -45.3 ± 1.6 mV after recovery. Thus, hypoxia reversibly depolarized neonatal WT cells by 6.3 ± 1.3 mV (n=3) and OD cells by 8.1 ± 1.5 mV (n=5; Figs. 4A and B).

In the absence of TTX, the majority (6/8 cells tested) of neonatal AMC in small clusters exhibited spontaneous action potentials (see Fig. 4). Both WT (Fig 4A) and OD (Fig 4B) cells showed this spontaneous activity. The inhibition of voltage-dependent K^+ currents by hypoxia suggests that modulation of action potential duration may also be a contributing factor to the overall hypoxic response, including the amount of CA secretion. Thus, we compared the rise time (T_{rise}), decay time (T_{decay}), spike width ($T_{1/2}$), and frequency of spontaneous action potentials and in control (normoxic) and hypoxic conditions. Hypoxia was found to increase T_{rise} (Fig. 4Ca), T_{decay} (Fig. 4Cb), and $T_{1/2}$ (Fig. 4Cc) in both WT and OD chromaffin cells.

Fig. 4. Hypoxia depolarizes and increases action potential duration, but does not affect frequency, in neonatal wild type and oxidase deficient mouse AMC.

Current clamp records in A and B are taken in zero current (I=0) mode using the Nystatin perforated patch clamp technique. A, effects of hypoxia on resting membrane potential recorded from a wild type neonatal AMC. Note that hypoxia reversible depolarized the cell by ~ 10 mV. B, hypoxia caused a similar membrane depolarization in transgenic mouse AMC. C, summary of the effects of hypoxia on the rise time (Ca; T_{rise}), decay time (Cb; T_{decay}), width (Cc; $T_{1/2}$) and frequency (Cd) of action potentials recorded from neonatal wild type and oxidase deficient AMC. Hypoxia (solid bar) was found to increase T_{rise}, T_{decay} and consequently $T_{1/2}$, but did not affect spike frequency relative to the control value (open bar). In most cases, the effects of hypoxia on action potential properties was reversible (hashed bar). For wild type mouse AMC, bars represent the mean action potential properties from 75 spikes (3 cells) and for transgenic mice they represent 95 spikes (3 cells). * significantly (P<0.05) from control.

A

−42 mV

hypoxia

15 mV

10 ms

B

−40 mV

hypoxia

C

a

T_{rise} (ms)

*

*

wild type   transgenic

b

T_{decay} (ms)

*   *

wild type   transgenic

c

$T_{1/2}$ (ms)

*

*

wild type   transgenic

d

spike frequency (Hz)

wild type   transgenic
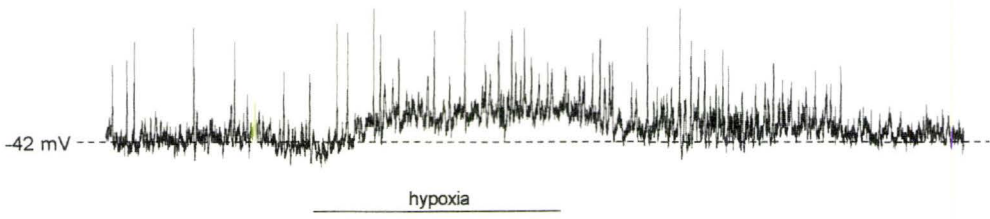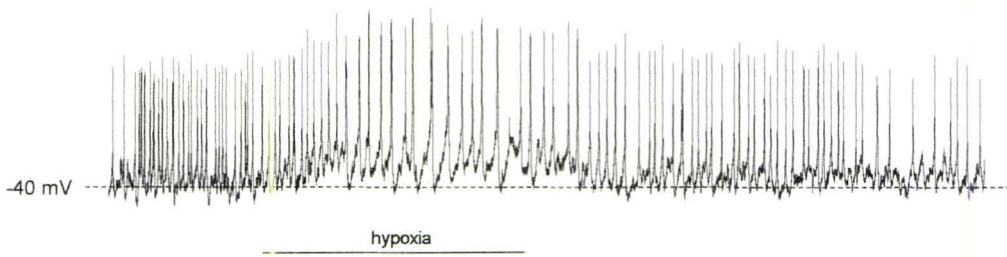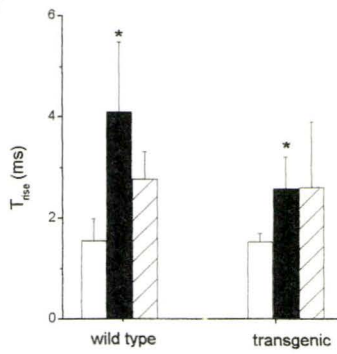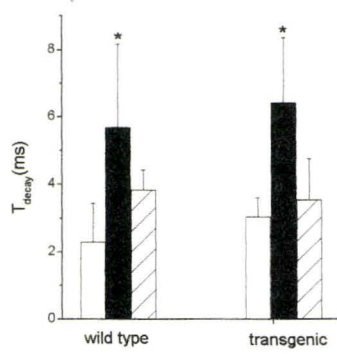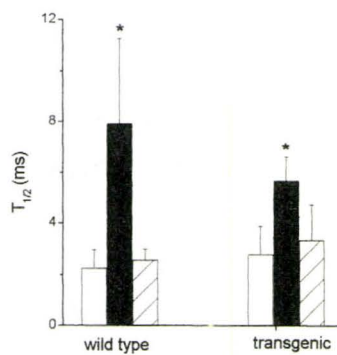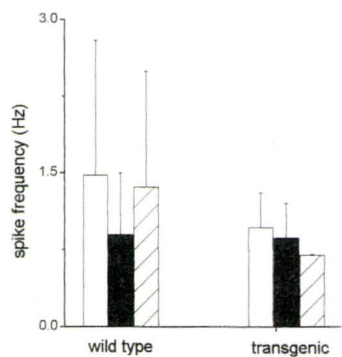
Increased action potential duration was not associated with a change in spike frequency (Fig. 4Cd) in either WT or OD cells. Therefore, these data suggest that inhibition of voltage-dependent currents by hypoxia contributes to broadening of the action potential in chromaffin cells.

Hypoxia-induced catecholamine secretion from neonatal mouse AMC

To test whether membrane responses of cultured neonatal WT and OD mouse AMC correlated with secretion, electrochemical detection by HPLC was used to compare CA secretion under basal ($20\%O_2$) and hypoxic ($5\%O_2$) conditions. Following release experiments, immunofluorescence staining for tyrosine hydroxylase (TH), a cytoplasmic marker for AMC, was used in order to normalize CA secretion to chromaffin cell number in each culture (see Fig. 5). Hypoxia-evoked CA release from neonatal WT cells was increased 3-4 times basal (Fig. 5A). The ratio of NE/EPI release was ~ 1 under both basal and hypoxia-evoked conditions, suggesting that sub-populations of AMC are equally stimulated by hypoxia (not shown).

Since the electrophysiology experiments presented above suggest that OD chromaffin cells are also sensitive to hypoxia. It was of interest to determine whether they release CA under these conditions. Both NE and E secretion was increased ~ 4 times basal (the ratio of NE/E was ~ 1) during 1 hr exposure of the OD chromaffin cell cultures to hypoxia (Fig. 6). Additionally, the percentage increase in hypoxia-evoked CA release was similar in WT and OD cultures, suggesting that the magnitude of the hypoxic response was unaffected in the knockout mouse.

Hypoxia does not evoke secretion from juvenile AMC

It was of interest to determine if mouse AMC exhibit a developmental loss of hypoxia-induced CA release, as predicted from the electrophysiology studies discussed above. To this end, we used HPLC to assay CA release from juvenile AMC cultures exposed to hypoxia for 1 hr. These release experiments were performed after 1 day in culture, since the electrophysiology studies suggested that AMC were not hypoxia-sensitive at this time. As expected, exposure to hypoxia ($5\%O_2$) failed to stimulate CA secretion in juvenile AMC (Figs. 5C and 6), consistent with the loss of O_2-sensing mechanisms in these cells. However, a high K^+ (30mM) stimulus evoked CA release, indicating that the secretory mechanisms were intact (Fig.5C). Similar to neonatal AMC, the ratio of NE/E release by high K^+ was ~ 1 (not shown). Further, as expected, hypoxia failed to stimulate CA secretion from juvenile OD chromaffin cells, though the high K^+ stimulus did (Fig. 6).

Fig. 5. Age-dependent effects of hypoxia on catecholamine secretion from wild type and oxidase deficient mouse adrenal chromaffin cells.

Catecholamine release was assayed by HPLC with electrochemical detection and normalized to 10 000 TH positive chromaffin cells identified by immunocytochemistry. A, normalized catecholamine (CA) release from neonatal wild type (WT) adrenal chromaffin cells. Note that hypoxia (Hox) and high K^+ (HK^+) stimulated CA release ~4-6 times basal (Nox). These effects were reversible (not shown). B, effects of hypoxia on normalized CA release from neonatal oxidase deficient chromaffin cells. Both hypoxia (Hox) and high K^+ (HK^+) stimulated CA secretion compared to basal (Nox), and the results are similar to those in WT cells. C and D, hypoxia (Hox) did not stimulate secretion from juvenile WT and oxidase deficient chromaffin cells. However, in both the WT and oxidase deficient cultures, high K^+ (HK^+) stimulate release. These results suggest the juvenile AMC are not O_2-sensitive, but they have functional secretory machinery.

newborn Control mice

juvenile control mice

Legend:
- NE (open bar)
- EPI (hatched bar)
- DA (filled bar)
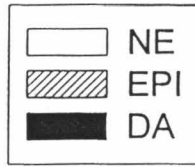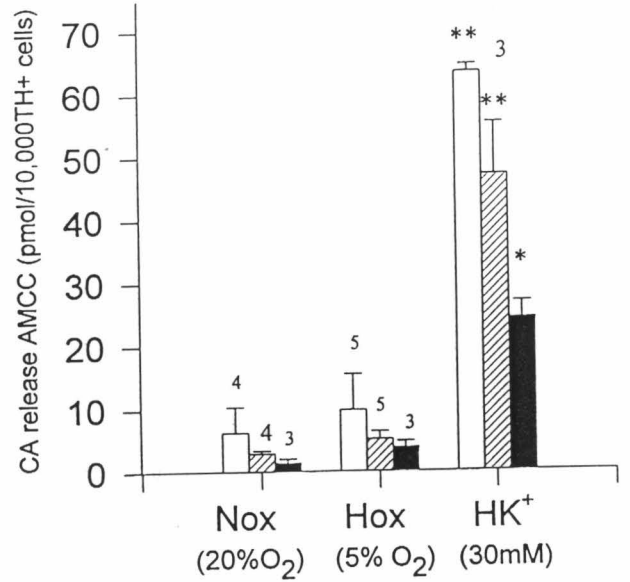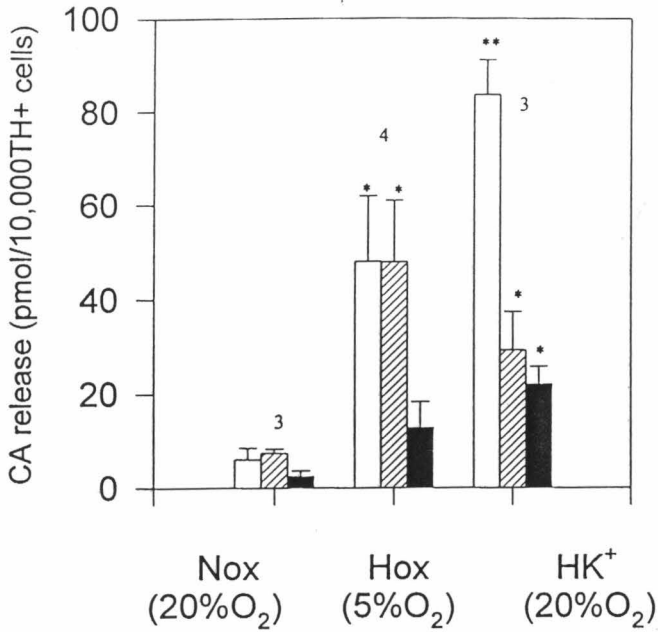
newborn gp91^phox

juvenile gp91^phox

Top left panel (newborn Control mice):
- Y-axis: CA release (pmol/10,000TH+ cells), 0 to 100
- X-axis: Nox (20%O₂), Hox (5%O₂), HK⁺ (20%O₂)

Top right panel (juvenile control mice):
- Y-axis: CA release AMCC (pmol/10,000TH+ cells), 0 to 70
- X-axis: Nox (20%O₂), Hox (5% O₂), HK⁺ (30mM)

Bottom left panel (newborn gp91^phox):
- Y-axis: CA release (pmol/10,000TH+ AMCs), 0 to 70
- X-axis: Nox (20% O₂), Hox (5% O₂), HK+ (20%O₂)

Bottom right panel (juvenile gp91^phox):
- Y-axis: CA release (pmol/10,000TH+ cells), 0 to 50
- X-axis: Nox (20%O₂), Hox (5%O₂), HK⁺ (20% O₂)

Fig. 6. Comparison of the ratio of basal and hypoxia-evoked epinephrine release between neonatal and juvenile wild type and oxidase deficient chromaffin cell cultures.

Ratio of basal – hypoxia-evoked CA release in NADPH oxidase deficient mice, lacking the gp91^{phox} component of the oxidase complex. Newborn (P1-2) wild type and oxidase deficient AMC secreted predominantly epinephrine (EPI) in response to hypoxia. Juvenile AMC from wild type and oxidase deficient chromaffin cells did not respond to the hypoxic stimulus, as indicated by a basal – hypoxia evoked ratio of 1. These data suggest that neonatal wild type and oxidase deficient chromaffin cells are O_2-sensitive and demonstrate that EPI release is enhanced during hypoxic stress. In contrast, O_2-sensing mechanisms appear to be absent in juvenile AMC, and may be related to the development of sympathetic innervation to the adrenal gland.
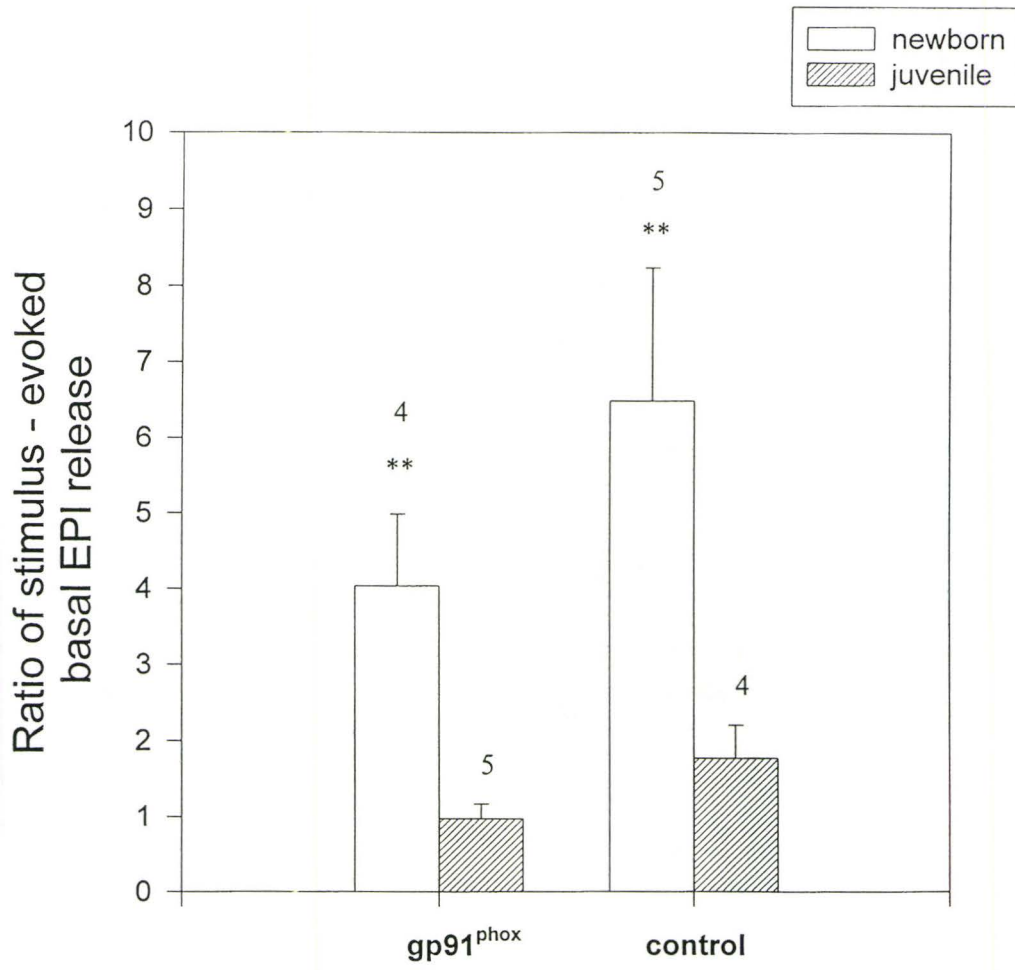
Discussion

In the perinatal period, CA secretion from adrenal chromaffin cells (AMC) during hypoxia is critical for the animal's adaptation to extrauterine life (Lagercrantz and Slotkin, 1986; Slotkin and Seidler, 1988). Several studies have identified mechanisms of O_2-sensing in rat AMC, which include reversible suppression of K^+ current (Thompson et al., 1997), membrane depolarization (Thompson and Nurse, 1998), Ca^{2+} influx (Mojet et al., 1997) and catecholamine secretion (Mojet et al, 1997; Mochizuki-Oda et al, 1997; Thompson et al, 1997). However, the mechanism by which AMC sense hypoxia is presently unknown. This study employed a transgenic mouse model, deficient in the gp91^{phox} subunit of the NADPH oxidase complex, to investigate a possible role for the oxidase in O_2-sensing. Such a role was recently identified in pulmonary neuroepithelial bodies using the same transgenic model (Fu et al, 2000). Here we demonstrate that O_2-sensing properties, as manifested by suppression of outward K^+ current, membrane depolarization, and CA secretion are expressed in wild type and oxidase deficient mouse chromaffin cells. Further, similar to rat AMC (Thompson et al, 1997), hypoxic responses were absent in the juvenile mouse shortly after the cells were brought into culture.

O_2-sensitive K^+ currents in wild type and oxidase deficient mouse AMC

Hypoxia reversibly inhibited outward K^+ current in both neonatal wild type and oxidase deficient AMC cultured for 1-6 days. The suppression of outward K^+ current appeared to consist of inhibition of both Ca^{2+}-dependent and independent components, as for neonatal rat AMC (Thompson and Nurse, 1998). Additionally, preliminary data

suggests that hypoxia can augment a glibenclamide-sensitive K^+ current (unpublished observations), similar to one described in neonatal rat AMC (Thompson and Nurse, 1998) and neurons of the substantia nigra (Jiang et al, 1994). Thus, it appears that similar K^+ channel subtypes are regulated by hypoxia in both WT and OD chromaffin cells, suggesting that the NADPH oxidase is not the main O_2-sensor for regulating any of these channel types. This contrasts with studies on pulmonary NEBs where hypoxia-sensitive Ca^{2+}-independent and -independent K^+ current appear to utilize NADPH oxidase as the main O_2-sensor (Youngson et al, 1993; Fu et al., 1999; 2000).

In contrast to neonatal wild type and oxidase deficient AMC, hypoxia-sensitive K^+ currents were not observed in juvenile AMC maintained in culture for 1-3 days. Interestingly, approximately half of the cells (n=2/4) showed hypoxic suppression of outward current on day 3 in culture, and all cells tested (n=4) showed this suppression on day 6. This suggests that when juvenile AMC are brought into culture they do not express O_2-chemosensitivity, but after a period of isolation this property may return. One possibility is that it occurs as a consequence of the denervation *in vitro* (see Seidler and Slotkin, 1988). Similar observations have been made on *adult* rat AMC maintained in culture for 7 days (Mochizuki-Oda et al, 1997; see however, Lee et al 2000). Indeed, transection of the splanchnic nerve in adult rats has been reported to cause return of the non-neurogenic hypoxic responses in adult AMC (Seidler and Slotkin, 1986), indicating that the expression of O_2-sensing mechanisms may be intimately related to sympathetic innervation (Slotkin and Seidler, 1988). It is not clear how sympathetic innervation to chromaffin cells may regulate O_2-chemosensitivity. However, it has been suggested that

activation of nicotinic receptors is responsible for down-regulation of the mechanism, since infusion of pregnant rats with nicotine causes loss of hypoxia-evoked CA secretion from the adrenal gland (Slotkin et al, 1995). A direct effect of nicotine on modulation of O_2-chemosensitivity in neonatal AMC still requires validation.

Hypoxia depolarizes and broadens action potentials in neonatal mouse AMC

In rat neonatal AMC, we have previously reported that hypoxia induces membrane depolarization (receptor potential), which is thought to increase Ca^{2+} influx through activation of L-type channels (Thompson et al, 1997). Though the exact mechanism of the receptor potential in neonatal AMC is unknown, freshly dissociated *adult* rat AMC appear to express an O_2- and apamin-sensitive, small conductance Ca^{2+}-dependent K^+ current (SK) that may be responsible for the receptor potential (Lee et al, 2000). Hypoxia-induced membrane depolarization was also observed in neonatal wild type and oxidase deficient chromaffin cells, though the underlying mechanism remains to be determined.

In addition to membrane depolarization, hypoxia was also found to cause a reversible broadening of the action potential. This was due to an increase in the depolarizing and repolarizing phases of the action potential. Broadening of the action potential through prolongation of repolarization is consistent with the hypoxic-suppression of large conductance Ca^{2+}-dependent K^+ channels (Pancrazio et al, 1994; Thompson and Nurse, 1998). The ability of AMC in clusters to fire spontaneously, as observed in the present study, means that changes in action potential duration can be

effectively coupled to CA secretion. Further, comparison of action potential duration demonstrated a reversible broadening of the spike by hypoxia in both the wild type and oxidase deficient chromaffin cells, suggesting that hypoxic-inhibition of K^+ currents leads to action potential prolongation, in WT and OD cells.

Catecholamine release from mouse AMC is developmentally regulated

Hypoxia-induced CA secretion has been described in several O_2-chemoreceptors of various species, including rat and rabbit glomus cells of the carotid body (Gonzalez et al., 1994; Jackson and Nurse, 1998), and rat and sheep AMC (Comline and Silver, 1961; Mojet et al., 1997; Thompson et al, 1997). In the present study, we found a similar magnitude of hypoxia-evoked CA secretion in AMC from neonatal wild type and oxidase deficient mice. Further, hypoxia did not evoke CA secretion from juvenile WT or OD cells, suggesting that this property is also developmentally regulated in mouse. The ratio of NE/E released during hypoxia from mouse AMC was similar, but is in contrast to rat AMC, which secrete predominantly E during hypoxia (Thompson et al, 1997). These likely reflect species differences in the CA content of the adrenal gland.

What is the O_2-sensor in AMC?

We have investigated if O_2-sensing in neonatal AMC involves modulation of K^+ channels through a putative O_2-sensor protein, NADPH oxidase. Several studies on other O_2-chemoreceptor systems, including glomus cells of the carotid body (Obeso et al, 1999), pulmonary artery smooth muscle cells (PASMC; Archer et al, 1999) and the

airway neuroepithelial bodies (Fu et al, 2000) suggest the NADPH oxidase does not function as a ubiquitous Po_2-sensor. Inhibitors of NADPH oxidase failed to prevent hypoxia-evoked CA secretion from the rat and rabbit glomus cells, suggesting NADPH oxidase is unlikely to be involved in O_2-sensing mechanisms in this system (Obeso et al, 1999). Studies on PASMC found that K^+ currents were inhibited by hypoxia in both WT and OD mice (Archer et al., 1999). In contrast, wild type NEBs, but not those from the gp91^{phox} knockout mouse, expressed hypoxia-sensitive K^+ currents, indicating that the NADPH oxidase system can function as the O_2-sensor in these cells (Fu et al, 2000). Taken together, these studies suggest that the NADPH oxidase is not a universal O_2-sensor.

In the present study, voltage clamp experiments revealed similar magnitudes of Ca^{2+}-dependent and -independent, hypoxia-sensitive K^+ currents in wild type and oxidase deficient chromaffin cells. Further, hypoxic activation of a glibenclamide-sensitive K^+ current (not shown), action potential broadening and CA secretion occurred in both cases. Therefore, it is concluded that the H_2O_2-generating NADPH oxidase is unlikely to be the primary O_2-sensing mechanism leading to K^+ channel closure and CA release from mouse chromaffin cells.

Studies on neonatal rat AMC have suggested that inhibition of the electron transport chain during hypoxia, coupled to either changes in reactive oxygen species generation or ATP levels may be the mechanism for hypoxic sensitivity (Mojet et al, 1997). This conclusion was based on the observation that cyanide can mimic the effects of hypoxia on changes in intracellular Ca^{2+} and CA secretion. However, the ability of

electron transport chain blockers to inhibit K^+ currents and depolarize AMC was not been investigated in the latter study. This idea is developed in greater detail in the next chapter of this thesis.

Chapter 4

O_2 Sensing in Neonatal Rat Adrenal Chromaffin Cells: Role of Mitochondrial Electron Transport Chain and Reactive Oxygen Species

The work in this chapter will be submitted to the *Journal of Biological Chemistry.*

The authors are: Roger J. Thompson, Linda Mills[1] and Colin A. Nurse.

I carried out all experiments. ROS measurements were done in the laboratory of Linda Mills, at Toronto Western Hospital.

Summary

Adrenal chromaffin cells from the neonatal rat express hypoxia-sensing mechanisms, resulting in a net suppression of outward K^+ current, membrane depolarization, and catecholamine secretion. Here, we tested the hypothesis that inhibition of the mitochondrial electron transport chain (ETC) and reactive oxygen species (ROS) generation by low oxygen ($PO_2 \sim 5$ mmHg) are intermediary steps in the signal transduction pathway. Outward K^+ current was inhibited in a dose-dependent manner by the proximal ETC inhibitors rotenone ($IC_{50} \sim 4$ μM) and antimycin A ($IC_{50} \sim 7$ μg/ml), but was unaffected by cyanide (CN^-; $5 - 5000$ μM) and 2,4-dinitrophenol (DNP; $2.5 - 2500$ μM). Further, rotenone and antimycin A attenuated the hypoxic inhibition of outward K^+ current, suggesting they all share a common pathway. Action potential duration in spontaneously firing chromaffin cells was increased by hypoxia, rotenone, and antimycin A (but not CN^-), and the combined effects of hypoxia and rotenone were non-additive. Measurements of ROS generation using 2,7-dichlorodihydrofluorescein (DCF) fluorescence indicated a decrease in ROS during hypoxia, rotenone and antimycin A, but not CN^-. The hypoxia-induced decrease in DCF fluorescence was attenuated in the presence of rotenone and antimycin A. Under voltage clamp, exogenous H_2O_2 (50 μM) reversed the inhibitory effect of hypoxia. Taken together, these results suggest that hypoxic chemosensitivity in neonatal rat chromaffin cells is mediated via inhibition of the mitochondrial ETC, upstream from the CN^- binding site, leading to a decrease in ROS

(e.g. H_2O_2) generation. This signal in turn appears to increase action potential duration, thereby facilitating calcium entry and catecholamine secretion.

Introduction

The ability to modulate metabolic and physiological responses to decreased O_2 availability is important for cell survival and adaptation, and implies cells must be endowed with machinery for sensing O_2. Hypoxia can modulate both gene expression (Semenza, 1999), and excitable membrane properties (Lopez-Barneo et al., 1996) in a variety of cell types. For example in Hep3B and PC12 cells, hypoxia activates transcription of erythropoietin and tyrosine hydroxylase respectively (Chandel et al., 1998; Czyzyk-Kreska et al., 1994), via the basic helix-loop-helix (bHLH) transcription factor, HIF-1. Additionally, in other specialized O_2-sensing cells, for example carotid body type 1 cells (Lopez-Barneo et al., 1996), neuroepithelial bodies of the lung (NEBs; Youngson et al., 1993), pulmonary myocytes (Archer et al., 1993), and neonatal rat adrenal chromaffin cells (Thompson et al., 1997; Thompson and Nurse, 1998), hypoxia reversibly inhibits outward K^+ currents, leading to or facilitating membrane depolarization.

The available evidence suggests that these specialized O_2-chemosensitive cells may not use a common mechanism for sensing O_2. Candidate sensors in these cells include heme and non-heme O_2 –binding proteins in the mitochondrial electron transport chain and a neutrophil-like NADPH oxidase (Duchen and Biscoe, 1992; Acher and Xue, 1995, Semenza, 1999). The latter was recently shown to be the primary O_2-sensor in pulmonary NEB cells (Fu et al., 2000), but apparently *not* in pulmonary myocytes (Archer et al., 1999), based on use of a knockout mouse model deficient in the O_2-binding gp91^{phox} subunit of the oxidase. More recent studies in our

laboratory using similar oxidase deficient mice suggest that NADPH oxidase is not an important O_2-sensor in neonatal rat chromaffin cells (Thompson, Farragher and Nurse, unpublished observations). Thus, other potential candidate O_2-sensors need to be considered.

It has been suggested that inhibition or uncoupling of the mitochondrial electron transport chain (ETC) mediates the physiological effects of hypoxia in pulmonary myocytes (Archer et al., 1993), cardiomyocytes (Duranteau et al., 1998), Hep3B cells (Chandel et al., 1998), carotid body type 1 cells (Biscoe and Duchen, 1992; Lahiri, 1994; Buckler and Vaughan -Jones, 1998) and neonatal adrenal chromaffin cells (Mojet et al., 1997). Though a change in reactive oxygen species (ROS) generation is proposed as one potential signalling pathway, both a decrease (Archer et al., 1993) and an increase (Duranteau et al., 1998) in ROS during hypoxia has been observed in pulmonary myocytes and cardiomyocytes respectively. Additionally, a change in ATP/ADP ratio has been proposed as the second messenger between the mitochondria and plasma membrane during hypoxic responses in neonatal rat chromaffin cells (Mojet et al., 1996) and carotid body type 1 cells (Buckler and Vaughan- Jones, 1998). Changes in ROS levels (or ATP/ADP ratio) may then modulate K^+ channel activity through a direct action on the channel or indirectly via a change in redox status.

Rat adrenal chromaffin cells (AMC) transiently express O_2-sensing mechanisms in the perinatal period (Siedler and Slotkin, 1985; Thompson et al., 1997; Mojet et al., 1997). The primary response to neonatal hypoxia is increased

catecholamine (CA) secretion, which promotes vital physiological adaptations that facilitate the transition to extra-uterine life (Siedler and Slotkin, 1985; Thompson et al., 1997; Mojet et al., 1997). Recent studies in our laboratory provided evidence for at least three O_2-sensitive K^+ currents in neonatal rat AMC (Thompson and Nurse, 1998). Anoxia inhibited both a large-conductance Ca^{2+}-dependent K^+ (I_{BK}) and a delayed rectifier K^+ (IK_v) current, but augmented a glibenclamide-sensitive K^+ current (IK_{ATP}). These studies, however, did not reveal the location or identity of the O_2-sensor, nor the signalling pathway that links the sensor to plasma membrane K^+ channels. Since Mojet et al. (1997) proposed that inhibition of the distal mitochondrial ETC with cyanide (CN) can mimic hypoxia, as measured by CA secretion, we investigated whether selective inhibitors of proximal vs distal ETC, as well as the uncoupler (DNP), can mimic the differential effects of hypoxia on K^+ currents and the action potential waveform. Moreover, we monitored changes in ROS generation in neonatal AMC by 2,7-dichlorodihydrofluorescein (DCF) fluorescence during hypoxia and inhibition of the ETC. Using these more stringent tests, we found that whereas the more proximal inhibitors of complex I (rotenone) and complex III (antimycin A) were good mimics of hypoxia, the more distal ETC inhibitor (CN) and the uncoupler DNP were not. In addition, we provide evidence that decreased ROS generation by the mitochondrial ETC may function as the second messenger during hypoxia-induced CA secretion from neonatal rat chromaffin cells.

Experimental Procedures

Cell Culture. Primary cultures enriched in adrenal chromaffin cells were prepared from postnatal 1-2 day old (P1-2; neonatal) rats as previously described (Thompson et al., 1997). Cells were grown at 37 °C in a humidified atmosphere of 95% air, 5% CO_2 for 1-3 days before they were used in patch clamp experiments. The growth medium consisted of F-12 nutrient medium supplemented with 10% fetal bovine serum (Gibco), 0.01% dexamethasone, and various additives (see Thompson et al., 1997).

Electrophysiology. All voltage and current clamp data were obtained using the Nystatin perforated-patch configuration of the patch clamp technique (see Thompson et al., 1997; Thompson and Nurse, 1998). Seal resistance was typically 2-10 GΩ and most (~ 75%) of the series resistance (range 10-40 MΩ) was compensated in voltage-clamp experiments; voltage errors due to series resistance were minimal because of the high input resistance (~ 2 GΩ) of the cells. Junction potentials, typically 2-5 mV were cancelled prior to seal formation. The pipette solution contained (mM) potassium gluconate, 95; KCl, 35; NaCl, 5; $CaCl_2$, 2; HEPES, 10; at pH 7.2, and Nystatin (300-450 μg ml^{-1}). The standard bathing solution contained in mM: NaCl, 135; KCl, 5; $CaCl_2$, 2; $MgCl_2$, 2; glucose, 10; HEPES, 10, at pH 7.4; 0.5 μM tetrodotoxin (TTX) was present during all voltage clamp experiments but was omitted during current clamp experiments.

All recordings were obtained at room temperature (20-23 °C) with an Axopatch-1D amplifier equipped with a 500 MΩ head stage feedback resistor (Axon

Instruments). Records were lowpass Bessel filtered at 2 kHz and digitized at 10 kHz using a Digidata 1200 interface (Axon) and pClamp software versions 6.0.3 or 8.0 (Axon Instruments). Hypoxia was generated by bubbling 100% N_2 into 150 ml of standard recording saline for 1 to 1.5 hrs. Measurement of the Po_2 in the recording chamber with a 25 μm O_2 microelectrode (Diamond General Electro-Tech Inc., Ann Arbor, MI) routinely yielded an O_2 partial pressure of ~ 5 mmHg during hypoxia and ~ 140 mmHg during normoxia (control). The solution in the recording chamber was exchanged by gravity flow and removed by suction at a rate of 4-6 ml min^{-1}.

In voltage clamp experiments, the holding potential was –60 mV and currents were recorded during 10 mV increments in voltage steps (duration 80 msec) between –50 and +50 mV. Membrane capacitance (pF) was determined by integrating the capacitative transient elicited by a hyperpolarizing voltage step from –60 to –100 mV, then dividing the charge by the magnitude of the step. Current density (pA/pF) was determined by dividing the mean current (pA), measured at 40 msec from three recordings averaged on-line during each stimulus, by the membrane capacitance. This allowed comparison of currents between cells of different sizes. All data are expressed as mean ± standard error of the mean. Patch clamp data were compared using the paired or independent Student's t tests (Microcal Origin version 6.0), with the level of significance set at $P < 0.05$. Voltage clamp data traces are shown without leak subtraction and current-voltage (I-V) plots are leak subtracted.

In current-clamp experiments, all measurements of membrane potential were obtained in zero current (I =0) mode. In cases where cells fired spontaneously, the

action potentials were analysed using pClamp software to determine 10-90% rise time (T_{rise}), 10-90% decay time (T_{decay}) and the width of the spike between 50% of the rise time and 50% of the decay time ($T_{1/2}$). These spike properties were determined for each individual action potential, and the average value (for 5 sec recording interval) calculated for each stimulus.

Measurement of Reactive Oxygen Species (ROS)

The generation of reactive oxygen species (ROS) was assayed in clusters of 3-15 chromaffin cells using the probe 2,7-dichlorodihydrofluorescein (DCF; Molecular Probes). Cells were loaded for 40 min (at 35-37 °C) with 10 μM DCF (in DMSO) dissolved in standard bathing solution. The dye was excited using an Argon laser Confocal Imaging System (Bio-Rad, MRC-600) and filtered with a fluorescein filter set before images were collected by a photomultiplier tube. One scan plane was used throughout each experiment and images were collected every 10 sec using Comos software (version 7.0) and stored on a personal computer. Images were then converted to TIF files with Confocal Assistant (version 4.02) and measurements of fluorescence (as mean pixel count in a cell cluster) were taken with ScionImage (ScionCorp). Changes in DCF fluorescence are reported as percent change from control (normoxia) after backgound subtraction.

Drugs. All chemicals were obtained from Sigma (unless otherwise indicated) and were made fresh on the day of recording. Sodium cyanide (CN) was diluted from a

100 mM stock solution in distilled water; pH was adjusted to 7.40 with HCl. 2,4-dinitrophenol (DNP) was diluted from a 10 mM stock solution in standard recording saline (pH adjusted to 7.4). Rotenone and antimycin A (a mixture of antimycin A_1, A_2, A_3 and A_4) were diluted into standard recording saline from 10 mM stock solutions in DMSO. Since the exact molecular weight of the antimycin A mixture was not known, concentrations are reported as μg/ml. Application of vehicle (DMSO) at the concentrations used in these experiments (0.1 to 1%) did not affect outward currents, membrane potential or DCF fluorescence.

Results

Effects of ETC inhibitors on voltage-dependent outward currents

The first step in determining whether the mitochondrial electron transport chain (ETC) can function as an O_2-sensor was to investigate whether inhibitors of the ETC mimic the effects of hypoxia in suppressing outward K^+ current in neonatal rat AMC. To this end, we tested the effects of the classical inhibitor of cytochrome oxidase (CN), a complex I inhibitor (rotenone), a complex III inhibitor (antimycin A), and an uncoupler of ATP production (DNP) on the voltage-activated K^+ current. Neither CN nor DNP significantly affected outward current at the doses tested (Figs. 1A,B; 2A,B). For the voltage step to +30 mV, outward current density was 120.2 ± 10.7 pA/pF (n=4) before (control) and 104.0 ± 8.9 pA/pF (n =4; P =0.9) during 5 mM CN. Similarly, outward current density (at +30 mV) was 100.6 ± 10.4 pA/pF (n =4) before, and 98.0 ± 13.0 pA/pF (n =4; P =0.9) during 250 μM DNP. These data suggest that neither inhibition of the ETC at cytochrome oxidase, nor uncoupling of ATP production from electron transport mimic the effects of hypoxia on outward currents in neonatal rat AMC.

In contrast the more proximal inhibitors of the ETC, antimycin A and rotenone, caused a dose-dependent inhibition of outward K^+ current (Figs. 1 C, D; 2 C,D). Outward K^+ current density (step to +30 mV) was significantly reduced from 96.4 ± 14.5 pA/pF (n =7) to 50.0 ± 11.6 (n =7; P< 0.05) by 10 μg/ml antimycin A. For a different group of cells, the outward K^+ current density was significantly reduced from 134.9 ± 20.8 pA/pF to 57.2 ± 11.9 pA/pF (n =7; P<0.01) by 5 μM

rotenone. Dose-response curves for the inhibition of outward current (at +30 mV) for each of the ETC inhibitors are plotted in Figs. 2 A, B. The concentration vs K^+ current inhibition curves for antimycin A and rotenone are plotted in Figs. 2C, D, and fitted with the Hill equation (dashed line) with IC_{50} values of 6.74 ± 0.6 μg/ml for antimycin A and 3.97 ± 0.3 μM for rotenone. Taken together, these data suggest that inhibition of the proximal ETC by rotenone or antimycin A, but *not* the distal ETC by CN, mimics hypoxia in causing a dose-dependent suppression of outward current. In addition, uncoupling of oxidative phosphorylation with DNP did not mimic hypoxia, suggesting a change in ATP/ADP ratio was not the major intracellular signal mediating this aspect of the hypoxic response.

Effects of hypoxia on outward current in the presence of ETC inhibitors

The fact that inhibitors of the proximal ETC (rotenone and antimycin A) mimicked hypoxia in suppressing outward K^+ current in neonatal rat AMC (see above) raises the question whether there is convergence of the signalling pathways. We therefore investigated whether the effects of ETC inhibitors and hypoxia are additive. As shown in Figs. 3,4 the proximal inhibitors caused a significant, dose-dependent reduction in the magnitude of the hypoxia-sensitive difference current, IK_{O2}. For example, in Figs. 3C, D and 4C, D, the magnitude of K^+ current suppression by hypoxia (at + 30 mV) was reduced in the presence of 10 μg/ml antimycin A and 10

Fig. 1. Dose-dependent effects of mitochondrial inhibitors and an uncoupler on voltage-dependent outward currents.

Current traces in the left panels are for the voltage step from the holding potential of − 60 mV to +30 mV. Each point in the current-voltage plots of the right panels represents the mean of three records for each step from the holding potential. Drugs were applied for 3-5 min before records were collected. A, cyanide did not affect outward currents in neonatal chromaffin cells at any dose tested. Symbols in the right panel are as follows, control, O; 5 µM, •; 50 µM, □; 500 mM, ■; 5 mM, Δ. B, DNP, an uncoupler of oxidative phosphorylation did not affect outward currents at any dose tested. Symbols are as follows: control, O; 2.5 µM, •; 25 mM, □; 250 µM, ■; 2.5 mM, Δ. C, antimycin A, an inhibitor of complex III, inhibited outward current in a dose-dependent manner. Symbols in C are as follows: control, O; 0.5 µM, •; 2 mM, □; 5 µM, ■; 10 mM, Δ; 50 mM, ▼; 100 µM, ∇. D, dose-dependent suppression of outward currents was also observed by rotenone, a complex I inhibitor. Symbols in D are: control, O; 0.5 mM, •; 2 µM, ∇; 3.5 µM, ▼; 7 µM, □; 50 µM, ■.

A cyanide

0-5 mM

current (pA) / voltage (mV)

B DNP

0 - 2.5 mM

current (pA) / voltage (mV)

C antimycin A

0 - 2 µM
5 µM
10 µM
50 µM
100 µM

current (pA) / voltage (mV)

D rotenone

0 µM
0.5 µM
2 µM
3.5 µM
5/7 µM

current (pA) / voltage (mV)
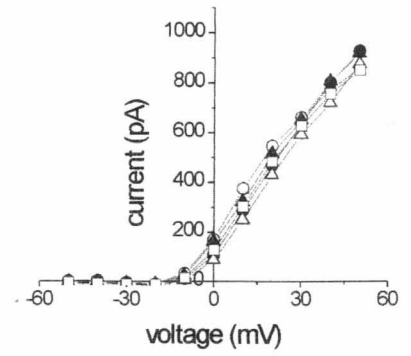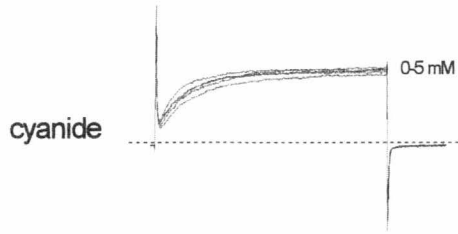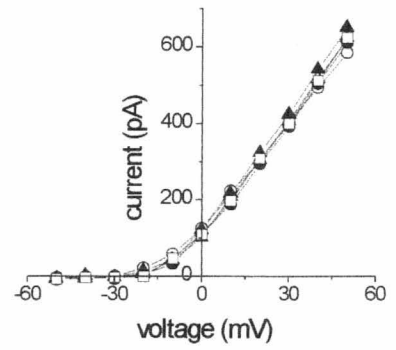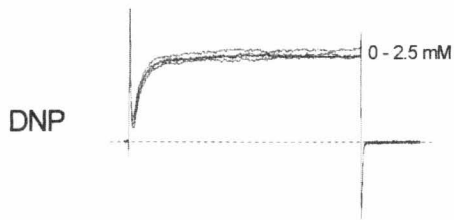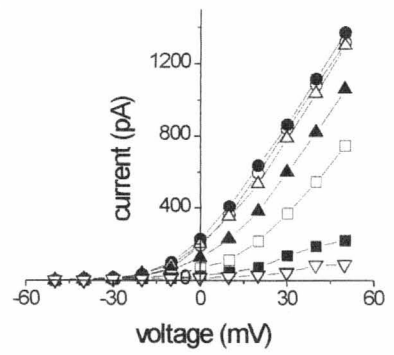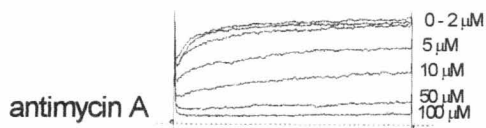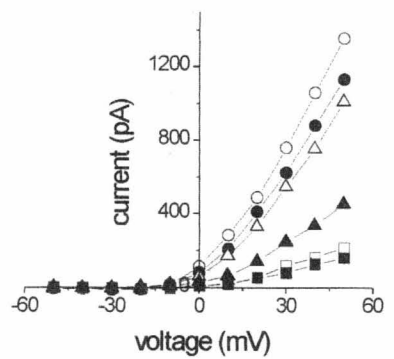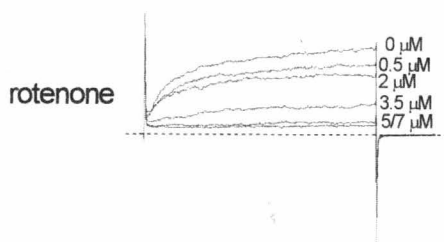
Fig. 2. Dose-response curves for the effects of mitochondrial inhibitors on outward currents at + 30 mV.

Mean outward current density +/- standard error of the mean are shown for each drug tested. Each cell was exposed to all doses of the drug and the percentage suppression of outward current estimated at + 30 mV was determined. A, cyanide did not affect outward currents at any dose tested (n=4). B, the uncoupler, DNP did not affect outward current at any dose tested (n=4). C, dose-dependent inhibition of outward current by antimycin A (n=7); smooth curve (dotted line) represents fit with the Hill equation, with IC_{50} = 6.74 ± 0.6 µg/ml . D, dose-dependent inhibition of outward current by rotenone (n=7 except for the point at 25 µM, where n=3); smooth curve (dotted line) represents fit with the Hill equation, with IC_{50} = 3.97 ± 0.3 µM.
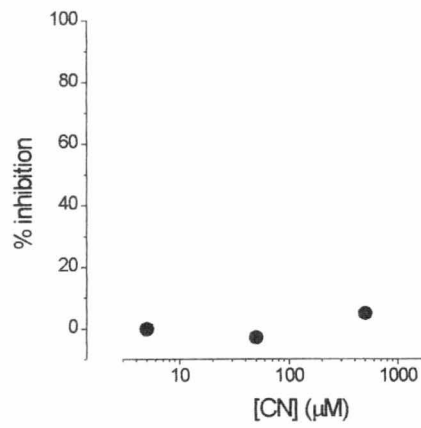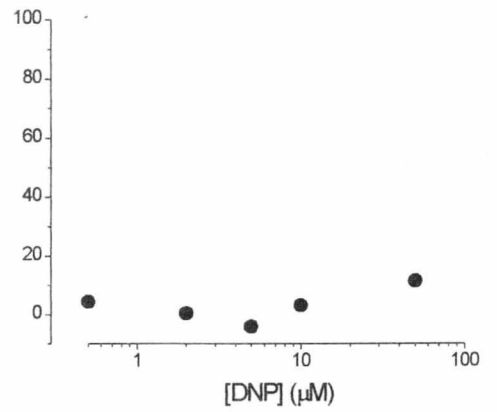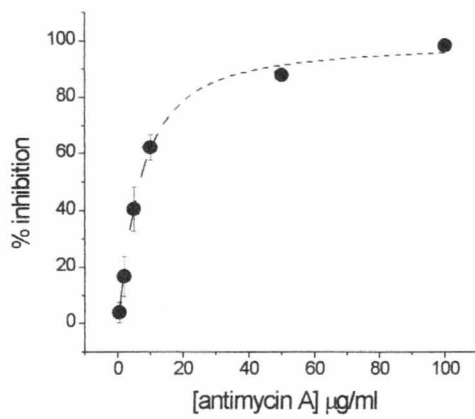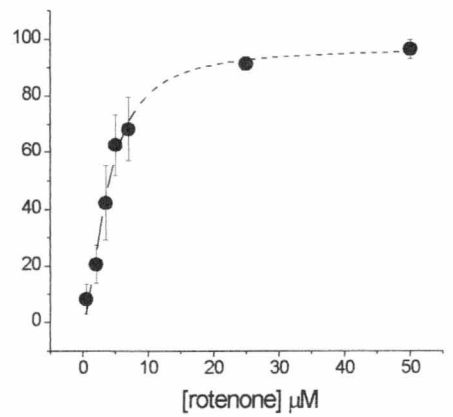
μM rotenone. In contrast, the hypoxia-sensitive difference current (IK_{O_2}) was unchanged in the presence of either 5mM CN or 250 μM DNP (Figs. 3A,B and 4A,B). These data suggest that hypoxia and inhibitors of the proximal ETC suppress voltage-dependent K^+ currents through a common signalling pathway. Further, the data are consistent with the presence of a putative mitochondrial O_2 sensor located upstream form the CN binding site (i.e. cytochrome c oxidase).

Rotenone and antimycin A activate a glibenclamide-sensitive K_{ATP} current

We previously reported that the hypoxia-sensitive K^+ current, IK_{O_2}, consisted of the sum of three components, i.e. inhibition of both a Ca-dependent (I_{BK}) and Ca-independent (IK_V) K^+ current, and activation of an ATP-sensitive K^+ current, IK_{ATP} (Thompson and Nurse, 1998). Thus, a stringent test as to whether ETC inhibitors are genuine mimics of hypoxia, rather than generalized non-specific inhibitors of K^+ current, was to determine whether they *activated* IK_{ATP}. This was the case for both rotenone (Fig. 5) and antimycin A (not shown). The effects of glibenclamide, an inhibitor of IK_{ATP}, on outward current (step to +30 mV) in the presence and absence of 5 μM rotenone are shown in Fig. 5A, and the corresponding I-V relationships in Fig. 5B. In the absence of rotenone, outward current density at +30 mV was unaffected by glibenclamide (Fig. 5A B); control current density was 154.3 ± 30.8 pA/pF before, and 157.5 ± 32.9 pA/pF (n=7; P=0.36) after 50 μM glibenclamide. In contrast, in the presence of 5 μM rotenone, glibenclamide (50 μM) caused a

Fig. 3. Effects of hypoxia on outward current in the presence of electron transport chain inhibitors.

All current traces are for the voltage-step to +30 mV from the holding potential of − 60 mV. A, hypoxia suppresses outward current in the presence of 5 mM CN. B, DNP does not affect the hypoxic suppression of outward current. C, rotenone (5 μM) attenuates the inhibitory effect of hypoxia on outward current. D, antimycin A (10 μM) attenuates the effects of hypoxia on outward current. Symbols in the I-V plots are as follows: control, O; hypoxia, ●; inhibitor plus normoxia, □; inhibitor plus hypoxia, ■.

A

c/ 5mM CN

h/ h + CN

current (pA)

voltage (mV)

B

c/ 250µM DNP

h / h + DNP

C

c

5µM rotenone

h

h + rotenone

D

c

h

10 µg/ml antimycin A / +h
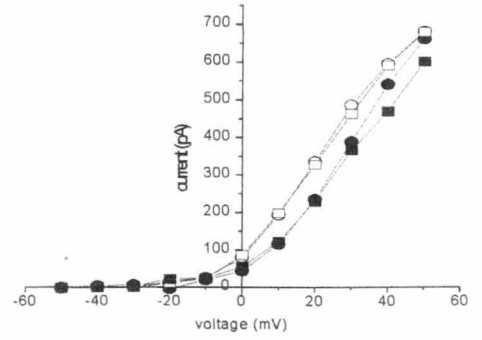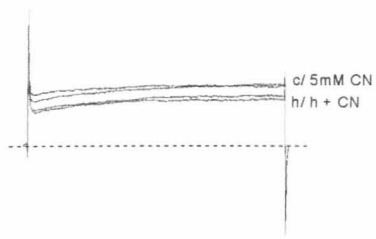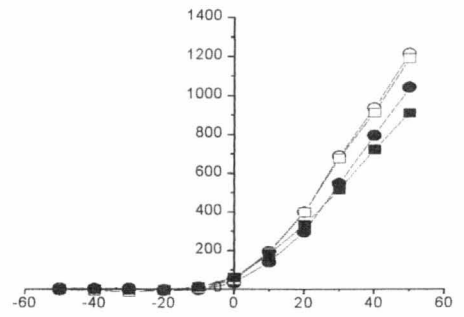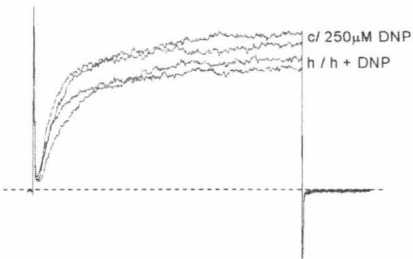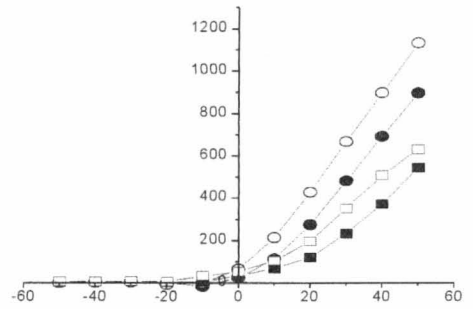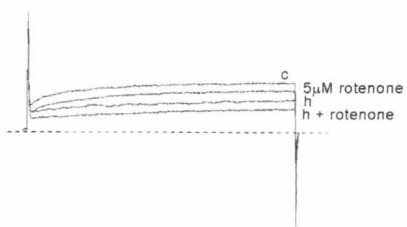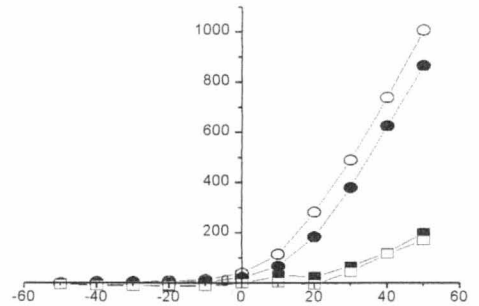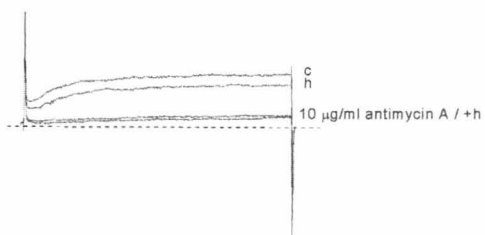
Fig. 4. Inhibitors of the more proximal electron transport chain selectively attenuate the hypoxia-induced suppression of outward current.

The magnitude of the hypoxia-sensitive outward current (IKo_2) was determined by subtracting the current density at +30 mV during hypoxia from that in normoxia. A, the magnitude of IKo_2 was not significantly affected by 5 mM cyanide (n=4). B, 2.5 mM DNP did not significantly affect IKo_2. C, the magnitude of IKo_2 was reduced in a dose-dependent manner by antimycin A (n=7). D, rotenone also caused a dose-dependent reduction in IKo_2 (n=7).
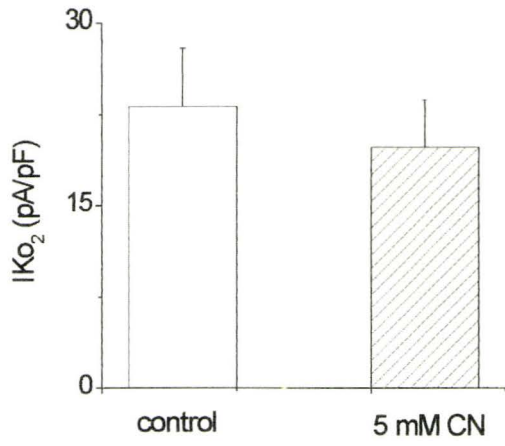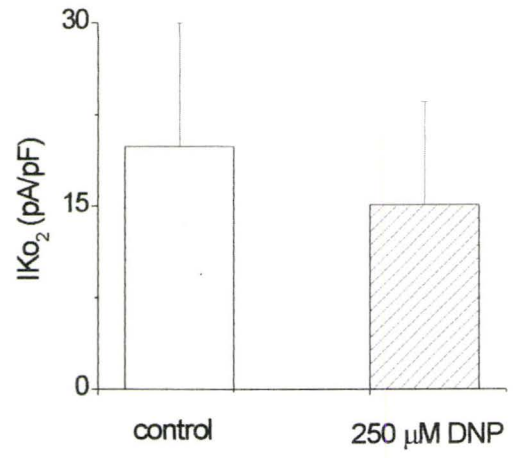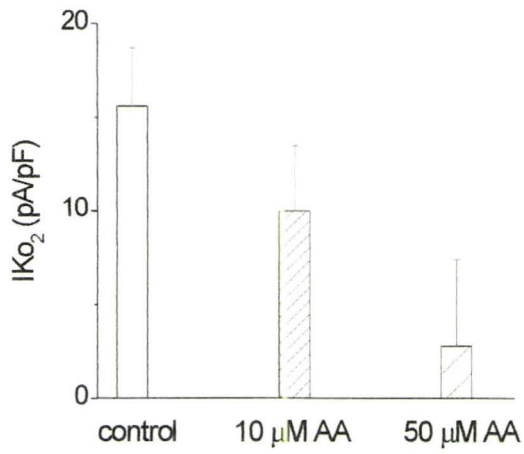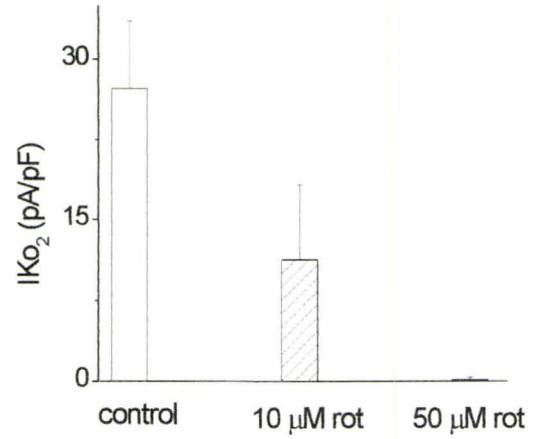
significant further reduction in outward current density in the same cells (n =7) from 111.3 ± 27.9 pA/pF to 73.9 ± 14.4 pA/pF (P< 0.05). Therefore, the glibenclamide-sensitive current was significantly increased by rotenone from −3.1 ± 3.2 pA/pF to 37.4 ± 14.6 pA/pF (n =7; P<0.05). Similar results were found during ETC inhibition with antimycin A (not shown). Thus, as was the case for hypoxia, the proximal ETC inhibitors appear to activate IK_{ATP} channels, the majority of which are closed in normoxia.

Hypoxia and proximal ETC inhibitors increase action potential duration

We previously suggested that hypoxia-induced catecholamine secretion from neonatal rat adrenal chromaffin cells (AMC) is triggered by membrane depolarization, and inhibition of voltage-dependent K^+ currents, including the Ca-dependent K^+ current, I_{BK} (Thompson et al., 1997; Thompson and Nurse, 1998). Since the latter is known to play a key role in action potential repolarization in chromaffin cells (Pancrazio et al., 1994), it was of interest to compare the shape of the action potential in neonatal AMC during hypoxia and following inhibition of the proximal ETC. To address this, we took advantage of the fact that neonatal AMC often fire spontaneously when present in clusters (~ 4-15 cells), in contrast to when they are singly-isolated (unpublished observations). In clustered AMC, exposure to hypoxia or rotenone (5 or 10 μM) resulted in a small depolarization as well as a broadening of the action potential (Figs. 6A, B; 7 A, B), without any significant effect on firing

Fig. 5. Rotenone actives a glibenclamide-sensitive K^+ current.

A, effects of glibenclamide on outward currents at $+ 30$ mV in the presence and absence of 5 µM rotenone. In the absence of rotenone, glibenclamide, an inhibitor of ATP-sensitive K^+ channels, did not affect outward current, indicating that these channels are not open under control conditions. In contrast, in the presence of rotenone the magnitude of the glibenclamide-sensitive current was increased, suggesting that metabolic inhibition can activate the ATP-sensitive K^+ current. B, current-voltage relationship for the cell in A, showing that the effects of glibenclamide in the presence of rotenone occur at all voltage-steps where currents are activated. Similar results were seen in 6 other neonatal chromaffin cells tested.

A

c / glib / w

rot
rot + glib

250 pA

10 ms

B

- control
- 50 μM glib
- 5 μM rot
- rot + glib
- wash

current (pA)

voltage (mV)
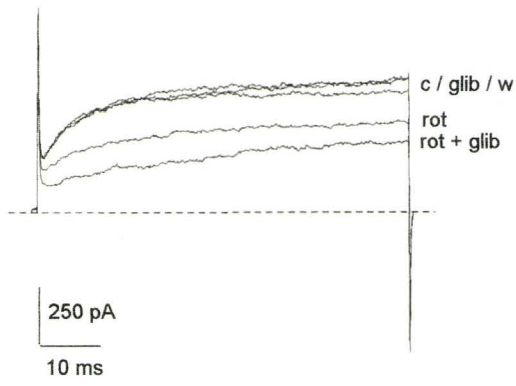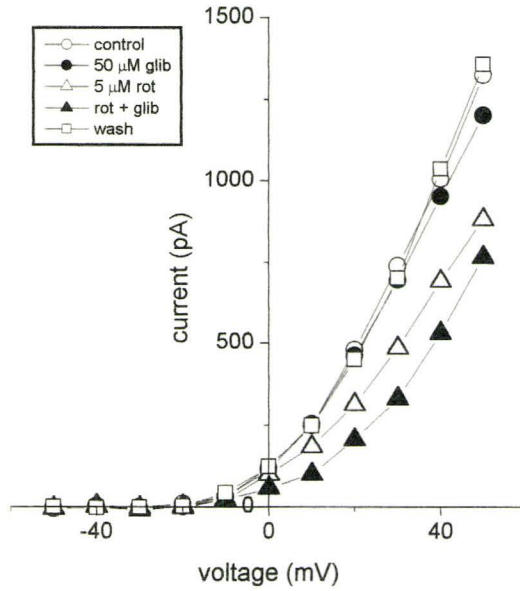
frequency (Fig. 7B). Moreover, the effect of the same hypoxic stimulus on action potential duration was attenuated when rotenone was present (see Figs. 6B; 7A, B). Hypoxia and rotenone increased the duration of the repolarizing or decay phase (T_{decay}) and, to a lesser extent, the depolarizing phase (T_{rise}) of the action potential; consequently, the half-width ($T_{1/2}$) of the action potential was increased (Fig. 7B). In general, the presence of rotenone attenuated the hypoxia-induced effects on action potential waveform (Fig. 7A, B). Similar results were obtained during ETC inhibition with antimycin A (not shown); however, this drug appeared more toxic to AMC and often irreversibly inhibited action potential generation. In contrast to these data on more proximal ETC blockers, application of the distal ETC blocker CN (500 μM) did not affect spike frequency or duration (Figure 6C 7B).

Exogenous H_2O_2 augments outward K^+ current and reverses the effects of hypoxia

The failure of CN and DNP to mimic hypoxia suggests that a change in ATP/ADP is not the important second messenger system during hypoxic chemotransduction in neonatal rat AMC. The ETC is thought to be the primary source of cellular reactive oxygen species (ROS), which have frequently been proposed as intracellular signal(s) mediating the effects of hypoxia in several systems (Archer et al., 1993; Semenza, 1999). We focussed on one ROS species, i.e. hydrogen peroxide (H_2O_2), which is known to regulate various K^+ channels (Michelakis et al., 1995; Lopez-Barneo et al., 1996), and intracellular H_2O_2 levels can be monitored using the fluorescent probe

Fig. 6. Effects of hypoxia, rotenone and cyanide on membrane potential in spontaneously active neonatal chromaffin cells.

All recordings were collected in current clamp mode (I=0) using the Nystatin perforated patch configuration of whole-cell recording (without addition of tetrodotoxin). A, representative current clamp recording of spontaneous action potentials in a neonatal chromaffin cell. Hypoxia caused a membrane depolarization and an increase action potential duration (shown more clearly in Fig. 7). B, rotenone (10 μM) causes a small depolarization, but hypoxia had no further effect in the presence of the drug. C, cyanide (500 μM) did not affect membrane potential and the depolarizing effect of hypoxia persisted in the presence of the drug. Horizontal scale bar represents 15 sec in A and C, and 30 sec in B. Vertical scale bar is 20 mV.

A

-45 mV ----

hypoxia

B

-40 mV ----

hypoxia

rotenone

C

-45 mV ----

hypoxia

cyanide
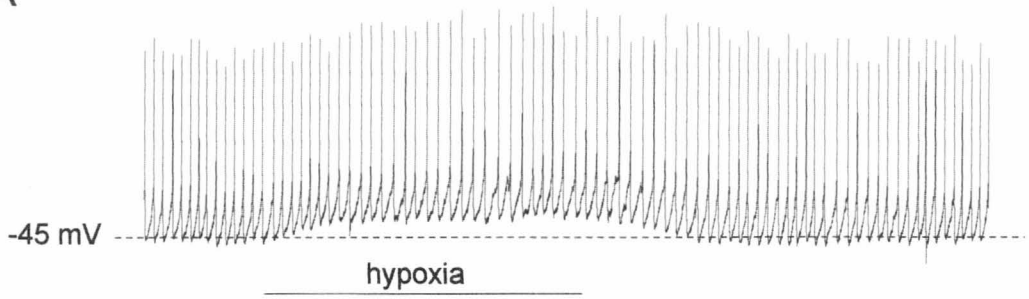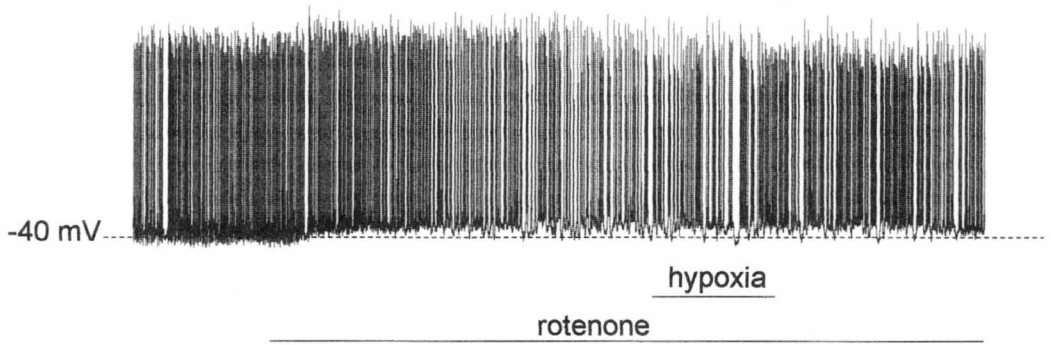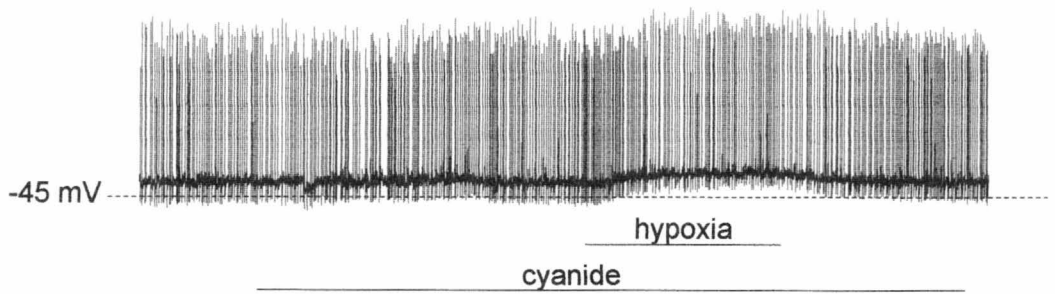
Fig. 7. Hypoxia causes an increase in duration without affecting the frequency of action potentials.

Histograms were generated by calculating the mean frequency, rise time (T_{rise}), decay time (T_{decay}), and half-width (T_{half}) of action potentials over 5 sec intervals. T_{rise} and T_{decay} were determined by fitting the rising and falling phases of the action potential with single exponential equations, and $T_{1/2}$ was determined as the time between 50% of the T_{rise} and 50% of T_{decay}. A, representative action potentials showing the broadening by hypoxia (left panel) and 5 µM rotenone (second panel). The effects of hypoxia on action potential duration were attenuated in the presence of 5 µM (third panel) and 10 µM rotenone (fourth panel). Action potentials were adjusted to start at the same membrane potential for each set of traces. B, comparison of action potential time constants and spike frequency between normoxia (open bar) and hypoxia (filled bar) under control conditions (n=90 spikes from 4 cells), in the presence of rotenone (n=50 spikes from 3 cells) or cyanide (n=30 spikes from 2 cells). Hypoxia and rotenone (10 µM) caused a slight reversible increase in the rise time of the action potential; hypoxia had no further effect on T_{rise} in the presence of rotenone (left panel). Hypoxia and rotenone, but not CN, prolonged the decay phase of the action potential, and hypoxia was without further effect in the presence of rotenone (second panel). Hypoxia and rotenone increased T_{half}, but cyanide was without affect (third panel). Hypoxia and rotenone, but not cyanide caused a slight decrease in action potential frequency (fourth panel).

A

control
hypoxia
recovery

control
5 μM rotenone

5 μM rotenone
5 μM rotenone
+ hypoxia

10 μM rotenone
10 μM rotenone
+ hypoxia

B

Trise (ms)

control   rotenone   cyanide

Tdecay (ms)

control   rotenone   cyanide

Thalf (ms)

control   rotenone   cyanide

spike frequency (Hz)

control   rotenone   cyanide
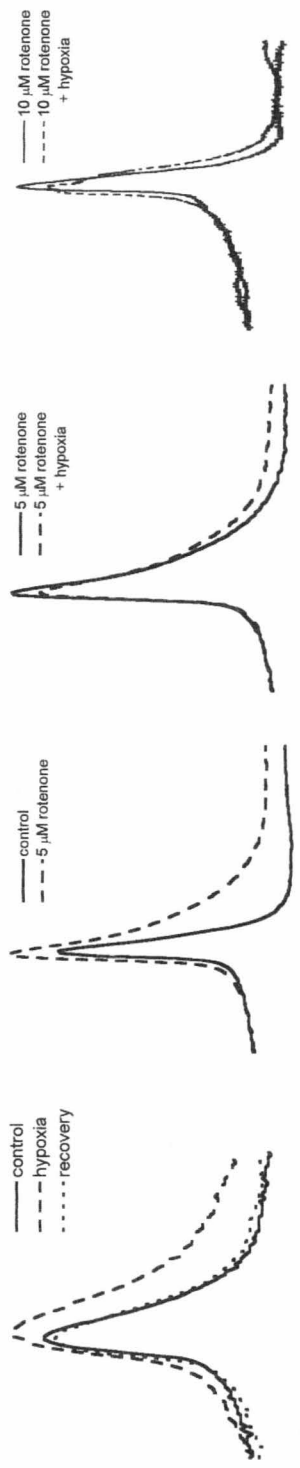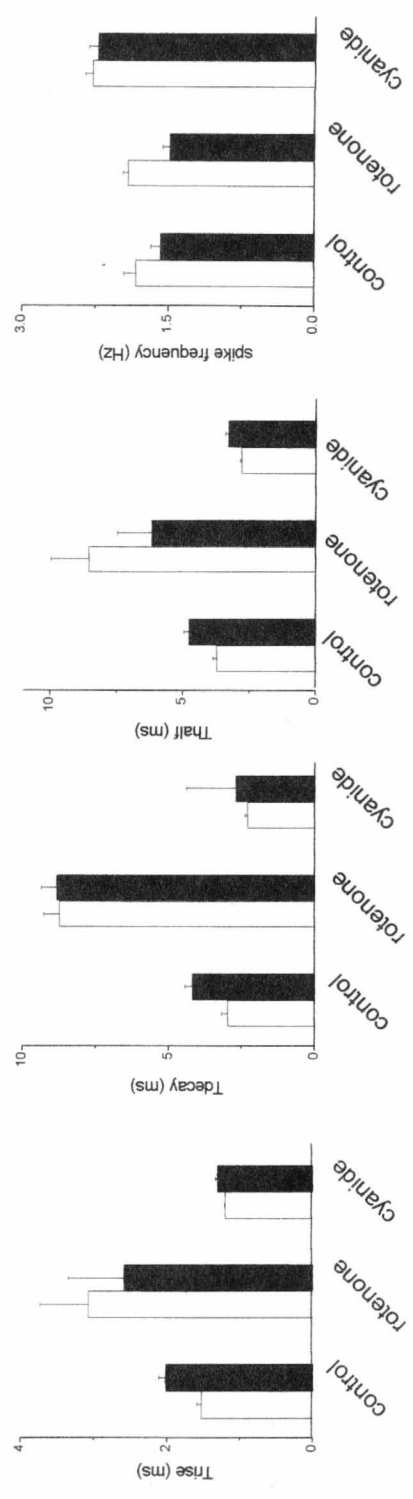
DCF (see below). To test whether hypoxia and H_2O_2 use the same pathway, cells were exposed sequentially to hypoxia followed by H_2O_2 plus hypoxia. As shown in Fig.8, hypoxia reduced outward current K^+ density from 119.1 ± 19.5 pA/pF to 101.9 ± 17.2 pA/pF (n =4; p< 0.05). The hypoxia-induced suppression of outward current was reversed upon addition of 50 µM H_2O_2. Outward current density in hypoxia plus 50 µM H_2O_2 was 127.6 ± 14.2 pA/pF, a value that is significantly different from hypoxia alone (P< 0.05) but not from control (P=0.23; Figure 8). After return to control normoxic conditions, the outward current density recovered to 116.0 ± 12.2 pA/pF (n=4), a value not significantly different from the initial control (p=0.25). These data raise the possibility that H_2O_2 may act as an intracellular signal in neonatal AMC during hypoxic chemotransduction.

Measurements of ROS during hypoxia and ETC inhibition using DCF fluorescence

In order to investigate whether changes in ROS can plausibly account for the effects of hypoxia and ETC inhibitors on neonatal chromaffin cells we used the fluorescent indicator, DCF as a probe (see, Semenza, 1999). As shown in Fig. 9A B, hypoxia caused a rapid and reversible decrease in DCF fluorescence in chromaffin cell clusters. Interestingly, in 5 of 9 cell clusters tested, there was a rebound generation of ROS following reperfusion with normoxic bathing solution, a phenomenon reminiscent of that seen during reperfusion after ischemia in many cell types (Vanden Hoek et al., 1998). Moreover, application of 10 µM rotenone (Fig. 9D) and 10 µg/ml antimycin A (Fig. 9E) under normoxic conditions mimicked the suppression of DCF

fluorescence seen during hypoxia. Application of hypoxia in the presence of these sub-saturating doses of rotenone or antimycin A (see Fig. 2) caused a further decrease in DCF fluorescence. However, the hypoxia-induced decrease in DCF fluorescence by rotenone and antimycin A did not exceed the level seen for hypoxia alone (~ 18%), suggesting that the mitochondria are the primary source for the reduced DCF fluorescence observed during hypoxia. In contrast, the distal ETC inhibitor 2 mM CN (for ~ 200 sec) had no significant effect on ROS generation in these cells (Fig. 9C).

Fig. 8. Exogenous hydrogen peroxide reverses the effects of hypoxia on outward current.

A, hypoxia ($\sim$ 5 torr) caused a reversible suppression of outward current, which was reversed by application of 50 μM H_2O_2 (steps to $+$ 30 mV are shown). B, application of H_2O_2 reverses the hypoxia-induced suppression of outward current at all voltages where outward currents are activated. Similar results were seen in 3 other cells, consistent with a decrease in H_2O_2 acting as the second messenger in the hypoxic inhibition of outward currents.

A

$c / h + H_2O_2 / w$

h

B

control
hypoxia
hyp + H_2O_2
wash

current (pA)

1000

750

500

250

-60   -30   30   60

voltage (mV)
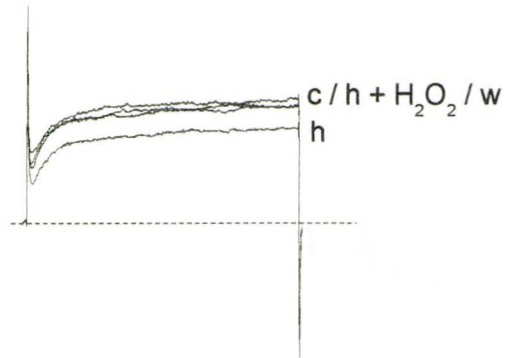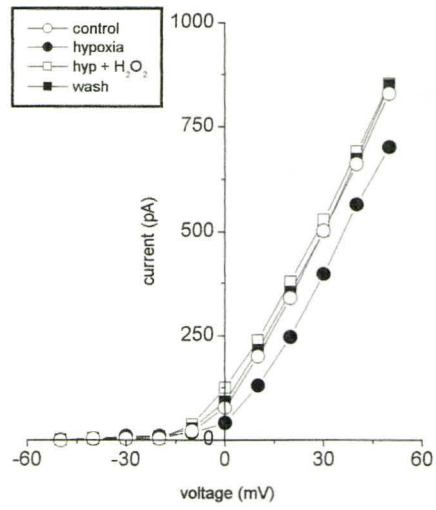
Fig. 9. Hypoxia and inhibitors of the proximal electron transport chain, but not cyanide, decrease reactive oxygen species generation in neonatal rat chromaffin cells.

Cultures were loaded with 10 µM DCF-diacetate for 40 min at 37 °C, in standard recording saline. DCF fluorescence was recorded every 10 sec and quantified as percentage change from that relative to normoxia (control). A B, hypoxia caused an inhibition of reactive oxygen species (ROS) generation in 9 clusters of chromaffin cells tested (~ 90 cells total). Note that the onset of the decrease in ROS levels was rapid and the effect was reversed upon return to normoxia. C, 2 mM cyanide did not affect DCF fluorescence and therefore ROS levels in chromaffin cells (n=4 clusters, ~ 40 cells). D, rotenone (10 µM) decreased ROS levels, the effect was slightly potentiated by hypoxia (n=6 clusters). E, antimycin A (10 µg/ml) reduced ROS levels in neonatal chromaffin cells (n=5 clusters), and the effect was further potentiated by hypoxia. In most cases, the effects of rotenone and antimycin A on DCF fluorescence were not completely reversible. It is unclear if this is due to failure of the drug to completely washout, or if it is the result of dye loss from the cells. Note that the decrease in DCF fluorescence by hypoxia in the presence of rotenone and antimycin A did not exceed the level seen in hypoxia alone, suggesting that ROS generation by hypoxia, rotenone and antimycin A converge on the same pathway.

A

phase normoxia hypoxia recovery

B

hypoxia

C

cyanide

D

rotenone
hypoxia

E

antimycin A
hypoxia
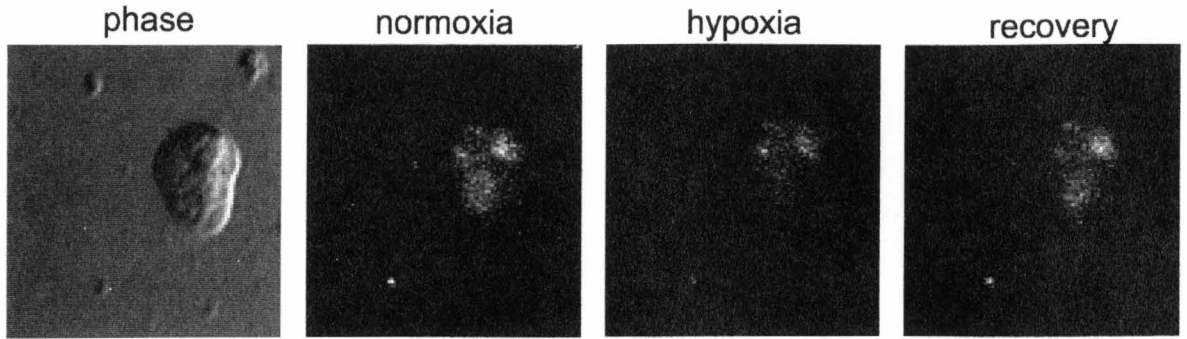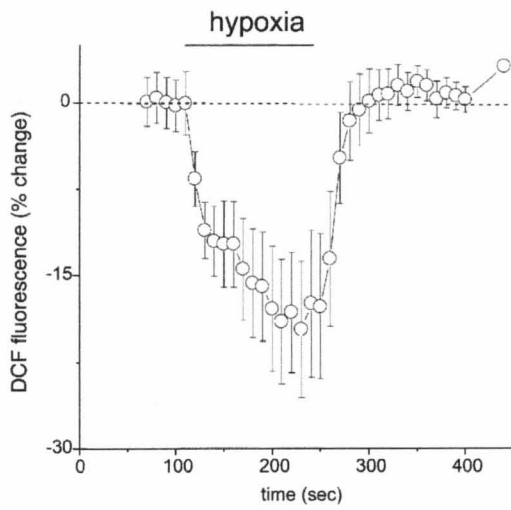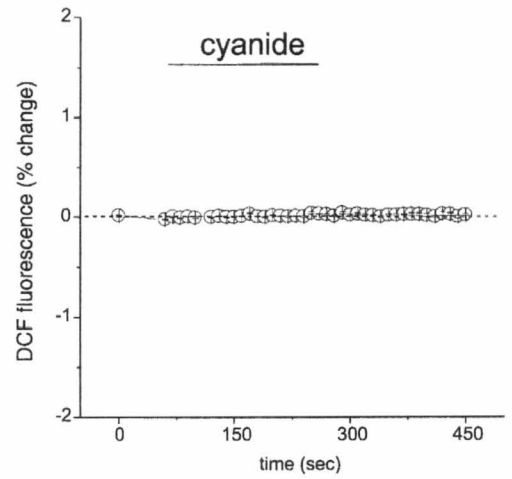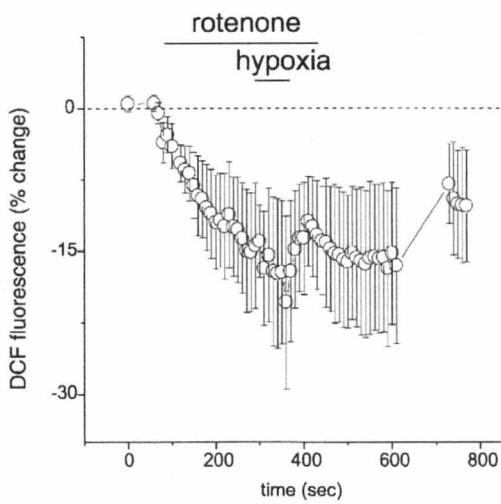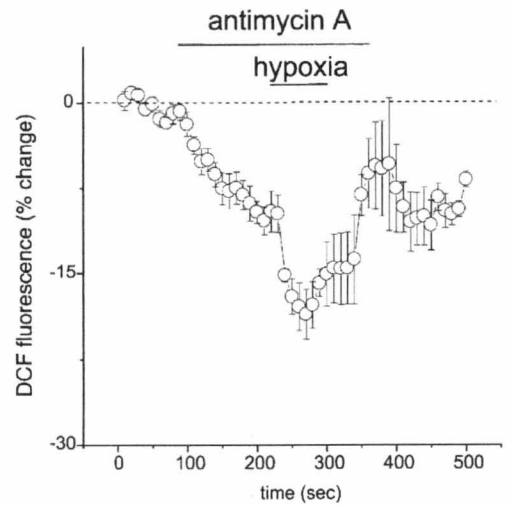
Figure 9: Thompson, Mills and Nurse

Discussion

These results strongly suggest that hypoxic chemosensitivity of neonatal rat adrenal chromaffin cells is mediated via inhibition of the proximal electron transport chain, at a site upstream of the cyanide binding site, i.e. cytochrome oxidase. The data further support the idea that a decrease in ROS generation functions as the signal that couples the mitochondrial O_2 sensor to the plasma membrane. Similar observations have been made in rat pulmonary myocytes by Archer et al. (1993), who concluded that the redox status of the cells changes during hypoxia and signals the plasma membrane. In the present study we found that exogenous H_2O_2 can reverse the inhibitory effects of hypoxia on outward K^+ current and that H_2O_2 levels, as revealed by the fluorescent probe DCF, decrease in neonatal chromaffin cells during hypoxia. In other preparations, it has been suggested that hypoxia causes an *increase* in ROS generation, which is responsible for activation of hypoxia-inducible factor (HIF-1) in HEP3b cells (Chandel et al., 1998) or muscle contraction in cardiomyocytes (Duranteau et al., 1998). However, tyrosine hydroxylase gene expression is thought to be negatively correlated with H_2O_2 levels in PC12 cells (Kroll and Czyzyk-Krzeska, 1998), a cell line derived from adrenal chromaffin cells. Interestingly, cyanide (CN) did not mimic hypoxia in any of the several tests employed in the present study (see however, Mojet et al., 1997), and similar results were reported for pulmonary myocytes (Archer et al., 1993).

We used several stringent criteria to determine whether hypoxia and ETC inhibition share a common pathway, and thereby test the hypothesis that the PO_2

sensor was located in the ETC and that changes in ROS generation were an integral part of the transduction process. Proximal ETC inhibitors, rotenone and antimycin A, but *not* the distal inhibitor CN nor the uncoupler DNP mimicked the hypoxia-induced modulation of K^+ currents. Both hypoxia and the proximal ETC inhibitors caused a net suppression of outward current, but most importantly, the effects of hypoxia were attenuated in a dose-dependent manner by rotenone and antimycin A (but not CN nor DNP). These effects of the proximal ETC inhibitors were not due to a non-specific inhibition of K^+ currents since, like hypoxia (Thompson and Nurse, 1998), rotenone and antimycin A *activated* a glibenclamide-sensitive K_{ATP} current, a component of total hypoxia-sensitive K^+ current, IKo_2.

Hypoxia and rotenone were also observed to increase action potential duration in neonatal chromaffin cells, through prolongation of the repolarizing, and to a slight extent, the depolarizing phase of the action potential. Further, the effects of hypoxia on action potential duration were attenuated in the presence of rotenone. The cause of action potential broadening is probably related to the inhibition of Ca^{2+}-dependent K^+ or BK channels. Inhibition of these channels has been shown to increase action potential duration in adult rat adrenal chromaffin cells by prolonging the depolarization of the action potential (Pancrazio et al., 1994), and indeed, we recently showed that BK channels are inhibited by hypoxia in neonatal rat chromaffin cells (Thompson and Nurse, 1997). The resulting broadening of the action potential is likely to be physiologically important, since it would be expected to facilitate calcium

entry and catecholamine secretion during perinatal hypoxic stress (see Thompson et al.,1997).

The model we propose for O_2-chemotransduction in neonatal chromaffin cells favors a hypoxia-induced decrease in mitochondrial electron transport, resulting in decreased ROS generation, which in turn signals modulation of K^+ channels, action potential broadening and catecholamine secretion. The actual O_2-binding site is not known, though it is unlikely to be at cytochrome oxidase, as suggested for carotid body type 1 cells (Biscoe and Duchen, 1992) and cardiomyocytes (Chandel et al., 1997), because CN, the classical inhibitor of cytochrome oxidase, did not mimic any of the effects of hypoxia in this study. This conclusion contrasts with that of Mojet et al. (1997), who reported that CN mimicked hypoxia in freshly-isolated neonatal rat chromaffin cells, insofar as both agents caused a rise in intracellular calcium and catecholamine secretion.

What is the site of ROS generation in the ETC that is functionally coupled to K^+ channel inhibition? Our study points to a site that lies between the antimycin A binding site of complex III and cytochrome aa_3 (O_2 acceptor and CN binding site), because inhibition of electron transport by antimycin A mimics the effects of hypoxia, whereas CN does not. We propose that during hypoxia, reduced O_2 availability causes a reduction in ROS generation at a site between complex III and cytochrome aa_3. Inhibition of the proximal ETC by rotenone or antimycin A mimics hypoxia because electron flow to the ROS generating site is reduced, which consequentially inhibits ROS generation causing a decrease in cellular H_2O_2. Cyanide may not affect electron

transport or O_2 availability to the ROS generating site, resulting in no change, an or increase in ROS levels. Indeed, increased ROS generation during CN treatment has been observed in pulmonary myocytes (Archer et al., 1993). It has been proposed that the V_{max} of cytochrome oxidase increases during hypoxia in cardiomyocytes (Chandel et al., 1997), though this does not appear to be the case in chromaffin cells. It remains to be determined whether this is due to expression of different ETC protein isoforms in different cell types.

How does a decrease in ROS generation modulate K^+ channels? The initial ROS generated is likely superoxide or hydroxyl radicals, but it is not clear whether these ROS modulate K^+ channels directly, or indirectly following conversion to H_2O_2 by superoxide dismutase. H_2O_2 may affect K^+ channel activity either directly or through a change in the cell's redox state (Lopez-Barneo et al., 1996). We observed that application of exogenous H_2O_2 reversed the effects of hypoxia on K^+ channels, though it is not clear which pathway is involved. Interestingly, H_2O_2 has been shown to directly activate BK channels (DiChiara and Reinhart, 1997) in isolated membrane patches and may inhibit ATP-sensitive K^+ channels (Roper and Ascroft, 1995). Since we previously showed that both these channels are oppositely regulated by anoxia in neonatal chromaffin cells (Thompson and Nurse, 1998), it is plausible that H_2O_2 could function as a key second messenger that co-ordinates the regulation of K^+ channels during hypoxic stress.

General Discussion

The ability to sense changes in blood oxygen tension (Po_2) and make appropriate physiological adjustments is vital for survival of all mammals. In adults, hypoxia is sensed by peripheral chemoreceptors, which relay information to the central pattern generator in the brain stem, resulting in increased respiration. Activation of the central pattern generator is also thought to initiate catecholamine (CA) secretion from adrenal chromaffin cells via activation of the sympathetic nervous system (Jones et al., 1988). In the newborn however, the sympathetic nervous system is immature, yet the rat adrenal gland still releases CA during episodes of hypoxia, such as those that accompany labour and birth (Lagercrantz and Slotkin, 1985). Hypoxia-evoked CA secretion from embryonic and neonatal AMC is 'non-neurogenic' and disappears along a time course similar to the development of sympathetic innervation (Seidler and Slotkin, 1985; Rhykov et al., 1999; Chapter 1 in this thesis). Therefore, it was hypothesised that rat adrenomedullary chromaffin cells (AMC) possess mechanisms for sensing hypoxia in the perinatal period and that these mechanisms are lost with postnatal maturation of sympathetic innervation. The cellular and molecular mechanisms of O_2-sensing in AMC were compared to carotid body glomus cells, which similarly are derived from the sympatho-adrenal sublineage of the neural crest.

Several methods were used to determine if rat AMC could respond directly to hypoxia. Embryonic (E16-18), neonatal (P1-2) and juvenile (P14-21) AMC were maintained in culture (for 1 to 5 days) and assayed for O_2-chemosensitivity using the

nystatin perforated-patch configuration of whole-cell recording (Horn and Marty, 1988). In particular, the effects of hypoxia on voltage-dependent currents and membrane potential were investigated. In parallel studies, high-pressure liquid chromatography (HPLC) was used by other members of the laboratory (A. Jackson and S. Farragher) to quantify CA release from cultured AMC. In addition, I used carbon fibre amperometry to measure hypoxia-evoked amine secretion from small clusters of neonatal AMC (Chapter 1). Though a minor component of the overall thesis, the latter study corroborated the main results obtained by HPLC.

It was observed that *embryonic* and *neonatal*, rat AMC responded to hypoxia with a suppression of outward current (Chapters 1 and 2), membrane depolarization (Chapters 1 and 2), action potential broadening (Chapter 3), increased Ca^{2+} influx through L-type Ca^{2+} channels (Chapter 1) and CA secretion (Chapters 1 and 3). Additionally, several K^+ currents were differentially modulated by hypoxia (Chapter 2) and had specific developmental patterns of expression (Appendix 1). In contrast, these effects of hypoxia were absent in juvenile rat AMC (Chapter 1). Similar results were obtained in the mouse. For example, neonatal mouse AMC showed hypoxic modulation of K^+ currents, membrane depolarization, action potential broadening and CA secretion. The juvenile mouse AMC, like those from the rat, were not O_2-sensitive when tested shortly after isolation (1-3 days). However, hypoxia-sensing mechanisms reappeared after 3 days in culture.

Strong evidence was obtained supporting a component of the mitochondrial electron transport chain (ETC) as the O_2-sensor in neonatal rat AMC (Chapter 4), and

tests on a transgenic mouse model suggested that putative O_2-sensor protein, NADPH oxidase, was not involved (Chapter 3). Finally, it was proposed that the second messenger which transduces the hypoxic signal from the ETC to the plasma membrane was a decrease in reactive oxygen species and evidence in support of hydrogen peroxide as the likely candidate was presented (Chapter 4).

Comparison of O_2-sensing between adrenal chromaffin and glomus cells

It is interesting to compare the mechanisms of O_2-sensing between AMC and the glomus cells of the carotid body, especially since the hypoxic sensitivity of AMC peaks around birth, when that of the carotid body is blunted (Hertzberg et al., 1990). Additionally, like AMC, glomus cells are of neural crest origin and share a chromaffin cell phenotype. They also occur in clusters *in vivo*, where they play a role in regulating cardiopulmonary physiology. Further, the responses of glomus cells to hypoxia are well characterized and thus, the comparison could provide information on whether neural crest-derived O_2-chemosensors use common signalling mechanisms.

At first glance, the mechanisms of O_2-sensing in the rat glomus cell and AMC appear similar. Following exposure to hypoxia, both cells show suppression of voltage-dependent outward K^+ current (Peers, 1990; Stea and Nurse, 1991; Thompson et al., 1997; Thompson and Nurse, 1998; Chapters 1, 2 and 3), membrane depolarization (Buckler and Vaughan-Jones, 1994; Thompson et al., 1997; Thompson and Nurse, 1998; Chapters 1 and 2), Ca^{2+} influx through L-type channels (Buckler and Vaughan-Jones, 1994; Thompson et al., 1997; Chapter 1), and neurotransmitter secretion (Donnelly,

1993; Gonzalez et al., 1994; Jackson and Nurse, 1997; Zhang et al., 1997; Thompson et al., 1997; Chapter 1). However, there are several differences between these two neural crest cell types that likely reflect their different phenotypes and functions in the organism.

O_2-sensitive K^+ currents in neural crest-derived chromaffin cells

Interesting differences are seen in the types of K^+ currents that are modulated by hypoxia in the glomus cell and AMC. Although, both the glomus cell and AMC respond to hypoxia with a net suppression of voltage-dependent outward current, this entire suppression can be accounted for by inhibition of large-conductance Ca^{2+}-dependent K^+ current in the rat glomus cells (BK; Peers, 1990; Lopez-Lopez et al., 1998). In addition, rat glomus cells also express an O_2-sensitive 'leak' K^+ conductance that may initiate membrane depolarization during hypoxia (Buckler, 1997, 1999; Buckler et al., 2000). Rat AMC in contrast, express three types of O_2-sensitive K^+ current that are differentially modulated by hypoxia (Chapter 2). These include BK and a delayed rectifier K^+ current (K_v) which are inhibited, and K_{ATP}, which is *activated* by hypoxia.

Hypoxic suppression of BK currents has been observed in rat glomus cells (Peers, 1990) and rat and mouse AMC (chapters 2 and 3). The precise role of this channel in evoking neurotransmitter release from the glomus cell during hypoxia is still unclear. However, blockade of these channels by iberiotoxin (IbTX) leads to CA secretion from glomus cells in thin carotid body slices (Pardal et al., 2000). In rat AMC, it appears that inhibition of BK currents by IbTX is intimately linked to broadening of action potentials, through a prolongation of the spike repolarizing phase (i.e. increased repolarizing time

constant; Pancrazio et al., 1994). Similar changes in action potential duration were seen during hypoxia in neonatal rat AMC (Chapter 4), suggesting that inhibition of O_2-sensitive BK currents causes action potential broadening, thereby facilitating Ca^{2+} influx through L-type channels and CA secretion. Glomus cells from the rat normally express a low density of Na^+ channels, and thus rarely fire spontaneous action potentials (Stea and Nurse, 1991; Stea et al., 1995; Peers and Buckler, 1995). Most of this work was performed on singly isolated glomus cells, which may be hyperpolarized relative to cells in their native clustered arrangement (Taylor et al., 1999; see also Pardal et al., 2000). However, a recent study suggests that glomus cells in large clusters may fire spontaneously and that inhibition of BK currents by hypoxia may also play a role in action potential broadening and neurotransmitter secretion (Zhang and Nurse, 2000). Interestingly, recordings from AMC in clusters (Chapters 3 and 4) suggests that singly isolated chromaffin cells may also be depolarized relative to those in a clustered arrangement.

Rat and mouse neonatal AMC have a Ca^{2+}-independent K^+ current (K_V) that is also inhibited by hypoxia. It is not known if this K_v current is mediated by the same channels in these cells, though the currents do appear macroscopically similar. In the rabbit glomus cell, inhibition of K_v is proposed to contribute to an increase in action potential frequency during hypoxia (Montoro et al., 1996). Increases in action potential frequency were not observed in neonatal rat or mouse AMC (chapters 3 and 4). Additionally, hypoxia has been reported to inhibit K_v 1.2 *shaker* K^+ channels in PC12 cells (Conforti and Millhorn, 1997; Conforti et al., 2000), a cell line derived from a rat

AMC tumour, and the channels are likely responsible for the hypoxia-induced membrane depolarization (receptor potential) seen in PC12 cells (Zhu et al., 1996).

It is possible that inhibition of *shaker*-like K^+ channels in rat and mouse AMC contributes to membrane depolarization and action potential broadening. This channel is sensitive to TEA, which depolarized neonatal rat AMC (Thompson and Nurse, 1998; Chapter 2). However, the hypoxia-induced membrane depolarization was similar in the presence of TEA suggesting that this channel is not the major contributor to the receptor potential in these cells (Thompson and Nurse, 1998; Chapter 2). However, PC12 cells appear to be more depolarized at rest than AMC (Zhu et al., 1996; Chapter 2) and hypoxic inhibition of K_v channels may be significant at lower resting membrane potentials.

In addition to hypoxia-sensitive BK and K_v currents, AMC also expressed a Ca^{2+} dependent K^+ current that was augmented by hypoxia and appeared to belong to the family of ATP-sensitive K^+ currents (K_{ATP}). These channels are either inward or outward rectifiers, Ca^{2+}-dependent or independent, inhibited by increasing ATP concentrations, and sensitive to the glibenclamide (Ashcroft and Ashcroft, 1990). This K_{ATP} current was not active during normoxia ($PO_2 \sim 150$ mmHg) since glibenclamide had no affect on outward currents at this PO_2. However, an outward current could be activated by pinacidil, an activator of K_{ATP}, suggesting that the underlying channels are present in neonatal AMC. Interestingly, anoxia (chapter 2) and hypoxia (not shown) were found to increase the glibenclamide-sensitive component of outward current. The effects of glibenclamide were absent in the presence of Cd^{2+}, which blocks Ca^{2+} entry and

indirectly, Ca^{2+}-dependent K^+ currents. A hypoxia-sensitive channel with similar pharmacology and Ca^{2+} dependence has been described in neurons of the substantia nigra (Jiang et al., 1994), but not in glomus cells (Peers and O'Donnell, 1990). However, electrophysiological studies on glomus cells traditionally involve conventional whole-cell recording, where the intracellular milieu is replaced with a high ATP containing solution. This would serve to inhibit K_{ATP} and make its presence difficult to detect under these recording conditions.

In substantia nigra neurons, activation of K_{ATP} is proposed to cause membrane hyperpolarization during hypoxia and appears to play a protective role during oxidative stress. In Chapter 2 of this thesis, a similar role is proposed for K_{ATP} in neonatal AMC, since the hypoxia-induced depolarization is larger in the presence of glibenclamide. Therefore, activation of K_{ATP} by hypoxia may serve to limit Ca^{2+} influx and CA secretion, thereby allowing AMC to respond to repetitive bouts of hypoxia or prolonged O_2 deprivation.

The presence of multiple hypoxia-sensitive K^+ currents in AMC provides these cells with a versatile mechanism for regulating CA secretion during hypoxia. Interestingly, the three voltage-dependent, hypoxia-sensitive currents do not appear to contribute significantly to the hypoxia-induced membrane depolarization, but K_{ATP} may play a role in limiting its magnitude (Thompson and Nurse, 1998; Chapter 2). These data suggest that there is another component to the O_2-sensing mechanism in neonatal AMC.

Origin of the receptor potential

The mechanism that is primarily responsible for the receptor potential (hypoxia-induced depolarization) in neonatal AMC was not identified in this thesis. Examination of the literature suggests that there are several possibilities that include both channels and electrogenic pumps.

The glomus cells of the rat carotid body express an O_2-sensitive, voltage-independent background K^+ conductance that is active at the resting membrane potential and may belong to a class of pH-sensitive K^+ leak conductances called TASK (Buckler, 1997; Kim et al., 1999; Buckler et al., 2000). This channel has a conductance of 14 pS and is half-maximally inhibited at a $PO_2 \sim 12$ mmHg. The glomus cell K^+ 'leak' channel is also inhibited by millimolar concentrations of Ba^{2+}, which appears to mimic hypoxia in these cells (Buckler, 1999; Buckler et al., 2000). These channels therefore, appear ideally suited to play a role in the hypoxia-induced depolarization of single quiescent glomus cells (Buckler, 1997; 1999). It has been suggested that the resting membrane potential of single glomus cells in culture is hyperpolarized relative to clustered cells (Taylor et al., 2000), so the relative importance of K^+ leak channels in the normal physiological responses of glomus cells during hypoxia remains to be determined. Further, clusters of cultured glomus cells may fire spontaneous action potentials (Zhang and Nurse, 2000) and CA secretion can be induced in thin carotid body slices by the specific BK channel blocker, IbTX (Pardal et al., 2000). It is not known whether similar hypoxia-sensitive

'leak' K^+ channels are expressed in AMC, though if present, they may play a role in depolarization of single AMC during hypoxia (see Chapter 2).

Additionally, a human ether-a-go-go (HERG) like channel has been described in the glomus cells of the rabbit carotid body (Kiehn et al., 1996; Overholt et al., 2000). This channel is an inward rectifier K^+ channel that is open at the resting membrane potential and inhibited by millimolar Ba^{2+} (Overholt et al., 2000). It is possible that inhibition of this channel during hypoxia can generate the receptor potential in rabbit glomus cells (Overholt et al., 2000). However, this channel has not been identified in rat AMC.

Other potential meechanisms for the receptor potential in neonatal AMC are the activation of a non-selective cation channel and inhibition of the Na^+/K^+ ATPase. These possibilities have been suggested for adult guinea pig AMC, which are O_2-sensitive (Inoue et al., 2000). In these cells CN, which is thought to mimic hypoxia (see Chapter 4 however), activates a non-selective cation (Na^+, Ca^{2+}, and K^+ permeable) conductance, which depolarizes the membrane and is inhibited by millimolar concentrations of Ba^{2+} (Inoue et al., 2000). Additionally, depletion of ATP during application of CN is proposed to inhibit a ouabain-sensitive Na/K pump, which further contributes to the receptor potential (Inoue et al., 2000).

At present, activation of cation channels during hypoxia in rat AMC cannot be ruled out. However, a role for these channels in rat AMC seems unlikely since the receptor potential was associated with a decrease in membrane conductance, consistent with the closure of channels that are open at rest (Thompson et al., 1997; Chapter 1).

Moreover, perfusion with a Na^+/Ca^{2+}-free solution hyperpolarized neonatal rat AMC and reduced the magnitude of the receptor potential (see Chapter 2). This suggests that at rest there is a cation leak current that contributes to the resting potential and that removal of the permeant cations may serve to reduce the receptor potential. However, an alternative explanation is that the hyperpolarization induced by removal of Na^+ and Ca^{2+} decreases the driving force on K^+ conductance, reducing the receptor potential. Inhibition of a Na^+/K^+ pump does not appear to be involved in generation of the receptor potential because ouabain and strophanthidin, inhibitors of p-type ATPases did not mimic the effects of hypoxia or prevent the hypoxia-induced depolarization (Chapter 2).

In PC12 cells, a cell line derived from a rat AMC tumour, inhibition of a TEA-sensitive, Ca^{2+}-independent K^+ channel (likely K_v 1.2) can account for the membrane depolarization seen during hypoxia. In the presence of TEA, the resting membrane potential depolarized and the receptor potential was ablated (Zhu et al., 1996; Conforti and Millhorn, 1997; Conforti et al., 2000). TEA was also found to depolarize neonatal rat AMC, however, the magnitude of the receptor potential was unaffected (chapter 2). Therefore, K_v 1.2 does not appear to play a major role in generation of the receptor potential in these cells.

A recent study suggests that a proportion of *adult* rat AMC are O_2-sensitive (Lee et al., 2000), which is in contrast to the lack of O_2-sensing observed in juvenile (14-21 day olds) rat and mouse AMC (Thompson et al., 1997; Chapters 1 and 3). It was proposed that inhibition of an apamin-sensitive, small conductance Ca^{2+}-dependent K^+ current (SK) was responsible for the receptor potential in *adult* AMC (Lee et al., 2000).

Exposure to apamin mimicked the hypoxic suppression of outward current, depolarized the membrane, and blocked the receptor potential (Lee et al., 2000). Further, these channels are known to be open at the resting membrane potential in adult rat AMC (Neely and Lingle, 1992), so they are excellent candidates for generating the receptor potential. To date, no information is available on whether these channels are present in neonatal AMC, but since the data presented in this thesis suggest involvement of a K^+ conductance in the receptor potential (see above), a role for SK cannot be ruled out.

Though the data currently available support either activation of a cation channel (Inoue et al., 2000) or inhibition of SK (Lee et al., 2000) as the mechanism underlying the receptor potential, other possibilities exist. It was observed in neonatal rat AMC that Ba^{2+}(5 mM) can mimic the effects of hypoxia on membrane potential (not shown). However, the effects of Ba^{2+} are relatively non-selective since this cation can inhibit the hypoxia-sensitive K^+ leak current in rat (Buckler, 1999; Buckler et al., 2000) and the HERG-like channel in rabbit (Overholt et al., 2000) glomus cells. Millimolar Ba^{2+} also blocks the non-selective cation channel in guinea pig AMC (Inoue et al., 2000), and SK channels in adult rat AMC (Park, 1996). Thus, further experiments are required to determine which channel(s) are involved in generation of the receptor potential in neonatal AMC.

Development of the O_2-sensing mechanism in adrenal chromaffin cells

In this thesis, it was shown that rat embryonic AMC as well as neonatal rat and mouse AMC are O_2-chemosensitive. Additionally, AMC isolated from juvenile animals

lacked hypoxia-sensitivity, indicating that this property is lost by 2-3 weeks of postnatal life. The O_2-sensing mechanisms involve the net suppression of outward currents, membrane depolarization, action potential broadening, Ca^{2+} influx through L-type channels, and catecholamine secretion. The developmental loss of O_2-chemosensitivity in AMC is consistent with the hypothesis that maturation of sympathetic innervation regulates the hypoxia-sensing mechanism. However, since a proportion of adult rat AMC were recently reported to be O_2-sensitive (Lee et al., 2000), it is of interest to determine the extent of functional innervation of chromaffin cells in the adult adrenal medulla.

It has been reported that neonatal rats exposed to hypoxia (5% for 1 hr) release adrenal CA and that this response is not inhibited by the nAChR blocker, chlorisondamine (Seidler and Slotkin, 1985). Further, release of CA in adult rats could be inhibited by chlorisondamine, suggesting that responses of AMC to hypoxia in the adult are mediated mainly through the central nervous system (Seidler and Slotkin, 1985; Slotkin and Seidler, 1988). Treatments that accelerate the development of sympathetic innervation (e.g. maternal stress) hasten the loss of the 'non-neurogenic' hypoxic responses in the neonate (Seidler and Slotkin, 1985). On the other hand, denervation of the adult rat adrenal gland causes a return of this non-neurogenic O_2-sensing mechanism (Slotkin and Seidler, 1988). Similarly, fetal sheep AMC respond directly to hypoxia before, but not after, the development of sympathetic innervation (Cheung, 1994). Consistent with a role of innervation in regulating O_2-sensing by AMC, denervation produced by culturing of these cells from juvenile rat (for 7 days) and mouse (for > 3 days) appears to cause a return of the direct hypoxic sensing mechanism

(Mochizuki-Oda et al., 1997; Chapter 3). Taken together, these studies suggest that maturation of sympathetic innervation to the adrenal gland results in a loss of the direct O_2-sensing mechanism in AMC.

How does innervation regulate the O_2-sensing mechanism? One possibility is that activation of the nicotinic AChR by ACh released from sympathetic nerves can down-regulate oxygen-sensing by AMC. Indeed, infusion of pregnant rats with nicotine via minipumps at a rate of 6 mg/kg/day causes the pups to loose their hypoxia tolerance. This is thought to be due to loss of the direct O_2-sensing response by AMC, since CA release was not augmented during hypoxia (Seidler and Slotkin, 1986; Slotkin et al., 1995).

Activation of the nAChR is thought to activate protein kinase C (PKC) via Ca^{2+} influx through the receptor (Huganir and Miles, 1989), which may regulate gene expression. The loss of hypoxic sensitivity likely represents loss of the O_2-sensor, or coupling mechanisms, rather than an alteration in ion channel expression, since a similar compliment of K^+ channels has been observed in neonatal (Thompson and Nurse, 1998; Chapter 2) and adult AMC (Neely and Lingle, 1992). Thus, it is possible that nAChR stimulation causes down-regulation of the oxygen sensor. Experiments performed during the course of this thesis, involving chronic exposure (1 week) of cultured neonatal rat AMC to nicotine (100 μM) or high K^+ (30 mM) did not eliminate O_2-chemosensitive properties (not shown). However, the concentration of nicotine used may be considered high, insofar as it likely causes nAChR desensitization (Huganir et al., 1986). This work does not support however, the idea that depolarization produced by sympathetic innervation (mimicked by high K^+) is the signal for loss of O_2-sensing.

Physiological relevance of a developmentally-regulated O₂-sensing mechanism

Release of CA from neonatal AMC during hypoxia has well-defined roles in protecting the animal from O_2-stress and in development of lung maturation after birth (Lagercrantz and Slotkin, 1986; see also section 4 in the General Introduction). Thus, the O_2-sensing mechanism in chromaffin cells seems to have its most important function for neonatal survival just after birth. Hypoxia-sensing mechanisms seem especially important in light of the observation that the animal's principle O_2-chemoreceptors, the glomus cells of the carotid body, are undergoing resetting of their sensitivity in the period immediately after birth (Hertzberg et al., 1990, 1997; Wasiko et al., 1999). This likely reflects the increase in blood PO_2 that accompanies the transition to air breathing life and loss of dependence on the placenta for gas exchange. At this early stage, the glomus cells are less sensitive to hypoxia, and after resetting, physiological responses to hypoxia are mediated through the carotid sinus reflex stimulation of respiration (Gonzalez et al., 1994). The resetting of the glomus cell's O_2-sensitivity, together with the immaturity of sympathetic innervation to the adrenal glands, suggests that the neonate must have alternative mechanisms for responding to hypoxia. Episodes of hypoxia (e.g. apnoea) are frequently encountered by the neonate and are common occurrences during lung development (Slotkin and Seidler, 1988). Thus, direct O_2-sensing and hypoxia-evoked CA release from AMC seems ideally suited to play a protective role in the neonate.

Why are embryonic AMC also sensitive to hypoxia? It would seem paradoxical to have a functional O_2-sensing mechanism releasing CA that could cause early maturation

of the cardiopulmonary system prior to birth. However, it appears that the O_2-sensing mechanism and the state of AMC development in the embryo are immature, which may function to limit CA release during fetal hypoxia. Evidence that the O_2-sensing mechanism is developing in embryonic E16-18 AMC comes from observations in this thesis that the major O_2-sensitive component of outward current (BK) is absent or non-functional, but other O_2-sensitive currents, K_v and K_{ATP} are present (see Appendix 1). Increased expression of BK currents over the next 4-6 days as the animal approaches birth may allow AMC to fire repetitive action potentials during stimulation (Solaro et al., 1995), and facilitate hypoxia-evoked CA release through modulation of action potential duration.

It was also observed that AMC from embryonic rats release predominantly NE during hypoxia, while those from neonatal rats secrete predominantly E (Jackson, 1997). This is likely due to the lack of expression of PNMT, the enzyme required for synthesis of E from NE, which does not appear in the rat until E18 (Verhofstad et al., 1985). PNMT expression is known to be strongly upregulated by corticosteroids, and the adrenal cortex (the primary source of GC) is immature in the embryo, but increases in size and GC content after birth (Phillippe, 1983). Thus, the predominant release of NE over E from embryonic AMC may function in a developmental role, rather than one involved in physiological protection (as in the neonate). Indeed, circulating NE is known to modulate adrenergic receptor expression (Hadcock and Malbon, 1993), and may serve to maintain the fetal complement of adrenergic receptors (e.g. high levels of α receptors in the heart).

In neonatal AMC, the O_2-sensing mechanism is fully developed. There are three, and possibly four, pharmacologically distinct K^+ currents that are differentially modulated by hypoxia. Why are there multiple O_2-sensitive K^+ currents in a single cell type? Conceivably, different K^+ currents may combine to provide fine regulation of CA release over a broad Po_2 range. For example, these channels may or may not be Ca^{2+}-dependent (i.e. BK and K_{ATP} are Ca^{2+}-sensitive, whereas K_v is not) and increases in intracellular Ca^{2+} during hypoxia can act in a negative feedback manner to limit CA secretion via activation of BK and K_{ATP}. Further, if the channels have different O_2-sensitivities, then dynamic modulation of action potential duration, membrane depolarization, and CA secretion can be achieved. The precise O_2-affinity of each channel has not been determined and must await single channel analysis. However, single channel analysis of O_2-dependence will be complicated by the observation that the sensor appears to be located in the mitochondria (Chapter 4), which are likely excluded during excised patch formation. Indeed, BK channels in excised patches from rat glomus cells are not modulated during hypoxia, unlike those in perforated vesicles, where a portion of the cytoplasm is retained (Wyatt and Peers, 1994). These data suggest that a cytoplasmic component is required for O_2-sensing.

Why do AMC from juvenile rats and mice lose O_2-sensitivity? From a physiological viewpoint, a 'direct' hypoxic response by AMC is no longer needed in the older animal. This is because both the carotid sinus reflex and sympathetic nervous system are mature, thereby allowing CA secretion from AMC to be under nervous control (Jones et al., 1988). CA secretion in adult rats, can be more precisely controlled

since different frequencies of splanchnic stimulation and activation of sub-populations of splanchnic neurons can evoke release of different CA species or peptidergic transmitters (Parker et al., 1993). This would allow the animal to tailor its stress response to the specific stressor encountered.

It appears that the loss of direct O_2-sensing in the juvenile rat and mouse (Seidler and Slotkin, 1985; Chapters 1 and 3) is due to down regulation of the sensor or uncoupling of the K^+ channels from the second messenger (e.g. ROS), since a similar complement of K^+ channels is observed in adult and neonatal rat AMC (Neely and Lingle, 1994; Chapter 2). However, it is possible that different isoforms of K^+ channels are expressed in the adult versus the neonate. Indeed, different proportions of BK channel types that may have varying sensitivities to ROS were observed in neonatal and adult AMC (Solaro et al., 1996; Chapter 2).

Cellular mechanisms of O_2-sensing

Two potential mechanisms of O_2-sensing were examined in this thesis. First, a knockout mouse model, deficient in gp91^{phox}, was used to ascertain the role of the NADPH oxidase complex in O_2-sensing. This model predicts that decreased O_2 availability decreases H_2O_2 generation by the oxidase, which then modulates K^+ channels either directly or through a change in the cell's redox status (Acker et al., 1989). The second mechanism tested was that hypoxia acts via inhibition of electron transport in the mitochondrial ETC, leading to increases or decreases in ROS generation, or changes the cellular ATP/ADP ratio. In the second model, ROS or a change in ATP/ADP ratio may

either directly modulate channels or affect the cell's redox status, which in turn modulates channel activity (Archer et al., 1993; Mojet et al., 1996; Chandel et al., 1997; Buckler and Vaughan-Jones, 1999). This model was tested using inhibitors of the ETC or uncouplers of ATP production to determine if they can mimic and attenuate the effects of hypoxia on K^+ channels.

NADPH oxidase does not function as the O_2-sensor in AMC

Evidence presented in Chapter 3 suggests that the NADPH oxidase is not the primary O_2-sensor in AMC. All three voltage- and O_2-sensitive K^+ currents found in the rat were also observed in wild type mouse AMC, suggesting that the mechanism of O_2-sensing is similar in these two species. The persistence of hypoxic suppression of BK and K_v, and activation of K_{ATP}, in AMC from oxidase deficient mice (Chapter 3) suggests that these cells continue to sense hypoxia similar to wild type cells. The data further suggest that all three types of O_2-sensitive K^+ channels use a single sensor (see below) and that multiple sensors (one for each channel type) are unlikely to be present. Evidence that all three O_2-sensitive K^+ currents are modulated by inhibition of the mitochondrial ETC in neonatal rat adds further support to the idea of a single O_2-sensor (see below).

Interestingly, pulmonary neuroepithelial body (NEB) cells from a similar oxidase deficient mouse lose sensitivity to hypoxia (compared to wild type cells), as assayed by hypoxic suppression of outward current (Fu et al., 2000). These data suggest that that the NADPH oxidase can function as the O_2-sensor in some cell types. In contrast, pulmonary smooth muscle cells, which produce vasoconstriction during hypoxia (Archer et al.,

1993), still retain hypoxic sensitivity in mice deficient in gp91^{phox} (Archer et al., 1999). Taken together, data from different O_2-sensitive cells isolated from control and oxidase deficient mice suggest that the NADPH oxidase can function as the sensor in NEB cells, but apparently not in other cell types.

Role of the electron transport chain as the O_2-sensor in AMC

The persistence of O_2-sensing in mouse AMC, deficient in NADPH oxidase function, means that AMC use a different O_2- sensor than NEB cells (see above). One possibility is that AMC sense hypoxia via inhibition of electron transport through the mitochondrial electron transport chain as proposed for other cell types (Biscoe and Duchen, 1992; Archer et al., 1993; Semenza, 1999). Decreased electron transport may be coupled to an increase (Chandel et al., 1998) or decrease (Archer et al., 1993) in ROS generation, or to a change in the ATP/ADP ratio (Mojet et al., 1996; Duchen, 1999).

Data are presented in Chapter 4 of this thesis suggesting that inhibition of the ETC by hypoxia, coupled to a decrease in ROS generation, functions as the O_2-sensor and second messenger signalling pathway during hypoxic chemotransduction. This hypothesis is supported by the observations that drugs which inhibit the more proximal electron transport, rotenone and antimycin A, mimic and attenuate the effects of hypoxia in a dose-dependent fashion. Sub-saturating doses of rotenone and antimycin A (5-10 μM) suppressed outward currents in neonatal AMC and reduced the magnitude of the hypoxia-sensitive outward current (IKo$_2$). On the other hand, saturating doses of these drugs (50 μM) ablated the effects of hypoxia on outward current. These data suggest that

hypoxia and proximal ETC inhibition modulate K^+ currents via a common pathway. This is further supported by the observation that rotenone can activate K_{ATP} while inhibiting BK and K_v currents. Thus, it is unlikely that the effects of the proximal ETC inhibitors, rotenone and antimycin A, on K^+ channels are due to a non-specific action of the drugs on the channel itself, since they can oppositely modulate distinct K^+ currents, as does hypoxia.

How does inhibition of electron transport during hypoxia and proximal ETC inhibition alter ROS generation by the mitochondria? The pharmacological data presented in Chapter 4, combined with the use of DCF fluorescence, provide insight into the mechanism of ROS generation by the mitochondria. The observations that rotenone and antimycin A, which inhibit electron transport up to the iron-sulphur (FeS^-) component of complex III (Hatefi, 1985), mimic hypoxia indicate that the important site of ROS generation in AMC lies between FeS^- and cytochrome aa_3 of complex IV (see Figure 1). The failure of CN, an inhibitor of cytochrome aa_3, to mimic or attenuate the effects of hypoxia further supports this hypothesis. A model for the decreased generation of ROS during hypoxia is presented in figure 1 of this section of the thesis, and an explanation is given below.

Under conditions of normal O_2 availability (normoxia), cytochrome aa_3 is in an oxidized state, and the proximal electron carriers are more reduced (Mitchell, 1961; Nicholls and Budd, 2000). This is important to ensure an electrochemical gradient for the transfer of electrons through the ETC to O_2 at cytochrome aa_3. The model proposes that during hypoxia, O_2 becomes less available to the ROS generating site between FeS- and

cytochrome aa3, which reduces ROS generation (possible O_2^-) and ultimately decreases H_2O_2 levels in the cytoplasm. Rotenone and antimycin A mimic the effects of hypoxia because they inhibit electron transport to the FeS^-/cytochrome aa_3 site of ROS generation and consequently decrease ROS production by the mitochondria. CN on the other hand, may not affect ROS generation because it competes with O_2 for the binding site on cytochrome aa_3, but does not accept electrons. This may serve to reduce cytochrome aa_3 relative to its redox state during normoxia and either produce no change, or increase ROS generation since electrons are still available for the FeS^-/cytochrome aa_3 site. Indeed, increased ROS generation by CN has been observed in pulmonary myocytes (Archer et al., 1993), which appear to have a similar O_2-sensor to AMC. However, in this thesis CN did not affect ROS generation by neonatal AMC (Chapter 4).

The evidence presented in Chapter 4 also suggests that a change in ATP/ADP ratio is not the functional second messenger during hypoxia chemotransduction in neonatal AMC. This was based on the observation that DNP, an uncoupler of ATP production, and CN, which is thought to decrease ATP levels in neonatal AMC (Mojet et al., 1996), did not mimic the effects of hypoxia. Therefore, the functional second messenger for hypoxic chemotransduction in neonatal AMC appears to be a decrease in ROS generation, leading to a decrease in H_2O_2 levels and K^+ channel modulation. The observation that exogenous H_2O_2 can reverse the effects of hypoxia on outward K^+ currents in neonatal AMC suggests that H_2O_2 alone can function as the second messenger (Chapter 4). Furthermore, application of reducing agents can augment cloned BK currents expressed in HEK 293 cells (DiChiara and Reinhart, 1997) and exogenous H_2O_2

can activate K_{ATP} current in hippocampal neurons (Roper and Ashcroft, 1995; Tokube et al., 1998), which are consistent with these channels being regulated by intracellular H_2O_2.

What is the site of O_2-binding, and thus the O_2-sensor? The experiments reported in this thesis did not identify the site of O_2-binding in the ETC that is coupled to hypoxic chemotransduction. However, it was determined that the functionally important site is not cytochrome aa_3, as suggested for glomus cells (Biscoe and Duchen, 1992) and cardiomyocytes (Duranteau et al., 1998), since CN, an inhibitor of cytochrome aa_3, did not mimic the effects of hypoxia. Thus, the O_2-sensor appears to be a component of the ETC that blocks electron transport to the FeS^-/cytochrome aa_3 site, and as such should lie proximal to complex III.

One interesting candidate for the O_2-binding site is the succinate-ubiquinone dehydrogenase (SDHD) component of complex II. This enzyme is anchored to the inner mitochondrial membrane via a b_{558} cytochrome (thus may bind O_2), and a naturally occurring mutation in SDHD has been associated with hereditary paraganglioma and blunted hypoxic responses in the human carotid body (Baysal et al., 2000). SDHD is found on chromosome 11q23 and carotid bodies from humans with one of five naturally occurring mutations in SDHD appear to show some characteristics similar to individuals exposed to chronic hypoxia (Baysal et al., 2000). However, other components of the proximal electron transport chain, such as complex I or ubiquinone cannot presently be excluded.

Figure 1. Proposed sites of reactive oxygen (ROS) species generation and the O_2-sensor in the mitochondrial electron transport chain of neonatal rat chromaffin cells.

Subunits of each complex are indicated in square parenthesis for each complex of the chain (labelled in standard parenthesis). Inhibitors of electron transport are denoted by flat-headed lines and the direction of electron flow by a standard arrow head. Note that the site of ROS generation that is functionally linked to hypoxic chemotransduction is likely found between complex III and complex IV, as indicated. The proposed O_2-binding site that represents the O_2-sensor is suggested to reside in complex II. (Modified from Hatefi, 1985).

NADH

Succinate

(Complex I)

$[FMN, FeS_{N-1}, FeS_{N-3}, FeS_{N-2}]$

$\begin{bmatrix} FeS_{-2} & FeSs_{-1} \\ B_{560} & FeS_{-3} \end{bmatrix}$ (Complex II)

Rotenone

O_2 sensor?

Ubiquinone; Q

Antimycin A

(Complex III)

$B_{562'}$
$b_{566'}$
FeS,
C1

ROS site?

Cytochrome C

(Complex IV) $\begin{bmatrix} a_3 & a \\ Cu & Cu \end{bmatrix}$

O_2

H_2O

CN
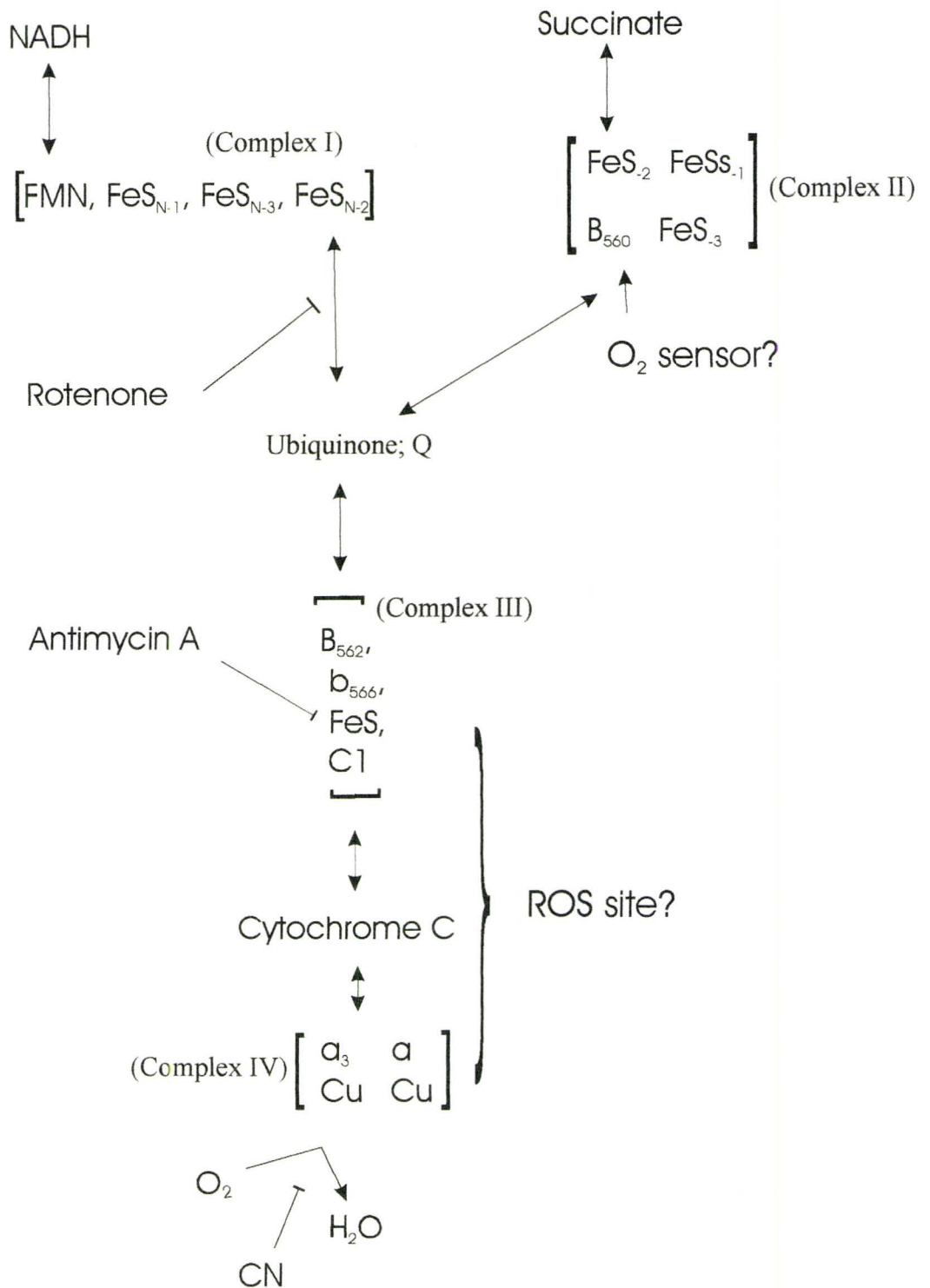
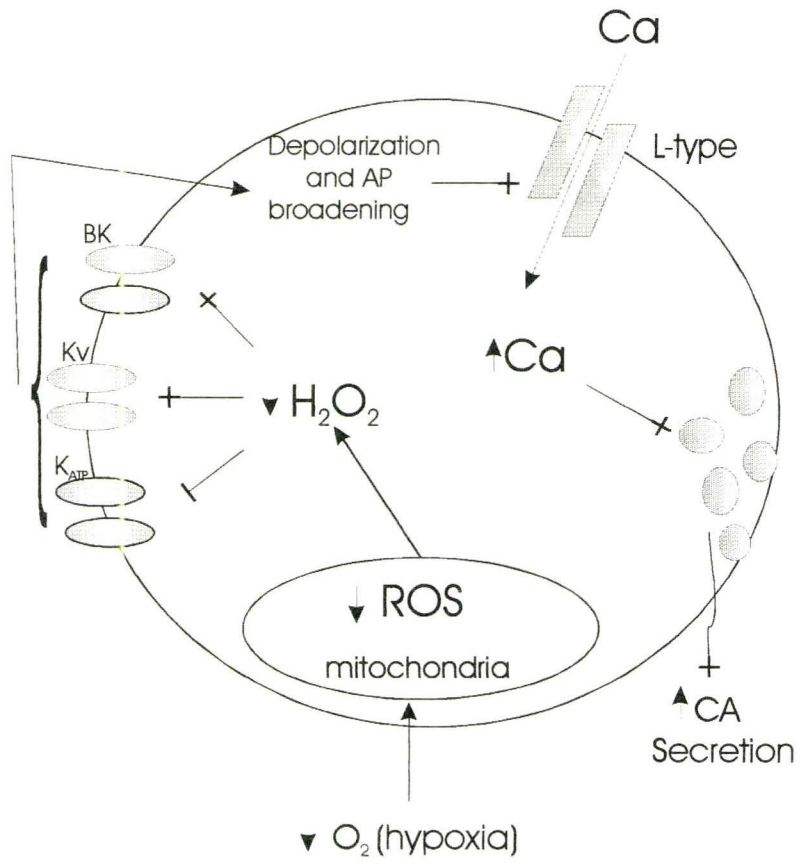**A model for O$_2$-chemotransduction by neonatal AMC**

A current model for O$_2$-chemotransduction in AMC is now presented in figure 2, which may also have relevance to other O$_2$-sensing cells. The general paradigm is that hypoxia is sensed by the proximal electron transport chain, possibly at complex II, resulting in reduced electron flow and decreased ROS generation. A fall in H$_2$O$_2$ functions as the second messenger between the sensor and plasma membrane K$^+$ channels, activating K$_{ATP}$ but inhibiting BK and K$_v$ (and possibly SK). This leads to membrane depolarization, broadening of the action potential and prolonged opening of L-type Ca^{2+} channels, which increase Ca^{2+} influx and CA secretion. Secreted CA enters the blood stream where they are transported towards adrenergic targets, e.g. lung, heart and liver, where they mediate the physiological adaptations of the neonate to hypoxia.

Future Research

This thesis investigated the cellular and molecular mechanisms of O$_2$-sensing by developing adrenal chromaffin cells. It would be of interest in the future to extend these studies to encompass single channel recordings to determine precisely how hypoxia modulates the various K$^+$ channels. This would best be achieved with perforated vesicles or cell-attached configurations of patch clamp recording, since the O$_2$-sensor appears to be located in the mitochondria which are excluded in conventional outside-out and inside-out patches. Single channel recording should also be able to determine if H$_2$O$_2$ or some other ROS can directly modulate K$^+$ channels in AMC, thereby confirming their suggested role as the second messenger.

Figure 2. A model of hypoxic chemotransduction in neonatal rat adrenal chromaffin cells.

In this model, hypoxia is sensed by the mitochondria via inhibition of electron transport in the electron transport chain (see Figure 1). Inhibition of the electron transport chain leads to a decrease in reactive oxygen species generation, e.g. H_2O_2, which modulates K^+ channels. Decreased ROS is proposed to inhibit BK and K_V channels, and activate K_{ATP}. The net result of K^+ channel modulation is membrane depolarization and action potential prolongation, increased Ca^{2+} influx through L-type channels and consequently, catecholamine (CA) secretion. Released CA are transported by the blood to adrenergic receptors, e.g. in the lung and heart, initiating the fight-or-flight response and promoting neonatal survival.

Ca

L-type

Depolarization
and AP
broadening

$+$

BK

$\times$

Kv

$+$ ▼H_2O_2

↑Ca

$\times$

K_{ATP}

⊥

↓ ROS

mitochondria

$+$

↑CA
Secretion

▼ O_2 (hypoxia)

Another direction for future research would involve determination of the precise O_2-binding site in the ETC. Does SDHD play this role? This may best be achieved using techniques to remove mitochondria (e.g. chronic ethidium bromide treatment) from an O_2-sensitive cell line similar to AMC, and then replace the mitochondria with those that contain mutations in SDHD. Methods for depleting and restocking cells with foreign mitochondria are available (King and Attardi, 1989). Furthermore, MAH cells, which are an immortalized embryonic AMC cell line, posses many of the O_2-sensing properties of AMC (see Appendix 2) and would make excellent candidates for these studies. Also, the use of differential display polymerase chain reaction could provide valuable information on the types of mRNA that are expressed by AMC prior to and after innervation.

Finally, an attractive direction for future studies could be correlating CA secretion with changes in K^+ channel activity and ROS levels in the cell. This could be achieved by concurrently recording membrane properties with the patch clamp technique and/or CA secretion in real-time with carbon fibre microelectrodes and monitoring ROS levels with fluorescent dyes. These studies would be both elegant and substantive in providing novel information on the cellular mechanisms of O_2-sensing.

References

Acker, H. (1989) Pc_2 chemoreception in arterial chemoreceptors. *Annual Review of Physiology*, **51**, 835-844.

Acker, H., Dufau, E , Huber, J. and Sylvester, D. (1989) Indications to an NADPH oxidase as a possible Po_2 sensor in the rat carotid body. *FEBS Letters*, **256**, 75-78.

Acker, H. and Xue, D. (1995) Mechanisms of oxygen sensing in the carotid body in comparison to other oxygen sensing cells. *NIPS* **10**, 211-216.

Ahlquist, R.P. (1948) A study of the adrenotropic receptors. *American Journal of Physiology*, **153**, 586-601.

Akaike, A., Mine, Y., Sasa, M. and Takaori, S. (1990) Voltage and current clamp studies of muscarinic and nicotinic excitation of the rat adrenal chromaffin cells. *The Journal of Pharmacology and Experimental Therapeutics*, **255(1)**, 333-339.

Anderson, D.J. (1993) Molecular control of cell fate in the neural crest: the sympathoadrenal lineage. *Annual Review of Neuroscience*, **16**, 129-158.

Anderson, D.J. (1993) Cell fate determination in the peripheral nervous system: the sympathoadrenal progenitor. *Journal of Neurobiology,* **24(2),** 185-198.

Archer, S.L., Huang, J., Henry, T., Peterson, D. and Weir, E.K. (1993) A redox-based O_2 sensor in rat pulmonary vasculature. *Circulation Research,* **73,** 1100-1112

Archer, S.L., Huang, J.M.C., Reeve, H.L., Hampl, V., Tolarova, S., Michelakis, E. and Weir, E.K. (1996) Differential distribution of electrophysiologically distinct myocytes in conduit and resistance arteries determines their response to nitric oxide and hypoxia. *Circulation Research,* **78,** 431-422.

Archer, S.L., Reeve, H.L., Michelakis, E., Puttagunta, L., Waite, R., Nelson, D.P., Dinauer, M.C. and Weir, E.K. (1999) O_2 sensing is preserved in mice lacking the gp91 phox subunit of NADPH oxidase. *Proceedings of the National Academy of Sciences, USA,* **96,** 7944-7949.

Artalejo, C.R., Adams, M.E. and Fox, A. P. (1994) Three types of Ca^{2+} channel trigger secretion with different efficacies in chromaffin cells. *Nature,* **367,** 72-76.

Ashcroft, S. J. H. & Ashcroft F. M. (1990). Properties and functions of ATP-sensitive K-channels. *Cell Signalling* **2,** 197-214.

Aunis, D. and Langley, K. (1999) Physiological aspects of exocytosis in chromaffin cells of the adrenal medulla. *Acta Physiologica Scandinavia,* **167,** 89-97.

Baysal, B.E., Ferrell, R.E., Willet-Brozick, J.E., Lawrence, E.C., Myssiorek, D., Bosch, A., van der May, A., Taschner, P.E.M., Rubenstein, W.S., Myers, E.N., Richard, C.W., Cornelisse, C.J, Devilee, P. and Devlin, B. (2000) Mutations in *SDHD*, a mitochondrial complex II gene, in hereditary paraganglioma. *Science,* **287,** 848-851.

Biesold, D., Kurosawa, M., Sato, A. and Trzebski, A. (1989) Hypoxia and hypercapnia increase the sympathoadrenal medullary functions in anesthetized, artificially ventilated rats. *Japanese Journal of Physiology,* **39,** 511-522.

Birren, S.J. and Anderson, D.J. (1990) A v-myc-immortilized sympathoadrenal progenitor cell line in which neuronal differentiation is initiated by FGF but not NGF. *Neuron,* **4,** 189-201.

Biscoe, T.J. and Duchen, M.R. (1989) Electrophysiological responses of dissociated type I cells of the rabbit carotid body to cyanide. *Journal of Physiology,* **413,** 447-468.

Buckler, K.J. (1997) A novel oxygen-sensitive potassium current in rat carotid body type I cells. *Journal of Physiology,* **498.3,** 649-662.

Buckler, K.J. (1999) Background leak K$^+$-currents and oxygen sensing in carotid body type 1 cells. *Respiration Physiology,* **115(2),** 179-188.

Buckler, K.J., Williams, B.A., and Honore, E. (2000) An oxygen-, acid- and anasthetic-sensitive TASK-like background potassium channel rat arterial chemoreceptor cells. *Journal of Physiology,* **525.1,** 135-142.

Buckler, K.J. and Vaughan-Jones, R.D. (1994) Effects of hypoxia on membrane potential and intracellular calcium in rat neonatal carotid body type I cells. *Journal of Physiology,* **476,** 423-428.

Buckler, K.J. and Vaughan-Jones, R.D. (1998) Effect of mitochondrial uncouplers on intracellular calcium, pH and membrane potential in rat carotid body type 1 cells. *Journal of Physiology,* **513.3,** 819-933.

Cambell, A.G.M., Dawes, G.S. and Fishman, A.P. (1967) Regional redistribution of blood flow in the mature fetal lamb. *Circulation Research,* **21,** 229-239.

Castellano, M. and Bohm, M. (1997) The cardiac α-adrenoreceptor-mediated signalling pathway and its alterations in hypertensive heart disease. *Hypertension,* **29,** 715-722.

Chandel, N.S., Budinger, G.R.S., Choe, S.H. and Schumacker, P.T. (1997) Cellular respiration during hypoxia: role of cytochrome oxidase as the oxygen sensor in hepatocytes. *The Journal of Biological Chemistry,* **272(30),** 18808-18816.

Chandel, N.S., Maltepe, E., Goldwasser, E., Mathieu, C.E., Simon, M.C. and Schumacker, P.T. (1998) Mitochondrial reactive oxygen species trigger hypoxia-induced transcription. *Proceedings of the National Academy of Sciences, USA,* **95,** 11715-11720.

Chantry, C.J., Seidler, F.J. and Slotkin, T.A. (1982) Non-neurogenic mechanism for reserpine-induced release of catecholamines from the adrenal medulla of neonatal rats: possible modulation by opiate receptors. *Neuroscience,* **7(3),** 673-678.

Cheung, C. (1989) Direct adrenal medullary catecholamine response to hypoxia in fetal sheep. *Journal of Neurochemistry,* **52,** 148-153.

Cheung, C. Y. (1990). Fetal adrenal medulla catecholamine response to hypoxia - direct and neural components. *American Journal of Physiology* **258**, R1340-R1346.

Chow, R.H. and von Ruden, L. (1995) Electrochemical detection of secretion from single cells. In Single Channel Recording, 2nd Edition. *Eds.* B. Sackmann and E. Neher. Plenum Press, New York. pp 245-277.

Chowdhury, P.S., Guo, X., Wakade, T.D., Przywara, D.A. and Wakade, A.R. (1994) Exocytosis from a single rat chromaffin cell by cholinergic and peptidergic neurotransmitters. *Neuroscience,* **59(1),** 1-5.

Comline, R.S. and Silver, M. (1961) The release of adrenaline and noradrenaline from the adrenal glands of the foetal sheep. *Journal of Physiology,* **156,** 424-444.

Conforti, L. & Millhorn D. E. (1997). Selective inhibition of slow-inactivating voltage-dependent K^+ channel in rat PC 12 cells by hypoxia. *Journal of Physiology* **502,** 293-305.

Conforti, L., Bodi, I., Nisbet, J.W. and Millhorn, D.E. (2000) O_2-sensitive K^+ channels: role of the Kv 1.2 alpha-subunit in mediating the hypoxic response. *Journal of Physiology,* **524,** 783-793.

Coupland, R.E., Parker, T.L., Keese, W.K. and Mohamed, A.A. (1989) The innervation of the adrenal gland III. Vagal innervation. *Journal of Anatomy,* **163,** 173-181.

Cross, A.R., Henderson, L., Jones, O.T.G., Delpiano, M.A., Hentschel, J. and Acker, H. (1990) Involvement of an NAD(P)H oxidase as pO_2 sensor protein in the rat carotid body. *Biochemical Journal,* **272,** 743-747.

Czyzyk-Krzeska, M.F., Furnari, B.A., Lawson, E.E., and Milhorn, D.E. (1994) *Journal of Biological Chemistry,* **269**, 760-764.

De Leo, F.R., Ulman, K.V., Davis, A.R., Jutila, K.L., Quinn, M.T. (1996). Assembly of the human neutrophil NADPH oxidase involves binding of p67[phox] and flavocytochrome b to a common functional domain in p47[phox]. *Journal of Biological Chememistry,* 27(29), 17013-17020.

Delpiano, M. A. & Hescheler, J. (1989). Evidence for a Po_2-sensitive K^+ channel in the type-I cell of the rabbit carotid body. *FEBS Letters* **249**, 195-198.

DiChiara, T.J., and Reinhart, P.H. (1997) Redox modulation of hslo Ca^{2+}-activated K^+ channels. *The Journal of Neuroscience,* **17,** 4942-4955.

Donnelly, D.F. (1993) Response to cyanide of two types of glomoid cells in mature rat carotid body. *Brain Research,* **630,** 157-168.

Doupe, A.J., Landis, S.C. and Patterson, P.H. (1985) Environmental influence in the development of neural crest derivatives: glucocorticoids, growth factors, and chromaffin cell plasticity. *The Journal of Neuroscience,* **5(8),** 2119-2142.

Dry, K.L., Phillips, J.H. and Dart, A.M. (1991) Catecholamine release from bovine adrenal chromaffin cells during anoxia or metabolic inhibition. *Circulation Research,* **69,** 466-474.

Duchen, M.R. and Biscoe, T.J. (1992) Mitochondrial function in type I cells isolated from rabbit arterial chemoreceptors. *Journal of Physiology,* **450,** 13-31.

Duchen, M.R. and Biscoe, T.J. (1992) Relative mitochondrial membrane potential and $[Ca^{2+}]_i$ in type I cells isolated from the rabbit carotid body. *Journal of Physiology,* **450,** 33-61.

Duchen, M.R. (1999) Contributions of mitochondria to animal physiology: from homeostatic sensor to calcium signalling and cell death. *Journal of Physiology,* **516.1,** 1-17.

Dun, N.J., Tang, H., Dun, S.L., Huang, R., Dun, E.C. and Wakade, A.R. (1996) Pituitary acenylate cyclase activating polypeptide-immunoreactive sensory neurons innervate rat adrenal medulla. *Brain Research,* **716,** 11-21.

Duranteau, J., Chandel, N.J., Kulisz, A., Shao, Z. and Schumacker, P.T. (1998) Intracellular signalling by reactive oxygen species during hypoxia and cardiomyocytes. *The Journal of Biological Chemistry,* **273(19),** 11619-11624.

Eberhard, D.A. and Holz, R.W. (1987) Cholinergic stimulation of inositol phosphate formation in bovine adrenal chromaffin cells: distinct nicotinic and muscarinic mechanisms. *Journal of Neurochemistry,* **49,** 1634-1643.

Federoff, H.J., Grabczyk, E. and Fishman, M.C. (1988) Dual regulation of GAP-43 gene expression by nerve growth factor and glucocorticoids. *Journal of Biological Chemistry,* **263,** 19290-19295.

Fenwick, E.M., Marty, A. and Neher, E. (1982) A patch-clamp study of bovine chromaffin cells and of their sensitivity to acetylcholine. *Journal of Physiology,* **331,** 577-597.

Fu, X.W., Nurse, C.A., Wang, Y.T., Cutz, E. (1999) Selective modulation of membrane currents by hypoxia in intact airway chemoreceptors from neonatal rabbit. *Journal of Physiology,* **514.1,** 139-150.

Fu, X.W., Wang, D., Nurse, C.A., Dinauer, M.C and Cutz, E. (2000) NADPH oxidase is an O_2 sensor in airway chemoreceptors: Evidence from K^+ current modulation in wild-type and oxidase-deficient mice. *Proceedings of the National Academy of Sciences, USA,* **97,** 4374-4379.

Galvez A. Gimenez-Gallego G. Reuben G. Roy-Contancin L. Fingenbaum P. Kaczorowski G. J. & Garcia M. L. (1990) Purification and characterization of a unique, potent, peptidyl probe for the high conductance calcium activated potassium channel from venom of the scorpion *Buthus tamulus*. *Journal of Biological Chemistry* **265**, 11083-11090.

Ganfornia, M.D. and Lopez-Barneo, J. (1992) Potassium channel types in arterial chemoreceptor cells and their selective modulation by oxygen. *Journal of General Physiology*, **100**, 401-426.

Gaspo, R., Yamaguchi, N. and De Champlain, J. (1993) Effects of nifedipine and BAY K 8644 on stimulation-induced adrenal catecholamine secretion in the dog. *American Journal of Physiology*, **265**, R28-R34.

Gonzalez, C., Almarez, L., Obeso, A. and Rigual, R. (1994) Carotid body chemoreceptors: from natural stimuli to sensory discharges. *Physiological Reviews*, **74**, 829-898.

Grimminger, F., Weissmann, N., Spriestersbach, R., Becker, E., Rosseau, S. and Seeger, W. (1995) Effects of NADPH oxidase inhibitors on hypoxic vasoconstriction in buffer-perfused rabbit lungs. *American Journal of Physiology*, **268**, L747-L752.

Ghysen, A. and Dambly-Chaudiere, C. (1988) From DNA to form: the *achete-schute* complex. *Genes and Development,* **2,** 495-501.

Guo, X. and Wakade, A.R. (1994) Differential secretion of catecholamines in response to peptidergic and cholinergic transmitters in rat adrenals. *Journal of Physiology,* **475.3,** 539-545.

Guyton, A.C. (1991) Textbook of medical physiology, eighth edition. W.B Saunders Company, Philadelphia. pp. 1014.

Hadcock, J.R. and Malbon, C.C. (1993). Agonist regulation of gene expression of adrenergic receptors and G proteins. *Journal of Neurochemistry,* **60,** 1-9.

Haddad G. G. & Jiang C. (1997). O_2-sensing mechanisms in excitable cells: role of plasma membrane K^+ channels. *Annual Review of Physiology,* **59,** 23-43.

Hamill, O.P., Marty, A., Neher, E., Sackmann, B. and Sigworth, F.J. (1981) Improved patch-clamp techniques for high-resolution current recording from cells and cell-free membrane patches. *Pflugers Archives,* **391,** 85-100.

Hatefi, Y. (1985) The mitochondrial electron transport and oxidative phosphorylation system. *Annual Review of Biochemistry,* **54,** 1015-1069.

Hatton, C.J., Carpenter, C., Pepper, D.R., Kumar, P., and Peers, C. (1997) Developmental changes in isolated rat type 1 carotid body cell K^+ current and their modulation by hypoxia. *Journal of Physiology,* **501.1,** 49-58.

Hernandez-Guijo, J.M., de Pascual, R., Garcia, A.G. and Gandia, L. (1998) Separation of calcium channel current components in mouse chromaffin cells superfused with low- and high-barium solutions. *Pflugers Archives,* **436,** 75-82.

Herrington, J., Solaro, C.R., Neely, A. and Lingle, C.J. (1995) the suppression of Ca^{2+}- and voltage-dependent K^+ current during mAChR activation in rat adrenal chromaffin cells. *Journal of Physiology,* **485.2,** 297-318.

Hertzberg, T., Hellstrom, S., Lagercrantz, H. and Pequinot, J.M. (1990). Development of the arterial chemoreflex and turnover of carotid body catecholamines in the newborn rat. *Journal of Physiology,* **425,** 211-225.

Hess. P. (1990) Calcium channels in vertebrate cells. *Annual Review of Neuroscience,* **13,** 337-356.

Hodgkin, A.L. and Huxley, A.H. (1952) A quantitative description of membrane current and its application to conduction and excitation in nerve. *Journal of Physiology,* **117,** 500-544.

Hole, J.W. (1993) Human anatomy and physiology, sixth edition. Wm. C. Brown Publishers, Oxford. pp 962

Holgert, H., Dagerlind, A., Hokfelt, T. and Lagercrantz, H. (1994) Neuronal markers, peptides and enzymes in nerves and chromaffin cells in the rat adrenal medulla during postnatal development. *Developmental Brain Research,* **83,** 35-52.

Hollins, B. and Ikeda, S.R. (1996) Inward currents underlying action potentials in rat adrenal chromaffin cells. *Journal of Neurophysiology,* **76(2),** 1195-1211.

Horn, R. and Marty, A. (1988) Muscarinic activation of ionic currents measured by a new whole-cell recording method. *Journal of General Physiology,* **92,** 145-159.

Hoshi, T. and Aldrich, R.W. (1988) voltage-dependent K^+ currents underlying single K^+ channels in pheochromocytoma cells. *Journal of General Physiology,* **91,** 73-106.

Huginar, R.L., Delcour, A.H., Greengard, P., and Hess, G.P. (1986) Phosphorylation of the nicotinic acetylcholine receptor regulates its rate of desensitization. *Nature,* **321,** 774-776.

Huginar, R.L., and Miles, K. (1989) Protein phosphorylation of nicotinic acetylcholine receptors. *Critical Reviews in Biochemistry and Molecular Biology,* **24(3),** 183-214.

Inoue M. Fujishiro N. & Imanaga I. (1998) Hypoxia and cyanide induce depolarization and catecholamine release in dispersed guinea-pig chromaffin cells. *Journal of Physiology,* **507,** 807- 818.

Inoue, M., Fujishiro, N., Imanaga, I. (1999). Na^+ pump inhibition and non-selective cation channel activation by cyanide and anoxia in guiney pig chromaffin cells. *Journal of Physiology,* **519.2,** 385-396.

Inoue, M., Fujisharo, N., and Imanaga, I. (2000) Retardation of cation channel deactivation by mitochondrial dysfunction in adrenal medullary cells. *American Journal of Physiology,* **278,** C26-C32.

Jackson A. & Nurse C. A. (1997) Dopaminergic properties of cultured rat carotid body chemoreceptors grown in normoxic and hypoxic environments. *Journal of Neurochemistry,* **69,** 645-654.

Jackson A., and Nurse, C.A. (1998). Role of acetylcholine receptors and dopamine transporter in regulation of extracellular dopamine in rat carotid body cultures grown in chronic hypoxia or nicotine. *Journal of Neurochemistry,* **70,** 653-662.

Jiang C. Sigworth F. J. & Haddad G. G. (1994). Oxygen deprivation activates an ATP-inhabitable K^+ channel in substantia nigra neurons. *Journal of Neuroscience,* **14,** 5590-5602.

Jones, S.W. (1990) Whole-cell and microelectrode voltage clamp. In, Neuromethods, Vol 14. Neurophysiological techniques: Basic methods and concepts. *Eds.* Boulton A.A., Baker, G.B., and Vanderwolf C.H. Humana press Inc., Clifton, N.J. pp 143-192.

Jones, C.T., Roebuck, M.M., Walker, D.W. and Johnston, B.M. (1988) The role of the adrenal medulla and peripheral sympathetic nerves in the physiological responses of the fetal sheep to hypoxia. *Journal of Developmental Physiology,* **10,** 17-36.

Kang, J., Huguenard, J.R., and Prince, D.A. (1996) Development of BK channels in neocortical pyramidal neurons. *Journal of Neurophysiology,* **76(1),** 188-198.

Keese, W.K., Parker, T.L. and Coupland, R.E. (1988) The innervation of the adrenal gland I. The source of pre- and postganglionic nerve fibres to the rat adrenal gland. *Journal of Anatomy,* **157,** 33-41.

Khalil, Z., Livett, B.G. and Marley, P.D. (1986) The role of sensory fibres in the rat splanchnic nerve in the regulation of adrenal medullary secretion during stress. *Journal of Physiology,* **370,** 201-215.

Khalil, Z., Livett, B.G. and Marley, P.D. (1987) Sensory fibres modulate histamine-induced catecholamine secretion from the rat adrenal medulla and sympathetic nerves. *Journal of Physiology,* **391,** 511-526.

Kiehn, J., Lacerda, A.E., Wible, B. and Brown, A.M. (1996) Molecular physiology and pharmacology of HERG: single channel currents and block by dofetilide. *Circulation,* **94(10),** 2572-2579.

Kim, Y., Bang, H. and Kim, D. (1999) TBAK-1 and TASK-1, two-pore K^+ channel subunits: kinetic properties and expression in rat heart. *American Journal of Physiology,* **277,** H1669-H1678.

Kim, S.J., Lim, W. and Kim, J. (1995) Contribution of L- and N-type calcium currents to exocytosis in rat adrenal medullary chromaffin cells. *Brain Research,* **675,** 289-296.

King, M.P. and Attardi, G. (1989) Human cells lacking mtDNA: Repopulation with exogenous mitochondria by complementation. *Science,* **246,** 500-503.

Kleinberg, M.E. and Finkelstein, A. (1984) Single-length and double length channels formed by nystatin in lipid bilayer membranes. *Journal of Membrane Biology,* **80,** 257-269.

Kroll,S.L. and Czyzyk-Crzeska (1998) Role of H_2O_2 and heme-containing O_2-sensors in hypoxic regulation of tyrosine hydroxylase gene expression. *American Journal of Physiology,* **43,** C167-174.

Kummer, W. and Acker, H. (1995) Immunohistochemical demonstration of four subunits of neutrophil NAD(P)H oxidase in type I cells of carotid body. *Journal of Applied Physiology,* **78(5),** 1904-1909.

Lagercrantz, H. and Bistoletti, P. (1973) Catecholamine release in the newborn infant at birth. *Pediatric Research,* **11,** 889-893.

Lagercrantz, H. and Slotkin T.A. (1986) The stress of being born. *Scientific American,* **254,** 100-107.

Lahiri, S. (1994) Chromophores in O_2-chemoreception: the carotid body model. *NIPS,* **9,** 161-165.

Lahiri, S., Ehleben, W. and Acker, H. (1999) Chemoreceptor discharges and cytochrome redox changes of the rat carotid body: role of heme ligands. *Proceedings of the National Academy of Sciences, USA,* **96,** 9427-9432.

Lee, J., Lim, W., Eun, S.-Y., Kim, S.J. and Kim J. (2000) Inhibition of apamin-sensitive K^+ current by hypoxia in adult rat adrenal chromaffin cells. *Pflugers Archives,* **439(60),** 700-705.

Leszczyszyn, D.J., Jankowski, J.A, Viveros, O.H., Diliberto, E.J. Jr., Near, J.A. and Wightman, R.M. (1990) Nicotinic receptor-mediated catecholamine secretion from single chromaffin cells. *Journal of Biological Chemistry,* **265,** 14763-14737.

Li, Y. and Trush, M.A. (1998) Diphenyleniodonium, an NAD(P)H oxidase inhibitor, also potently inhibits mitochondrial reactive oxygen species production. *Biochemical and Biophysical Research Communications,* **253,** 295-299.

Lo, L., Johnson, J.E., Wuenschell, C.W., Saito, T. and Anderson, D.J. (1991) Mammalian achaete-schute homolog 1 is transiently expressed by spatially-restricted subsets of early neuroepithelial and neural crest cells. *Genes and Development,* **5,** 1524-1537.

Lopez, M.G., Alibillos, A., de la Fuente, M.T., Borges, R., Gandia, L., Carbone, E., Garcia, A.C. and Artalejo, A.R. (1994) Localized L-type calcium channels control exocytosis in cat chromaffin cells. *Pflugers Archives*, **427**, 348-354.

Lopez-Barneo, J. (1996) Oxygen-sensing by ion channels and the regulation of cellular functions. *Trends in Neuroscience*, **19(10)**, 435-439.

Lopez-Barneo, J., Lopez-Lopez, J.R., Urena, J. and Gonzalez, C. (1988) Chemotransduction in the carotid body: K current modulated by pO_2 in type I chemoreceptor cells. *Science*, **241**, 580-582.

Lopez-Barneo, J., Ortega-Saenz, P., Molina,A., Franco-Obregon, A., Urena, J., and Castellano, A. (1997) *Kidney Internat.* **51**, 454-461.

Lopez-Lopez J. Gonzalez C. Urena J. & Lopez-Barneo J. (1989). Low Po_2 selectively inhibits K channel activity in chemoreceptor cells of the mammalian carotid body. *Journal of General Physiology*, **93**, 1001-1015.

Lopez-Lopez, J.R., Gonzalez, C. and Perez-Garcia, M.T. (1998) Properties of ionic currents from isolated adult rat carotid body chemoreceptor cells: effects of hypoxia. *Journal of Physiology*, **499.2**, 429-441.

Lovell, P.V., James, D.G. and McCobb, D.P. (2000) Bovine versus rat adrenal chromaffin cells: big differences in BK potassium channel properties. *APStracts* **7**, *0174J.*

Malhotra, R.K. and Wakade, A.R. (1987) Non-cholinergic component of rat splanchnic nerves predominates at low neuronal activity and is eliminated by naloxone. *Journal of Physiology,* **383,** 639-652.

McCormack, T. and McCormack, K. (1994) Shaker K^+ channel β subunits belong to an NAD(P)H-dependent oxidoreductase superfamily. *Cell*, **79,** 1133-1135.

Michelakis, E.D., Archer, S.L. and Weir, E.K. (1995) Acute hypoxic pulmonary vasoconstriction: a model of oxygen sensing. *Physiol. Res.,* **44(6),** 361-367.

Michelshon, A. and Anderson, D.J. (1992) Changes in competence determine the timing of two sequential glucocorticoid effects on sympathoadrenal progenitors. *Neuron,* **5,** 589-604.

Mitchell, P. (1961) Coupling of phosphorylation to electron and hydrogen transfer by a chemi-osmotic type of mechanism. *Nature,* **191,** 144-148.

Mochizuki-Oda N. Takeuchi Y. Matsumura K. Oosawa Y. & Watanabe Y. (1997) Hypoxia-induced catecholamine release and intracellular Ca^{2+} increase via suppression of K^+ channels in cultured rat adrenal chromaffin cells. *Journal of Neurochemistry,* **69,** 377-387.

Mohamed, A.A., Parker, T.L. and Coupland, R.E. (1988) The innervation of the adrenal gland II. The source of spinal afferent nerve fibres to the guinea-pig adrenal gland. *Journal of Anatomy,* **160,** 51-58.

Mojet, M.H., Mills, E. and Duchen, M.R. (1996) Hypoxia-induced catecholamine secretion by adrenal chromaffin cells isolated from newborn rats is mediated by a fall in $[ATP]_i$ and influx of extracellular Ca^{2+}. *Journal of Physiology,* **487.P,** 80-81P (abstract).

Mojet, M.H., Mills, E. and Duchen, M.R. (1997) Hypoxia-induced catecholamine secretion in isolated newborn rat adrenal chromaffin cells is mimicked by inhibition of mitochondrial respiration. *Journal of Physiology,* **504.1,** 175-189.

Montoro, R.J., Urena, J., Fernandez-Chacon, R., Alvarez de Toledo, G. and Lopez-Barneo, J. (1996) Oxygen sensing by ion channels and chemotransduction in single glomus cells. *Journal of General Physiology,* **107,** 133-143.

Neely, A. and Lingle, C.J. (1992) Two components of calcium-activated potassium current in rat adrenal chromaffin cells. *Journal of Physiology,* **453,** 97-131.

Nicholls, D.G. and Budd, S.L. (2000) Mitochondria and neuronal survival. *Physiological Reviews,* **80(1),** 315-356.

Nurse, C. A. (1990) Carbonic anhydrase and neuronal enzymes in cultured glomus cells of the carotid body of the rat. *Cell and Tissue Research,* **261**, 65-71.

Obeso, A., Gomez-Nino, A. and Gonzalez, C. (1999) NADPH oxidase inhibition does not interfere with low Po_2 transduction in rat and rabbit CB chemoreceptor cells. *American Journal of Physiology*, **276,** C593-C601.

Oomori, Y., Habara, Y. and Kanno, T. (1998) Muscarinic and nicotinic-mediated Ca^{2+} dynamics in rat adrenal chromaffin cells during development. *Cell Tissue Research,* **294(1),** 109-123.

Overholt, J.L., Ficker, E., Yang, T., Shams, H., Bright, G.R., and Prabhakar, N.R. (2000) HERG-Like potassium current regulates the resting membrane potential in glomus cells of the rabbit carotid body. *Journal of Neurophysiology,* **83(3),** 1150-1157.

Pancrazio, J.J., Johnson, P.A. and Lynch III, C. (1994) A major role for calcium-dependent potassium current in action potential repolarization in adrenal chromaffin cells. *Brain Research,* **668,** 246-251.

Pardal, R., Ludewig, U., Garcia-Hirschfeld, J., and Lopez-Barneo, J. (2000) Secretory responses of intact glomus cells in thin slices of rat carotid body to hypoxia and tetraethylammonium. *Proceedings of the National Academy of Sciences,* **97(5),** 2361-2366.

Park Y. (1994). Ion selectivity and gating of small conductance Ca^{2+}-activated K^+ channels in cultured rat adrenal chromaffin cells. *Journal of Physiology* **481,** 555-570.

Parker, T.L., Keese, W.K., Mohamed, A.A. and Afework, M. (1993) The innervation of the mammalian adrenal gland. *Journal of Anatomy,* **183,** 265-276.

Peers, C. (1990) Hypoxic suppression of K^+ currents in type I carotid body cells: selective effect on the Ca^{2+}-activated K^+ current. *Neuroscience Letters,* **119,** 253-256.

Peers C. Buckler K. J. (1995). Transduction of chemostimuli by the type 1 carotid body cell. *Journal of Membrane Biology*, **144,** 1-9.

Peers, C. and O'Donnell, J. (1990) Potassium currents recorded in type 1 carotid body cells isolated from the neonatal rat and their modulation by chemoexcitatory agents. *Brain Research,* **522,** 259-266.

Pelto-Huikko, M., Saminen, T. and Hervonen, A. (1985) Localization of enkephalins in adrenaline cells and the nerves innervating adrenaline cells in rat adrenal medulla. *Histochemistry,* **82,** 377-383.

Phillippe, M. (1983) Fetal Catecholamines. *American Journal of obstetrics and Gynecology,* **146,** 840-855.

Post J. M. Hume J. R. Archer S.L. & Weir E. K. (1992) Direct role for potassium channel inhibition in hypoxic pulmonary vasoconstriction. *American Journal of Physiology,* **262,** C882-C890.

Reeve, H..L., Weir, E.K., Nelson, D.P., Peterson, D.A. and Archer, S.L. (1995) Opposing effects of oxidants and antioxidants on K+ channel activity and tone in vascular tissue. *Exp. Physiol,* **80,** 825-834

Roper, J., and Ashcroft, F.M. (1995) Metabolic inhibition and low internal ATP activate K-ATP channels in rat dopaminergic substantia nigra neurons. *Pflugers Archives,* **430,** 44-54.

Rychkov, G.Y., Adams, M.B., McMillon, I.C. and Roberts, M.L. (1998) Oxygen-sensing mechanisms are present in the chromaffin cells of the sheep adrenal medulla before birth. *Journal of Physiology,* **509.3,** 887-893.

Sackmann, B. and Neher, E. (1995) Single-channel recording, second edition. Plenum Press, New York. pp 700.

Seidler, F.J. and Slotkin, T.A. (1985) Adrenomedullary function in the neonatal rat: responses to acute hypoxia. *Journal of Physiology,* **385,** 1-16.

Seidler, F.J. and Slotkin, T.A. (1986) Ontogenty of adrenomedullary responses to hypoxia and hypoglycemia: role of splanchnic innervation. *Brain Research Bulletin,* **16,** 11-14.

Seidler, F.J. and Slotkin, T.A. (1986) Non-neurogenic adrenal catecholamine release in the neonatal rat: exocytosis or diffusion? *Brain Research,* **393,** 274-277.

Seidler, F.J., Brown, K., Smith, P.G. and Slotkin, T.A. (1987) Toxic effects of hypoxia on neonatal cardiac function in the rat: α-adrenergic mechanisms. *Toxicology Letters,* **37,** 79-84.

Semenza, G.L. (1999) Perspectives on oxygen sensing. *Cell,* **98,** 281-284.

Shao, L., Halvorsrud, R., Borg-Graham, L. and Storm, J.F. (1999) The role of BK-type Ca^{2+}-dependent K^+ channels in spike broadening during repetitive firing in rat hippocampal pyramidal cells. *Journal of Physiology,* **521.1,** 135-146.

Slotkin T.A. and Seidler, F.J. (1988) Adrenomedullary catecholamine release in the fetus and newborn: secretory mechanisms and their role in stress and survival. *Journal of Developmental Physiology,* **10,** 1-16.

Slotkin, T.A., Lappi, S.E., McCook, E.C., Lorber, B.A., and Seidler, F.J. (1995) Loss of hypoxia tolerance after prenatal nicotine exposure: implications for sudden infant death syndrome. *Brain Research Bulliton,* **38(1),** 69-75.

Solaro, C.R., Prakriya, M., Ding, J.P. and Lingle, C.J. (1995) Inactivating and non-inactivating Ca^{2+} and voltage-dependent K^+ current in rat adrenal chromaffin cells. *Jounal of Neuroscience,* **15,** 6110-6123.

Stea, A. & Nurse, C. A. (1991) Whole-cell and perforated-patch recordings from O_2-sensitive rat carotid body cells grown in short- and long-term culture. *Pflügers Archives,* **418,** 93-101.

Stea, A., Jackson, A., Macintyre, L., and Nurse, C.A. (1995) Long-term modulation of inward currents in O_2 chemoreceptors by chronic hypoxia and cyclic AMP *in vitro*. *Journal of Neuroscience,* **15,** 2192-2202.

Stemple, D.L., Mahanthappa, N.K. and Anderson, D.J. (1988) Basic FGF induces neuronal differentiation, cell division, and NGF dependence in chromaffin cells: a sequence of events in sympathetic development. *Neuron,* **1,** 517-525.

Strosberg, A.D. (1993) Structure, function, and regulation of adrenergic receptors. *Protein Science,* **2,** 1198-1209.

Summers, R.J. and McMartin, L.R. (1993) Adrenoreceptors and their second messenger systems. *Journal of Neurochemistry,* **60(1),** 10-23.

Taylor, S.C. and Peers, C. (1999) Chronic hypoxia enhances the secretory response of rat phaeochromocytoma cells to acute hypoxia. *Journal of Physiology,* **514.2,** 483-491.

Thompson R. J. Jackson A. & Nurse C. A. (1997). Developmental loss of hypoxic chemosensitivity in rat adrenomedullary chromaffin cells. *Journal of Physiology,* **498,** 503-510.

Thompson R. J. & Nurse C. A. (1997) Hypoxia-sensitive K^+ channels in rat adrenal chromaffin cells. *Society for Neuroscience Abstracts,* **23,** 1746.

Thompson, R.J. and Nurse, C.A. (1998) Anoxia differentially modulates multiple K^+ currents and depolarizes neonatal rat adrenal chromaffin cells. *Journal of Physiology,* **512.2,** 421-434.

Tokube, K., Kiyosue, T. and Arita, M. (1998) Effects of hydroxyl radicals on K_{ATP} channels in guinea-pig ventricular myocytes. *Pflugers Archives-European Journal of Physiology,* **437,** 155-157.

Tortora, G.J. and Grabowski, S.R. (1992) Principles of anatomy and physiology, seventh edition. Harper Collins College Publishers, New York. pp 999.

Tsapatsaris, N.P. and Breslin, D.J. (1989) Physiology of the adrenal medulla. *Urologic Clinics of North America,* **16(3),** 439-445.

Vanden Hoek, T.L., Becker, L.B., Shao, Z., Changqing, L. and Schumacker, P.T. (1998) *Journal of Biological Chemistry,* **273,** 18092-18098.

Verhofstad, A.A.J., Coupland, R.E., Parker, T.R. and Goldstein, M. (1985) Immunohistochemical and biochemical study on the development of the noradrenaline-

and adrenaline-storing cells of the adrenal medulla of the rat. *Cell Tissue Research,* **242,** 233-243.

Wang, D., Youngson, C., Wong, V., Yeger, H., Dinauer, M.C., Vega-Saenz De Miera, E., Rudy, B. and Cutz, E. (1996) NADPH-oxidase and a hydrogen peroxide-sensitive K^+ channel may function as an oxygen sensor complex in airway chemoreceptors and small cell lung carcinoma cell lines. *Proceedings of the National Academy of Sciences USA,* **93,** 13182-13187.

Wann, K.T. and Richards, C.D. (1994) Properties of single calcium-activated potassium channels of large conductance in rat hippocampal neurons in culture. *European Journal of Neuroscience,* **6,** 607-617.

Wasiko, M.J., Sterni, L.M., Bamford, O.S., Montrose, M.H. and Carroll, J.L. (1999) Resetting and postnatal maturation of oxygen chemosensitivity in rat carotid chemoreceptor cells. *Journal of Physiology,* **514.2,** 493-503.

West, G.B., Shepherd, D.M. and Hunter, R.B. (1953) The function of the organs of Zuckerkandl. *Clinical Scientist,* **12,** 317-325.

Wilson, D.F., A. Mokashi, D. Chugh, S. Vinogradov, S. Osanai, and S. Lahiri. (1994) The primary oxygen sensor of the cat carotid body is cytochrome a3 of the mitochondrial repsiratory chain. *FEBS Letters,* **351,** 370-374.

Wyatt, C.N. and Peers, C. (1995) Ca^{2+}-activated K^+ channels in isolated type I cells of the neonatal rat carotid body. *Journal of Physiology,* **483.3,** 559-565.

Wyatt, C. N., Wright, C., Bee, D. & Peers, C. (1995) O_2-sensitive K^+ currents in carotid body chemoreceptor cells from normoxic and chronically hypoxic rats and their roles in hypoxic chemotransduction. *Proceedings of the National Academy of Sciences of the USA,* **92,** 295-299.

Youngson, C., Nurse, C. A., Yeger, H. & Cutz, E. (1993) Oxygen sensing in airway chemoreceptors. *Nature* **365,** 153-155.

Yu, L., Quinn, M.T., Cross, A.D., Dinauer, M.C. (1998) $Gp91^{phox}$ is the heme binding subunit of the superoxide-generating NADPH oxidase. *Proceedings of the National Academy of Sciences, USA,* **95,** 7993-7998.

Zhong, H., Zhang, M., and Nurse, C.A. (1997) synapse formation and hypoxic signalling in co-cultures of rat petrosal neurones and carotid body type 1 cells. *Journal of Physiology,* **503,** 599-612.

Zhang, M. and Nurse, C.A. (2000) Does endogenous 5-HT mediate spontaneous rhythmic activity in chemoreceptor clusters of rat carotid body? *Brain Research, submitted.*

Zhu W. H. Conforti L. Czyzyk-Kreska M. F. & Millhorn D. E. (1996). Membrane depolarization in PC-12 cells during hypoxia is regulated by an O_2-sensitive K^+ current. *American Journal of Physiology,* **271,** C658-C665.

Zulueta, J.J., Aawhney, R., Yu, F.S., Cote, C.C., Hassoun, P.M. (1997). Intracellular generation of reaction oxygen species in endothelial cells exposed to anoxia-reoxygenation. *American Journal of Physiology,* **272,** L897-902.

Appendix 1

Development of O_2-sensitive large conductance Ca^{2+}-dependent K^+ currents in perinatal rat adrenal chromaffin cells

Adrenal medullary chromaffin cells (AMC) from the rat express O_2-sensitive properties in the perinatal period. The work in this thesis has demonstrated that AMC from the neonatal rat 'directly' sense hypoxia, as assayed by the effects on ionic currents and membrane potential. The pinnacle event of the hypoxia-sensing response of AMC is catecholamine (CA) secretion into the blood. Increased plasma CA are thought to play a physiological protective role and promote the transition to air breathing life (Slotkin and Seidler, 1988). The fetal arterial Po_2 is ~ 20 mmHg, equivalent to a moderate hypoxic stimulus in the adult, which raises the question as to how the fetus manages to regulate CA release from AMC and prevent early maturation of the cardiovascular system. Thus it was of interest to determine the development of O_2-sensing mechanisms in AMC during late fetal to early postnatal stages. It is reported here that E16-18 (embryonic) AMC are hypoxia-sensitive, but the O_2-sensing mechanism appears only partially developed relative to neonatal AMC, insofar as functional O_2-sensitive BK channels are absent.

Primary cultures of embryonic and neonatal rat AMC were prepared as previously described (Thompson et al., 1997; Chapter 1). Enzymatic solutions used for cell isolation and culture conditions were the same as those described in Chapter 1. Further, electrophysiological experiments on embryonic AMC were performed on cells cultured for 1-3 days, and techniques were similar to those described in the main body of the thesis (e.g. Chapter 2).

The main goal of this study was to determine if embryonic chromaffin cells from the rat adrenal medulla express O_2-sensitive properties similar to those in neonatal cells. Also, we wished to determine if these hypoxia-sensing mechanisms were fully

developed, and whether embryonic AMC possess any mechanisms to restrict CA release in the fetus. No difference in the passive properties (i.e. whole cell capacitance and input resistance) of embryonic and neonatal AMC was observed. Interestingly, hypoxia reversibly inhibited outward currents in AMC from both age groups. Figure 1 compares the effects of hypoxia on outward current (step to +30 mV) and current–voltage relationships between embryonic (Fig. 1A) and neonatal (Fig. 1B) AMC. The control outward current density in embryonic AMC was 72.1 ± 13.8 pA/pF (n=8; step to +30 mV), which was significantly reduced by hypoxia to 54.0 ± 12.6 pA/pF (n=8; P<0.05). The current density recovered to 71.1 ± 15.1 pA/pF (n=8; P>0.05 compared to control) upon return to a normoxic bathing solution (compare to neonatal cells in Chapter 2). It is interesting to note that there was a significant difference in the control outward current density (P<0.05) and IKo_2 (P<0.05) in embryonic AMC compared with neonatal cells (see Figure 4 for a summary of these data).

The reduced outward current density and smaller magnitude of IKo_2 raises the question whether all hypoxia-sensitive K^+ currents are present in embryonic AMC. One possibility is that there is a difference in expression of a functional O_2-sensitive Ca^{2+}-dependent K^+ current (I_{BK}). Figure 2 compares the effects removing extracellular Ca^{2+} (Ca^{2+}-free) on outward currents and I-V relationships between embryonic (Fig. 2A) and neonatal (Fig. 2B) AMC. Control outward current density (step to +30 mV) for a group of 7 embryonic AMC was 71.5 ± 15.1 pA/pF in 2mM bathing Ca^{2+} and 64.1 ± 11.4 pA/pF (n=7; P>0.05) in the Ca^{2+}-free bathing solution, suggesting that embryonic AMC lack functional Ca^{2+}-dependent K^+ currents (compare to neonatal cells in Figure 2B and

Chapter 2). By comparison, removal of extracellular Ca^{2+} reduced outward currents (at +30 mV) by $6.3 \pm 0.4\%$ (n=7) in embryonic and $60.1 \pm 7.9\%$ (n=8) in neonatal AMC. To confirm the possibility that embryonic AMC lack functional O_2-sensitive Ca^{2+}-dependent K^+ currents we compared the magnitude of IK_{O2} in the presence and absence of extracellular Ca^{2+}. For embryonic AMC, the total hypoxia-sensitive outward current, IK_{O2}, was similar in the presence of 2 mM Ca^{2+} (18.1 ± 2.2 pA/pF; n=7) and in the absence of extracellular Ca^{2+} (26.7 ± 6.7 pA/pF; n=7; P>0.05; see Figure 4A). In contrast, IK_{O2} was significantly reduced in neonatal AMC (see Chapter 2 and Figures 2 and 4).

To determine if the absence of O_2-sensitive, Ca^{2+}-dependent K^+ currents reflects a lack of I_{BK}, we used 50 nM ChTX or 50 nM IbTX to directly inhibit BK currents. Figure 3 compares outward currents and I-V plots between embryonic and neonatal AMC in the presence and absence of ChTX or IbTX. For, embryonic AMC, control outward current density was 65.2 ± 8.8 pA/pF (n=8) without, and 66.9 ± 12.6 pA/pF (n=8; P>0.05) with ChTX or IbTX in the bath (compare this to the significant effect of these toxins on outward currents in neonatal AMC as shown in Chapter 2 and Figure 3, and summarized in Figure 4).

The above voltage-clamp data suggests that embryonic AMC express O_2-sensing mechanisms that are immature compared to those in the neonate. Thus it was of interest to determine if hypoxia could depolarize embryonic AMC, as has been reported for neonatal cells (Thompson and Nurse, 1998; Chapters 1 and 2). The mean resting membrane potential in singly isolated embryonic and neonatal AMC was not significantly different; resting potential in embryonic AMC was -51.7 $\pm$ 3.7 mV (n=6),

compared to -59.2 ± 4.9 mV (n=5; P>0.05) in neonatal cells. Hypoxia reversibly depolarized embryonic and neonatal AMC by 10.8 ± 1.1 mV (n=6) and 16.6 ± 4.9 mV (n=5; P>0.05), respectively. These data suggest that embryonic and neonatal AMC possess a similar mechanism for generating the receptor potential.

Two criteria were used to assay embryonic and neonatal AMC for O_2-sensitive, large-conductance Ca^{2+}-dependent K^+ currents (I_{BK}). First, cells were bathed in a Ca^{2+}-free solution to block Ca^{2+} influx, and indirectly I_{BK}. Second, we used direct inhibitors of BK channels, iberiotoxin (IbTX) and charybdotoxin (ChTX) to block I_{BK}. Both the Ca^{2+}-free solution and IbTX/ChTX had no significant effect on outward current in embryonic AMC, but suppressed outward current in neonatal cells (see Chapter 2). Additionally, the magnitude of the hypoxia-sensitive outward current (IK_{O2}) in embryonic AMC was similar during control conditions and after BK blockade (see Figure 4). However, blockade of BK currents reduced IK_{O2} in neonatal cells (Chapter 2 and Figure 4), indicating that BK channels carry the majority of O_2-sensitive outward K^+ current in these cells. In addition, we have observed that the percentage of hypoxia-sensitive outward current in embryonic AMC (~25%) is less than that seen in neonatal cells (~40%), supporting the hypothesis that embryonic AMC lack functional O_2-sensitive BK currents.

In glomus cells of the rat carotid body, the mammals primary O_2-sensitive cell, BK currents have been reported to be absent at birth and increase in density by the first postnatal week (Hatton et al., 1997). This change in BK current density appears correlated with an increase in the sensitivity of glomus cells to hypoxia (Hatton et al.,

1997; Wasiko et al., 1999). Similar changes in BK current density have been reported with development in pyramidal cells from the neocortex (Kang et al., 1996) and hippocampus (Wann and Richards, 1994).

What is the physiological role of regulating expression of O_2-sensitive BK channels in the perinatal period? The large-conductance Ca^{2+}-dependent K^+ channel has a well-defined role in regulating the rate of action potential repolarization and in permitting adult rat AMC to fire repetitive action potentials during a single suprathreshold stimulus (Pancrazio et al., 1994; Solaro et al., 1995; Shao et al., 1999). Regulation of expression of BK channels during development could play a role in restricting catecholamine release during hypoxia by preventing cells from firing repetitive action potentials during hypoxia. Indeed, hypoxia-evoked catecholamine secretion from embryonic AMC appears blunted, and E16-18 AMC release predominantly norepinephrine, as opposed to the secretion of epinephrine from neonatal cells (S. Farragher and C.A. Nurse, unpublished observations). In summary, embryonic adrenal chromaffin cells lack functional O_2-sensitive large-conductance Ca^{2+}-dependent K^+ currents. It is proposed that development of BK currents is associated with reduced sensitivity of embryonic AMC to hypoxia and this may function to restrict catecholamine release during hypoxic stress in the fetus.

Figure 1. Comparison of the effects of hypoxia on outward current and current-voltage relationships between embryonic and neonatal adrenal chromaffin cells.

All current traces in the top two panels are for the voltage step to +30 mV from the holding potential of −60 mV. A, hypoxia (h) suppresses outward current from the control/normoxic (c) value in an embryonic (E18) chromaffin cell. Current magnitude recovered (r) upon re-perfusion with a normoxic solution. Bottom panel is the current-voltage relationship for the cell in the top panel and hypoxia (closed circles) reversibly (open triangle) inhibited outward currents from the control value (open circles) at all activating potentials. Similar results were seen in 7 other embryonic AMC tested this way. B, hypoxia (h) reversibly (r) suppresses outward current from the control/normoxic (c) value in a neonatal adrenal chromaffin cell. Bottom panel is the current-voltage relationship for the cell in the top panel. Note that hypoxia (closed circles) inhibited outward currents from the control values (open circles) at all potentials where currents are activated, and the effects are reversible (open triangle). These data indicate that both embryonic and neonatal chromaffin cells are hypoxia-sensitive.

A   embryonic

B   neonatal

500 pA

10 ms

c / r
h

c / r
h

current (pA)

1500

1000

500

-40   0   40   80

voltage (mV)

current (pA)

1500

1000

500

-40   0   40

voltage (mV)
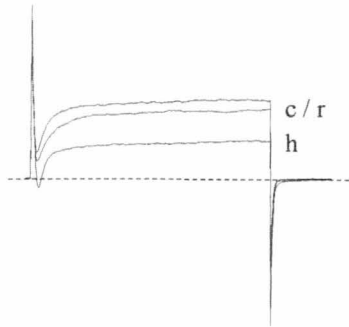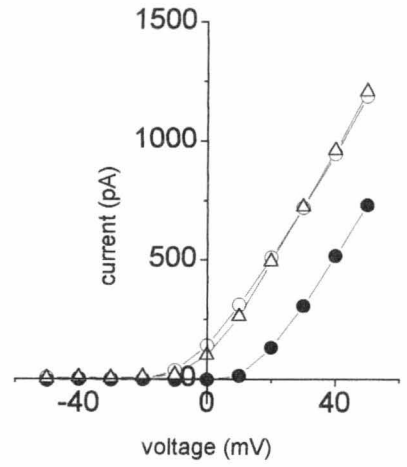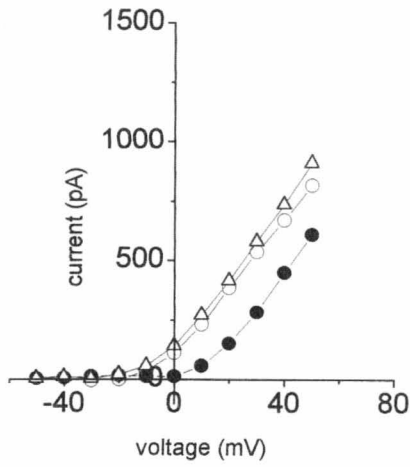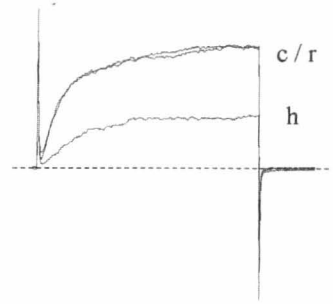
Figure 2. Embryonic and neonatal chromaffin cells possess Ca^{2+}-independent O_2-sensitive outward currents.

A, effects of removing extracellular Ca^{2+} (Ca-free) on control (c) outward currents and suppression by hypoxia (h), and hypoxia in the absence of extracellular Ca^{2+} (Ca-free + h) in an embryonic chromaffin cell. Note that the suppression of outward current (step to +30 mV shown) is similar in the presence and absence of 2mM bathing Ca^{2+}. Outward currents returned to the control value after Ca^{2+} was washed (w) back into the bath. Bottom panel is the current-voltage plot for the cell in the top panel, and note that removal of extracellular Ca^{2+} (open squares) did not significantly affect outward current from the control (open circle) level. Additionally, the magnitude of inhibition of outward current by hypoxia (closed circle) and hypoxia in the absence of extracellular Ca^{2+} (closed squares) were similar. Current levels returned to a value similar to the control level upon return to normoxia and 2 mM bathing Ca^{2+} (open triangle). These results indicate that the O_2-sensitive outward K^+ current in embryonic chromaffin cells is predominantly Ca^{2+}-independent. B, effects of hypoxia on outward currents (top panel; step to + 30 mV) and current-voltage relationships (lower panel) in a typical neonatal adrenal chromaffin cell. Labels in the top panel and symbols in the bottom panel are as in A. Removal of extracellular Ca^{2+} significantly suppressed outward current and reduced the magnitude of the hypoxia-sensitive outward current, indicating that the majority of O_2-sensitive outward current in neonatal chromaffin cells is Ca^{2+}-*dependent* (see Chapter 2).

A   embryonic

B   neonatal

c / Ca-free / w

h / Ca-free + h

c / w
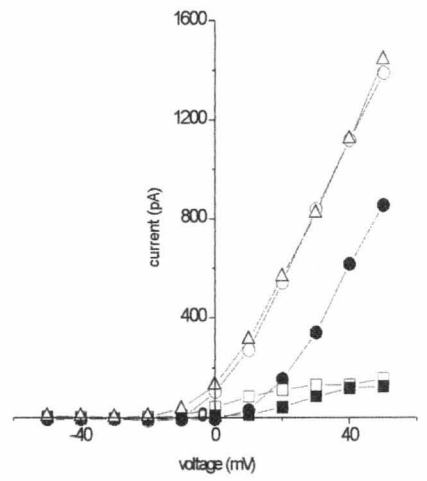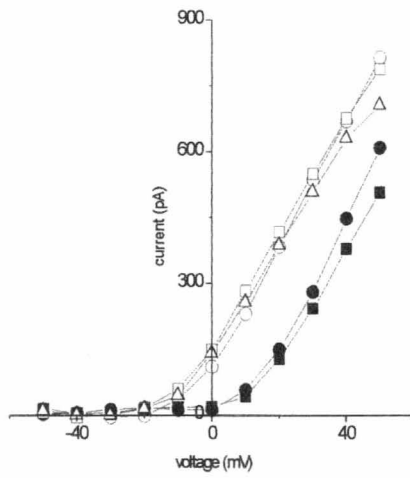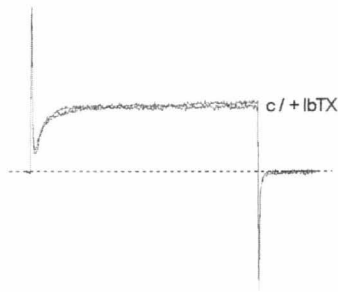
h

Ca-free c / h
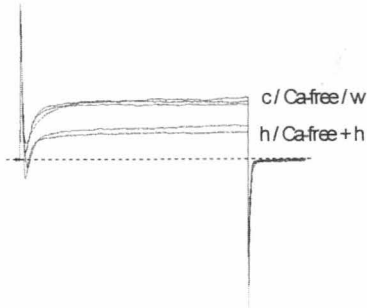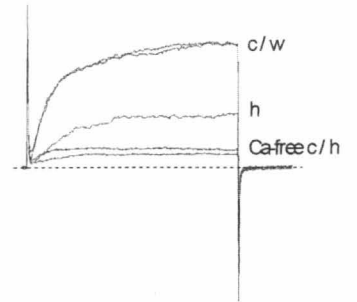
800 pA | 500 pA

15 ms

Figure 3. Embryonic chromaffin cells lack large-conductance Ca^{2+}-dependent K$^+$ currents.

A, exposure of an embryonic chromaffin cell to iberiotoxin (IbTX; 50 nM) did not affect outward current (step to + 30 mV shown). The bottom panel is a current voltage plot for the cell in the top panel. Note that IbTX (closed circles) did not affect outward currents compared to the control value (open circles) at any potential where currents are activated, indicating that embryonic chromaffin cells lack large-conductance Ca^{2+}-dependent K$^+$ currents (BK). Similar results were seen in 3 other cells exposed to IbTx and 4 cells exposed to the BK blocker, charybdotoxin. B, by contrast, a major portion of the outward current is sensitive to IbTX in neonatal chromaffin cells. Labels in the top panel, and symbols in the current-voltage plot are the same as in A. Similar results were observed in 3 other cells exposed to IbTX and 4 cells where BK currents were blocked with charybdotoxin. These data suggest that neonatal, but not embryonic chromaffin cells express functional BK currents.
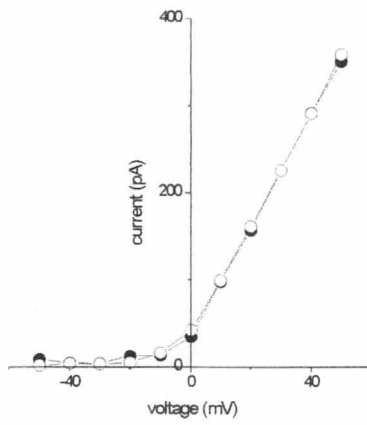
A
embryonic

c / + IbTX

200 pA | 300 pA

15 ms

current (pA)

400

200

-40   0   40
voltage (mV)

B
neonatal

c

+ IbTX

current (pA/pF)

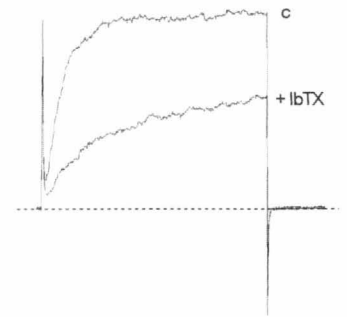1600

1200

800

400

-40   0   40
voltage (mV)
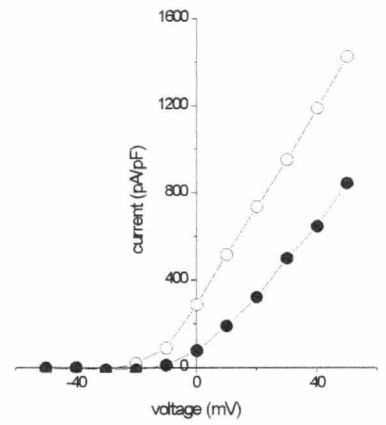
Fig. 4. Comparison of outward current density between embryonic and neonatal chromaffin cells.

These data are a summary of the mean outward current density (at + 30 mV) for 7 embryonic and 8 neonatal chromaffin cells. Current density was determined by dividing the steady-state outward current (at 40 ms) by the whole cell capacitance. A, outward current density measured in embryonic chromaffin cells in the presence and absence of extracellular Ca^{2+}, or with the BK channel blockers ChTx or IbTX in the bath. Note that K^+ current density was not affected by removal of extracellular Ca^{2+} and the hypoxia-sensitive component of outward current was unchanged. Furthermore, neither iberiotoxin (IbTX) nor charybdotoxin (ChTX), blockers of large-conductance Ca^{2+}-dependent K^+ channels affected outward current density. Difference bars represent the hypoxia or IbTX/ChTX current density subtracted from the control values. B, comparison of outward current density in a group of 8 neonatal adrenal chromaffin cells exposed to similar conditions as the embryonic cells in A. Note that control current density and the magnitude of the hypoxia-sensitive current were reduced upon removal of extracellular Ca^{2+}. Additionally, neonatal chromaffin cells had a significant IbTX/ChTX-sensitive component to the outward current. These data suggest that neonatal AMC posses both Ca^{2+}-dependent and –independent O_2-sensitive K^+ currents, whereas embryonic chromaffin cells express predominantly Ca^{2+}-*independent* hypoxia-sensitive outward currents.

A

embryonic

B

neonatal

control
hypoxia
recovery
difference
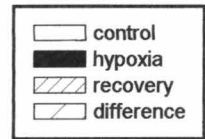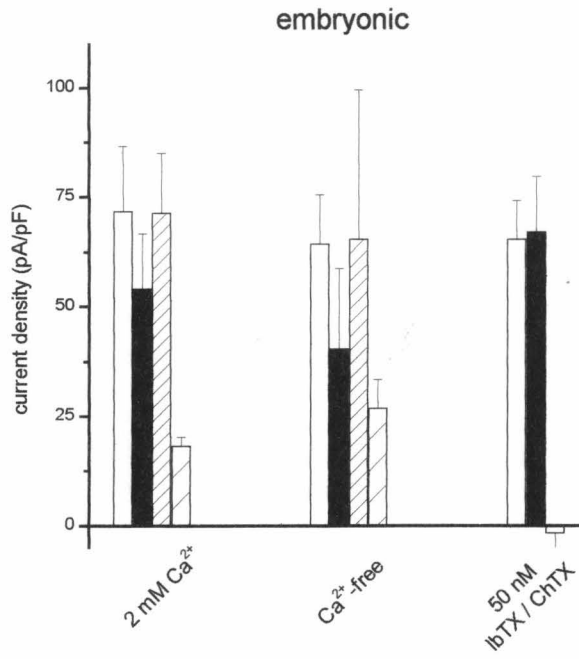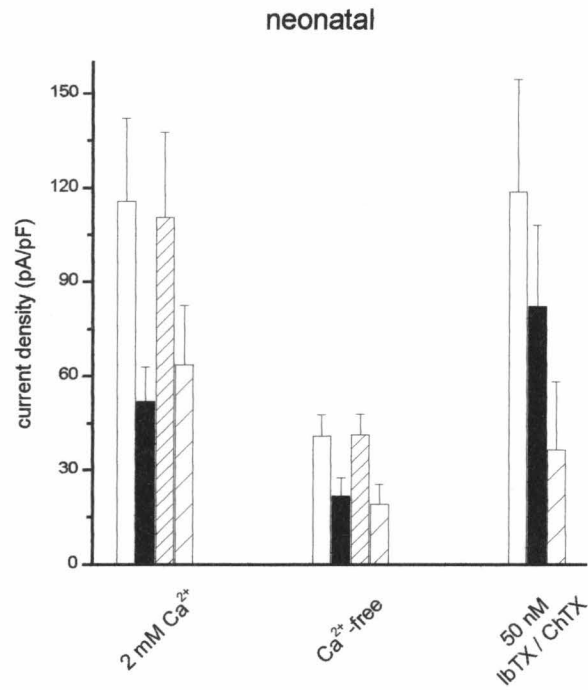
Appendix 2

O_2-chemosensitivity in an embryonic adrenal chromaffin cell derived cell line, the MAH cell

Studies of oxygen-sensitive cells have been extended to include cell lines in addition to primary cultures from hypoxia-sensitive tissues. This is because cell lines are easy to maintain and can be readily manipulated to delineate the molecular mechanisms of O_2-sensing. Perhaps the best-characterized O_2-sensitive excitable cell line is the phaeochromocytoma (PC12) cell, which are derived from an adult rat adrenomedullary tumour (see Millhorn et al., 1994). Although the PC12 cells express several aspects of the O_2-sensing mechanism seen in adrenal chromaffin cells (AMC), some interesting differences are apparent. The PC12 cells appear to lack functional O_2-sensitive Ca^{2+}-dependent K^+ currents, which comprise the major component of hypoxia-sensitive outward current in AMC (Zhu et al., 1996; Thompson and Nurse, 1998; Conforti et al., 2000). Furthermore, hypoxic inhibition of shaker type (K_V 1.2) K^+ channels appears to be responsible for generating the receptor potential in these cells, but not in AMC (see Chapter 2). Thus PC12, and other cell lines, may express some aspects of the O_2-sensing mechanism seen in primary cultures of AMC, but they seem to be relatively incomplete insofar as the entire mechanism may not be present. Thus, we chose to investigate if a cell line derived from embryonic E14.5 rat AMC, the MAH cell (Birren and Anderson, 1990), are O_2-sensitive, and whether these cells are suitable for further characterization.

Passive properties in MAH cells were similar to those in neonatal AMC. Mean input resistance was 2.0 ± 0.3 GΩ (n=7) and mean whole cell capacitance was 7.4 ± 1.3 pF (n=7; compare to neonatal cells in Chapter 1). Figure 1 illustrates that MAH cells are O_2-sensitive, as assayed by hypoxic inhibition of outward current. Control outward K^+

current density was 51.2 ± 6.9 pA/pF (n=7), which was reduced to 38.7 ± 6.2 pA/pF (n=7) by hypoxia. Outward current density returned to 51.4 ± 7.4 pA/pF (n=7) upon return to a normoxic bathing solution. Additionally, MAH cells appear to be similar to embryonic AMC insofar as the majority of cells tested (5/7) lack hypoxia sensitive Ca^{2+}-dependent K^+ currents. Outward current density was 51.7 ± 11.1 pA/pF for a group of 5 cells, and addition of 200 μM Cd^{2+} to the bath, to block Ca^{2+}-dependent K^+ currents, did not significantly effect outward current density in these cells to (44.7 ± 11.7 pA/pF; $P > 0.05$). Furthermore hypoxia (in the presence of Cd^{2+}) decreased outward current density to 28.2 ± 11.5 pA/pF (n=5; $P < 0.05$; see Figure 1) and this returned to 34.8 ± 14.5 pA/pF (n=5; $P > 0.05$ compared to control) upon reperfusion with a normoxic solution.

This suggests that MAH cells have a similar O_2-sensing mechanisms as PC12 cells and embryonic AMC. Thus, they may be suitable for studies to delineate the mechanisms that regulate BK channel expression during fetal development, or ones that involve cellular manipulation at the molecular level, (e.g. to identify of the O_2-sensor).

Figure 1. Effects of hypoxia and cadmium on outward currents in MAH cells.

A, hypoxia (h) reversibly (r) suppresses outward current from the control level (c; step to +30 mV shown) in a MAH cell. The lower panel is a current-voltage plot for the cell in the top panel. Note that hypoxia inhibits outward current at all potentials where they are activated and the effects are qualitatively similar to those seen in AMC (see Chapter 1). B, effects of 200 μM Cd^{2+}, and Cd^{2+} plus hypoxia on outward current in the same cell depicted in A. note that a outward K^+ current was not affected when Ca^{2+}-dependent outward currents are blocked with Cd^{2+}. Furthermore, the hypoxia-induced suppression of outward current is similar in the presence and absence of 200 μM Cd^{2+}. These data indicate that MAH cells are O_2-sensitive, but lack hypoxia-sensitive Ca^{2+}-dependent K^+ currents, similar to embryonic AMC (see Appendix 1). Similar results were seen in 5 of 7 cells tested this way.
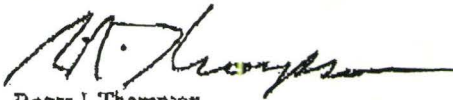
A

2 mM Ca²⁺

c / r
h

B

0.2 mM Cd²⁺

c / r
h

control
hypoxia
recovery
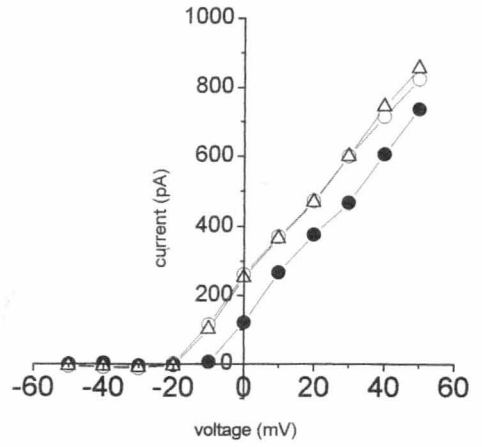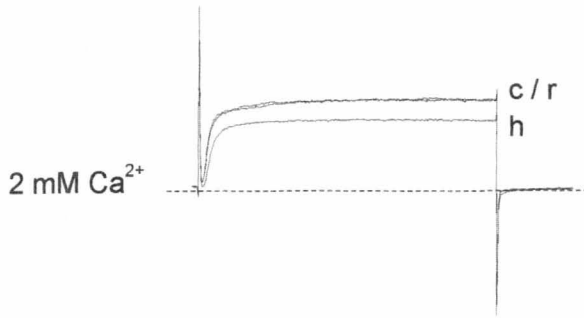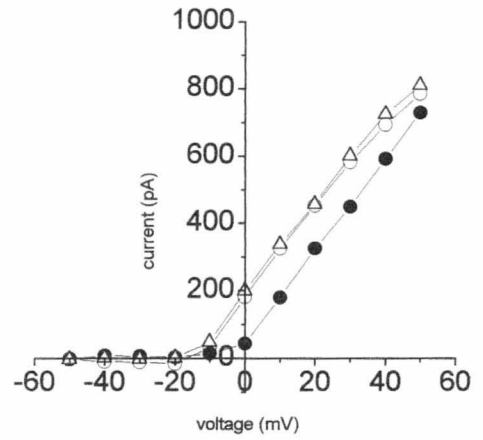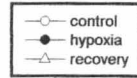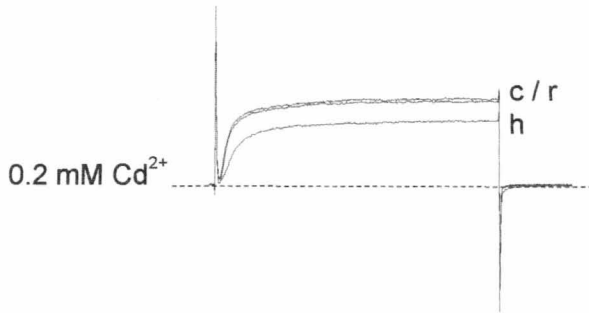
PO Box 11319
London
WC1E 7JF

Dear Miss Chapas,

I am currently writing my Ph.D. thesis at McMaster University in Hamilton, Canada and would like to request permission to reproduce two articles that I have published in the Journal of Physiology. They are Thompson, Jackson, and Nurse (1997) 498.2: 503-510 and Thompson and Nurse (1998) 512.2: 421-434. Permission is needed by both McMaster University and the National Library of Canada.

Thank you for your assistance and I look forward to you prompt reply.

Sincerely,

Roger J. Thompson
LSB 526
McMaster University
1280 Main Street West
Hamilton, Ontario, Canada
L8S 4K1
Phone: (905) 525-9140 ext. 27412
Fax: (905) 522-6066
Email: thompsrj@mcmaster.ca